MOL.19980724.0390

WBS: 1.2.5.4
QA: L

Civilian Radioactive Waste Management System
Management & Operating Contractor

Chapter 1
Total System Performance Assessment-Viability Assessment (TSPA-VA) Analyses Technical Basis Document

Introduction

B00000000-01717-4301-00001 REV 00

August 14, 1998

Prepared for:

U.S. Department of Energy
Yucca Mountain Site Characterization Office
P.O. Box 30307
North Las Vegas, Nevada 89036-0307

Prepared by:

TRW Environmental Safety Systems Inc.
1261 Town Center Drive
Las Vegas, Nevada 89134

Under Contract Number
DE-AC08-91RW00134

Civilian Radioactive Waste Management System
Management & Operating Contractor

Chapter 1
Total System Performance Assessment-Viability Assessment (TSPA-VA)
Analyses Technical Basis Document

Introduction

B00000000-01717-4301-00001 REV 00

August 14, 1998

Prepared by:

Holly Dockery
Performance Assessment Operations

14 Aug 98
Date

Checked by:

Robert Baca
Performance Assessment Operations

8/14/98
Date

Approved by:

Robert W. Andrews
Performance Assessment Operations

14 Aug 98
Date

INTENTIONALLY LEFT BLANK

INTENTIONALLY LEFT BLANK

INTENTIONALLY LEFT BLANK

CONTENTS

FIGURES

TABLES

ACRONYMS

AML	areal mass load
CAM	corrosion allowance material
CRM	corrosion resistant material
DOE	U.S. Department of Energy
EBS	Engineered Barrier System
EPA	U.S. Environmental Protection Agency
FEPs	features, events, and processes
LA	License Application
NRC	U.S. Nuclear Regulatory Commission
PA	performance assessment
PACE	Performance Assessment Calculated Exercise
SCP	Site Characterization Plan
SNF	Spent Nuclear Fuel
TSPA-VA	Total System Performance Assessment for the Viability Assessment
UZ	unsaturated zone
VA	Viability Assessment
WP	waste package

1. INTRODUCTION TO THE TSPA-VA TECHNICAL BASIS DOCUMENT

This report was prepared for the specific purpose of augmenting the documentation of the Total System Performance Assessment (TSPA) methodology, results, and information contained in Volume 3 of the Viability Assessment (VA) (DOE 1998). While Volume 3 represents a relatively comprehensive compendium of analyses and results, this Technical Basis Document goes further into the technical details regarding modeling approaches, assumptions, data base, computer codes, and process-level model sensitivity analyses. This document was primarily written for regulatory agencies and scientific review groups such as the U.S. Nuclear Regulatory Commission (NRC) and their contractors, the U.S. Department of Energy (DOE) TSPA-VA Peer Review Panel, the Nuclear Waste Technical Review Board, the Advisory Committee on Nuclear Waste, the State of Nevada and affected units of government groups, as well as for other interested parties in industry and academia. A directed effort was made to document the component performance analyses in a manner that would be transparent, traceable, and thus facilitate its review.

This first chapter discusses the broad objectives of the TSPA-VA as defined in Public Law 104-206. To aid the reader, this introductory chapter explains the primary objectives of the TSPA-VA Technical Basis Document. It outlines the organization of this document, and explains how various chapters of this document are correlated with corresponding sections of Volume 3 of the VA. In addition to defining terms such as "performance assessment" (PA) and "total-system performance assessment" (TSPA), this chapter also describes the general TSPA process as implemented by the DOE and NRC repository programs in the United States and by high-level waste programs and regulatory agencies elsewhere in the world. The chapter also discusses the role of TSPA as a tool for integrating the knowledge base from diverse disciplines and its use as a systematic process for analyzing a nuclear waste repository system. To provide a historical background, this chapter discusses the evolution of TSPA iterations for the Yucca Mountain site, starting with the Performance Assessment Calculated Exercise (PACE 90) exercise (Barnard and Dockery 1991) and the progressions of the TSPA iterations to the current TSPA-VA. The last part of this chapter describes the current reference design for the proposed repository and provides the specific design data used in TSPA calculations for the VA.

1.1 OBJECTIVE OF THE TSPA-VA TECHNICAL BASIS DOCUMENT

The Technical Basis Document provides the supporting documentation for Volume 3 of the VA. In the TSPA-VA, the results of the total-system analyses and the supporting sensitivity analyses were reported in detail. However, documentation of the component models was written at a generalized level to only provide a synopsis of the development, implementation, and results of the subsystem analyses. Also, the details of the TSPA code architecture and the methodology associated with the sensitivity and uncertainty analyses were not described in Volume 3 of the VA. The purpose of this document is to provide the underlying details for the topics that were only briefly covered in Volume 3.

1.1.1 Objectives of Total System Performance Assessment for the Viability Assessment

The overall scope and objective of the TSPA for the VA are contained in the 1997 Energy and Water Development Appropriations Act (Public Law 104-206):

> ...a total system PA based upon the design concept and the scientific data and analysis available by September 30, 1998, describing the probable behavior of the repository in the Yucca Mountain geological setting relative to the overall system performance standards.

Assessing the overall performance of the proposed repository system at Yucca Mountain required the following:

- Assimilating all the available scientific data and examining prior analyses for the geological setting
- Preparing a discrete representation of the reference design concept for the repository facility, waste package (WP), and hydrogeologic setting for use in the assessment
- Developing appropriate models and input data sets to forecast the probable behavior of the proposed repository system
- Selecting the interim performance standards to be used in comparisons with the TSPA results.

Since the inception of the DOE Yucca Mountain project, the scientific data produced by site characterization activities have been compiled, documented, analyzed, and reviewed by both internal and external groups. This data and information is largely contained in several computer data bases under the Yucca Mountain Project's Technical Data Management system, which is accessible through the internet. These and more recent data have been examined by project scientists and input data sets developed for use in the TSPA-VA.

Concurrent with the collection of site data, the design efforts have produced a reference design for the underground facility, the WP, as well as for the emplacement geometry to achieve the appropriate thermal design. The reference design for the proposed repository is described in Volume 2 of the VA (DOE 1998). Some of the major aspects of the reference design are summarized at the end of this chapter.

Since the early 90s, DOE PA model development efforts have produced a set of process-level models applicable to different components and subsystems of the proposed repository. These sophisticated and detailed models have been used in developing a system-level model that integrates all the component models, accounts for major phenomenological couplings, and propagates uncertainty (i.e., using a probabilistic technique) for both input parameters and future system states (i.e., disruptive scenarios). In addition to analyzing the isolation capability of the natural and engineered barriers of the repository system, the total system model produces statistical distributions of the performance indicator (e.g., peak dose) for the designated receptor location (e.g., 20 km) and containment period (e.g., 10,000 yr).

At present, the U.S. Environmental Protection Agency (EPA) is continuing to develop and finalize the new environmental standard for the proposed Yucca Mountain high-level waste repository. Similarly, the NRC is preparing a new high-level waste regulation which will revise the technical criteria in 10 CFR Part 60. In order to fulfill the objective mandated in Public Law 104-206, the DOE has adopted an interim postclosure performance goal for the proposed repository system. Specifically, the interim goal consists of an expected dose to an average individual in a critical group at a location 20 km from the repository not to exceed 25 mrem/yr from all pathways and all radionuclides during the first 10,000 years after closure (Barnes 1997). In addition, TSPA calculations beyond 10,000 years are to be performed to gain insight into longer term system performance.

1.1.2 Organization of This Document

Following this introductory chapter, the technical basis for each of the component models that comprise the TSPA-VA is presented. The TSPA-VA components presented in Chapters 2 through 9 consist of (1) unsaturated zone (UZ) flow, (2) thermal hydrology, (3) near-field geochemical environment, (4) WP degradation, (5) waste form alteration and mobilization, (6) unsaturated zone transport, (7) saturated zone flow and transport, and (8) biosphere. For each of these components, the associated chapter:

- Introduces the conceptualization of each individual process
- Discusses the key issues associated with the process model for that component
- Describes the abstraction approach and implementation in the TSPA analysis
- Provides the TSPA base case description for that component
- Describes the data sources
- Models parameter development and computer simulation methods
- Shows results and interpretation of the results
- Provides the approach, assumptions, description, results and interpretation of any sensitivity analyses performed for that component.

Chapter 10 describes the analyses and results associated with disruptive events (i.e., seismicity, volcanism, nuclear criticality, and human intrusion). Chapter 11 defines the TSPA-VA base case and then describes how the information produced in Chapters 2–10 is incorporated into the total-system model to provide evaluations of system performance. This chapter also includes a detailed discussion of the TSPA-VA model and computer code architecture and describes the uncertainty and sensitivity analysis methods used to determine the components and parameters contributing the most uncertainty to the evaluation of system performance. Finally, Appendix A gives the parameter values and distributions used in the TSPA-VA.

Table 1-1 cross-correlates the location of various types of information in Volume 3 of the VA (DOE 1998) and the chapters and subsections of this Technical Basis Document. As stated above, the sections on the individual TSPA components and some of the details of the total-system codes and methods are reported in much more detail in this volume. However, Volume 3 of the VA is the primary source for the results and interpretations of the total-system analyses and the associated sensitivity and uncertainty analyses. Volume 4 of the VA is also the primary reference containing the DOE guidance for PA model development for the License Application (LA).

1.2 DEFINITION AND USES OF PERFORMANCE ASSESSMENT AND TOTAL SYSTEM PERFORMANCE ASSESSMENT

As used in the nuclear waste management field, the terms PA and TSPA have very specific meanings. PA, the more generic term, is a method of forecasting how well a disposal or storage system (or component of that system) will isolate the nuclear waste (e.g., low-level, high-level, transuranic) over time. Its goal is to aid in determining whether the system or component being analyzed can achieve the specified design and/or regulatory requirements. A TSPA is a special type of PA in which all of the components of a system are linked into a single analysis.

1.2.1 What is a Total System Performance Assessment?

A TSPA, like other systematic safety assessment methodologies, is an analytic tool to aid decision making. It is unique from other methodologies, however, in that a TSPA for a geologic repository considers the combined behavior of disposal system as a function of significant features, events, and processes (FEPs), for time periods of thousands of years. These FEPs are represented in models of varying complexity for both the engineered and the natural system. The uncertainty and variability inherent in FEPs must also be included and evaluated. With these concepts in mind, a TSPA can formally defined as:

> A systematic analysis methodology that: (1) identifies the significant FEPs that may significantly affect the isolation capability of the system, (2) examines the effects of the FEPs on overall performance, and (3) estimates the radiologic risk to a hypothetical receptor group, taking into account the uncertainties associated with the FEPs , and (4) for the regulatory period of concern, provides a quantitative estimate of the regulatory risk measure and/or performance indicator in the form a probability distribution.

Another important output of a TSPA is a rank ordering of the FEPs, which delineates those components, scenarios classes, and uncertainties that determine overall repository performance.

The process of constructing and implementing a TSPA for a specific repository system is often explained using a pyramid, where detailed information representing the various processes and components of a total system are distilled and linked into progressively more abstracted models used to analyze system performance. The findings of a TSPA are also used to prioritize the information gathering activities of site characterization and design investigators. The results from prior TSPAs such as sensitivity studies performed on individual parameters or processes give insight into the areas in which additional information will decrease uncertainty to the greatest extent. This process is usually iterative, so incorporation of the revised and updated information into the subsequent TSPAs allows a progression toward more reasonable and defensible total-system models. The evolution of this process for the proposed Yucca Mountain repository is described in more detail in Section 1.3 of this chapter.

The word "forecast" rather than "predict" is used to describe the expected outcome of a TSPA. "Predict" implies "inference from facts or accepted laws of nature." Forecast has a similar meaning but also implies anticipating eventualities and differs from predict in being usually concerned with probabilities instead of certainties (Merriam-Webster 1993, pp. 457). As discussed in Section 1.3, incorporation of probabilities and uncertainty is a critical aspect of TSPA, which allows determination of reasonable assurance, as defined by regulatory agencies.

In certain respects, the process of TSPA is distinct from that of safety assessments and probabilistic risk assessments. Safety assessments generally use a conservative "bounding" assessment of the entire system; PAs analyze the best understanding of the system and its components (NEA 1995 pp. 28-36). In a safety assessment, which is often based on a deterministic approach, a set of FEPs are assumed to occur, regardless of the likelihood of their occurrence. A TSPA incorporates more information than a safety assessment because it assumes some processes or events are more likely to happen than others. They are then treated accordingly using mathematical models (however, for some processes or events where information is limited, bounding analyses may be used in the PA). The benefit of a TSPA in this case, is that a more realistic and, therefore, more defensible case is used.

It must be noted that, in the community of nuclear waste management professionals, this distinction between a safety assessment and a PA has become blurred, such that in informal usage they are often used interchangeably. However, it is important to differentiate the two philosophies, that is, the use of a "conservative" bounding cases versus using the most realistic models possible. In addition, a safety case, as made before a licensing authority, could include both safety assessments and PAs, as defined above.

"Probabilistic risk assessment" (PRA) is a term generally applied to safety studies of nuclear power plants (Lewis 1997) or other engineered systems, (Henley and Kumamoto 1991) but can be applied to any system that could fail in well-known and identifiable ways. Although this type of analysis incorporates variations in probability for different processes, the system and the time periods are very different between a reactor system and geologic repository system as studied by a PA. A PRA is usually considers discrete events of limited duration involving an engineered system and its components. Natural events such as earthquakes and volcanic eruptions are considered initiating events that may have an effect on overall system behavior, but are not a part of the system. Many reactor components, such as pumps and valves, can be tested on a time scale similar to that for the operational life of the system.

A PA for a geologic repository system includes both engineered and natural components as integral parts of the system. The variability and heterogeneity introduced in the system is much larger than that in a reactor system. Also, unlike the reactor system, the responses of the total-system extend over periods of time for which completely representative data has not or can not be obtained. It is important to emphasize that a TSPA, although based on the use of sophisticated computational models and probabilistic methods, only provides a rationale means of demonstrating a "reasonable expectation" of repository compliance with safety requirements. It can not be expected to provide a unique answer about the specific state of the repository system during various points in the future.

1.2.2 Philosophy of Total System Performance Assessment

The TSPA has become the internationally recognized method for analyzing system behavior for nuclear waste repositories. It is important to understand why TSPAs are performed, why a TSPA is unique, when compared to other types of analyses, and why the confidence in TSPA as a process has been established at such a global level.

1.2.2.1 Why Total System Performance Assessments are Performed

Performance assessments are used to forecast how a specific system and all of its components evolve over time. Comparing the results to performance requirements allows analysts to estimate whether the amount of harmful material that may become accessible in the environment is acceptably low. The requirements, usually in the form of regulatory criteria, are generally established by governmental oversight agencies. The ultimate determination of whether a system complies with the requirements lies with the legally responsible regulatory group. The task of those proposing a nuclear waste repository is to provide reasonable assurance that the safety standard will be met, which in turn requires that they:

- Understand the behavior of the proposed system and all of its components
- Can demonstrate the capability to model the system
- Can adequately account for and treat the uncertainties in the analysis
- Can show that the information in the model provides reasonable assurance that safety standards will be met.

In addition to providing a tool for demonstrating the disposal system's ability to meet regulatory requirements, TSPA also provides a rigorous method for aiding management in establishing the priority of information-gathering activities during the site selection, site characterization, and design phases. As more information is gathered, the TSPA process iterates to incorporate revised and updated information into successive TSPA models and allows a program to progress toward more reasonable and defensible total-system models. Results of each TSPA, particularly the sensitivity and uncertainty studies, provide information about the relative importance of ongoing or proposed information-gathering activities addressing site characterization and design development. Each successive TSPA requires that the total system models become more representative of the site and engineering design. Several TSPAs by the YMP have been completed to date on the Yucca Mountain repository system (Sinnock et al. 1984; Barnard and Dockery 1991; Barnard et al. 1992; Eslinger et al. 1993; Wilson et al. 1994; Andrews et al. 1994; CRWMS M&O 1995). These efforts, along with studies done by other organizations (NAS/NRC 1995; Kessler and McGuire 1996), have contributed to the iterative process of the TSPA for the VA.

A TSPA is unique because it is the analysis that links all the system components together. This linkage is important because it allows each component to be viewed in the context of the behavior of the entire system. Even the simplest system has various aspects that are easier to understand when studied separately. For example, WP material degradation may be characterized by laboratory tests of corrosion. However, the geologic system in which the WP is to be emplaced is analyzed using field studies of the host rock for properties that are only observed on a large scale (such as fracture density), as well as laboratory studies of other aspects (such as water chemistry). In a functioning system, these elements provide feedback to one another. The interaction of the water with the corroded WP would likely change the water chemistry, which may in turn change the fractures and the way water flows through them. This very simple example shows an obvious potential for feedback. When a very complex system with numerous components is simulated as a single system in a TSPA, interactions among the components that would not otherwise be observed are often found in the analysis.

As discussed in Volume 1 of the VA, the repository safety strategy for the YMP relies on a multiple barrier system. This isolation strategy means that all the components of the natural and engineered systems work together to form a series of barriers. Because the behavior of each component in the series is governed by a different set of physical or chemical processes, this strategy provides a strong argument that the entire system is very unlikely to fail in response to a single mechanism. Also, the use of different types of barriers lessens reliance on complete knowledge about any one process. Therefore, the incorporation of multiple barriers helps to answer the question that frequently arises, how can the analysis account for what is not known? Given the uncertainty inherent in a forecast, one way to deal with an unanticipated response by one component of the system is to have multiple additional components that will still operate as barriers.

"The concept of reasonable assurance" does not require absolute certainty in the results of an analysis. The incorporation of uncertainty into the TSPA, using various mathematical methods, allows the regulator and others to determine if the goal of reasonable assurance has been met. The study of uncertainty is documented in chapters of this document; however, some of the general methods of treating uncertainty include developing distributions to represent various types of data and also assigning probabilities to different conceptual models to encompass a range of potential behaviors or responses of certain components.

1.2.2.2 Why Total System Performance Assessments are the Appropriate Tool for Analyzing Repository Systems

A question that often arises is whether or not PA is a useful tool for the purpose of analyzing safety. The consensus of the international waste management community is that, PA is an adequate tool in the realm of providing reasonable assurance. In support of this consensus, the Nuclear Energy Agency Radioactive Waste Management Committee and the International Atomic Energy Agency International Radioactive Waste Management Advisory Committee issued a collective opinion (NEA 1991 p. 7) that they:

> "confirm that safety assessments are available today to evaluate adequately the potential long-term radiological impacts of a carefully designed radioactive waste disposal system on humans and the environment, and consider that appropriate use of

safety assessment methods, coupled with sufficient information from proposed disposal sites, can provide the technical basis to decide whether specific disposal systems would offer to society a satisfactory level of safety for both current and future generations."

Although TSPAs can never provide precise predictions, there are still many environmental problems that require modeling of the long-term interactions between man-made and geologic systems. Using the term "model" acknowledges that only approximate descriptions of geologic FEPs are possible and how well they represent absolute reality cannot be fully demonstrated. "Validation" of a long-term assessment model means that, on the basis of tests of the assumptions, inputs, outputs, and sensitivities, the model adequately reflects the recognized behavior of the portion of the system it is intended to represent. Adequacy of model is driven by the needs of the application for which it is specifically developed (Boak and Dockery 1998, pp. 178-180.).

Scientists assessing long-term risk (Kaplan and Garrick 1981) use the following mechanisms to establish the adequacy of their models (Boak and Dockery 1998, pp. 181-182):

- Expert judgment to assign appropriate ranges of parameters where data are sparse, controversial, or unobtainable
- Conservatism in assigning parameter values and process descriptions, including ignoring some potentially mitigating processes
- Stochastic simulation to assess the effect of uncertainty in descriptions and the sensitivity of performance predictions to uncertainty and to examine alternative scenarios and process models.

The following measures are undertaken to demonstrate that the effort to ensure validity has been comprehensive (Boak and Dockery 1998, p. 182):

- Documentation of the model structures, including justification for assumptions and simplifications as well as the examination of alternative conceptualizations for the system
- Review by the scientific community and those who have a stake in the decisions that these models support.

Uncertainty is an inherent part of all total system studies and, to the extent possible, is captured in statistical distributions selected to represent the randomness in future system states and variability of media properties. In some cases, information gathering activities are directed at reducing uncertainty as much as is practical, while in others, it is aimed at better characterizing the statistical representation of random behavior.

1.2.3 Role of Performance Assessment in the Nuclear Waste Management Program

The analysis of the Yucca Mountain total-system was performed, in part, to determine whether the system, using a reference design and current understanding of the natural system processes, is expected to comply with regulatory requirements. However, another goal of the YMP is to assess total system performance quantitatively defining the significance of each of the key components in the repository-safety strategy to assist in a systematic refocusing of Project resources in the areas of site characterization and system design. The statutory goal of the TSPA-VA is to address the probable behavior of the repository system. However, the available scientific information can also suggest alternative interpretations that may also be plausible. When propagated through a quantitative tool such as PA, these alternative interpretations can illustrate the significance of the uncertainty in the base-case interpretation chosen to represent the repository's probable behavior. The information about uncertainty will assist the U.S. Department of Energy (DOE) in defining the work required either to minimize uncertainty or to modify the repository design to accommodate for this uncertainty before submitting the LA for constructing the repository system. The quantitative performance analyses assist in identifying those areas where additional scientific and technical work are required to evaluate the site and to prepare a complete, cost-effective, and timely LA. The additional scientific investigations and design analyses necessary for developing the LA are summarized in Volume 4 of the VA (DOE 1998).

Another indirect use of the TSPA is to provide a vehicle for pre-licensing discussions with NRC. The NRC pre-licensing program focuses interactions on the key technical issues most important to repository performance. An important role of the TSPA is to evaluate the potential significance of these issues to find a common basis for understanding the need for additional scientific and technical work.

Although the goal of the TSPA is to provide a quantitative assessment of the probable behavior of the repository system, it is important to recognize the uncertainties inherent in such analyses. The EPA and NRC have recognized the care required in defining the degree of confidence needed from the analyses. EPA says that:

> "Because of the long time period involved and the nature of the events and processes of interest, there will inevitably be substantial uncertainties in projecting disposal system performance. Proof of the future performance of a disposal system is not to be had in the ordinary sense of the word in situations that deal with much shorter time frames" (EPA 1985; 40 CFR 191.13[a]).

According to NRC—The Commission anticipates that licensing decisions will be complicated by the uncertainties that are associated with predicting the behavior of a geologic repository over the thousands of years during which HLW [high-level waste] may present hazards to public health and safety (NRC 1983, 10 CFR 60).

These inherent uncertainties were recognized in developing the analysis tools that are described in Chapters 2–11 of this volume. The potential effects of many of these uncertainties are presented in Sections 5 and 6 of the Volume 3 of the VA.

An important goal of a post-closure PA is to produce document that is transparent with regards to the assumptions, results, and conclusions of the analyses. External review groups have defined what they mean by transparent. The Nuclear Waste Technical Review Board states that "transparency is the ease of understanding the process by which a study was carried out, which assumptions are driving the results, how they were arrived at, and the rigor of the analyses leading to the results" (Nuclear Waste Technical Review Board 1997, p. 21). The TSPA Peer Review Panel notes that "transparency is achieved when a reader or reviewer has a clear picture of what was done in the analysis, what the outcome was, and why" (Whipple et al. 1997, p. 10).

For there to be broad confidence in the PA, the presentation of the methodology and results must illustrate with sufficient clarity the following attributes:

- The conceptual basis for the individual components in the quantitative analyses
- How the individual components are combined into an assessment of system behavior
- The scientific understanding used to develop the quantitative analysis tools that describe the system's expected evolution
- The system's expected evolution as defined by the spatial and temporal response of the system to waste emplacement
- Uncertainty in the system's expected evolution and the significance of that uncertainty to the system performance goals.

This Technical Basis Document attempts to achieve the level of transparency expected by these oversight groups and the regulatory agencies. However, the YMP PA staff and management realize that there still remains a significant amount of work to be done to fully accomplish the level of traceability and transparency required for a defensible LA.

1.3 EVOLUTION OF YUCCA MOUNTAIN TSPA

A number of comprehensive but preliminary TSPAs (Sinnock et al. 1984; Barnard and Dockery 1991; Barnard et al. 1992; Eslinger et al. 1993; Wilson et al. 1994; Andrews et al. 1994; and M&O 1995) have been performed and documented for the proposed repository system at Yucca Mountain. In addition, several subsystem analyses have been performed. As more information about the site and design components of the potential repository system has become available, these TSPA analyses evolved into progressively more complex representations of the system.

The representation of some of the elements of the total system analysis included in each of the iterations has remained fundamentally the same, although the models and parameters have been revised and refined each time. However, as the collective scientific understanding of the FEPs specific to Yucca Mountain has progressed, the representation of certain process areas has been significantly updated. Perhaps the largest change has occurred in the understanding of unsaturated-zone groundwater flow at the potential repository site. Clearly, the rate and distribution of the movement of groundwater through the unsaturated-zone is important to the performance of the system. In every TSPA, regardless of the details of the performance measure used, performance is highly correlated to unsaturated-zone flow. In earlier assessments of Yucca Mountain, groundwater was assumed to flow downward, almost exclusively in the matrix. This assumption resulted in extremely slow flow through the entire system, and thus to very low cumulative releases during the regulatory period. Sensitivity studies at higher fluxes suggested it to be an important parameter. The evolution of the understanding of unsaturated-zone groundwater flow has required changes in the DOE models and the representation of the system. The most current model for this process is described in detail in Chapter 2 of this document and in Section 6.1.

In addition, the design has been evolving in response to experimental data and a changing understanding of site characteristics. In particular, TSPA analyses have been required to change from representation of a small, in-floor, vertically emplaced WP, as specified in the Site Characterization Plan (SCP), to a significantly larger WP emplaced horizontally in the drift. For a postclosure TSPA, this change has required inclusion of analyses concerning

- Drift stability with time
- Performance effects of backfill, pedestals, and invert materials
- Amount and location of seepage into the drift
- Lifetime of alternative container materials
- The possibility of single or common mode failures of multiple WPs due to circumstances in the drift.

Another large change in the design has been establishment of a high temperature region, utilizing the thermal output of the large WPs. In an attempt to form a long-lived "dry-out zone" from the heat of the packages, and thus to extend package lifetimes by curtailing corrosion from inflowing groundwater, areal power densities of up to 114 kW/acre have been studied. The change to higher thermal load and larger WPs, as well as other design changes related to use of concrete drift liners, drip shields, etc., have all required accommodation by the TSPA models.

Changes in regulatory guidelines have also resulted in major changes in the TSPA modeling activities. For instance, TSPA analyses that assessed the release of gaseous C-14 against the guidelines in 10 CFR Part 60 and 10 CFR Part 960 showed that this process provided the major contribution to the TSPA results when expressed in terms of cumulative releases over 10,000 years. However, the upper limit on releases of C-14 in these standards are far below annual release limits established by the Clean Air Act. If the new regulations, when repromulgated, are consistent with the Clean Air Act, C-14 is no longer expected to contribute significantly to the TSPA results. Another major change in TSPA models has resulted from the possibility of conversion to a dose standard, resulting in increased significance of the saturated-zone flow. The analyses presented here were predicated on the assumption that the Yucca Mountain repository system would be regulated using a dose-based standard. When the performance standard only addressed cumulative release, details of saturated-zone flow (e.g., dispersion, dilution) were relatively unimportant. Under a dose standard however, radionuclide transport through the saturated zone is very important. Thus, TSPA models and analyses have changed to reflect these and other changes required by the dose standard that is expected to be promulgated by the EPA in response to the Energy Policy Act of 1992. Table 1-2 contains a synopsis of the various features in each of the YMP TSPAs (including the TSPA-VA) to allow for comparison. This table generally shows an increase in sophistication in the model representation, however, this is not universally true.

1.3.1 Precursors to Recent YMP TSPA Modeling Activities

One early study of the Yucca Mountain repository system utilized deterministic calculations of radionuclide release from the system using a one-dimensional transport code (Sinnock et al. 1984). This study also included some additional analyses to estimate the importance of the effects of dimensionality, particularly in terms of lateral diversion of unsaturated flow. This study considered primarily "nominal conditions", based on the then current site knowledge. However, it also assessed the effects of increasing groundwater flux up to 20 mm/yr and of decreasing radionuclide retardation (due to interaction with the rock minerals) to zero. The releases calculated along the groundwater pathways under nominal conditions were more than seven orders of magnitude below the EPA release limits. Uncertainties were not explicitly included in the TSPA, nor were gaseous releases. The authors recognized that both incorporation of fast-path flow and changes in the assumptions about fracture-matrix interactions, as well as different treatment of geochemical retardation and of the source term could have major implications in terms of meeting the standard then applicable (EPA 1985). No disruptive processes or events were included in this calculation. Analyses performed for the Environmental Assessment (DOE 1986) evaluating the postclosure system guideline also concluded that releases, even over a period of 100,000 years, would not exceed the EPA's 10,000 year release guideline. However, it was recognized that a great deal of uncertainty remained in the representation of the groundwater flow system and in the performance of the engineered system in oxidizing conditions in the unsaturated-zone.

A number of subsystem analyses were performed in the subsequent years, including initial assessment of disturbances such as volcanism and human intrusion (Sinnock 1989; Doctor et al. 1992), WP lifetime (Farmer and McCright 1989), and performance of spent fuel (Apted et al. 1989). However, the predecessors to the current set of iterative PA were the PACE-90 conducted in 1989 and 1990 (Barnard and Dockery 1991) and the initial total systems analyses (Doctor et al. 1992, reporting 1988 work). PACE-90 was defined to simulate nominal-case groundwater flow and transport over a modeling period of 100,000 years. Deterministic analyses were run in both one- and two- dimensions. Four radionuclides were used to represent classes of behavior of long-lived nuclides present in the inventory (Np-237, Tc-99, I-129, and Cs-135). Percolation flux through the repository horizon was set at 0.01 mm/yr. Waste was mobilized from two major water-contact modes: "wet-drip" and "moist-continuous." The nuclides then traveled through a 19-layer hydrostratigraphy with laterally homogeneous properties that was developed from limited information from four boreholes. There were no calculated releases to the water table during the specified time period; therefore, movement in the saturated zone was not included. Also, gaseous releases, thermal effects, and disturbed scenarios were not included.

1.3.2 TSPA-91

The first in the "comprehensive" TSPA studies conducted by YMP was TSPA-1991 (Barnard et al. 1992; Eslinger et al. 1993) constructed using PACE-90 as a basis. Its objective was to develop a framework for probabilistic total-system calculations and it was the first set of stochastic analyses for YMP. The analyses were run in one- and two-dimensions using distributions of hydrogeologic parameters based on site and analog data. Two conceptual models for UZ flow were analyzed: composite porosity that represented fracture-matrix equilibrium, and the "weeps" model that assumed flow occurred exclusively in the fractures. The calculations also included disturbances to the nominal system caused by basaltic volcanism, human intrusion, and climate change. The radionuclide inventory was expanded to include those nuclides prevalent in the inventory (Pu, U, and Am isotopes), those expected to be important to dose (Se-79, Sn-126), and C-14 to represent the gaseous component. Radionuclide transport from the WP also included some near-field interactions. The saturated zone was also included explicitly and modeled out to the accessible-environment (5 kilometers). A simple drinking water dose was calculated, in addition to the cumulative releases.

No attempt was made to evaluate regulatory compliance. Qualitatively, however, comparisons were made with the EPA standard and NRC technical criteria. Results for TSPA-91 suggested that aqueous releases for both the weeps and composite porosity models and gaseous release using the weeps model did not exceed the EPA standard's (EPA 1985) cumulative release limits. Gaseous release, calculated with the composite porosity model, did exceed these limits. However, it was anticipated that a more realistic Engineered Barrier System (EBS) model for WP and waste form failure (i.e., taking credit for gradual degradation of these engineered components) would reduce these releases to below the EPA limit. Releases due to human intrusion and to volcanism were also both well below these regulatory limits.

1.3.3 TSPA-93

The primary purpose of TSPA-1993 (Wilson et al. 1994; Andrews et al. 1994) was to provide feedback concerning the relative importance of specific site-characterization and design information. Its secondary goal was to make progress in developing more defensible TSPA models for use in a demonstration of compliance.

There were a number of enhancements and revisions of the TSPA-1991 models and information including:

- A more geohydrologically representative model of the repository
- A 3-D geostatistically correlated stratigraphy
- An expanded hydrologic data set, explicit inclusion of wetter future climates
- Discrete modeling of individual stratigraphic units in the saturated zone
- Modification of retardation and sorption parameters
- Introduction of thermal dependence, spatial and temporal variation in fracture apertures (in the Weeps model)
- Inclusion of waste-package failure modes due to corrosion and dry oxidation
- Updated waste-form dissolution and oxidation models

- Analysis of both the SCP containers and the multi-purpose canisters, and inclusion of spent fuel and vitrified waste.

The analyses investigated sensitivities using both cumulative releases and dose results for up to 1,000,000 years. Percolation flux was the single most sensitive parameter. Again, as in TSPA-1991, all releases were below the EPA's 1985 standard, except for gaseous C-14 releases. However, longer-term (>100,000 years) peak doses for drinking water pathways were shown to be significantly above background. These analyses were being performed prior to the remanded EPA 1985 standard (i.e., 40 CFR Part 191), and were not designed to evaluate regulatory compliance with a dose or risk-based standard.

1.3.4 TSPA-95

The objectives of TSPA-1995 (M&O 1995) were primarily to enhance the representation of the engineered system, although some improvements of the natural system models were also incorporated. Specific changes to TSPA-1995 models included:

- Inclusion of a drift-scale thermohydrologic environment to derive relative humidity and temperature information adjacent to the WP
- A more detailed waste-package-degradation model, including corrosion of both inner and outer waste-package layers and galvanic protection of the inner layer
- Calculation of releases both with and without backfill
- Modification of solubility and retardation values for radionuclide transport
- Consideration of two alternative ranges of percolation flux (high flux: 0.5– 2.0 mm/yr; low flux: 0.01–0.05 mm/yr).

Disruptive events and gaseous releases were not included in TSPA-1995. A simple climate-change model was also incorporated into the analyses. The time period for the calculation of release and dose was up to 1,000,000 years.

TSPA-1995 also reported percolation flux to be the single most important factor to performance of a Yucca Mountain repository in the context of a 10,000-year standard. However, many elements of the EBS also were key to performance, as shown through sensitivity analyses such as galvanic protection, varying thermal load and backfill configurations, and assumptions about radionuclide transport through the EBS. As in TSPA-1993, sensitivities were calculated in terms of system-level performance measures (such as dose and cumulative release), and no attempt was made at evaluating regulatory compliance with a dose or risk-based standard.

1.3.5 Other Recent Yucca Mountain TSPAs

A number of other organizations have performed TSPAs for Yucca Mountain in the past several years. The most recent iterations include TSPAs run by the NRC (NUREG-1464) and by the Electric Power Research Institute (Kessler and McGuire 1996). A TSPA was also conducted by

Sandia National Laboratories (Rechard 1995) on a hypothetical "Yucca Mountain-like" tuff site. The suite of scenarios analyzed by each of these groups was essentially the same as those used in the YMP TSPAs. In each case, assumptions about conceptual models and parameter distributions differed somewhat from those used in the YMP TSPAs. However, the conclusions reached about the importance of particular processes and parameters (with the possible exception of basaltic volcanism in the case of the NRC analysis) with respect to performance of the repository system were very similar to those determined by the various YMP TSPA analyses.

1.4 SUMMARY DESCRIPTION OF TSPA-VA REFERENCE DESIGN

The base case repository design (i.e., underground facility a, WP, and thermal loading) used for TSPA-VA analyses is described in this section. The basis for the base case design is presented in this section. It is also described in detail in Volume 2 of the VA (DOE 1998). Design options analyses are included in Volume 3 of the VA (DOE 1998). Much of the text that follows was extracted from CRWMS M&O (1997). The design has been formulated with the intention of enhancing system performance with respect to the attributes of the repository safety strategy including (1) limited water contacting WPs, (2) long WP lifetime (containment), (3) low rate of release of radionuclides (mobilization) from breached WPs, and (4) radionuclide concentration reduction during transport from the WPs. The design strategy seeks to use engineered components to tailor the environmental variables (i.e., temperature, relative humidity, seepage flux) to be as benign as possible.

A schematic of the base case design at the time of repository closure is presented in Figure 1-1. In general, the major components of the base case design include a high areal mass load (AML) (85 MTU/acre), with "point loading" of the WPs. Figure 1-1 shows the repository layout design that covers ~740 acres and a schematic of the WP layout in the drift. The EBS will include a drift liner (concrete), an initial air gap in the drift (no backfill), two-layer WP (10 cm corrosion allowance material [CAM] and 2 cm corrosion resistant material [CRM]), in-drift emplacement of the WPs, placement of the WPs on steel support system, and a concrete invert at the base of the drift. Figure 1-2 shows representative WPs and waste forms for the reference design. The following discussion provides more detail as to the basis for each of these design components.

Drift Liner (Normal Concrete) - A drift liner (10 cm thick) has been included in the design, primarily in support of pre-closure safety. While it is intact, the liner is a potential barrier to water seeping into the drift. An intact liner could allow the water that might otherwise seep into the drift to drain along the perimeter of the drift in the small space between the liner and the host rock, or to flow as a film directly along the inside surface of the liner. Both of these modes of flow could reduce or eliminate dripping directly onto the WP. Normal concrete is used in the current reference design for lining 9 out of 10 drifts, with steel liner in the other drifts.

Air Gap (Capillary Barrier) - The air gap between the liner or drift wall and the WPs provides a means by which the percolating water may be diverted around the opening as matrix or film flow. This advantageous property will be in effect until the drift collapses and fills with rubble.

Waste Package—Corrosion Allowance Material - Because the WP is the single component that is expected to have absolute containment at the time of emplacement, the design strategy is to make the WP robust. The outer layer of the WP is 10 cm thick and serves three functions.

First, it provides structural strength to resist falling rock, to support the internal components, to be supported by the steel support systems, and to allow handling without damage. Second, the CAM provides radiation shielding to reduce the WP exterior surface contact dose rate. Coupled with the transportation overpack, the shielding is expected to be sufficient to protect workers during handling. Third, the CAM, in conjunction with the inner layer described below, acts as a containment barrier for the radioactive waste inside the WP. The current CAM material in the design is a carbon steel, Alloy A516.

Waste Package—Corrosion Resistant Material - The inner layer of the WP is a nickel-based alloy that is very resistant to aqueous corrosion and almost completely resistant to humid-air corrosion. The current reference CRM is 2 cm of Alloy 22. Because the CRM is inside the CAM, the corrosion environment can be much different than that induced by the ambient seeping water (potentially higher pH and crevice corrosion), thus requiring a more corrosion-resistant material than the outer barrier.

Large Waste Packages - A large WP reduces cost, handling, closure operations, non-destructive evaluation operations, and allows efficient use of the drift length. The current large WP reference design is based on a 21 PWR Spent Nuclear Fuel (SNF) Assembly WP. Roughly the same size WP can also accommodate 44 of the smaller Boiling Water Reactor SNF Assemblies or five Defense High-Level Waste glass "logs" surrounding a central canister of DOE SNF. For high heat producing or high criticality potential assemblies, a smaller WP, for 12 PWR SNF Assemblies, is used.

In-Drift Emplacement of Waste Packages - The design calls for in-drift emplacement. This is a consequence of large WPs being well suited to in-drift emplacement; consequently, the amount of excavation is minimized. Non-drift emplacement would require additional excavation.

Invert - The invert is designed to provide support for the WP pedestals during the pre-closure period. It will be composed of normal concrete.

Steel Support System for Waste Packages - The carbon steel support system provides support for the WPs during the pre-closure period. The support systems will be installed at a pre-determined spacing such that each WP is guaranteed to have at least three support systems under it, independent of WP spacing. Because the support system thickness is less than the CAM, it is expected that the support system will degrade prior to complete degradation of the CAM.

Thermal Design—Areal Mass Load (High) - The AML for the base case is 85 MTU/acre. This was determined by consideration of cost, expectation of water driven away during the high temperature period, and preservation of the zeolites below the repository. Clearly, if performance were independent of AML, it would be most cost effective to load the waste as densely as possible (high AML). Thus, the goal is to load the repository at as high an AML as feasible for acceptable performance, in order to minimize cost. In May 1995, the Office of Civilian Radioactive Waste Management Director decided to focus on a reference AML range of 80–100 MTU/acre, while maintaining the flexibility to use alternate AMLs should performance calculations find the reference range to be unacceptable. The current reference design AML is set by the temperature maximum which won't degrade the zeolites below the repository, which are a class of minerals that can potentially retard radionuclide transport.

Thermal Design—Waste Package Spacing (Point) - Once an AML is determined, the repository design team has the option to either place closely spaced WPs in widely spaced drifts or to place the WPs farther from each other in drifts that are more closely spaced. The latter option is termed "point loading" because each WP acts relatively independently of its neighbors in shedding its heat (this independence is strongest at very early times, before the rock between the WPs becomes hot). There is a large range of combinations of WP spacing and drift spacing that meets this definition of "point." The current reference design has a drift spacing of 28 m, which was determined by setting a limit of 200°C on the drift wall temperature.

Thermal Design—SNF Assembly Blending—To Meet 18 kW Limit - Each SNF assembly has a specific set of characteristics: enrichment, burnup, and age. These characteristics determine the amount of thermal power each assembly produces. A limit of 18 kW has been set for the thermal power produced by the collection of assemblies in a WPs to prevent heating the cladding beyond 350°C, which could cause the cladding to split. For the 18 kW "Design Basis" WP at a drift spacing of 28 m, enough aluminum is used in the basket design to ensure the cladding does not exceed the temperature limit. SNF assemblies will be packaged appropriately to meet the thermal power limit of 18 kW.

Thermal Design—SNF Assembly Blending—To Meet Criticality Limit - Each SNF assembly also has a specific potential to contribute to nuclear criticality, again based on enrichment, burnup, and age. This potential is quantified by the criticality constant in an infinite lattice, "k." Based on the finite number of assemblies in the WP and the overall effective criticality constant constraint, $k_{eff} < 0.95$, limits have been set for assembly values of k. SNF assemblies will be packaged to meet the limit.

INTENTIONALLY LEFT BLANK

1.5 REFERENCES

Andrews, R.W., T.F. Dale, and J.A. McNeish, 1994. *Total System Performance Assessment - 1993: An Evaluation of the Potential Yucca Mountain Repository,* DI B00000000-0717-220-00099-Rev. 01, Civilian Radioactive Waste Management System, Management and Operating Contractor, Las Vegas, Nevada. NNA.19940406.0158

Apted, M.J., A.M. Liebetrau, and D.W. Engel, 1989. *The Analytical Repository Source Term (AREST) Model: Analysis of Spent Fuel as a Nuclear Waste Form*, PNL-6347, Pacific Northwest Laboratory, Richland, Washington. NNA.19940406.0158

Barnard, R.W. and H.A. Dockery, (eds.), 1991. *Technical Summary of the Performance Assessment Calculational Exercises for 1990 (PACE-90), Volume 1: Nominal Configuration" Hydrogeologic Parameters and Calculational Results,"* SAND90-2726, Sandia National Laboratories, Albuquerque, New Mexico. NNA.19910523.0001

Barnard, R.W., M.L. Wilson, H.A. Dockery, J.H. Gauthier, P.G. Kaplan, R.R. Eaton, F.W. Bingham, and T.H. Robey, 1992. *TSPA 1991: An Initial Total-System Performance Assessment for Yucca Mountain,"* SAND91-2795, Sandia National Laboratories, Albuquerque, New Mexico. NNA.19920630.0033

Barnes, W.E., 1997 Letter to L.D. Foust, Concerning Interim Postclosure Requirement and Goal, U. S. Department of Energy, Office of Civilian Radioactive Waste Management, Yucca Mountain Site Characterization Office, Las Vegas, Nevada.

Boak and Dockery, 1998

CRWMS M&O (Civilian Radioactive Waste Management System Management and Operating Contractor) 1995a. *Total System Performance Assessment-1995: An Evaluation of the Potential Yucca Mountain Repository.* B00000000-01717-2200-00136 REV 01. Las Vegas, Nevada: Author. MOL.19960724.0188.

CRWMS M&O, 1997. *Year-End Status Report on Design Basis Models,* B00000000-01717-5703-00006, Las Vegas, Nevada.

Doctor, P., P. Eslinger, D. Elwood, D. Engel, M. Freshley, A. Liebetrau, P. Reimus, D. Strange, J. Tanner, and A. VanLuik, 1992. *An Example of Postclosure Risk Assessment Using the Potential Yucca Mountain Site,* PNL-8081, Pacific Northwest Laboratory, Richland, Washington. 208862

DOE (U.S. Department of Energy), 1998. *Viability Assessment of a Repository at Yucca Mountain.* DOE/RW/XX-XXXX, 5 Volumes. Washington, D.C.: U.S. Government Printing Office.

DOE [U.S. Department of Energy], 1986. *Environmental Assessment, Overview, Yucca Mountain Site, Nevada Research and Development Area, Nevada,"* DOE/RW-0079, U.S.

Department of Energy, Office of Civilian Radioactive Waste Management , Washington, D.C. 202194

Energy and Water Development Appropriations Act, 1997. Public Law 104-206. 110 Stat. 2984. 104th Congress. September 30, 1996. Full text available at http://www.gpo.ucop.edu/cgi-bin/gpogate?w...is/data/104_cong_pub_laws/publ206.104

EPA [U.S. Environmental Protection Agency] 1985. "40 CFR 191: Environmental Standards for the Management and Disposal of Spent Nuclear Fuel, High-Level and Transuranic Radioactive Wastes; Final Rule." *Federal Register,* 50 (182), 38066-38089. TIC Catalog Number: 221863

Eslinger, P.W., L.A. Doremus, D.W. Engel, T.B. Miley, M.T. Murphy, W.E. Nichols, M.D. White, D.W. Langford, and S.J. Ouderkirk, 1993. *Preliminary Total-System Analysis of a Potential High-Level Nuclear Waste Repository at Yucca Mountain,*" PNL-8444, Pacific Northwest Laboratory, Richland, Washington. 205581

Farmer, J.C. and R.D. McCright, 1989. *Review of Models Relevant to the Performance of High-Level Radioactive-Waste Disposal Containers,*" UCRL-100172, Lawrence Livermore National Laboratory, Livermore, California. NNA.19890725.0139

Kessler, J. And R. McGuire, 1996. "*Yucca Mountain Total System Performance Assessment, Phase 3,*" EPRI TR-107191, Electric Power Research Institute, Palo Alto, California. MOL.19980211.0367

Lewis, E. E. 1977, Nuclear Power Reactor Safety. John-Wiley and Sons, New York, NY

Merriam-Webster, 1993. Merriam-Webster's *Collegiate Dictionary (Tenth Edition).* Springfield, Massachusetts: Merriam-Webster Inc. 8883

NAS/NRC [National Academy of Sciences/National Research Council] 1995. *Technical Bases for Yucca Mountain Standards.* Committee on Technical Bases for Yucca Mountain Standards, Board on Radioactive Waste Management. Washington, DC: National Academy Press. 205 p. TIC Catalog Number: 217588

NEA 1995. *The Role of Conceptual Models in Demonstrating Repository Post-Closure Safety, Proceedings of an NEA Workshop.* November 16-18, 1993. 190 pages. Paris, France: Nuclear Energy Agency, Organization for Economic Co-Operation and Development. NUMBER.

Rechard, R.P., 1995. *Performance Assessment of the Direct Disposal in Unsaturated Tuff of Spent Nuclear Fuel and High-Level Waste Owned by U.S. Department of Energy, Volume 1: Executive Summary,*" SAND94-2563/1, Sandia National Laboratories, Albuquerque, NM.

NEA 1991. *Disposal of Radioactive Waste: Review of Safety Assessment Methods, Report of the Performance Assessment Advisory Group.* Paris, France: Radioactive Waste Management Committee, Nuclear Energy Agency, Organization for Economic Co-Operation and Development. NUMBER.

NWTRB [Nuclear Waste Technical Review Board] 1997. *Report to the U.S. Congress and The U.S. Secretary of Energy, January to December 1996 (1996 Findings and Recommendations).* Arlington, Virginia: Nuclear Waste Technical Review Board. TIC Catalog Number: 232686.

Rechard, R.P., 1995. *Performance Assessment of the Direct Disposal in Unsaturated Tuff of Spent Nuclear Fuel and High-Level Waste Owned by U.S. Department of Energy, Volume 1: Executive Summary,"* SAND94-2563/1, Sandia National Laboratories, Albuquerque, NM. TIC Catalog Number: 237101

Sinnock, S., Y.T. Lin, and J.P. Brannen, 1984. *Preliminary Bounds on the Expected Performance of the Yucca Mountain Repository Site, Southern Nevada,"* SAND84-1492, Sandia National Laboratories, Albuquerque, NM. NNA.19920131.0332

Sinnock, 1989 –

NRC [U.S. Nuclear Regulatory Commission], 1995. *NRC Iterative Performance Assessment Phase 2,"* NUREG-1464, U.S. Nuclear Regulatory Commission, Washington, D.C. 221527

NRC 1983, 10 CFR Part 60. Energy: Disposal of High-Level Radioactive Wastes in Geologic Repositories; Technical Criteria; Final Rule. *Federal Register,* 48 (120), 28194-28229 NNA.19891018.0190.

Whipple, C.; Budnitz, R.; Ewing, R.; Moeller, D.; Payer, J.; Witherspoon, P. 1997. *Peer Review of the Total System Performance Assessment - Viability Assessment, First Interim Report.* Las Vegas, Nevada: Total System Performance Assessment Peer Review Panel. MOL.19980127.0134.

Wilson, M.L., J.H. Gauthier, R.W. Barnard, G.E. Barr, H.A. Dockery, E. Dunn, R.R. Eaton, D.C. Guerin, N. Lu, M.J. Martinez, R. Nilson, C.A. Rautman, T.H. Robey, B. Ross, E.E. Ryder, A. R. Schenker, S.A. Shannon, L.H. Skinner, W.G. Halsey, J. Gansemer, L.C. Lewis, A.D. Lamont, I.R. Triay, A. Meijer, and D.E. Morris, 1994. *Total-System Performance Assessment for Yucca Mountain- SNL Second Iteration (TSPA-1993),"* SAND93-2675, Sandia National Laboratories, Albuquerque, NM. NNA.19940112.0123

Codes and Regulations:

10 CFR [Code of Federal Regulations] 60. *(date)* Energy: Disposal of High-Level Radioactive Wastes in Geologic Repositories; Technical Criteria; Final Rule. *Federal Register,* 48 (120), 28194-28229 NNA.19891018.0190.

10 CFR Part 960, 1984, Title 10, Energy, Part 960, *General Guidelines for the Recommendation of Sites for the Nuclear Repositories*, U.S. Government Printing Office, Washington, D.C. Available Electronically.

Public Law 104-206

Chapter 1
Tables

Table 1-1. Correlation of location of specific information in the TSPA in Volume 3 of the V-A Technical Basis Document.

Information	Location in Viability Assessment-Volume 3	Location in Technical Basis Document
Definition and Uses of TSPA	Sections 1.1-1.2	Chapter 1.2
Evolution of YMP TSPA	NA	Chapter 1.3
Description of Reference Design	Section 4.1	Chapter 1.4
Definition of TSPA-VA Base Case	Section 4.1	Chapter 11.1
Unsaturated-Zone Hydrology Model	Section 3.1	Chapter 2
Thermal Hydrology Model	Section 3.2	Chapter 3
Near-Field Geochemical Environment Model	Section 3.3	Chapter 4
Waste Package Degradation Model	Section 3.4	Chapter 5
Waste Form Degradation and Mobilization and EBS Transport Model	Section 3.5	Chapter 6
Unsaturated Zone Transport Model	Section 3.6	Chapter 7
Saturated Zone Flow and Transport Model	Section 3.7	Chapter 8
Biosphere Model	Section 3.8	Chapter 9
Disruptive Events Models	Section 4.4	Chapter 10
Effects of Design Options	Section 4.5	NA
TSPA-VA Methodology	Section 2.3	Chapter 11.1-11.2
Deterministic TSPA-VA Results	Section 4.2	Chapter 11.4
Probabilistic TSPA-VA Results	Section 4.3	Chapter 11.4
Uncertainty/Sensitivity Analyses	Section 5	NA
Uncertainty/Sensitivity Analysis Methods	Section 2.3.3	Chapter 11.3
TSPA-VA Conclusions	Section 6.4	NA
TSPA Model Development for the LA	Section 6.5	Chapter 11.5
Base Case Parameter Distribution	NA	Appendix A

Table 1-2. Analysis Approach to Selected Previous TSPA Evaluations.

Feature	Sinnock et. al. 1984	Pace-90	TSPA-91	TSPA-93	TSPA-95	TSPA-VA
Infiltration	Up to 20 mm/yr	Min: .01 mm/yr Max: 0.5 mm/yr	0 - 39 mm/yr	dry: 0.5 mm/yr mean wet: 10 mm/yr mean	lo: 0.01-0.05 mm/yr hi: 0.5-2.0 mm/yr	dry: 7.7 mm/yr mean LTA: 42 mm/yr mean SP: 110 mm/yr mean
Number of Radionuclides	17	4	10	43 (direct) 8 (aqueous)	39	9
Time Period of evaluation	up to100,000 yrs	up to 100,000 yrs	up to 100,000 yrs	up to 1,000,000 yrs	up to 1,000,000 yrs	up to 1,000,000 yrs
Waste Forms	CSNF	CSNF	CSNF	CSNF and HLW	CSNF and HLW	CSNF, HLW, DSNF
Distance to AE	.5 km	n/a	5 km	5 km	5 km 30 km	20 km
Saturated Zone	yes	n/a	single composite medium	multiple layers	single composite medium	effective continuum, 1-D, six stream tubes
Stratigraphic Discretization in UZ	n/a	19 layers	5 layers	10 layers	5 layers	28 layers
UZ flow model	1-D, matrix	1-,2-D 5 codes	1-,2-D; ECM and Weeps	1-,2-D; ECM and Weeps	2-D; ECM	3-D; DKM
Release Model	n/a	2 water contact modes	simple failure distribution for WP	simple failure distribution for WP	3 alternative conceptual models in EBS	diffusive, advective release from dripping and no dripping zones
^{14}C gaseous release	no	no	2-D steady state	2-D transient	no	no
Thermal effects	no	no	no	dry-out zone	dry-out zone	mountain and drift scale T-H
Disruptive Events	no	no	volcanism, human intrusion	volcanism, human intrusion	no	volcanism seismicity, human intrusion, nuclear criticality
Fracture Flow	no	in ECM	ECM, weeps	ECM, weeps	yes	DKM
Dose	no	no	no	Drinking water and irrigation	Drinking water	3 receptor scenarios, all pathways
Climate Change	through range of fluxes	no	through range of fluxes	100,000-year random periods	100,000-year random periods	3 climate cycles: Dry, LTA, SP

Table 1-2. (continued).

Feature	Sinnock et. al. 1984	Pace-90	TSPA-91	TSPA-93	TSPA-95	TSPA-VA
Galvanic Protection	no	no	no	no	yes	no
Uncertainty	through range of analysis parameters	no	in pdf's and flow models	in pdf's and flow models	in pdf's and flow models	in pdf's and flow models
Near field Geochemistry	no	no	no	no	no	limited

AE = Accessible Environment
LTA = Long Term Average Climate
SP = Super-Pluvial Climate
CSNF = Commercial Spent Nuclear Fuel
DSNF = Defense Spent Nuclear Fuel
HLW = High-level Waste
ECM = Equivalent Continuum Model
Weeps = Unsaturated flow model assumes stochastic flowing fractures
DKM = Dual-Permeability Model
WP = Waste Package
EBS = Engineered Barrier System
T-H = Thermal Hydrology
pdf = Probability Distribution Function

INTENTIONALLY LEFT BLANK

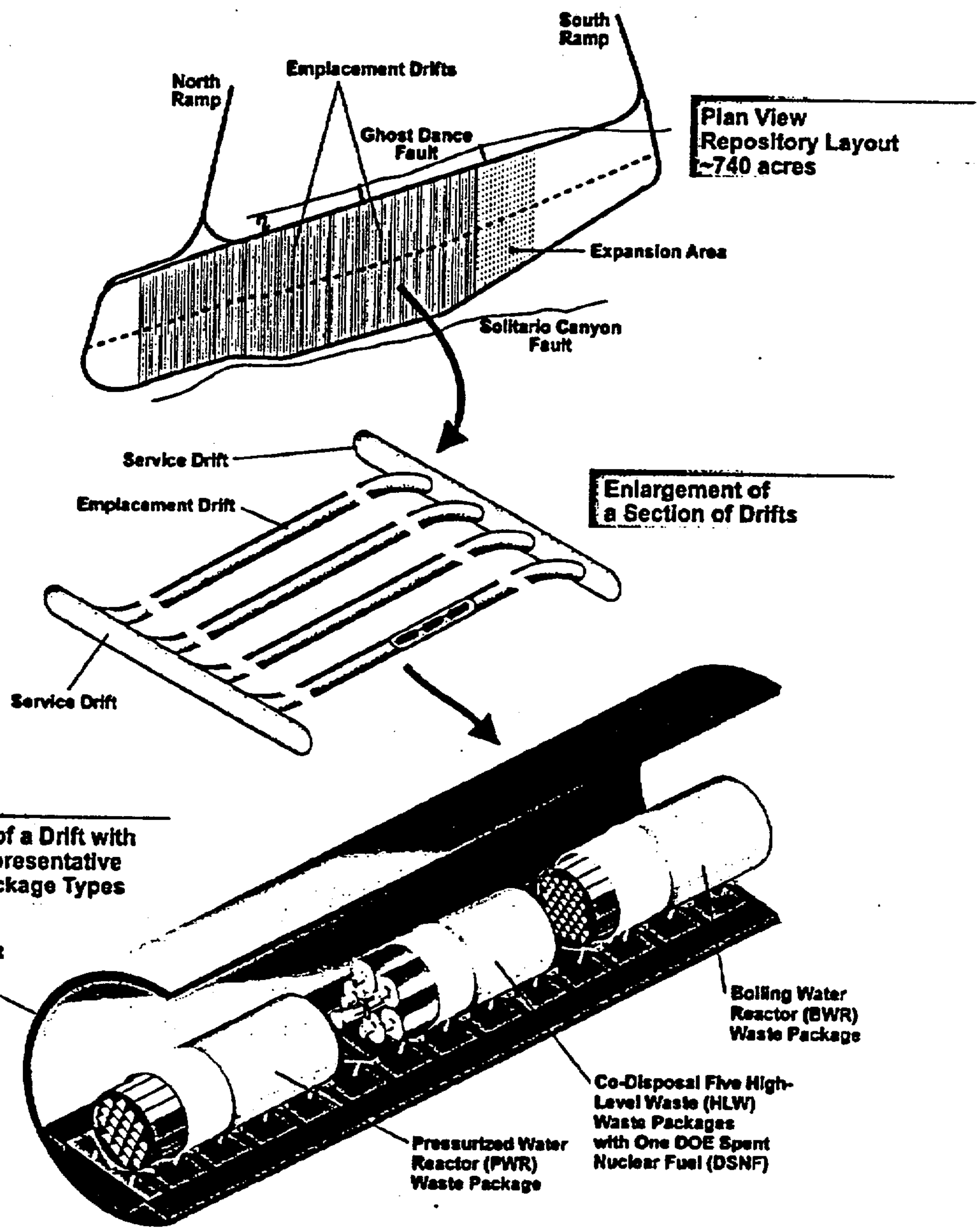

Figure 1-1. Schematic of the Reference Repository and Engineered Barrier System Designs used in the TSPA-VA. This figure illustrates the general drift layout within Yucca Mountain to contain the 70,000 metric tons of waste. Also illustrated is the emplacement of the waste packages on support system placed on the drift inverts.

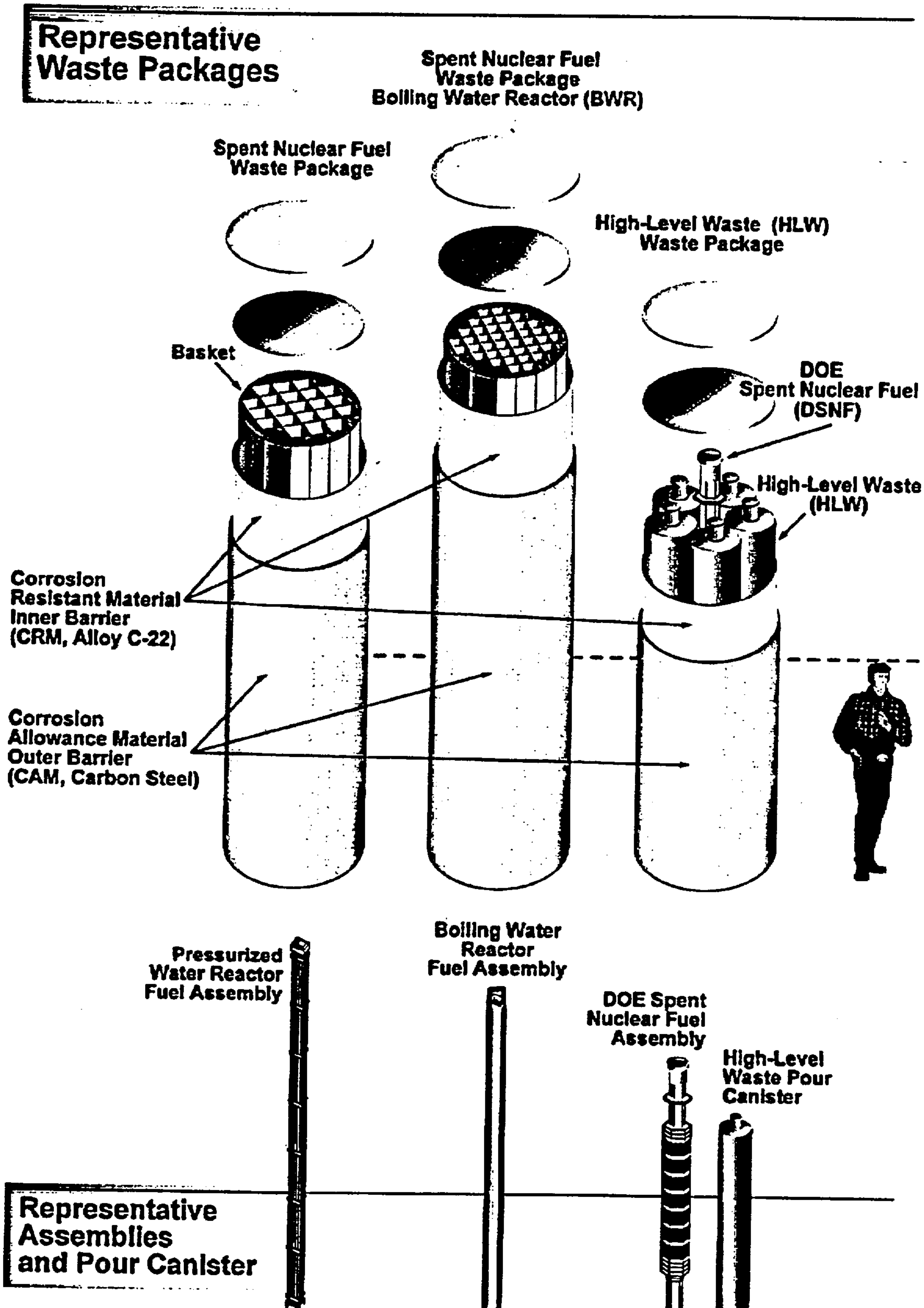

Figure 1-2. Representative Waste Forms and Waste Packages. This figure illustrates the three major waste form types: commercial spent nuclear fuel (CSNF), [existing as either Pressurized Water Reactor (PWR) fuel or Boiling Water Reactor (BWR) fuel], high level waste (HLW), or DOE-owned spent nuclear fuel (DSNF).

INTENTIONALLY LEFT BLANK

Chapter 1
Figures

INTENTIONALLY LEFT BLANK

DRAFT DISCLAIMER

CRWMS/M&O

Design Analysis Cover Sheet

Complete only applicable items.

(1.) QA: L

2. DESIGN ANALYSIS TITLE			
Evaluation of Ground Support Heating and Cooling Cycles			
3. DOCUMENT IDENTIFIER (Including Rev. No.) BCAA00000-01717-0200-00010 REV 00			4. TOTAL PAGES 69
5. TOTAL ATTACHMENTS 2	6. ATTACHMENT NUMBERS - NO. OF PAGES IN EACH I-4, II-3		
	Printed Name	Signature	Date
7. Originator	Yiming Sun	Yiming Sun	9/30/98
8. Checker	John F. Beesley David H. Tang	John F. Beesley David H. Tang	9-30-1998 9-30-98
9. Lead Design Engineer	Richard M. Nolting III	Richard M. Nolting III	9/30/98
10. Department Manager FOR	Kalyan K. Bhattacharyya	[illegible]	9/30/98

11. REMARKS

1. The following TBVs are contained in this analysis:

TBV-228	TBV-276	TBV-278	TBV-279	TBV-329	TBV-333	TBV-335	TBV-378	TBV-379
TBV-382	TBV-383	TBV-384	TBV-387	TBV-388	TBV-389	TBV-394	TBV-402	TBV-461

2. Checking of the Design Analysis:

   A. John F. Beesley: Responsible for discipline and compliance checking of the overall document.

   B. David H. Tang: Responsible for discipline checking of the computer input files (Reference 5.15).

CRWMS/M&O

Design Analysis Revision Record

Complete only applicable items.

1.

2. DESIGN ANALYSIS TITLE	
Evaluation of Ground Support Heating and Cooling Cycles	
3. DOCUMENT IDENTIFIER (Including Rev. No.)	
BCAA00000-01717-0200-00010 REV 00	
4. Revision No.	5. Description of Revision
00	Initial Issue.

TABLE OF CONTENTS

Page

TABLE OF CONTENTS (Continued)

LIST OF FIGURES

LIST OF FIGURES (Continued)

LIST OF TABLES

1.0 PURPOSE

The purpose of this analysis is to evaluate the effects of multiple heating and cooling cycles on rock mass and selected ground support systems in emplacement drifts. The analysis considers the multiple cooling caused by rapid ventilation to lower temperatures in the emplacement drifts for equipment access. The scope of this analysis is to assess the thermal and mechanical behavior of rock mass and ground supports affected by multiple thermal cycles in the emplacement drifts during the repository preclosure period of 150 years. The analysis only evaluates two options recommended for permanent ground supports of the emplacement drifts from an analysis for the Viability Assessment (VA) (Reference 5.1). The two ground support options recommended are precast concrete segmental lining and steel set lining.

The main objectives of this analysis are listed in the following:

- To determine the temperature distribution, both in time and location, due to multiple cycles of cooling and heating;
- To perform the stability analyses for affected openings considering the effects of thermal cycles on both rock mass and ground support materials;
- To determine the number and magnitude of heating and cooling cycles affecting the stability of emplacement drift openings.

2.0 QUALITY ASSURANCE

The emplacement area ground support items that are the subject of this analysis have been classified per QAP-2-3 as QA-1 and QA-2 in the Classification of the Preliminary MGDS Repository Design (Reference 5.2, Table 8.2-1) (TBV-228). Therefore, emplacement area ground support items are subject to QA controls.

This design analysis activity has been evaluated in accordance with the QAP-2-0 procedure, and It was determined that the QA program was applicable. Therefore, this activity is subject to QA controls. Input data used in this analysis that require further verification are designated as "To Be Verified" (TBV) in Sections 4.1 and 4.3. The tracking system described in NLP-3-15 is applicable.

3.0 METHOD

Analytical method is used in this analysis. Details on the approaches and their application in this analysis are discussed in Section 7.

4.0 DESIGN INPUTS

The majority of the input data presented in this section is considered preliminary and unqualified. The outputs from this analysis cannot be used for procurement, fabrication, or construction prior to qualification of all input data. Input data requiring TBV designation are identified in respective subsections.

4.1 DESIGN PARAMETERS

4.1.1 Stefan-Boltzmann Constant

For thermal calculations the Stefan-Boltzmann constant value of 5.669×10^{-8} $W/m^2 \cdot K^4$ is used (Reference 5.3, p. 396).

4.1.2 Average Ground Surface Temperature and Thermal Gradient (TBV-387)

The average ground surface rock temperature is 18.7°C (Reference 5.4, TDSS 002). The rock thermal gradients used in this analysis are listed in Table 4-1.

Table 4-1. Rock Thermal Gradient (Reference 5.4, TDSS 002).

Depth (m)	Value (°C /m)
0 - 150	0.020
150 - 400	0.018
400 - 541	0.030

4.1.3 Lithostratigraphy (TBVs-378 and 382)

The depth and thickness of the lithostratigraphic units listed in Table 4-2 (TBV-378) are the average values at the center point of the repository emplacement area based on Reference 5.1, Figure 4-1 and Table 4-3. The average elevations of the surface and the repository levels are 1407.2 m and 1072.3 m, respectively (Reference 5.1, Figure 4.1) (TBV-382). Therefore, the depth of the repository level (the invert) is at 334.9 m (1407.2 - 1072.3 = 334.9 m) from the surface.

4.1.4 Rock Mass Density, Thermal Conductivity, and Specific Heat (TBVs-279 and 378)

The rock mass dry bulk density, thermal conductivity and specific heat values (TBVs-279 and 378) are used in the thermal modeling. The values for each lithostratigraphic unit are listed in Table 4-2 based on Reference 5.1, Table 4-3.

Table 4-2. Lithostratigraphic Units and Their Density, Thermal Conductivity, and Specific Heat (Reference 5.1, Table 4-3).

T/M Unit	SNL Unit	Thickness	Bulk Density	Thermal Conductivity		Specific Heat		
				T<=100C	T>100C	T<=94C	94C<T<=114C	T>114
		(m)	(kg/m^3)	(W/m-K)		(J/kg-K)		
TCw	Tpcrv	Not Present						
TCw	Tpcrn	Not Present						
TCw	Tpcpul	Not Present						
TCw	Tpcpmn	Not Present						
TCw	Tpcpll	28.4	2300	1.92	1.69	883.17	4076.00	912.13
TCw	Tpcpln	60.9	2300	1.88	1.28	883.17	4076.00	912.13
TCw	Tpcpv	0.0						
PTn	Tpcpv1	13.8	1460	1.07	0.51	1526.44	20076.03	1043.56
PTn	Tpbt4	1.4	1310	0.50	0.35	1701.22	22374.81	1163.05
PTn	Tpy	1.4	1790	0.97	0.44	1245.03	16374.86	851.17
PTn	Tpbt3	0.4	1390	1.02	0.48	1603.31	21087.05	1096.12
PTn	Tpp	15.0	1130	0.82	0.35	1972.21	25938.94	1348.32
PTn	Tpbt2	5.5	1200	0.67	0.23	1857.17	24425.83	1269.67
PTn	Tptrv	4.7	1200	1.00	0.37	1814.58	19624.25	1410.00
TSw1	Tptrv	2.4						
TSw1	Tptrn	41.1	2380	1.62	1.06	872.90	5153.57	849.54
TSw1	Tptrl	10.9	2130	1.68	1.27	975.35	5758.45	949.25
TSw1	Tptpul	62.5	2130	1.97	1.07	975.35	5758.45	949.25
TSw2	Tptpmn	29.7	2250	2.33	1.56	951.73	4657.16	949.25
TSw2	Tptpll	96.5	2210	2.13	1.50	968.96	4741.45	970.62
TSw2	Tptpln	56.6	2270	1.84	1.43	943.35	4616.12	988.19
TSw3	Tptpv	19.1	2270	2.08	1.74	1018.63	8229.30	962.07
CHn1	Tptpv	16.2						1008.33
CHn1	Tpbt1	3.6	1660	1.31	0.68	1577.11	21311.27	1190.87
CHn1	Tac(v)	71.8	1520	1.18	0.59	1722.37	23274.14	1300.56
CHn1	Tac(z)							
CHn2	Tacbt	11.8	1790	1.34	0.70	1424.53	15131.62	1316.82
TSw2		182.8	2235	2.06	1.49	958.12	4688.41	977.14

4.1.5 Intact Rock Mechanical Properties (TBV-461)

The intact rock mechanical properties for TSw2 unit given in Table 4-3 are used in the analysis based on Reference 5.1, Table 4-6.

Table 4-3. Intact Rock Mechanical Properties for TSw2 Unit (Reference 5.1, Table 4-6).

Parameter	Value
Elastic Modulus (GPa)	33.03
Poisson's Ratio	0.21
Cohesion (MPa)	36.9
Friction Angle (degrees)	46
Tensile Strength (MPa)	8.91

4.1.6 Rock Mass Mechanical Properties (TBV-461)

Table 4-4 lists the rock mass parameters and properties for the TSw2 unit used in the analyses based on Reference 5.1, Table 4-7.

Table 4-4. Rock Mass Mechanical Properties for TSw2 Unit (Reference 5.1, Table 4-7).

Parameter	Rock Mass Quality Category	
	1	5
Elastic Modulus E (GPa)	7.76	32.61
Poisson's Ratio ν	0.21	0.21
Cohesion c (MPa)	1.5	5.2
Friction Angle (degrees)	43	46
Shear Modulus G (GPa)	3.21	13.48
Bulk Modulus B (GPa)	4.46	18.74
Tensile Strength (MPa)	1.32	4.21

4.1.7 Rock Mass Coefficient of Thermal Expansion for TSw2 Unit (TBV-279)

The temperature dependent coefficient of thermal expansion for the TSw2 unit listed in Table 4-5 is used in the analyses based on Reference 5.1, Table 4-8.

Table 4-5. Rock Mass Coefficient of Thermal Expansion for TSw2 Unit (Reference 5.1, Table 4-8).

Temperature Range (°C)	Value (10^{-6}/°C)
25 - 50	7.14
50 - 75	7.47
75 - 100	7.46
100 - 125	9.07
125 - 150	9.98
150 - 175	11.74
175 - 200	13.09

4.1.8 Concrete Thermal/Mechanical Properties

In analyzing the concrete lining system the parameter values listed in Table 4-6 are used based on Reference 5.1, Table 4-9. A concrete lining thickness of 0.2 m is used in the analyses. For the 0.20 m thick concrete lining (TBV-384), an area of 0.20 m^2/meter along the drift and corresponding moment of inertia of 6.6667×10^{-4} m^4/meter of drift are used in the analyses.

Table 4-6. Concrete Thermal/Mechanical Properties (Reference 5.1, Table 4-9).

Parameter	Value
Density (kg/m^3)	2323
Thermal Conductivity (W/m·K)	2.5
Specific Heat (J/kg·K)	1005
Emissivity	0.9
Elastic Modulus E (GPa)	27.58
Poisson's Ratio ν	0.25
Coefficient of Thermal Expansion (10^{-6}/°C)	9.9
Reference Compressive Strength (MPa)	34.48
Shear Modulus G (GPa)	11.03

4.1.9 Steel Set Thermal/Mechanical Properties

The parameter values listed in Table 4-7 are used in the analyses for the steel set lining based on Reference 5.1, Table 4-10. The steel set used in the analyses is W6×20. For W6×20 a cross-sectional area of 3.7871×10^{-3} m^2 and corresponding moment of inertia of 1.72320×10^{-5} m^4 is used from Reference 5.10 (p. 1-32). The cross-sectional areas and moments of inertia are divided by 1.2 m spacing and used in the analyses.

Table 4-7. Steel Set Thermal/Mechanical Properties (Reference 5.1, Table 4-10).

Parameter	Value
Density (kg/m^3)	7859
Thermal Conductivity (W/m·K)	50.67
Specific Heat (J/kg·K)	502.5
Emissivity	0.8
Elastic Modulus E (GPa)	200
Poisson's Ratio ν	0.3
Coefficient of Thermal Expansion (10^{-6}/°C)	11.24 at 25°C 11.40 at 50°C 11.71 at 100°C 12.01 at 150°C 12.32 at 200°C
Reference Strength (MPa)	248
Shear Modulus G (GPa)	76.92

4.1.10 Waste Package Steel Thermal Properties

The thermal properties for waste package steel listed in Table 4-8 are used in the thermal computations based on Reference 5.1, Table 4-11.

Table 4-8. Thermal Properties for Waste Package Steel (Reference 5.1, Table 4-11).

Parameter	Value
Density (kg/m^3)	8131
Thermal Conductivity (W/m·K)	41.71
Specific Heat (J/kg·K)	487.90
Emissivity	0.8

4.2 CRITERIA

The criteria that are related to this analysis are listed in the following, based on the Ground Control System Description Document (SDD) (Reference 5.8).

4.2.1 Ground Support System Performance

4.2.1.1 The emplacement drift ground support system shall maintain the envelope of 5.1 m diameter circle (TBV-329). [SDD 1.2.1.1]

4.2.1.2 The ground support system shall confine and support the rock surrounding each opening so as to minimize the potential for rock falls, fracturing, loosening of blocks, other deleterious rock movements, and surface deterioration of the rock mass. [SDD 1.2.1.2]

4.2.2 Safety

4.2.2.1 The ground support system shall be designed for the appropriate worst case combination of the corresponding loads including those induced by the cooling and reheating cycles in emplacement drifts. [SDD 1.2.2.1.2]

4.2.2.2 The ground support system shall fulfill the emplacement drift functions during the operational life of 150 years. [SDD 1.2.2.1.6]

4.2.3 Interface

The ground support system shall accommodate the subsurface ventilation, performance confirmation, emplacement, and retrieval. [SDD 1.2.4.1]

4.2.4 Maintenance

The emplacement drifts shall be designed to minimize maintenance, so that no more than 5% (TBV-335) of the emplacement drifts will require maintenance during the operational life with a level of confidence of 95% (TBV-335). [SDD 1.2.5.1]

4.3 ASSUMPTIONS

The following assumptions have been made in order to complete this analysis. These assumptions are used throughout the analyses.

4.3.1 In situ Stresses (TBV-278)

(This assumption is used in Section 7.)

The vertical stress value of 10 MPa at the repository drifts is assumed and used based on detailed explanation in Section 7.4.2 of Reference 5.1. The horizontal stresses are assumed to be in the range of 0.3 to 1.0 times the vertical stresses based also on the discussions in Section 7.4.2 of Reference 5.1.

4.3.2 Thermal Loads

(This assumption is used throughout the analysis.)

The following assumptions are required to perform the thermal computations. The assumed values and basis for assumptions are as follows:

Areal Mass Loading (TBV-394)

An AML of 85 MTU/acre is assumed as the emplacement drift thermal load in the analyses. This thermal load is based on recommendation of the Repository Thermal Loading Management Analysis for the Viability Assessment design (Reference 5.20, Section 8, p. 53).

Waste Package Diameter (TBV-379):

A diameter of 1.664 m for 21 PWR waste packages is used in the analyses based on Reference 5.12, p. 3.

Drift Spacing and Waste Package Spacing:

A drift spacing of 28.0 meters is assumed and used in the analyses based on the current repository configuration (Reference 5.21, p. 33) (TBV-276). Using this value and considering horizontal in-drift emplacement mode and the areal mass loading of 85 MTU/acre, an average waste package spacing of 15.18 meters is calculated in Attachment I.

Initial Rock Temperature (TBV-387):

Initial rock temperature is assumed to be 25°C based on reference average rock surface temperature of 18.7°C in Reference 5.4 (TDSS 002), and after accounting for thermal gradient at emplacement drift depth.

Waste Stream and Decay Heat Values (TBVs-383 and 389):

The waste stream information used in this analysis is stated in CDA Key Assumptions 003 and 004 (TBV-389). Based on this assumed waste stream, the decay characteristics of the 21-PWR waste packages are given in Reference 5.9. The heat flux values of the waste packages used in thermal model is calculated in Attachment I (TBV-383).

4.3.3 Emplacement Drift Locations (TBV-388)

(This assumption is used throughout the analysis.)

The emplacement drifts are assumed to be located mainly in the TSw2 unit based on Reference 5.4 (Key 022).

4.3.4 Physical Parameters and Properties for Rock Joints in TSw2 Unit (TBV-461)
(This assumption is used in Section 7.)

Rock joint parameters and properties include joint geometry, strengths, and stiffness values. The rock joint parameter and property values are assumed for the category-1 rock mass, as listed in Table 4-9, and used in the analyses based on Reference 5.1, Table 4-12.

Table 4-9. Physical Parameters and Properties for Rock Joints in TSw2 Unit (Reference 5.1, Table 4-12).

Parameter	Value
Cohesion (MPa)	0.07
Friction Angle (degrees)	56
Tensile Strength (MPa)	0
Normal Stiffness (MPa/m)	5×10^4
Shear Stiffness (MPa/m)	5×10^4
Orientation	85° for vertical joint set 15° for horizontal joint set
Spacing (m)	0.5 for vertical joint set 1.0 for horizontal joint set

4.3.5 Ground Support for Emplacement Drifts (TBV-402)
(This assumption is used throughout the analysis.)

Based on Reference 5.1, Sections 4.3.6 and 8.4, the ground support for emplacement drifts is assumed to include (1) a 200-mm-thick concrete lining and (2) 1.2-m-spaced W6×20 steel sets with steel lagging.

4.3.6 Retrievability Period
(This assumption is used throughout the analysis.)

The repository will be designed for a retrievability period of up to 100 years after initiation of emplacement Reference 5.4 (Key 016).

4.3.7 Emplacement Drift Diameter (TBV-333)
(This assumption is used throughout the analysis.)

The emplacement drift diameter is assumed to be 5.5 m based on present configuration for the repository openings (Reference 5.21, Section 4.3.10).

4.3.8 Initial Ground Relaxation

(This assumption is used in Section 7.)

An initial ground relaxation value of 60% is assumed and used in the ground support analysis of emplacement drifts based on Reference 5.5, Section 7.12.4.1. This value is related to the ground support loads induced by excavation and considered not critical to the results of this analysis. Therefore, this assumption is not required to be tracked by TBV.

4.3.9 Circumferential Contact Element Parameters

(This assumption is used in Section 7.)

A circumferential interface (discontinuity) between the precast concrete or steel set lining and the rock is assumed based on Reference 5.1, Section 4.3.17. The physical and numerical parameters associated with the interface are obtained from Reference 5.1, Section 4.3.17, and listed in Table 4-10.

Table 4-10. Physical and Numerical Parameters for Circumferential Contact Element (Reference 5.1, Section 4.3.17).

Parameter	Contact between Concrete and Rock	Contact between Steel and Rock
Coefficient of Friction	0.7	0.7
Penetration Tolerance (mm)	0.1	0.5
Normal Contact Stiffness (MPa/m)	15×10^3	3×10^3
Sticking Contact Stiffness (MPa/m)	5×10^3	3×10^3

4.3.10 Emplacement Drift Ventilation Parameters

(This assumption is used in Sections 7 and 8 and Attachment II.)

Ventilation air quantity values of 2.5 m^3/s and 50 m^3/s are assumed based on Reference 5.7, Table 3. Intake air for ventilation is assumed to be 25°C (298 K). By using interpolation from Reference 5.3, p. 646, the property values for ventilation air, as presented in Table 4-11, are obtained.

The cooling is assumed to be called for every 10 years beginning at 10 years after waste emplacement. The duration of each cooling period is assumed to be two weeks and two months for the air quantities of 2.5 m^3/s and 50 m^3/s, respectively.

Table 4-11. Property Values for Ventilation Air at 25°C (298 K) (Reference 5.3).

Parameter	Value
Density (kg/m^3)	1.1868
Thermal Conductivity (W/m·K)	0.02608
Dynamic Viscosity (kg/m·s)	1.8363×10^{-5}
Prandtl Number (dimensionless)	0.709

4.4 CODES AND STANDARDS

Not used.

5.0 REFERENCES

5.1 CRWMS M&O 1998. *Repository Ground Support Analysis for Viability Assessment.* BCAA00000-01717-0200-00004 REV 01. Las Vegas, Nevada: CRWMS M&O. MOL.19980512.0714.

5.2 CRWMS M&O 1997. *Classification of the Preliminary MGDS Repository Design.* B00000000-01717-0200-00134 REV 00. Las Vegas, Nevada: CRWMS M&O. MOL.19980211.1192.

5.3 Holman, J.P. 1997. *Heat Transfer.* Eighth Edition. New York, New York: McGraw-Hill, Inc. CRWMS M&O TIC No.: 239954.

5.4 CRWMS M&O 1998. *Controlled Design Assumptions Document.* B00000000-01717-4600-00032 REV 05, ICN 0. Las Vegas, Nevada: CRWMS M&O. MOL.19980804.0481.

5.5 CRWMS M&O 1995. *ESF Ground Support Design Analysis.* BABEE0000-01717-0200-00002 REV 00. Las Vegas, Nevada: CRWMS M&O. MOL.19960409.0355.

5.6 Owen, D. R. and Hinton, E. 1980. *Finite Elements in Plasticity: Theory and Practice.* Swansea, U.K.:Pineridge Press Limited. CRWMS M&O TIC No.: 208975.

5.7 CRWMS M&O 1997. *Emplacement Drift Air Control System.* BCAD00000-01717-0200-00005 REV 00. Las Vegas, Nevada: CRWMS M&O. MOL.19980102.0034.

5.8 CRWMS M&O 1998. *Ground Control System Description Document.* BCA000000-01717-1705-00011 REV 00. Las Vegas, Nevada: CRWMS M&O. MOL.19980825.0286.

5.9 CRWMS M&O 1997. *Preliminary Design Basis for WP Thermal Analysis.* BBAA00000-01717-0200-00019 REV 00. Las Vegas, Nevada: CRWMS M&O. MOL.19980203.0529.

5.10 AISC 1995. *Manual of Steel Construction.* Allowable Stress Design, 2nd Revision, 9th Edition, American Institute of Steel Construction, Inc. CRWMS M&O. TIC No.: 236850.

5.11 CRWMS M&O 1997. *Software Qualification Report for ANSYS Revision 5.2SGI.* CSCI: 30013 V5.2SGI. DI: 30013-2003 REV 00. Las Vegas, Nevada: CRWMS M&O. MOL.19970815.0536.

5.12 CRWMS M&O 1998. *Preliminary List of Waste Package Designs for VA.* BBA000000-01717-3300-00008 REV 02. Las Vegas, Nevada: CRWMS M&O. MOL.19980409.0021.

5.13 CRWMS M&O 1994. *Software V&V Package for UDEC Software Version 2.0.* RPI: QRP1.2.12. Las Vegas, Nevada: CRWMS M&O. NNA.940407.0188.

5.14 ANSYS 1994. *ANSYS User's Manual Version 5.2*. Volumes I, II, III, and IV. Canonsburg, PA: ANSYS, Inc. CRWMS M&O TIC No.: 233067.

5.15 Computer Input Files for the *Evaluation of Ground Support Heating and Cooling Cycles*, BCAA00000-01717-0200-00010 REV 00. Las Vegas, Nevada: CRWMS M&O. MOL.19980929.0060.

5.16 ITASCA 1993. *UDEC (Universal Distinct Element Code) User's Manual, Volumes I and II, Version 2.0.* Minneapolis, MN: ITASCA Consulting Group, Inc. CRWMS M&O TIC Numbers: 232815 and 232816.

5.17 CRWMS M&O 1997. *Subsurface Repository Performance Confirmation Facilities*. BCA000000-01717-0200-00011 REV 00. Las Vegas, Nevada: CRWMS M&O. MOL.19970723.0142.

5.18 CRWMS M&O 1998. *Repository Subsurface Waste Emplacement and Thermal Management Strategy*. B00000000-01717-0200-00173 REV 00. Las Vegas, Nevada: CRWMS M&O. MOL.19980918.0084.

5.19 CRWMS M&O 1997. *Performance Confirmation Data Acquisition System*. BCAI00000-01717-0200-00002 REV 00. Las Vegas, Nevada: CRWMS M&O. MOL.19980513.0133.

5.20 CRWMS M&O 1997. *Repository Thermal Loading Management Analysis*. B00000000-01717-0200-00135 REV 00. Las Vegas, Nevada: CRWMS M&O. MOL.19971201.0601.

5.21 CRWMS M&O 1997. *Repository Subsurface Layout Configuration Analysis*. BCA000000-01717-0200-00008 REV 00. Las Vegas, Nevada: CRWMS M&O. MOL.19971201.0879.

5.22 CRWMS M&O 1997. *Drift Ground Support Design Guide*. BCAA00000-01717-2500-00001 REV 00. Las Vegas, Nevada: CRWMS M&O. MOL.19980109.0104.

6.0 USE OF COMPUTER SOFTWARE

Two commercially available computer programs, ANSYS and UDEC, are used in this analysis. All codes were qualified for use for quality affecting work in accordance with M&O software procedures.

6.1 ANSYS COMPUTER SOFTWARE

ANSYS Version 5.2 is a general purpose finite element analysis (FEA) code, and is used in many disciplines of engineering that deal with topics including structural, geotechnical, mechanical, thermal, and fluids. ANSYS is installed on the SiliconGraphics (SGI) and Sun Microsystems workstations with the Unix operating system. ANSYS Version 5.2 has been verified and validated (CSCI#: 30013 V5.2SGI, Reference 5.11) according to applicable M&O procedures (Reference 5.11). ANSYS was used in thermal and coupled thermomechanical analyses for both emplacement and non-emplacement drifts. The input files are presented in Reference 5.15. The outputs are presented and described throughout Section 7.0. The output files generated by ANSYS are archived and submitted as part of the record package for this analysis. A detailed discussion on the general features and fields of application of ANSYS code is presented in the User's Manual (Reference 5.14).

The ANSYS Version 5.2 software was obtained from the Software Configuration Management (SCM) in accordance with the applicable M&O procedures. The software was appropriate for the applications used in this analysis. The software was used within the range of validation as specified in the software qualification report (Reference 5.11).

6.2 UDEC COMPUTER SOFTWARE

UDEC (Universal Distinct Element Code) Version 2.0 is a two-dimensional numerical program based on the distinct element method for discontinuum modeling (Reference 5.16). The program simulates the response of discontinuous media (such as a jointed rock mass) subjected to thermal, static or dynamic loading. In UDEC, the discontinuous medium is represented as an assemblage of discrete blocks. The discontinuities between blocks are treated as boundary conditions that permit large displacements along the discontinuities and block rotations. Individual blocks behave as either rigid or deformable material. Deformable blocks are subdivided into a mesh of finite difference elements, and each element responds according to a prescribed linear or non-linear stress-strain law. The relative motion of discontinuities is also governed by linear or non-linear force-displacement relations for movement in both the normal and shear directions. UDEC has several built-in material behavior models for deformable blocks, which simulate discontinuous geologic materials. UDEC is also based on a Lagrangian calculation scheme that is well-suited to model the large movements and deformations of blocky system. A more detailed discussion on general features and fields of applications of UDEC computer software is presented in the User's Manual (Reference 5.16). A complete listing of the input files used in the design analysis are provided in Reference 5.15. The outputs are presented and described in Section 7.0 and its subsections. The output files generated by UDEC are archived and submitted as part of the record package for this analysis.

UDEC is installed and run on Pentium PCs. UDEC Version 2.0 has been qualified for use in design in accordance with M&O Computer Software Quality Assurance procedures (CSCI#: B00000000-01717-1200-30004, Reference 5.13). UDEC was obtained from the SCM in accordance with the applicable M&O procedures. UDEC was appropriate for the applications used in this analysis. The UDEC software was used within the range of validation as specified in software qualification documentation.

6.3 SPREADSHEET SOFTWARE

Microsoft Excel 97 spreadsheet software was used in demonstrating some of the ANSYS results graphically. The results from the ANSYS models are used as inputs, and the outputs are presented in the forms of figures in Section 7. User defined formulas and/or algorithms are displayed where used. No additional information is identified from the Attachment VI of QAP-SI-0, Revision 4, that is applicable to the use of Microsoft Excel 97 in this analysis.

7.0 DESIGN ANALYSIS

7.1 INTRODUCTION

This analysis evaluates the effects of multiple heating and cooling cycles on rock mass and ground support systems in emplacement drifts during the repository preclosure period of 150 years. The cooling considered in the analysis is caused by rapid ventilation to lower temperature in order to allow for monitoring or personnel and equipment access. The interfaces that are related to the emplacement drift cooling include, but are not limited to, performance confirmation, waste retrieval, and ventilation design.

7.1.1 Performance Confirmation

Performance confirmation (PC) activities will be conducted to evaluate subsurface conditions encountered and changes in those conditions during construction and waste emplacement operations. The goals of the PC programs include confirmation of geotechnical and design parameters, design testing, and monitoring and testing of waste packages (References 5.17 and 5.19).

Some of the PC activities may be performed remotely without interfering with emplacement drift conditions, such as collecting data from boreholes at the performance confirmation drifts (Reference 5.17). But some may require a direct access to the emplacement drifts, in which ventilation may be required to lower the drift temperature before an access for monitoring or data acquisition is granted.

For some drift monitoring activities, such as to check for radiation leaks from waste packages, no equipment is required to operate inside the emplacement drifts, and therefore a low ventilation rate is sufficient. In this system, the ventilation air can blow contamination to the detecting instruments, and at the same time will not allow the radioactive leakage to travel far from the drift to pose any possible risk to the environment. This type of ventilation may be applied periodically, and potential perturbation to the drift temperature field is likely small.

Recovery of a specific waste package for performance confirmation may also occur during the preclosure period of the repository. The ventilation requirements for this operation will be the same as for waste retrieval, and will be discussed in the following section. The frequency of this waste removal operation during the lifetime of the repository is expected to be low.

7.1.2 Waste Retrieval

Retrieval of the waste packages in an entire emplacement drift may occur during the preclosure period of 150 years. This operation will require access to the emplacement drift to remove waste packages to surface handling facilities or a spare emplacement drift.

In order to provide personnel and equipment access to the emplacement drift and remove waste package from emplacement drift, the temperature in the emplacement drift must be lowered to a level at which the retrieval operations can be performed. Based on the current CDA, a drift temperature of 50°C will be required for maintenance and retrieval operations (Reference 5.4, DCSS 019). Options for lowering temperatures include continuous ventilation during emplacement and/or blast cooling prior to entry for maintenance. Use of continuous ventilation to maintain a low temperature throughout the preclosure period is beyond the scope of this analysis, but is addressed in Reference 5.18. Blast cooling with air of a previously unventilated emplacement drift is an effective means to provide a climate-controlled environment for support of the retrieval activities. However, it requires a large ventilation air quantity.

Blast cooling and multiple temperature cycles (cooling and reheating) may degrade drift components, such as ground support and rock mass in the vicinity of drift opening. These effects will be evaluated in this analysis.

7.1.3 Ventilation Design

The ventilation system for emplacement drifts is designed to accommodate the requirements for drift monitoring, waste emplacement, retrieval, and abnormal conditions. Based on the current design equipment capacity, the ventilation rates may vary from zero to a maximum of 100 m^3/s in a single drift (Reference 5.7, Section 7.1.1).

Selection of a ventilation rate depends upon its situation or the purpose of an operation, the drift condition such as humidity and temperature, and the anticipated impact. Reference 5.7 (Table 3) indicates that a range of 30 m^3/s to 50 m^3/s can satisfy the ventilation requirements for most conditions. This information is used as guidance in this analysis for selection of the ventilation rate for the cooling and heating cycles.

7.2 PHYSICAL RESPONSE DURING HEATING AND RAPID COOLING CYCLES

Physical responses involved in rapid cooling and reheating cycles include heat transfer and thermally-induced mechanical deformation in rock mass and ground support systems.

7.2.1 Thermal Response

Heat transfer involves conduction, convection, and radiation. Heat transfer in an unventilated waste emplacement drift occurs by thermal radiation from the waste packages to the drift wall as a result of temperature differences between the higher temperature waste packages and the lower temperature drift wall. In the rock mass, heat flow will occur by conduction due to the thermal gradient between the higher temperature drift wall and the lower temperature rock away from the drift. Heat transfer in a ventilated waste emplacement drift will involve not only radiation and conduction, but also convection between the higher temperature waste packages and drift wall and the lower temperature ventilating air.

The overall effect of convection can be evaluated using Newton's law of cooling (Reference 5.3, p. 12):

$$q = hA(T_w - T_a) \tag{7-1}$$

where
- q = heat flow rate, W
- h = convection heat transfer coefficient, $W/m^2 \cdot K$
- A = surface area, m^2
- T_w = drift wall temperature, K
- T_a = ventilation air temperature, K

It is noted that thermal response, such as the ventilating air and drift wall temperatures, in the ventilated emplacement drifts varies with time and location. This is because when the ventilating air travels along an emplacement drift, it will remove the heat from waste packages and drift wall. As a result, the air temperature will increase and the drift wall and waste package temperatures will decrease. The temperatures of air, waste packages, and wall near the intake of a drift will be lower than those near the exhaust. Simulation of the cooling and reheating effect in a ventilated emplacement drift is a time-dependent and three-dimensional problem. Despite these complexities, a two-dimensional modeling approach is used herein for simplicity and considered to be of sufficient accuracy to simulate the heat transfer process occurring during the cooling and reheating cycles in the emplacement drift.

7.2.2 Thermomechanical Response

The physical process in the rock mass near a waste-emplaced drift involves the coupled thermomechanical, hydrothermal and hydro-thermo-mechanical responses. This analysis considers only the thermomechanical process due to the rapid cooling and reheating cycles in the preclosure period of 150 years. The hydrothermal response during the cooling and reheating cycles may also affect the behavior of rock mass and ground support systems. This issue is beyond the scope of this analysis, and therefore is not addressed.

As mentioned previously, the temperature will change in the rock mass and ground supports caused by the waste package emplacement and cooling and reheating cycles, resulting in deformation and stress. An assessment of rock mass and ground support response requires that the thermomechanical effect be combined with in-situ stress and deformation. Depending on mechanical properties and the magnitude of the induced response, the rock mass or ground supports may behave elastically or elasto-plastically with the results being judged by appropriate performance criteria specified in the Drift Ground Support Design Guide (Reference 5.22, Sections 4.2.5 and 5.5.4).

In ANSYS code, the Drucker-Prager yield criterion is used and it is expressed as (Reference 5.6, p. 220):

$$\eta J_1 + (J_2')^{\frac{1}{2}} = \kappa' \tag{7-2}$$

where

$$\eta = \frac{2\sin\phi}{\sqrt{3}(3-\sin\phi)}$$

$$\kappa' = \frac{6c\cos\phi}{\sqrt{3}(3-\sin\phi)}$$

$$J_2' = \frac{1}{6}\left[(\sigma_1-\sigma_2)^2 + (\sigma_2-\sigma_3)^2 + (\sigma_3-\sigma_1)^2\right]$$

c = cohesion, Pa
ϕ = friction angle, degree
σ_1, σ_2, and σ_3 = principal stresses

In UDEC code, the Mohr-Coulomb yield criterion is used and it is defined as (Reference 5.6, p. 219):

$$\tau_f = c - \sigma_n \tan\phi \qquad (7\text{-}3)$$

where τ_f = shear stress on a failure plane, Pa
σ_n = normal stress on a failure plane, Pa

7.3 NUMERICAL SIMULATION OF MULTIPLE CYCLES OF HEATING AND RAPID COOLING

Numerical simulation of multiple cycles of rapid cooling and reheating involves thermal and thermomechanical analyses. This section discusses in detail the approaches, such as the assumptions, model configurations, boundary conditions, and loads (thermal and stress), employed in the thermal and thermomechanical models.

7.3.1 Thermal Analysis

The thermal analysis only calculates time-dependent temperature distributions in rock mass and ground supports, which is part of the thermomechanical analysis to determine the temperature-induced stress and displacement. For each thermal analysis, the temperature calculation is conducted under two conditions, as follows: For Condition I, the entire model shown in Figure 7-1, which includes all of the rock mass units considered to be significant to the analysis, is used. For Condition II, only part of the TSw2 thermal/mechanical unit, as shown in Figure 7-2, is modeled, and the temperatures at the top and bottom boundaries from Condition I are set as time-dependent boundary conditions. The latter calculation enables the subsequent coupled thermomechanical models to more accurately evaluate the near-field stress and displacement distributions. The ANSYS program is used in the temperature calculation.

7.3.1.1 Basic Assumptions

In evaluation of time-dependent temperature distributions in drifts, the thermal loads generated by waste packages are modeled based on the following three conservative assumptions:

(1) The waste packages are emplaced simultaneously in all emplacement drifts;
(2) The emplacement area covers the entire horizontal plane, meaning that the edge effect on the temperature distribution is neglected; and
(3) The ventilating air temperature remains constant, equal to the intake air temperature, as the air travels along the drift, meaning that the variation of ventilating air temperature along a drift is ignored. This assumption allows the use of two-dimensional model to simulate the complex three-dimensional drift cooling problem, and is considered to be conservative concerning the thermomechanical response of rock mass and ground supports during the cooling and reheating cycles.

7.3.1.2 Thermal Load

An areal mass load of 85 metric tons of uranium (MTU) per acre is used in this analysis (Section 4.3.2). The waste packages considered for the commercial spent fuel contain 21 PWR assemblies per package. The average MTU and the average initial heat output values for the 21 PWR waste packages are 8.93 MTU/package and 9.26 kW/package, respectively. In the model, the thermal loads, decaying with time, are represented by a series of heat flux values which are applied to the surfaces of the waste packages. The heat flux values are calculated by smearing the heat output at a given time from a single waste package over a length of package spacing. The computed flux is then applied in a piece-wise linear approximation of the flux-time curve over a specified time period. Details on the calculation of heat flux are described in Attachment I.

7.3.1.3 Ventilation Air Flow Rate

Two ventilation air flow rates (Q), 50 m^3/s and 2.5 m^3/s, are considered in this analysis (Section 4.3.10). The high flow rate of 50 m^3/s represents an emergency case scenario in which the drift temperature is required to be lowered to about 50°C within one or two months following the initiation of ventilation. The low flow rate of 2.5 m^3/s is selected to demonstrate a normal case scenario in which the drift temperature is only required to be lowered by about 15°C over a duration of a few weeks.

The duration of ventilation used in the analysis is two (2) weeks and two (2) months (Section 4.3.10), corresponding to the air flow rates of 2.5 m^3/s and 50 m^3/s, respectively. These durations are chosen based on the temperature reduction targets and some trial-and-error computer runs.

The number of cooling cycles used in the analysis is ten (10) and the cooling is initiated every 10 years with the first cycle started at 10 years after the waste emplacement (Section 4.3.10). Ten cycles of cooling and reheating are considered to be sufficient to evaluate the overall effect of multiple cycles of cooling and reheating on the stability of rock mass and ground supports.

The convection heat transfer coefficients (h) corresponding to the ventilation rates of 50 and 2.5 m^3/s are 6.45 and 0.59 $W/m^2 \cdot K$, respectively. Details on the calculation of these coefficient values are presented in Attachment II.

7.3.1.4 Model Configuration and Boundary Conditions

Figure 7-1 illustrates the configuration for a thermal model with ANSYS for calculating the boundary temperature histories. The boundary conditions for the thermal model are also shown in Figure 7-1. Only one-half (14.0 m) of the drift spacing (28.0 m) is employed in the model by taking advantage of thermal symmetries. The top of the model extends to surface while the bottom boundary is set far enough (more than 40 times the drift diameter) to minimize boundary effects on the temperature distributions in the vicinity of drift opening. Rock temperatures at the top and bottom boundaries of the thermal model (Figure 7-1) are set at 18.7°C and 30.81°C, respectively, based on the average ground surface temperature and the thermal gradient presented in Section 4.1.2.

7.3.2 Thermomechanical Analysis

The coupled thermomechanical analysis calculates the stress and deformation induced in rock mass and ground supports by the in-situ stress and changes of temperature in emplacement drifts experiencing the multiple cooling and reheating cycles. Details of discussion on the approach, assumptions, configuration, load, and boundary conditions follow.

7.3.2.1 Basic Assumptions

The following assumptions are incorporated in the thermomechanical models:

(1) A 60% of initial ground relaxation is completed before the application of ground supports (Section 4.3.8);
(2) For precast concrete segment and steel set linings, there exists a circumferential interface (discontinuity) between the lining and the rock, which provides neither bonding nor gaps (Section 4.3.9);
(3) Four deformable elements are embedded in the precast concrete segment and steel set linings, and their locations along a lining ring are illustrated in Figure 7-3, and
(4) Rock mass behaves elasto-plastically governed by either the Drucker-Prager yield criterion described by Equation 7-2 in ANSYS models or the Mohr-Coulomb yield criterion described in Equation 7-3 in UDEC models.

7.3.2.2 In Situ Stress Load

A vertical stress value of 10 MPa, applied at the drift center, is used in the analysis (Section 4.3.1). The values of the horizontal to vertical stress ratio (K_o) used in the UDEC models are 0.3 and 1.0 (Section 4.3.1), which are considered the lower and upper bounds at the repository horizon.

7.3.2.3 Model Configurations and Boundary Conditions

Figure 7-2 illustrates the configuration and boundary conditions for a thermomechanical model with ANSYS for calculating the stress and displacement distributions. The time-dependent temperatures on the drift wall, the top and bottom boundaries are obtained from the Condition I model, as discussed in Section 7.3.1.

As is shown in Figure 7-3, a UDEC model is constructed with three equally-spaced emplacement drifts. In doing so, the mutual effect of adjacent emplacement drift excavation is accounted for, and the introduction of symmetrical lateral boundaries may result in minimal impact on the behavior of the center drift. Therefore, only the results related to the center drift are subjected to interpretation. In the UDEC model, all three drifts are located within a jointed region. There are two sets of joints, as illustrated in Figure 7-3. The nearly vertical joint set dips at 85 degrees with a uniform spacing of 0.5 meters (Section 4.3.4). The nearly horizontal joint set dips at 15 degrees and has a uniform spacing of 1 meter (Section 4.3.4).

7.3.2.4 Simulation of Ground Support

Ground support is simulated with both beam and solid elements in ANSYS models. With beam elements, thrust (axial force) and bending moment of a lining are the results of calculation, and while with solid elements, the variation in stress over the lining thickness can be obtained directly.

The stress relief deformable elements are modeled with 2D point-to-point contact elements. The point-to-point contact elements are capable of supporting compression in the normal direction. The numerical parameter that controls the amount of compression or so called "penetration" under loading is the normal stiffness. The value of the normal stiffness can be estimated from the allowable stress for concrete or steel divided by the allowable displacement (compressible distance) of a deformable element, and is provided in Section 4.3.9.

The circumferential interface is simulated with 2D point-to-surface contact elements. The contact elements represent two surfaces of the concrete or steel set lining and the rock, and are capable of supporting only compression in the direction normal to the surfaces and shear in the tangential direction. No initial "gap" is assigned to the contact elements representing a full initial contact between the lining and the rock. The only physical property related is the coefficient of friction μ (Section 4.3.9). In addition, two numerical parameters, called the normal contact stiffness k_n and the sticking contact stiffness k_t, are also associated with the contact elements. The values of these parameters used in the ANSYS models are provided in Section 4.3.9.

7.3.3 Sign Convention

The sign convention for normal stresses is "tension is positive and compression is negative". However, all lining stresses in this analysis are plotted as positive in compression and negative in tension. For drift closures, changes in diameter, a positive closure indicates that two reference points located on the tunnel circumference move toward to each other, resulting in a reduction in the distance between these two points.

7.4 EFFECT OF MULTIPLE CYCLES OF HEATING AND RAPID COOLING

This section discusses the effect of multiple cycles of rapid cooling and reheating on the emplacement drift stability and ground support performance. Focus is on the resulting stress and displacement due to the significant change in temperature.

7.4.1 Calculation of Drift Temperature

Temperatures in rock were calculated with ANSYS based on a thermal load of 85 MTU/acre for a period of 300 years after waste emplacement. Three cases were considered as described in the following:

Case A: Heating only. This case serves as a basis for comparison to evaluate any impact caused by ventilation.

Case B: Ten cooling and heating cycles with a ventilation air flow rate of 2.5 m^3/s. Initial cooling starts at 10 years after waste emplacement, lasting for two weeks. The cycle repeats every 10 years.

Case C: Ten cooling and heating cycles with a ventilation air flow rate of 50 m^3/s. Initial cooling starts at 10 years after waste emplacement, lasting for two months. The cycle repeats every 10 years.

7.4.1.1 Drift Wall Temperature

Figures 7-5 and 7-6 show the time histories of rock temperatures for Cases A through C. For Case A, the peak wall temperature is about 165°C, which occurs at about 48 years following waste emplacement. For Cases B and C, the peak temperatures experienced on the drift wall are about 164°C and 159°C and occur at about 49 and 40 years, respectively, indicating the influence of multiple cooling and heating cycles on the wall temperatures.

When a ventilation air quantity of 2.5 m^3/s is used, the drift wall temperature can be reduced to about 126°C at 10 years and about 143°C at 100 years, resulting in a maximum reduction of about 17°C (Figure 7-5). Due to the low air quantity and short duration of ventilation, the disturbance in temperature caused by the cooling cycles is minimal once the ventilation is stopped.

With a ventilation air quantity of 50 m^3/s, the drift wall temperature can be lowered from about 159°C to about 47°C during a cycle, a reduction of 122°C (Figure 7-6). Apparently, the goal to reduce the maximum allowable rock surface temperature to 50°C can be achieved using this ventilation air quantity. It can also be seen that a lower wall temperature is indicated even beyond the completion of the cooling cycles, as a result of the heat removal from rock by a high quantity of ventilation air.

7.4.1.2 Rock Temperature Distribution

Temperature distributions in the middle-of-pillar rock at 10, 50 and 300 years following waste emplacement are presented in Figures 7-7 through 7-9, respectively. These plots show the disturbed zones in temperature field over time near an emplacement drift that has experienced the cooling cycle(s).

As indicated in Figure 7-7, the disturbed zones at 10 years following one cooling cycle are about 1 and 3.5 meters into rock for Cases B and C, respectively, and the majority of the temperature field is nearly undisturbed. At 50 years following five cooling cycles, the disturbed zones are expanded to about 1.5 and 4.5 meters for Cases B and C, respectively. Cumulative effect of heat removal by the multiple cooling cycles is also demonstrated by the temperature distribution curve for Case C (Figure 7-8). This effect clearly cannot be reversed by reheating process over a period of 200 years following the cooling cycles, indicated by an overall lower temperature in the rock for Case C (Figure 7-9).

7.4.2 Stability of Emplacement Drift Opening

Stability of the emplacement drift openings is examined by conducting thermomechanical analysis with ANSYS and UDEC to determine the stress and displacement in rock mass. The ANSYS code is used to model the behavior of rock mass as a continuous medium, while the UDEC code is employed to simulate the jointed rock mass. The configurations and boundary conditions used in the ANSYS and UDEC models are illustrated in Figures 7-2 and 7-3, respectively. Thermally-induced rock mass displacements and stresses were calculated based on the boundary temperatures shown in Figures 7-5 and 7-6 for Cases A through C.

7.4.2.1 Opening Displacement

Horizontal and vertical closures of an unsupported emplacement drift are presented in Figures 7-10 through 7-13 for Cases A through C based on the ANSYS models. Without the cooling cycles (Case A), maximum horizontal closures under combined in-situ stress and thermal loads, as shown in Figures 7-10a and 7-11a, are about 13 to 14 mm (inward) for the rock mass categories of 1 and 5, respectively. Maximum vertical closures during heating, as shown in Figures 7-10b and 7-11b, are outward, varying from about 0.3 to 11 mm for the rock mass categories of 1 and 5, respectively. These results indicate that the deformed drift opening shape changes from a horizontal oval initially to a vertical oval as a result of continuous heating of rock by waste packages.

When subjected to the multiple cycles of cooling and heating with a ventilation quantity of 50 m^3/s (Case C), the drift will experience less deformation or thermal expansion, as shown in Figures 7-10 and 7-11. This is because part of the heat generated by the waste packages will be removed by ventilation, resulting in a relatively cooler rock. Maximum horizontal closures during the cooling and heating cycles, as shown in Figures 7-10a and 7-11a, are about 6 to 7 mm for the rock mass categories of 1 and 5, respectively, indicating a reduction of about 7 mm by the cooling cycles. Maximum vertical closures at the same time vary from about 8 mm (inward) for the rock mass category of 1 (Figure 7-10b) to about 4 mm (outward) for the rock mass category of 5 (Figure 7-11b). A net reduction in the vertical closures by the cooling cycles is about 8 mm for both rock mass categories of 1 and 5.

It is noted that during each cooling and heating cycle, the rock mass will contract or expand as the temperature decreases or increases, showing that in general it behaves elastically. After the cooling and heating cycles are completed, the drift is expected to rebound in deformation. Eventually the drift closures, both horizontal and vertical, are predicted to be very close to those for the drift without experiencing the cooling cycles (Figures 7-10 and 7-11). The results also indicate that the effect of the cooling and heating cycles on the drift closures is not dependent on these mechanical properties of the rock mass.

When the ventilation quantity is 2.5 m^3/s (Case B), similar patterns in the horizontal and vertical closures are anticipated, as shown in Figures 7-12 and 7-13. However, the reduction in the closures by the cooling cycles is much less, about 1 mm in both directions, because the decrease in temperature is much smaller in this case. After the cooling and heating cycles are completed, the difference in the drift closures for Cases A and B is very small (Figures 7-12 and 7-13).

The results suggest that, if judged by the drift closures, the cooling and heating cycles, no matter what ventilation quantity is used, are not expected to have any adverse effect on the stability of drift opening. No limitation should be set on the maximum number of cooling and heating cycles.

7.4.2.2 Rock Mass Stress

Time histories of tangential stresses at the crown and springline of unsupported emplacement drifts are presented in Figures 7-14 through 7-17 for Cases A through C. Tangential stress at the crown is expected to decrease during the cooling cycles, from about -151 MPa (compression) for Case A to about -146 and -127 MPa (compression) for Case B and C, respectively, for the rock mass category of 5 (Figures 7-15a and 7-17a). The magnitude of stress reduction caused by the cooling cycles varies with time and is very sensitive (proportional) to the rock mass modulus (Figures 7-14a and 7-15a). Once the cooling and heating cycles are completed, the stress is shown to increase to a level that is close to what is predicted for Case A.

Tangential stress at the springline is also expected to decrease when the drift is cooled down. However, the stress is shown to rebound, once the ventilation is stopped, to a level that exceeds what is predicted for Case A at about the same time for the same rock mass category (Figures 7-14b and 7-15b). This may imply that the reheating process during each cooling and heating cycle would probably enhance the confinement of rock mass near the springline. It is worth mentioning that tensile stresses near the springline, as shown in Figures 7-15b and 7-17b, are indicated during the cooling phase of each cycle when the rock mass modulus is high (RMQ=5). This suggests that precaution measures need to be taken to prevent the rock mass from tensile failure when the rapid cooling is considered.

7.4.2.3 Jointed Rock Mass Behavior

Behavior of jointed rock mass near the unsupported emplacement drifts is evaluated using the discontinuum models with UDEC. Cases A and C are considered in the UDEC models.

Figures 7-18 and 7-19 illustrate the rock block displacement vectors, joint shear displacements and potential failure zone development around the opening for Case A and the initial horizontal-to-vertical stress ratios (K_o) of 0.3 and 1.0, respectively. A potential yield zone of about 2.0 m into the rock, as shown in Figures 7-18b and 7-19b, has developed surrounding the opening after 100 years of thermal loading. Some of rock blocks show a potential to tensile failure as indicated in Figures 7-18b and 7-19b by a "T" symbol. In addition, noticeable shear displacements on joints occur where the Mohr-Coulomb yield criterion is exceeded.

Multiple cooling and heating cycles have shown a significant impact on the behavior of jointed rock mass near the drifts. This can be seen by comparing Figures 7-20 and 7-21 for Case C with Figures 7-18 and 7-19 for Case A. The potential yield zone developed around the opening extends to a depth of about 3 and 4 m at 10 and 100 years following one and ten cooling cycles, respectively, compared to a depth of about 2 m at 100 years for Case A. Especially, the shear displacements on joints for Case C, as shown in Figures 7-20b and 7-21b, are predicted to be nearly an order of magnitude greater than those for Case A. This may be an indication of rock block loosening near the opening due to the drastic temperature decreases during the cooling cycles. This also suggests that the installation of ground supports in the emplacement drifts is necessary in order to prevent any potential rock falls.

7.4.3 Performance of Ground Supports

Supported emplacement drifts are modeled with ANSYS for Cases A and C. Ground supports considered in this analysis include a 200-mm-thick concrete lining and 1.5-meter-spaced W6×20 steel sets. The concrete lining is modeled with either a perfect bonding to the rock or an interface between them. For the former case, the creep/stress relaxation of concrete is introduced and the modeling of the creep/stress relaxation of concrete is discussed in detail in Reference 5.1, Attachment II. For the latter case, the stress relief deformable elements are incorporated in the models, as discussed in Section 7.3.2.4. The steel sets are modeled with an interface between the lining and the rock, and the deformable elements are considered.

7.4.3.1 Concrete Lining with Full Bonding

Time histories of tangential stresses at the crown and springline of a 200-mm-thick concrete lining modeled with full bonding to the rock are shown in Figures 7-22 and 7-23 for rock mass categories of 1 and 5. Results indicate that stresses in the lining are very sensitive to the surrounding rock mass properties, such as the modulus of elasticity. This demonstrates the dependency of the thermally-induced stresses on the modulus of elasticity. Without the cooling and heating cycles, the maximum tangential stresses at the crown are about 40 and 48 MPa (compression) for the rock mass categories of 1 and 5, respectively (Figures 7-22a and 7-23a). Tensile stresses, however, are expected to develop at the springline of lining after about 50 years of thermal loading (Figures 7-22b and 7-23b) due to the full bonding between the lining and the rock.

During the multiple cooling and heating cycles (Case C), the tangential stresses at the crown are shown to be lower (Figures 7-22a and 7-23a), oscillating between 9 to 25 MPa and 12 to 28 MPa (compression) corresponding to the rock mass categories of 1 and 5, respectively. Once the cooling cycles are completed, the stresses are shown to rebound as the temperature increases. It is predicted to take about 100 years for the stresses to reach the level which the lining in a heating-only drift may experience.

The adverse effect of cooling and heating cycles is shown in the development of tensile stresses at the springline of the lining due to the cooling (Figures 7-22b and 7-23b). The tangential stresses oscillate during each cooling and heating cycle. They range from about 11 MPa (compression) to about -9 MPa (tension) for RMQ=1 (Figure 7-22b) and from about 6 MPa (compression) to about -23 MPa (tension) for RMQ=5 (Figure 7-23b). It should be noted that though longitudinal cracks may be induced by the tensile stresses in the lining, they are expected to be limited to a small area near the springline.

Normal stresses in the longitudinal direction of the lining are illustrated in Figures 7-24 and 7-25 for the rock mass categories of 1 and 5. Since the plane strain assumption is used in the models, these stresses can be calculated directly from the stress components in the tangential and radial directions, and the temperature based on the Hooke's law (Reference 5.22, Section 5.5.4). Again, tensile stresses are indicated in the longitudinal direction, which implies that circumferential cracks are likely to be developed near the springline during the cooling.

7.4.3.2 Concrete Lining with Deformable Elements

Time histories of the stresses at the crown, invert and springline of the concrete lining with deformable elements are shown in Figures 7-26 and 7-27 for Cases A and C and the rock mass categories of 1 and 5. It is indicated that the stresses calculated are generally higher for the case of rock mass category of 1 and also sensitive to the location of the deformable elements. As shown in Figures 7-26a and 7-27a, the stresses at the crown are lower than at the invert owing to the fact that the deformable elements used in the models are closer to the crown than to the invert.

Compared to the results for Case A, the stresses at the crown and invert of the lining are lower during the cooling and heating cycles. They oscillate at each cycle, for example, from about 7 to 11 MPa for RMQ=1 and about 7 to 9 MPa for RMQ=5 at the crown (Figures 7-26a and 7-27a). It is also noted that the range of oscillation in the stress at the invert is greater than that at the crown. This observation may indicate that the stresses are sensitive to the location of the deformable elements and the stress level that the lining might experience without cooling.

Stresses at the springline of the lining with deformable elements are shown to increase during the cooling and heating cycles (Figures 7-26b and 7-27b). These stresses are predicted to be about one to two orders of magnitude higher than those for Case A. No tensile stresses are indicated in the lining when the deformable elements are considered.

7.4.3.3 Steel Sets with Deformable Elements

Time histories of stresses at the crown, invert and springline of steel sets (W6×20) with deformable elements are illustrated in Figures 7-28 and 7-29 for rock mass categories of 1 and 5. The stresses and their range of variation during the cooling and heating cycles, similarly to those in the precast segment concrete lining, are sensitive to the location of deformable elements. In general, a lower stress is expected at the crown or invert when the steel sets experience rapid cooling.

Stresses at the springline are shown to increase or decrease during the cooling and heating cycles depending on the rock mass categories, or the modulus of elasticity. With a poor rock (RMQ=1), higher stresses are predicted (Figure 7-28a), while with a good rock (RMQ=5), lower stresses are indicated (Figure 7-29a). Tensile stresses are likely to develop at the springline of the steel sets (Figure 7-29b).

8.0 CONCLUSIONS

Effects of multiple heating and cooling cycles on rock mass and ground support systems in emplacement drifts are evaluated in this analysis. The study concentrates on the thermal and mechanical behavior of rock mass and ground support systems affected by multiple thermal cycles due to rapid ventilation. Two ventilation scenarios are considered in this analysis, one corresponding to an emergency case with an air flow rate of 50 m^3/s and the other corresponding to a normal case with an air flow rate of 2.5 m^3/s. The duration of ventilation is two months and two weeks, respectively (Section 4.3.10). The number of cooling cycles used in this analysis is ten (10) and the cooling is initiated every 10 years with the first cycle started at 10 years following the waste emplacement (Section 4.3.10). Interfaces with performance confirmation, ventilation design, waste retrieval, and maintenance are also discussed.

The following conclusions can be drawn from this analysis:

- Rapid ventilation can effectively lower the drift wall temperatures, and the magnitude of temperature reduction depends on the ventilation air quantity and duration. With a ventilation air quantity of 50 m^3/s, the maximum reduction is about 122°C, resulting in a wall temperature of 47°C (Figure 7-6).

- Perturbation to the temperature field by multiple heating and cooling cycles is limited to a depth of about 1.5 and 4.5 meters into rock for the cases with ventilation air quantities of 2.5 m^3/s and 50 m^3/s, respectively. Cumulative effect of heat removal on the rock temperature is demonstrated only when the ventilation air rate is high ($Q=50\ m^3/s$).

- Rapid ventilation is expected to result in a reduction in rock deformation near a drift opening during the heating and cooling cycles (Section 7.4.2.1). The reduction is not very sensitive to the rock mass mechanical properties, i.e. the modulus of elasticity. Impact on the long-term rock deformation due to cooling cycles is minimal.

- Decrease in rock mass stresses is predicted during the heating and cooling cycles due to overall lower temperatures (Section 7.4.2.2). However, tensile stresses are indicated at the springline of a drift opening. This suggests that precautionary measures need to be taken to prevent the rock mass from tensile failure when the rapid cooling is considered.

- Rock block loosening is predicted near the opening due to the temperature decrease during the cooling cycles (Section 7.4.2.3). This suggests that the installation of ground supports in the emplacement drifts is necessary to prevent any potential rock falls.

- Possible adverse effect of the cooling cycles is not indicated on the performance of ground supports when they are not perfectly bonded to the rock, because lower stresses are predicted (Sections 7.4.3.2 and 7.4.3.3). However, the stresses in the tangential and longitudinal directions at the springline of a lining ring are expected to be in tension due to cooling when the lining is fully bonded to the rock (Section 7.4.3.1). This suggests that debonding between the lining and the rock will alleviate the stresses thermally-induced by either expansion or contraction.

- The magnitude of cooling rate may affect the changes in stress and deformation of rock mass and ground support during the cooling and heating cycles, but they are considered manageable.

- Number of cooling and heating cycles (10) used in this analysis is hypothetical. No change is expected in the results or conclusions of this analysis as a result of the increase or decrease of this number.

- An initial average rock temperature of 25°C is assumed and used in this analysis (Section 4.3.2). Thermal and mechanical effect based on a lower or higher initial temperature is not evaluated in this analysis, and is considered to be insignificant.

In general, multiple cycles of heating and cooling in the emplacement drifts can produce increased deformation adjacent to emplacement drifts but do not produce more extensive deformation or failure. Overall stability is maintained. No limitation is suggested on the number and magnitude of heating and cooling cycles as a result of this analysis.

9.0 ATTACHMENTS

I CALCULATION OF HEAT OUTPUT DECAY VALUES OF WASTE PACKAGE

II CALCULATION OF CONVECTION HEAT TRANSFER COEFFICIENT

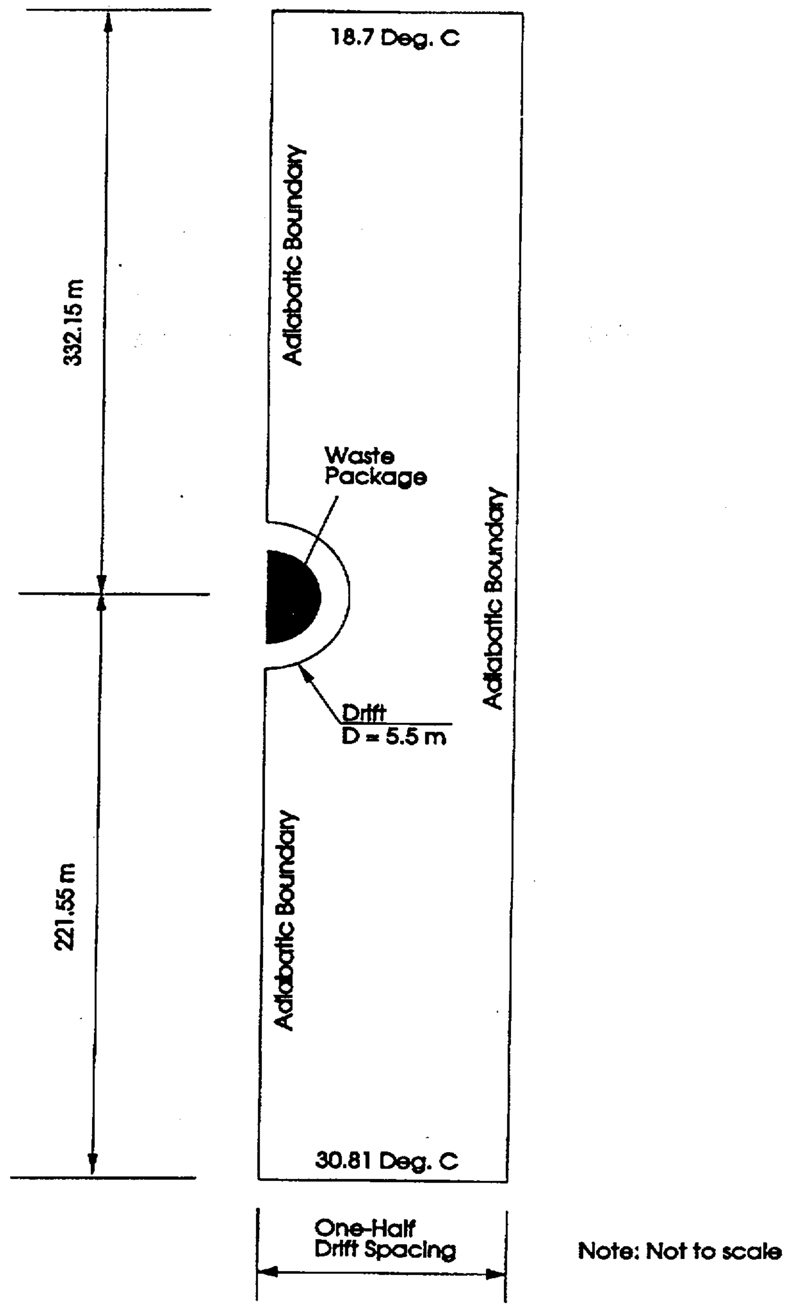

Figure 7-1 Geometry and Boundary Conditions for Thermal Modeling Using ANSYS

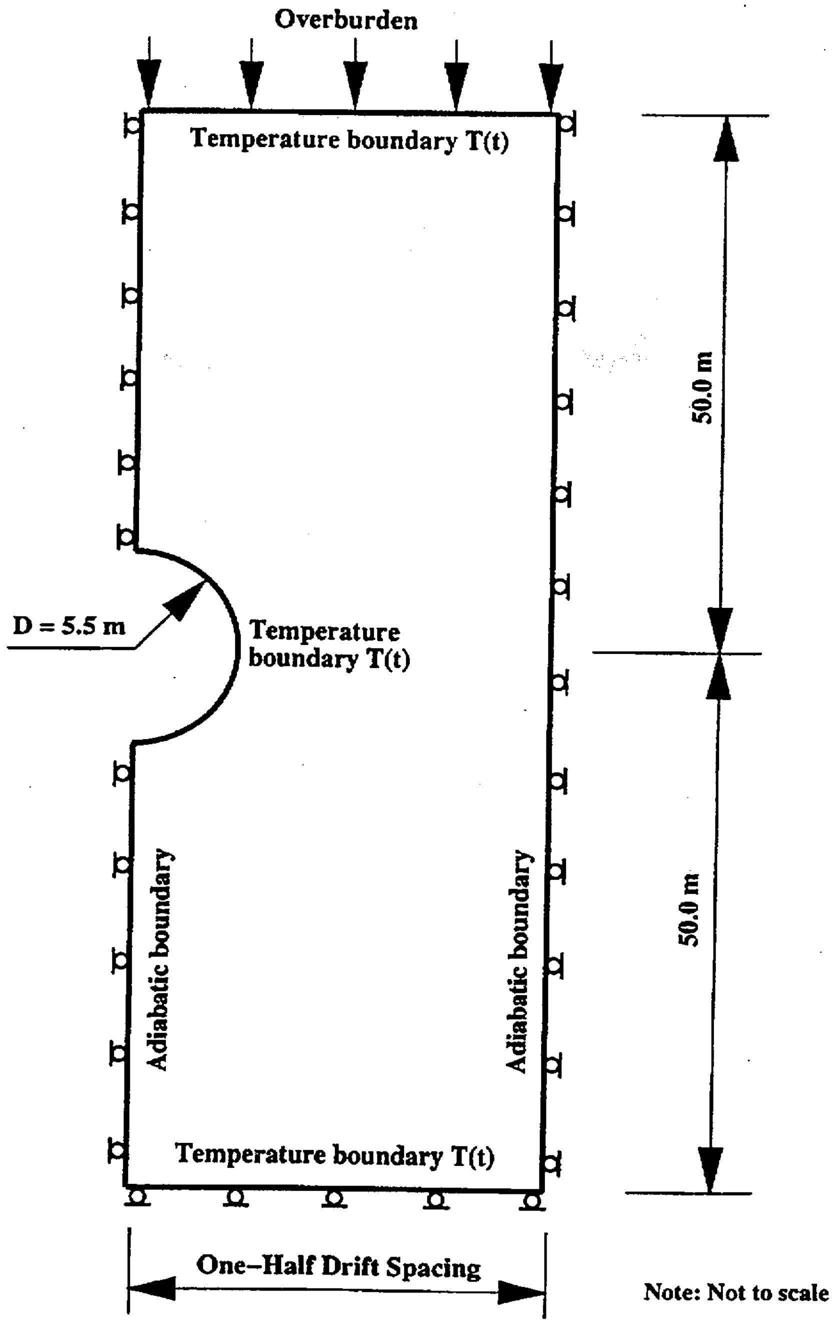

Figure 7-2 Geometry and Boundary Conditions for Thermomechanical Modeling Using ANSYS

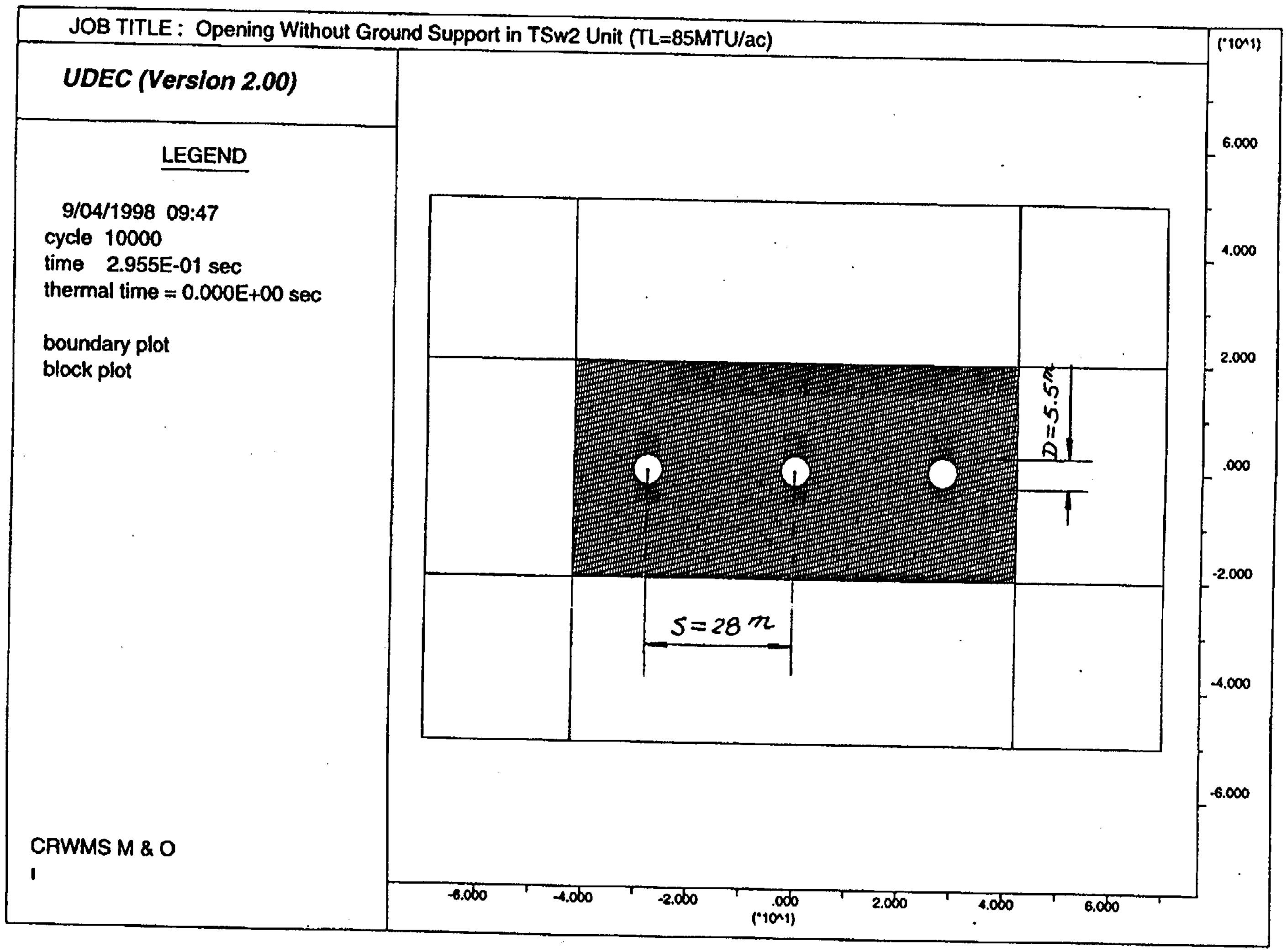

Figure 7-3 Configuration of a UDEC Model of Emplacement Drifts (Unit: Dimensions in Meters)

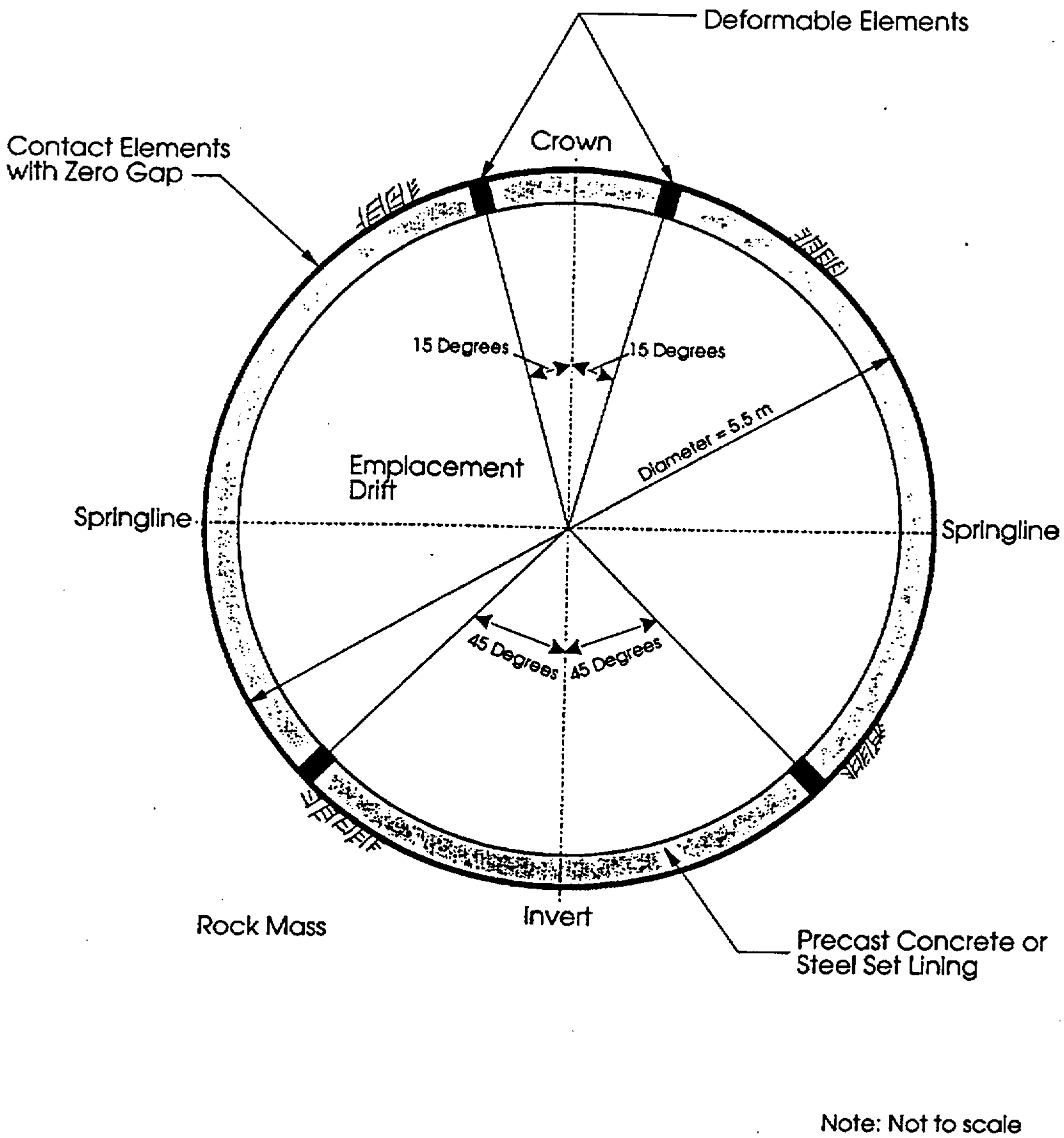

Figure 7-4 Ilustration of Deformable Element Concept for Precast Concrete and Steel Set Linings

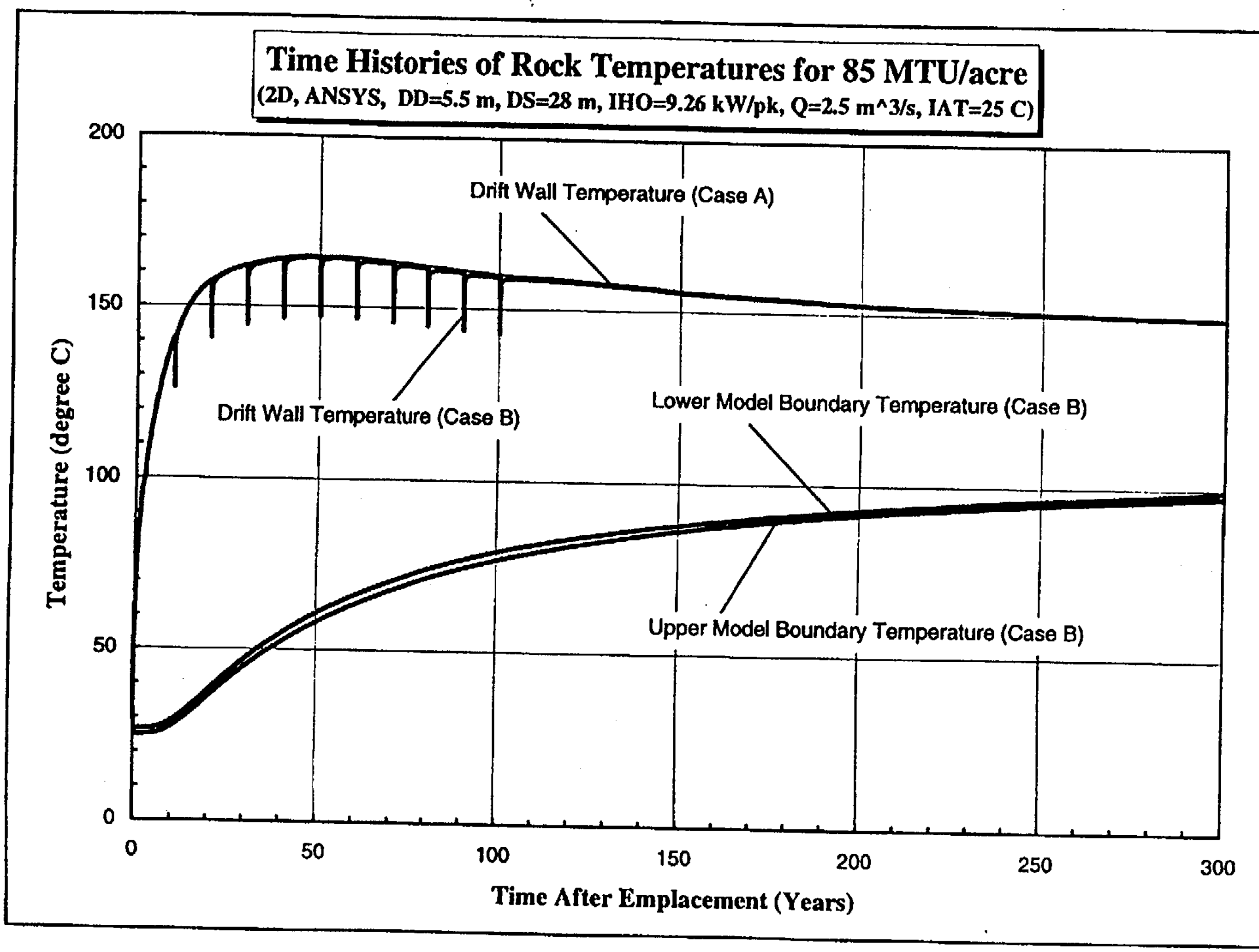

Figure 7-5 Time Histories of Rock Temperatures for Cases A (No Cooling) and B ($Q=2.5m^3/s$) (DD=Drift Diameter, DS=Drift Spacing, IHO=Initial Heat Output, IAT=Intake Air Temperature)

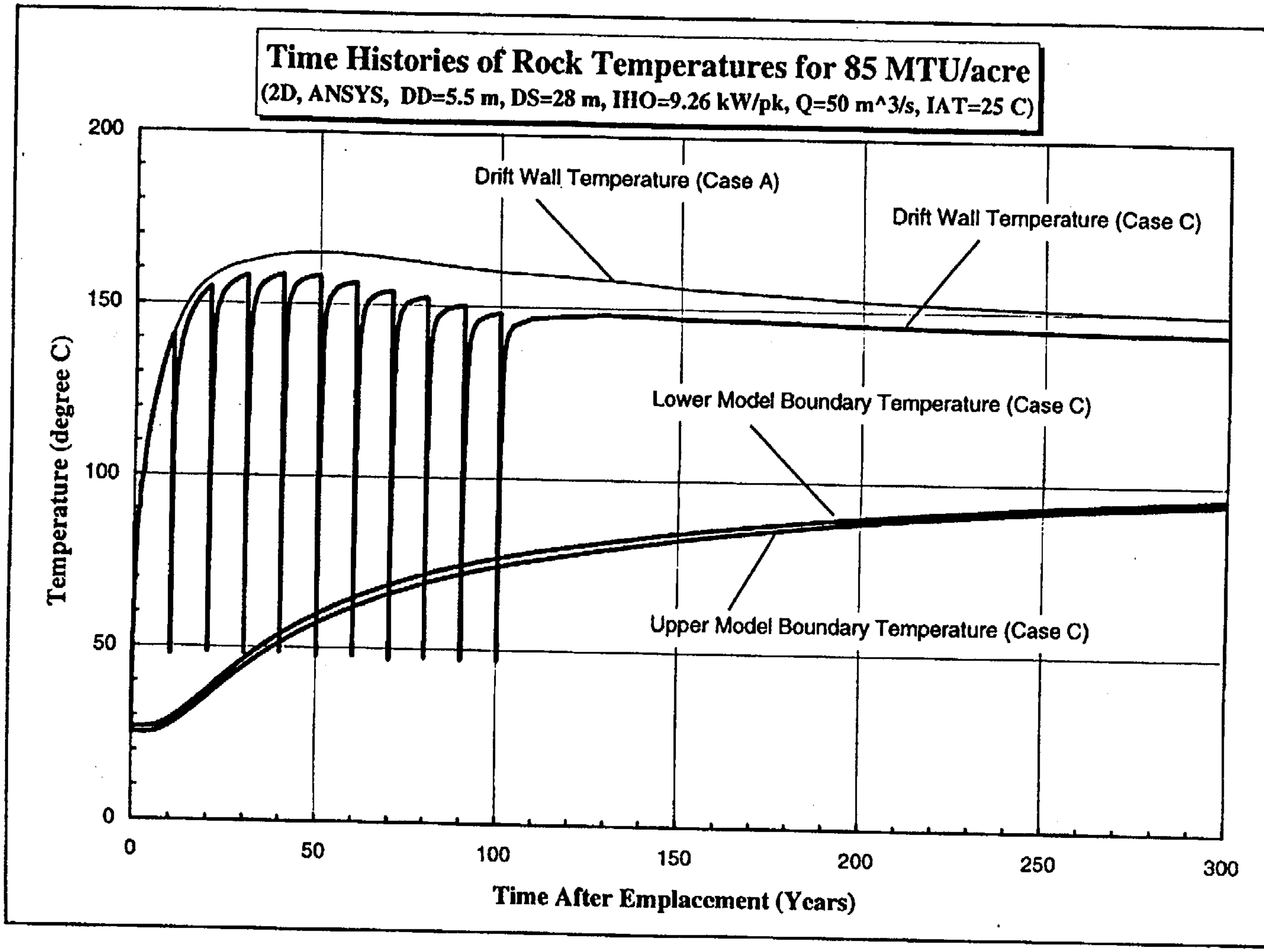

Figure 7-6 Time Histories of Rock Temperatures for Cases A (No Cooling) and C ($Q=50 m^3/s$) (DD=Drift Diameter, DS=Drift Spacing, IHO=Initial Heat Output, IAT=Intake Air Temperature)

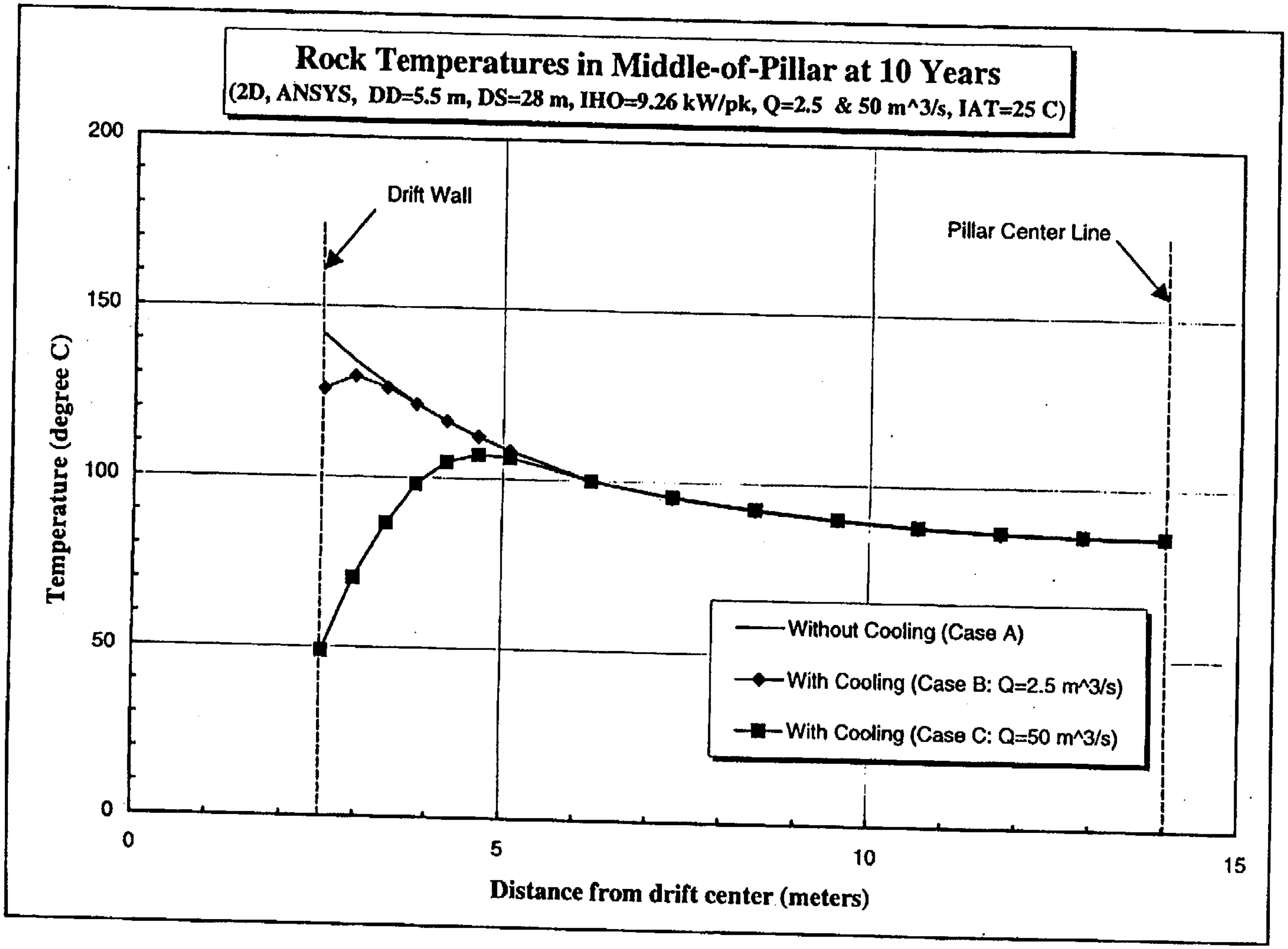

Figure 7-7 Rock Temperatures in Middle-of-Pillar at 10 Years after Waste Emplacement (DD=Drift Diameter, DS=Drift Spacing, IHO=Initial Heat Output, IAT=Intake Air Temperature)

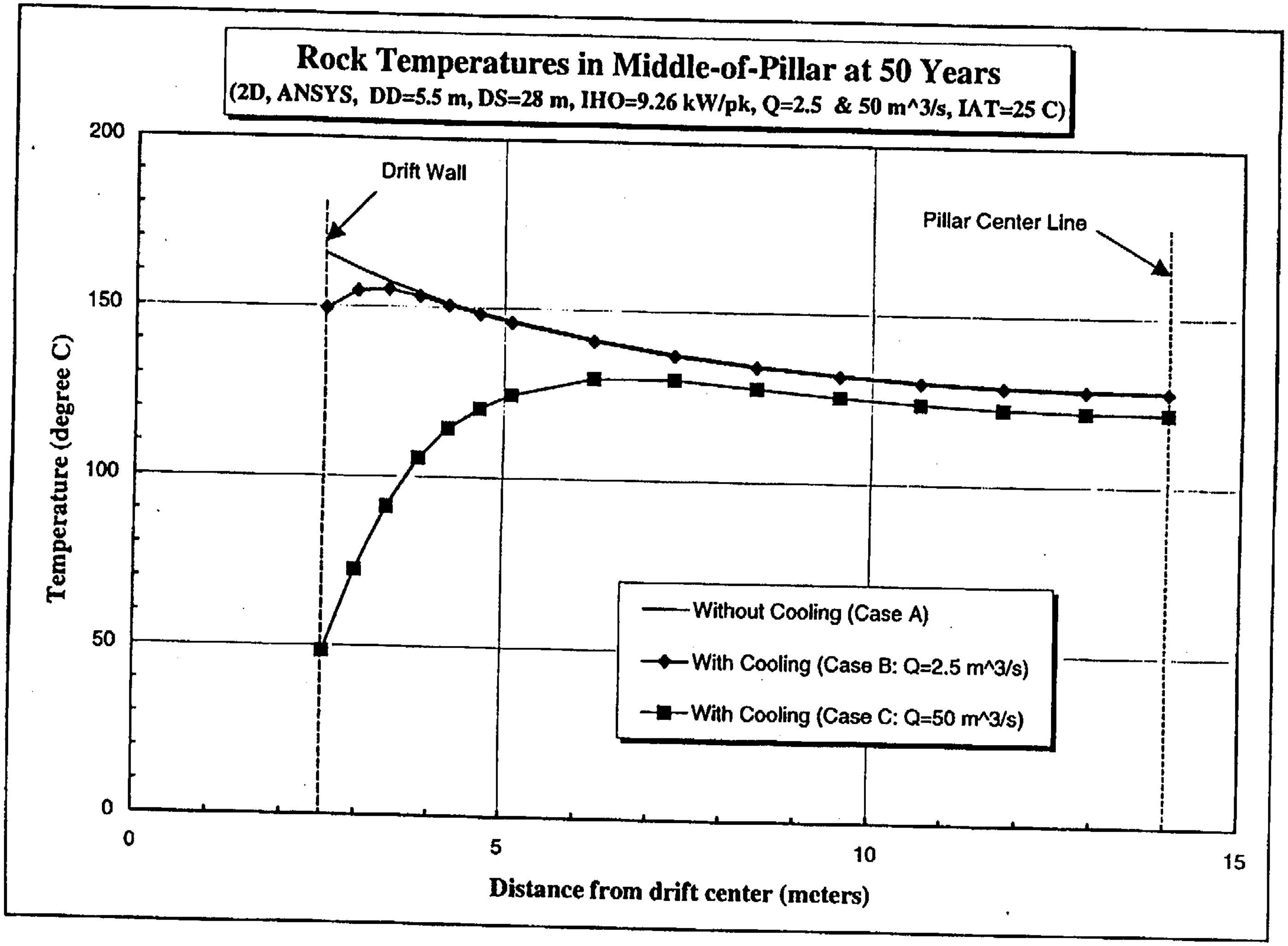

Figure 7-8 Rock Temperatures in Middle-of-Pillar at 50 Years after Waste Emplacement (DD=Drift Diameter, DS=Drift Spacing, IHO=Initial Heat Output, IAT=Intake Air Temperature)

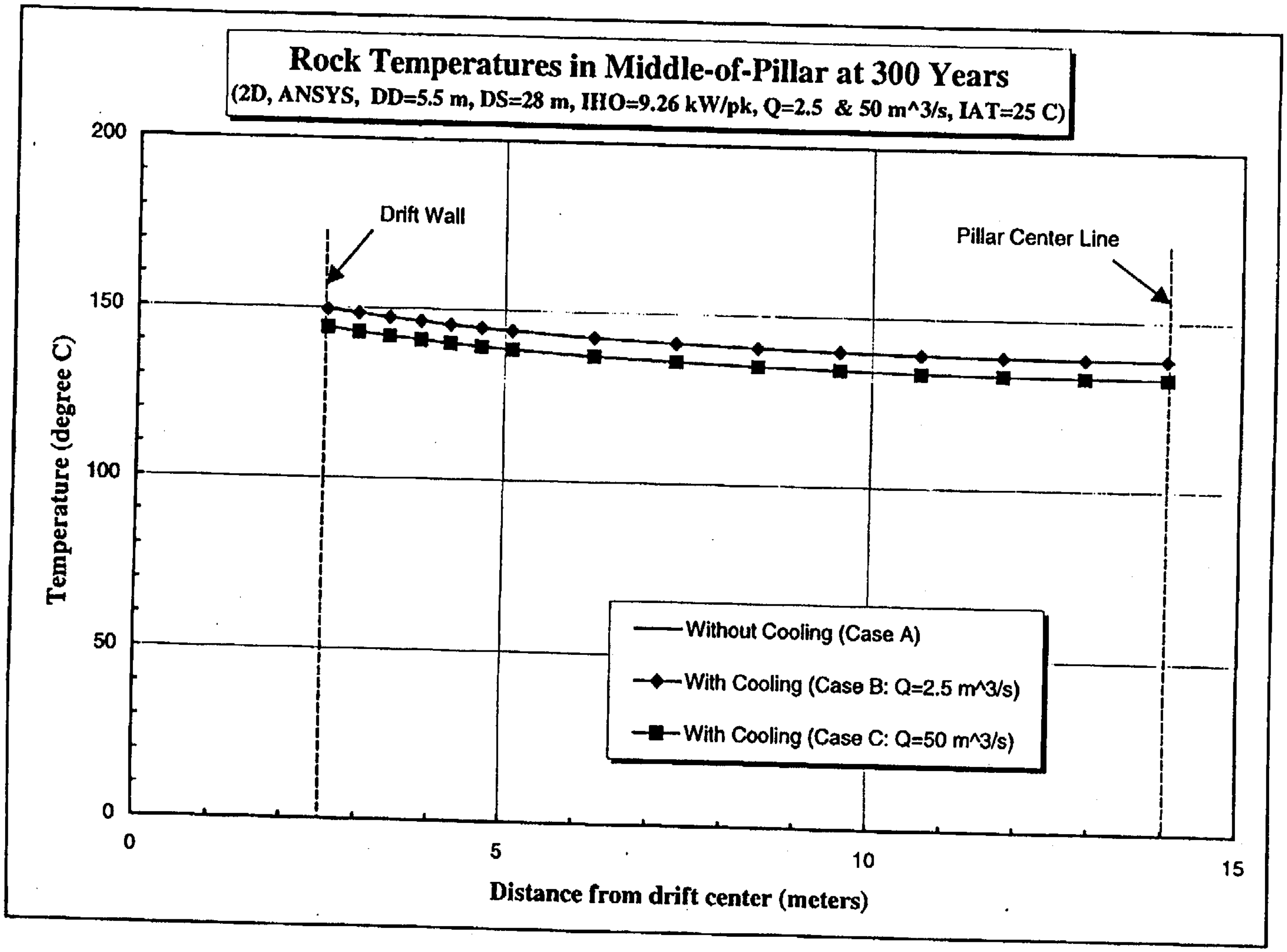

Figure 7-9 Rock Temperatures in Middle-of-Pillar at 300 Years after Waste Emplacement (DD=Drift Diameter, DS=Drift Spacing, IHO=Initial Heat Output, IAT=Intake Air Temperature)

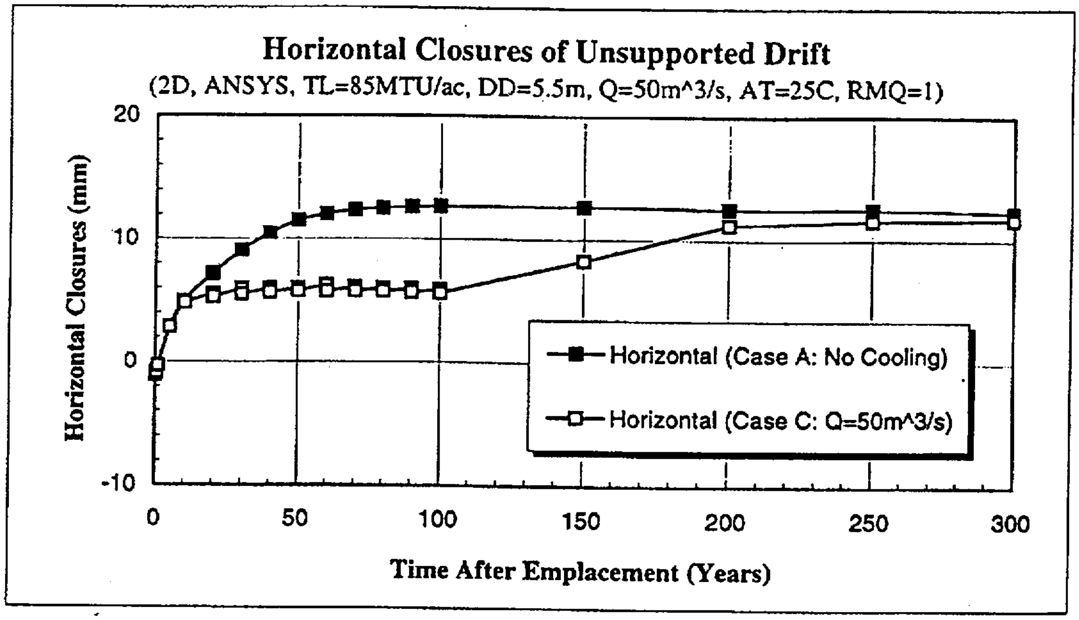

(a)

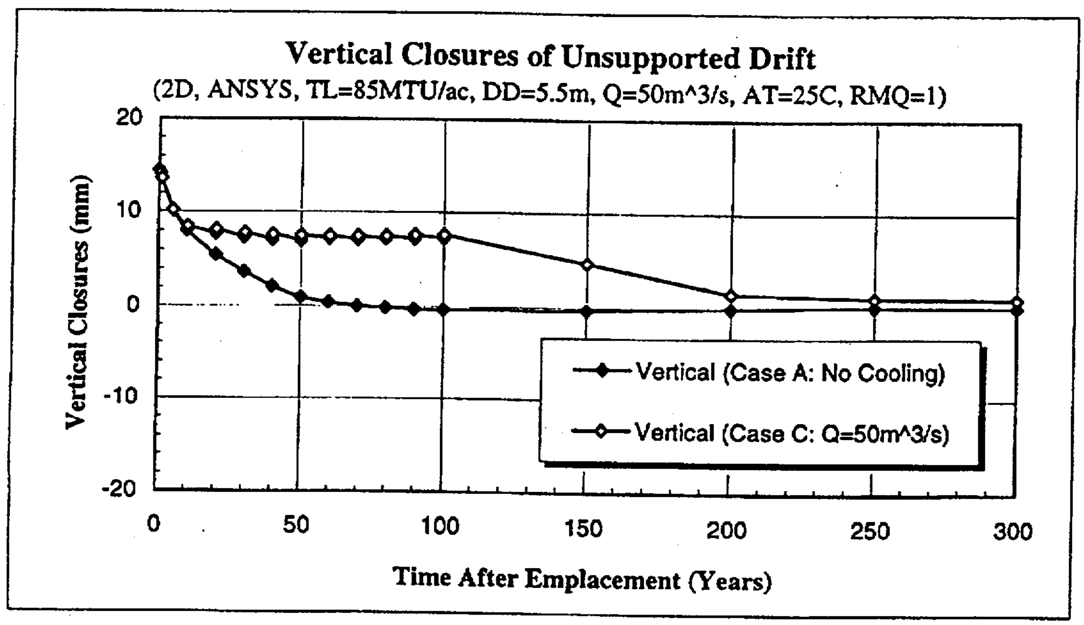

(b)

Figure 7-10 Closures of Unsupported Drift for Cases A and C and RMQ=1: (a) Horizontal; (b) Vertical. (Note: Positive Closure Indicates Drift Diameter Decrease. TL=Thermal Load, DD=Drift Diameter, Q=Air Quantity, AT=Air Temperature, RMQ=Rock Mass Quality Category)

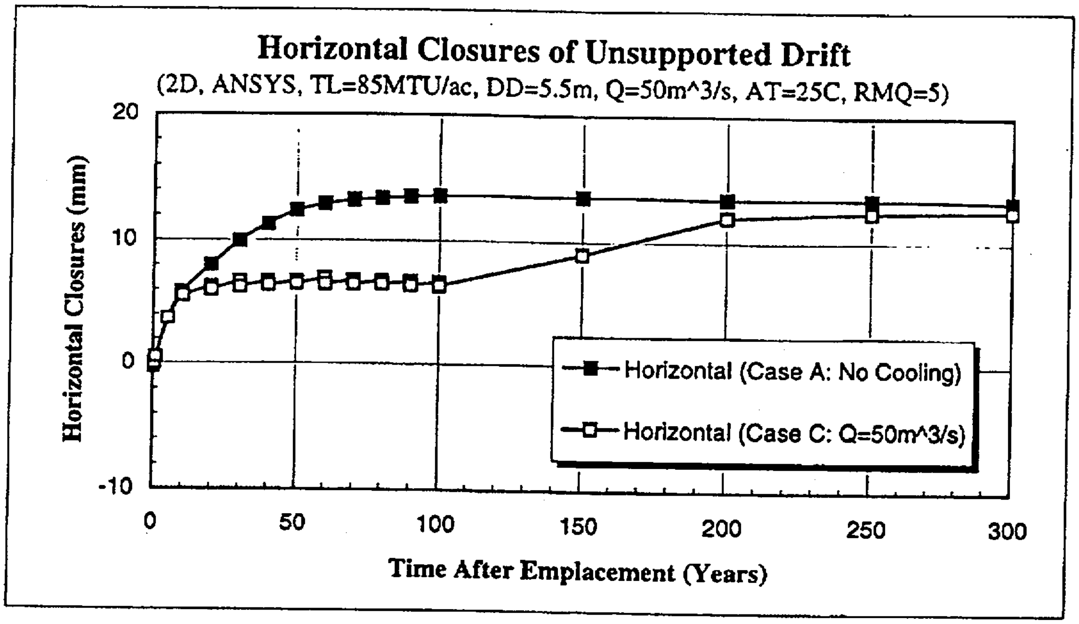

(a)

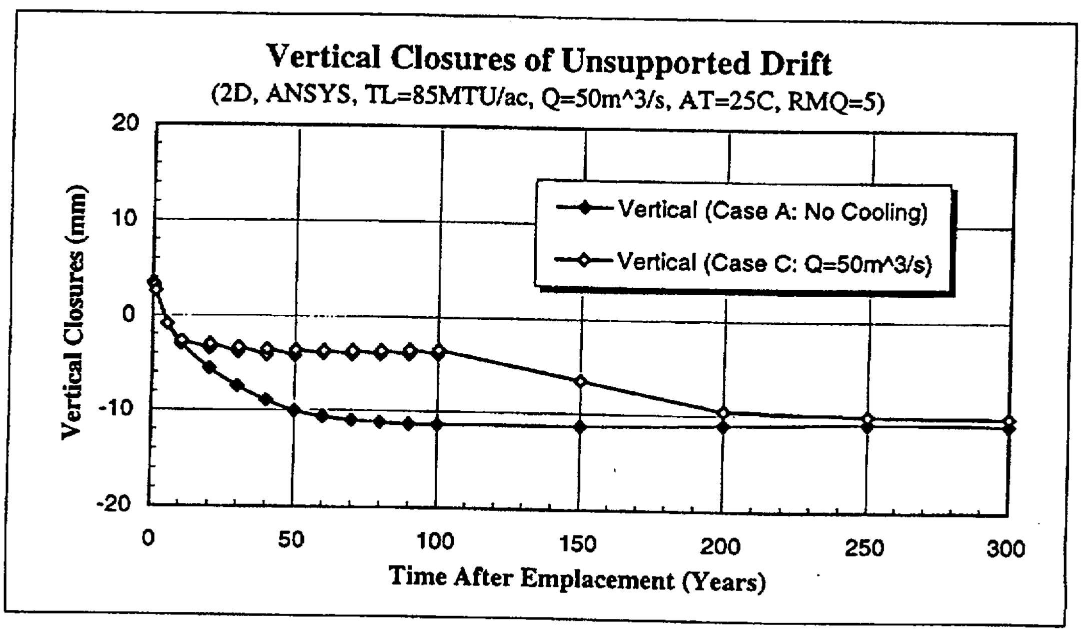

(b)

Figure 7-11 Closures of Unsupported Drift for Cases A and C and RMQ=5: (a) Horizontal; (b) Vertical. (Note: Positive Closure Indicates Drift Diameter Decrease. TL=Thermal Load, DD=Drift Diameter, Q=Air Quantity, AT=Air Temperature, RMQ=Rock Mass Quality Category)

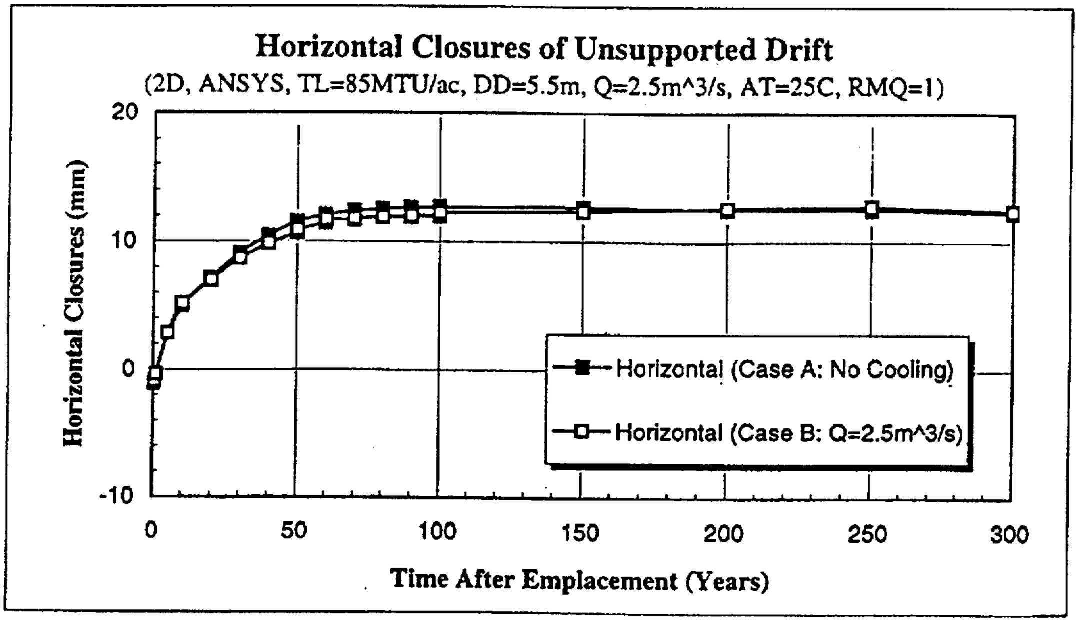

(a)

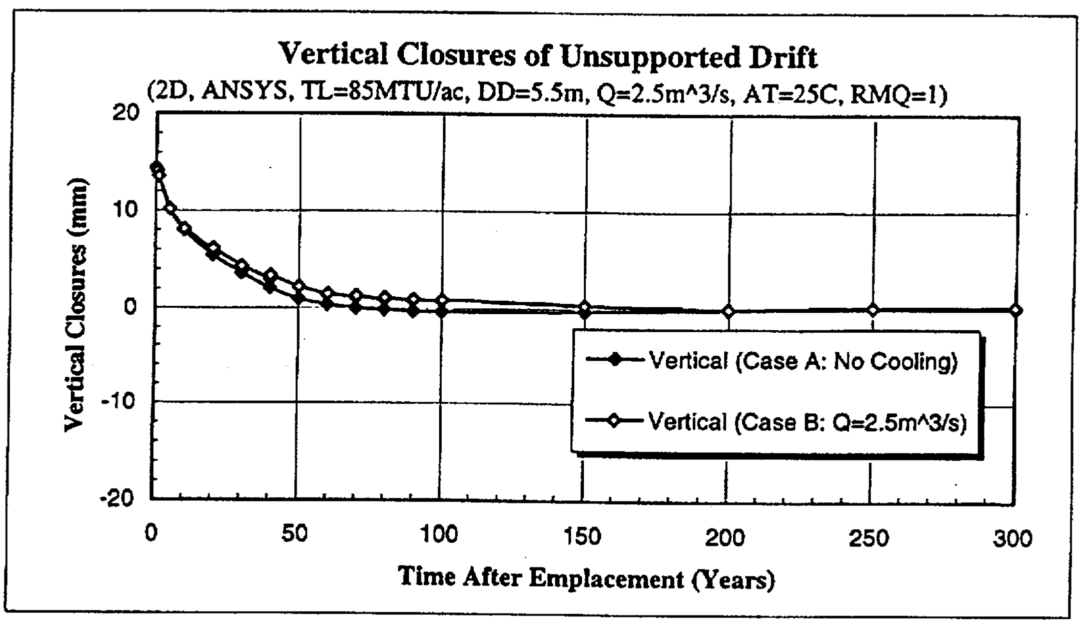

(b)

Figure 7-12 Closures of Unsupported Drift for Cases A and B and RMQ=1: (a) Horizontal; (b) Vertical. (Note: Positive Closure Indicates Drift Diameter Decrease. TL=Thermal Load, DD=Drift Diameter, Q=Air Quantity, AT=Air Temperature, RMQ=Rock Mass Quality Category)

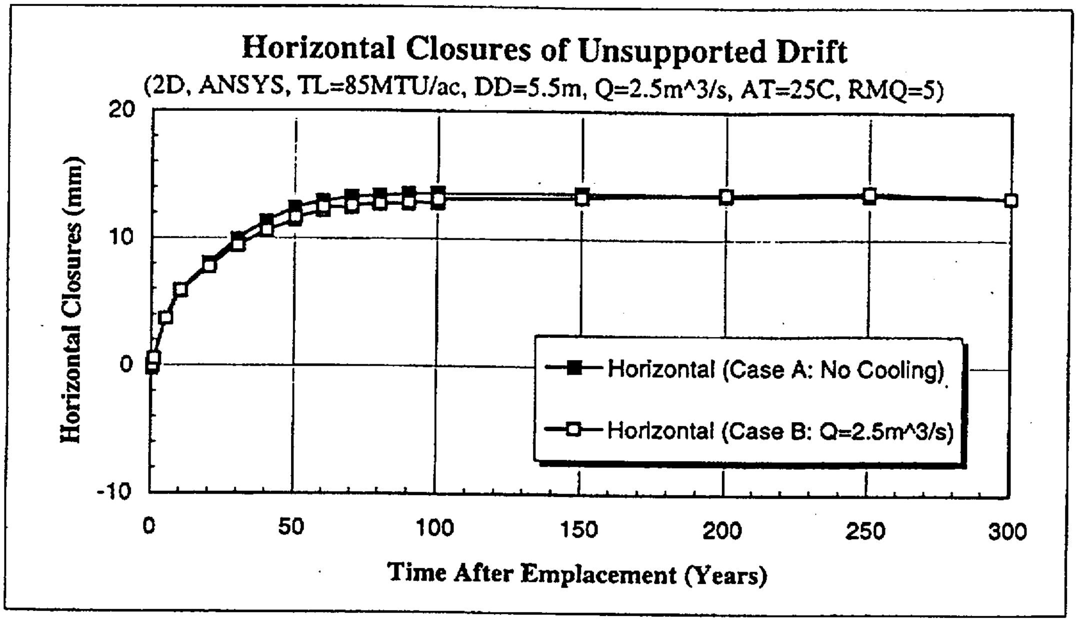

(a)

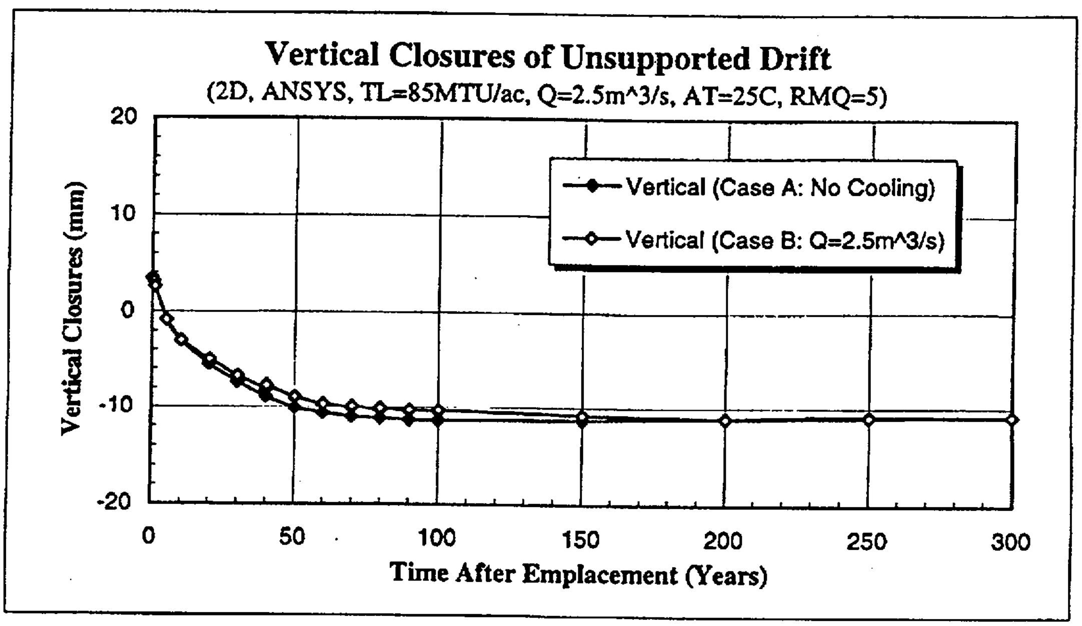

(b)

Figure 7-13 Closures of Unsupported Drift for Cases A and B and RMQ=5: (a) Horizontal; (b) Vertical. (Note: Positive Closure Indicates Drift Diameter Decrease. TL=Thermal Load, DD=Drift Diameter, Q=Air Quantity, AT=Air Temperature, RMQ=Rock Mass Quality Category)

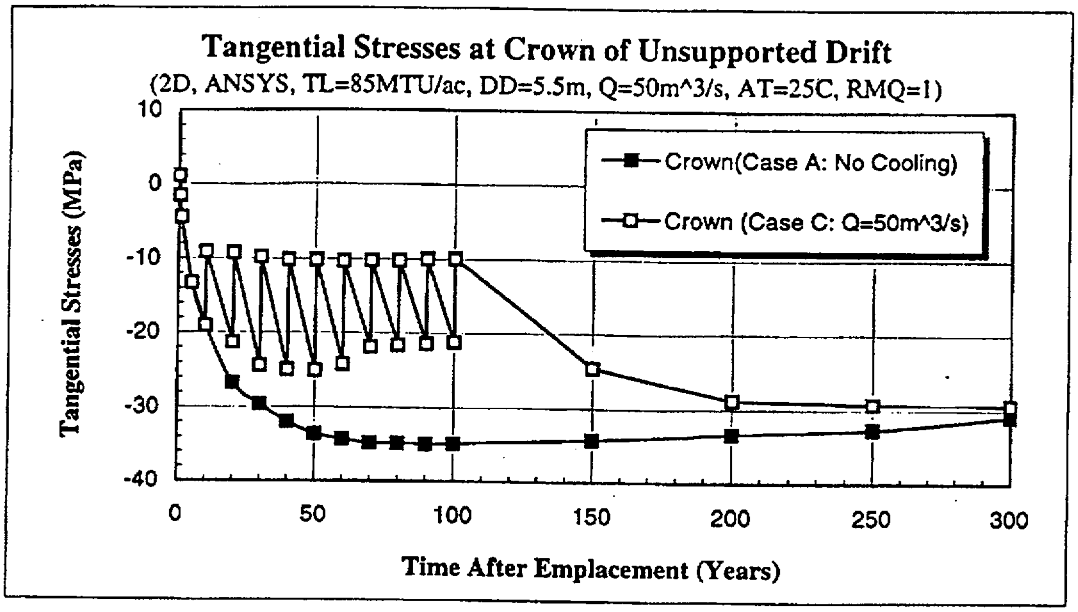

(a)

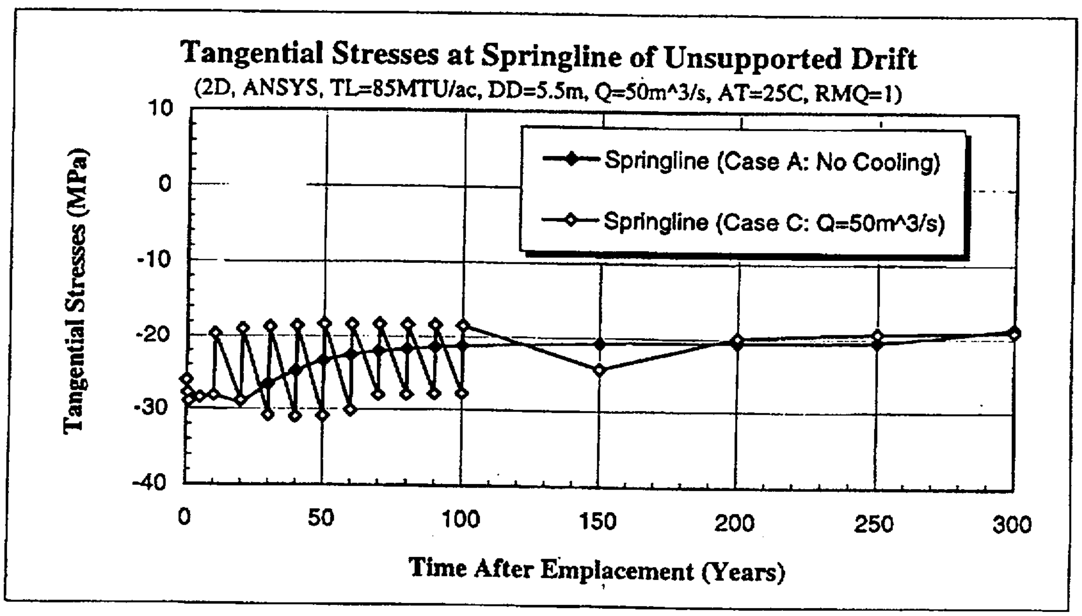

(b)

Figure 7-14 Tangential Stresses at Unsupported Drift for Cases A and C and RMQ=1: (a) Crown; (b) Springline. (Note: Compression Is Negative. TL=Thermal Load, DD=Drift Diameter, Q=Air Quantity, AT=Air Temperature, RMQ=Rock Mass Quality Category)

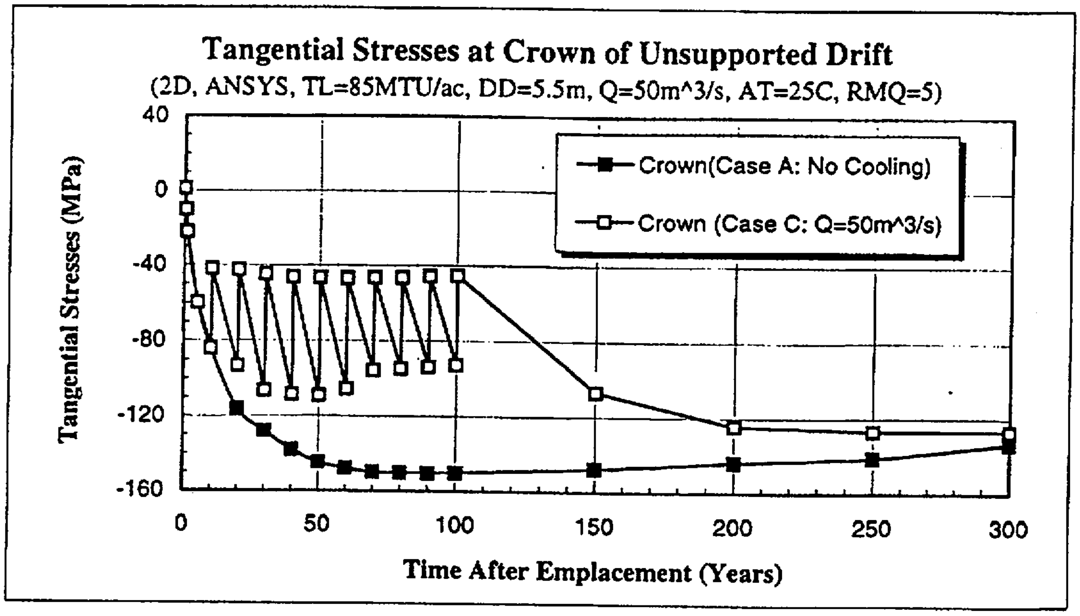

(a)

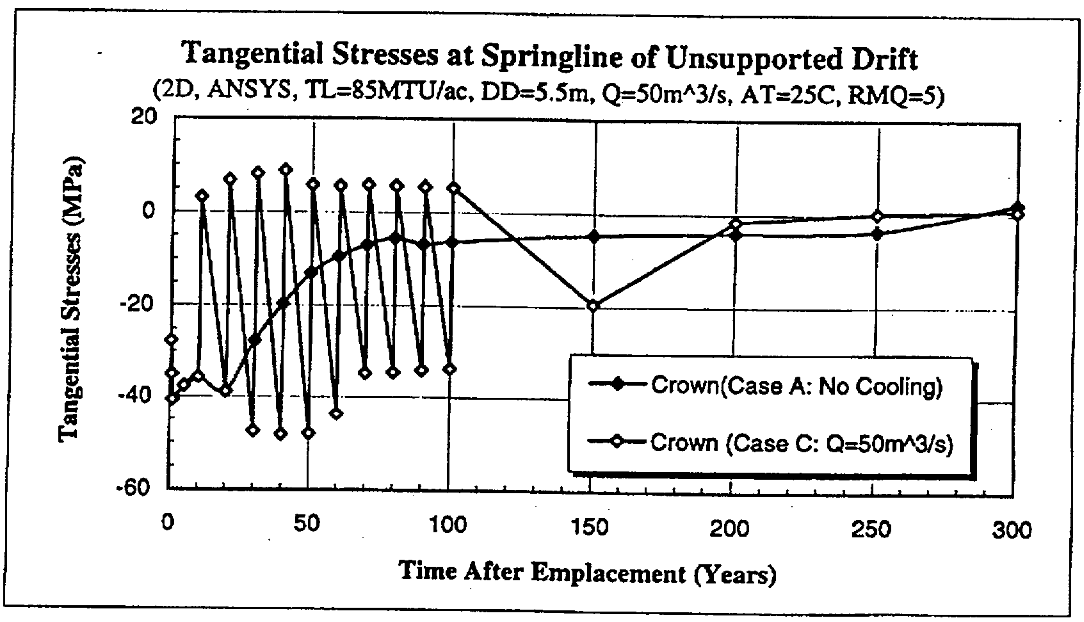

(b)

Figure 7-15 Tangential Stresses at Unsupported Drift for Cases A and C and RMQ=5: (a) Crown; (b) Springline. (Note: Compression Is Negative. TL=Thermal Load, DD=Drift Diameter, Q=Air Quantity, AT=Air Temperature, RMQ=Rock Mass Quality Category)

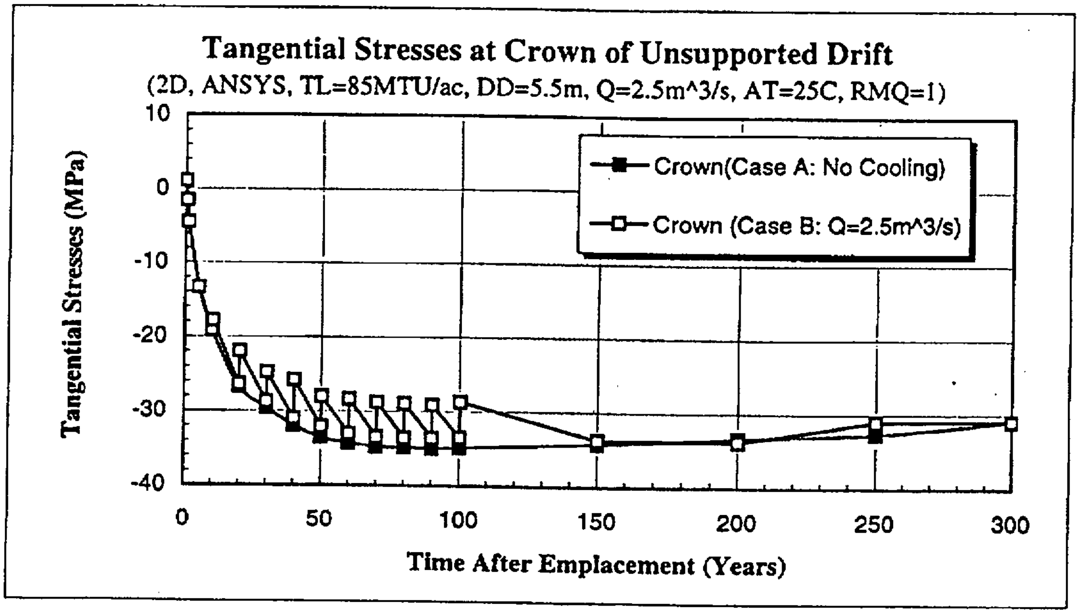

(a)

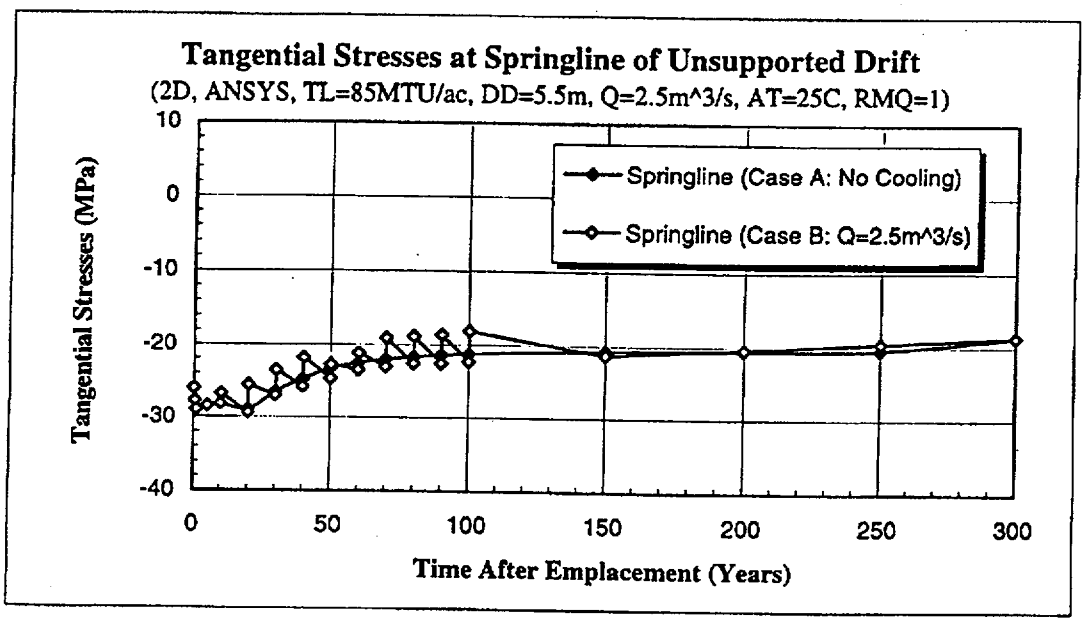

(b)

Figure 7-16 Tangential Stresses at Unsupported Drift for Cases A and B and RMQ=1: (a) Crown; (b) Springline. (Note: Compression Is Negative. TL=Thermal Load, DD=Drift Diameter, Q=Air Quantity, AT=Air Temperature, RMQ=Rock Mass Quality Category)

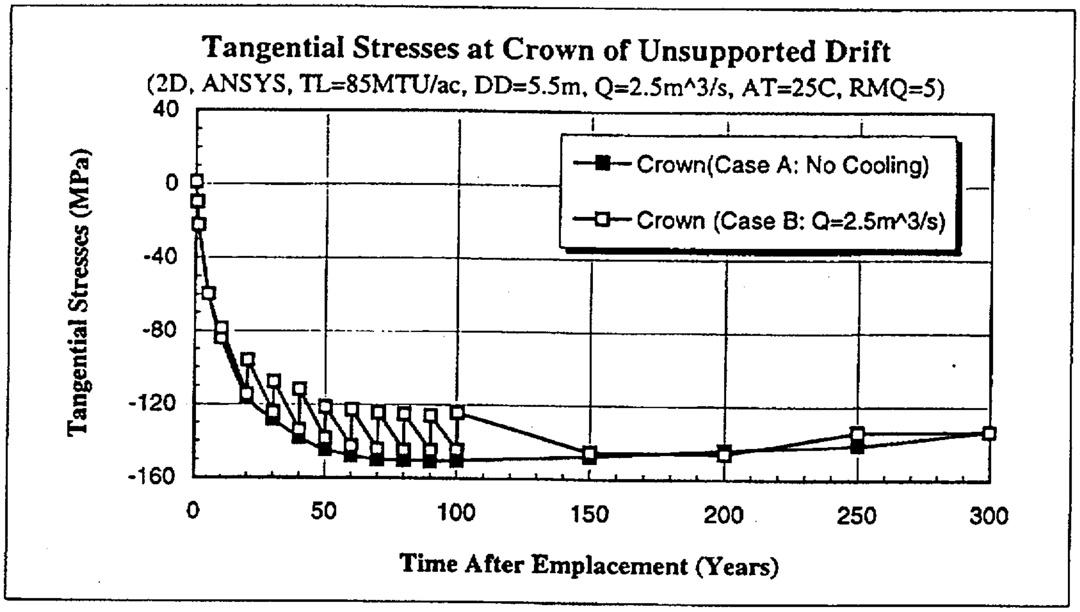

(a)

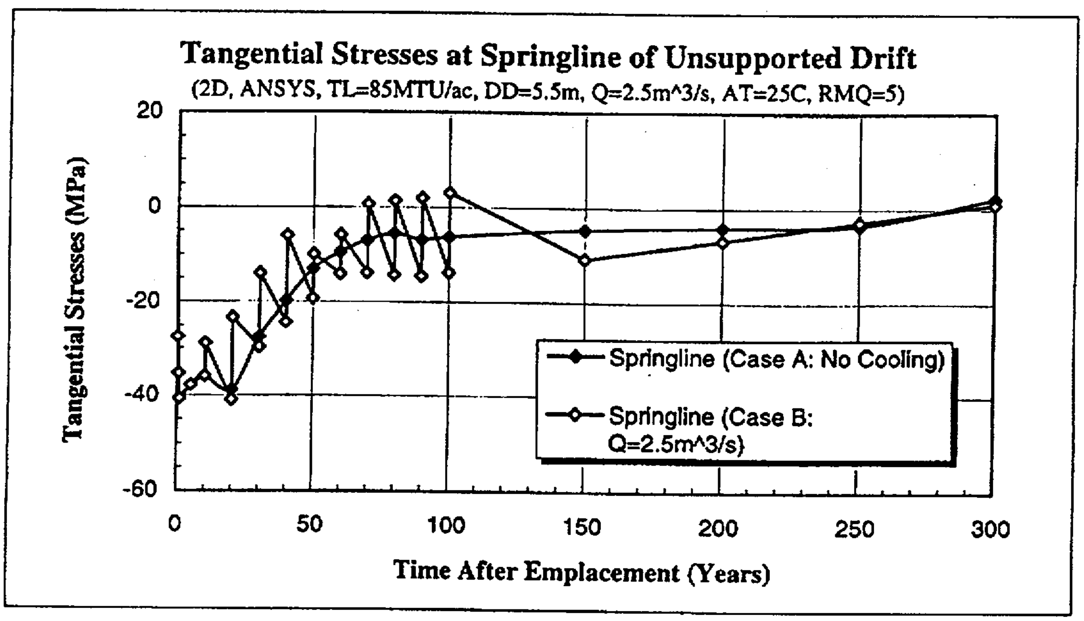

(b)

Figure 7-17 Tangential Stresses at Unsupported Drift for Cases A and C and RMQ=5: (a) Crown; (b) Springline. (Note: Compression Is Negative. TL=Thermal Load, DD=Drift Diameter, Q=Air Quantity, AT=Air Temperature, RMQ=Rock Mass Quality Category)

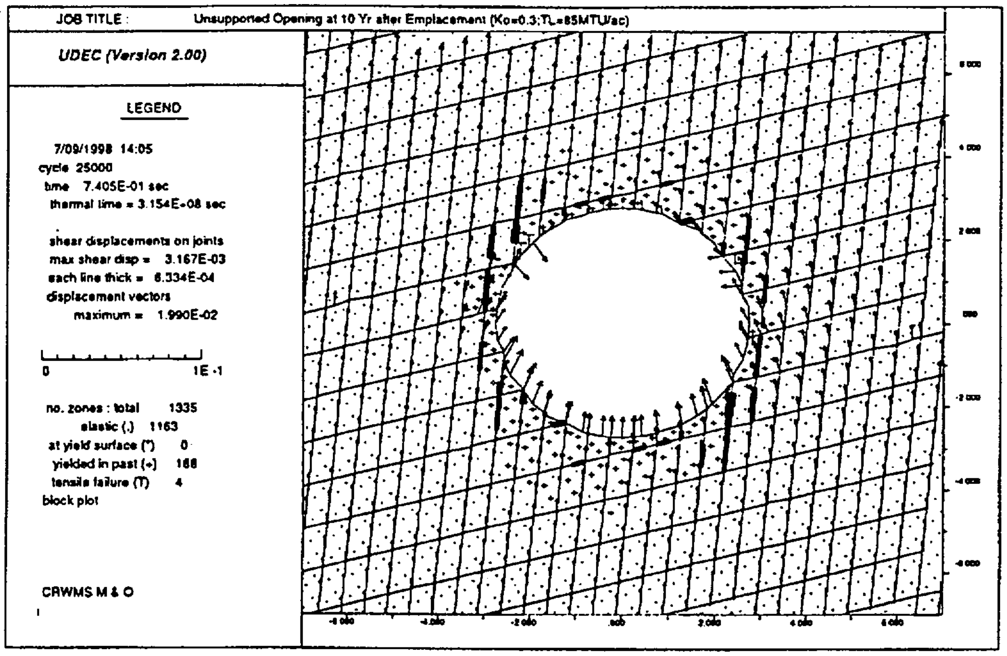

(a)

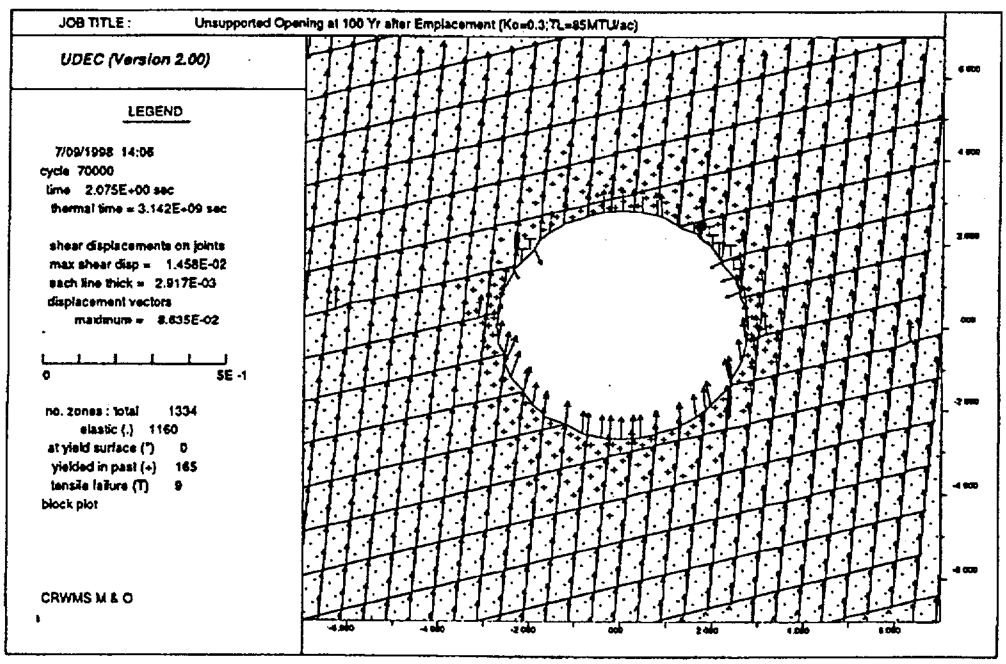

(b)

Figure 7-18 Rock Block Displacements and Potential Rock Yield around an Emplacement Drift for Case A and Ko=0.3: (a) at 10 Years; (b) at 100 Years. (Dimensions are in Meters, Displacements in Meters)

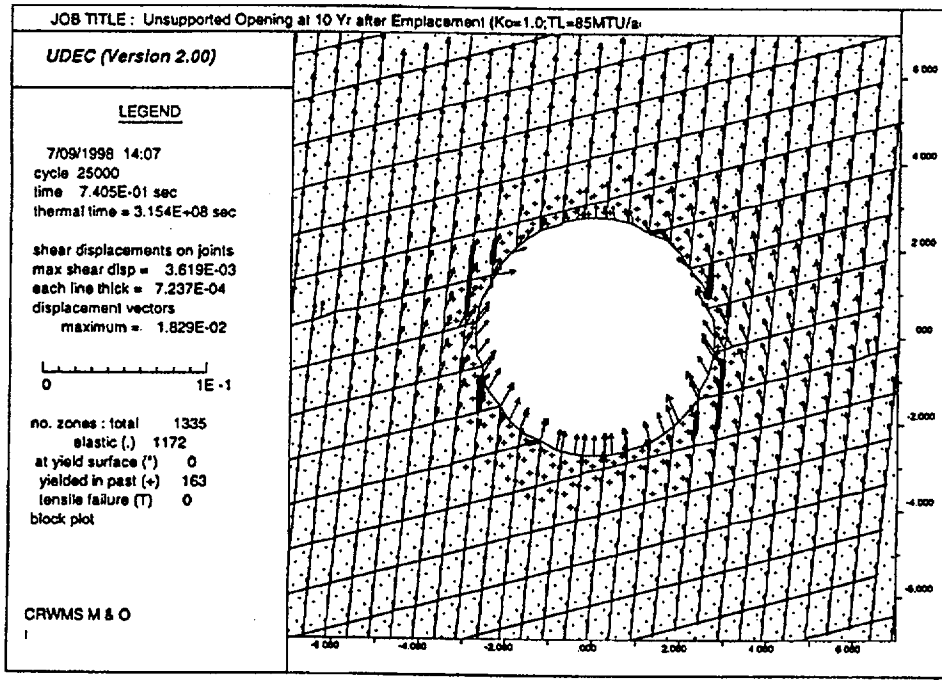

(a)

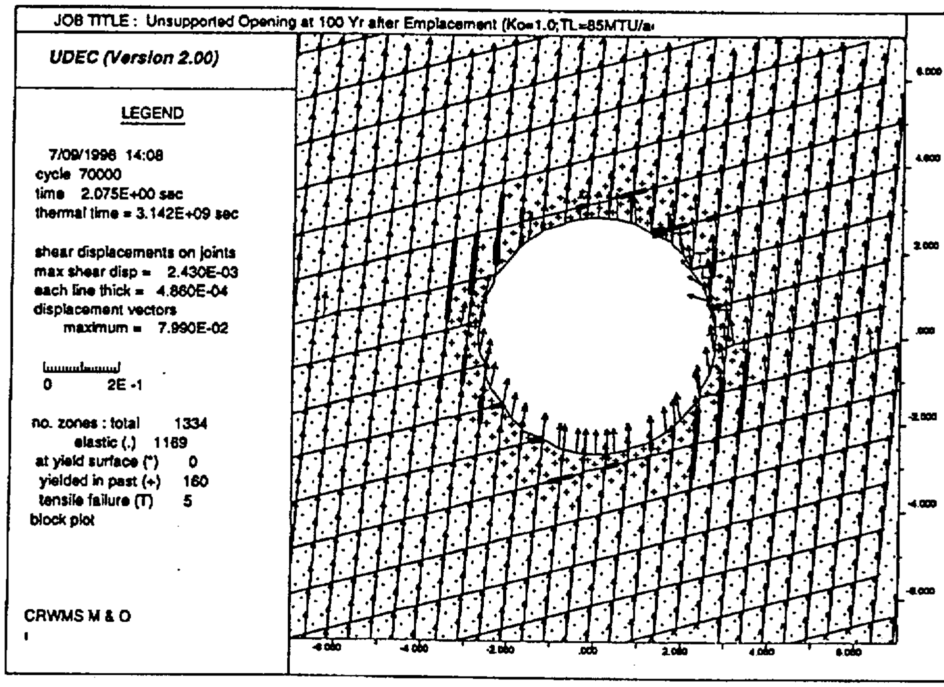

(b)

Figure 7-19 Rock Block Displacements and Potential Rock Yield around an Emplacement Drift for Case A and Ko=1.0: (a) at 10 Years; (b) at 100 Years. (Dimensions are in Meters, Displacements in Meters)

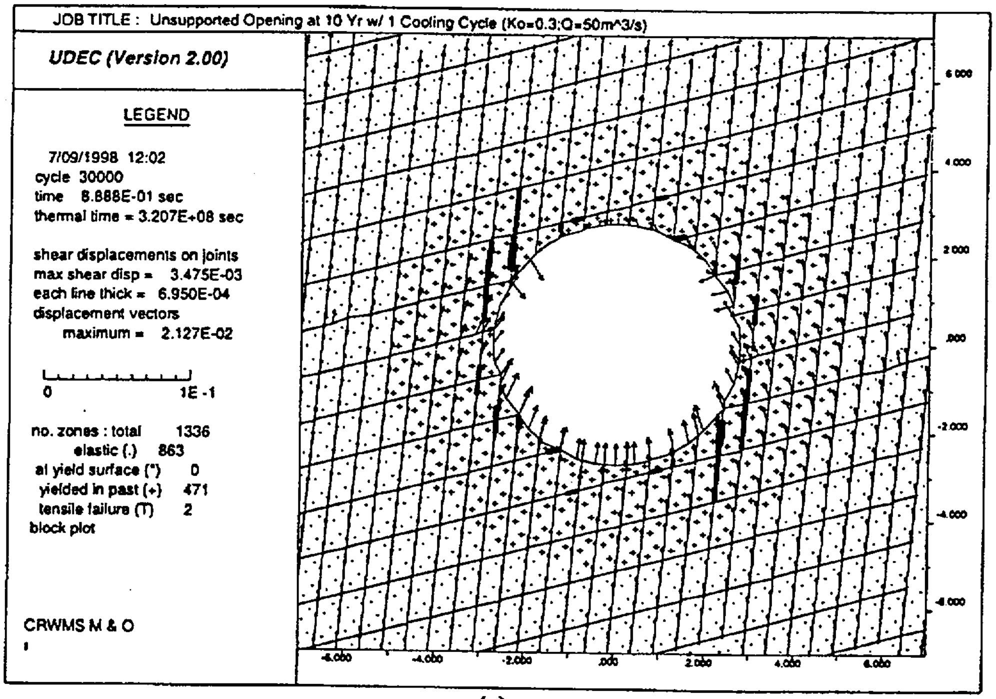

(a)

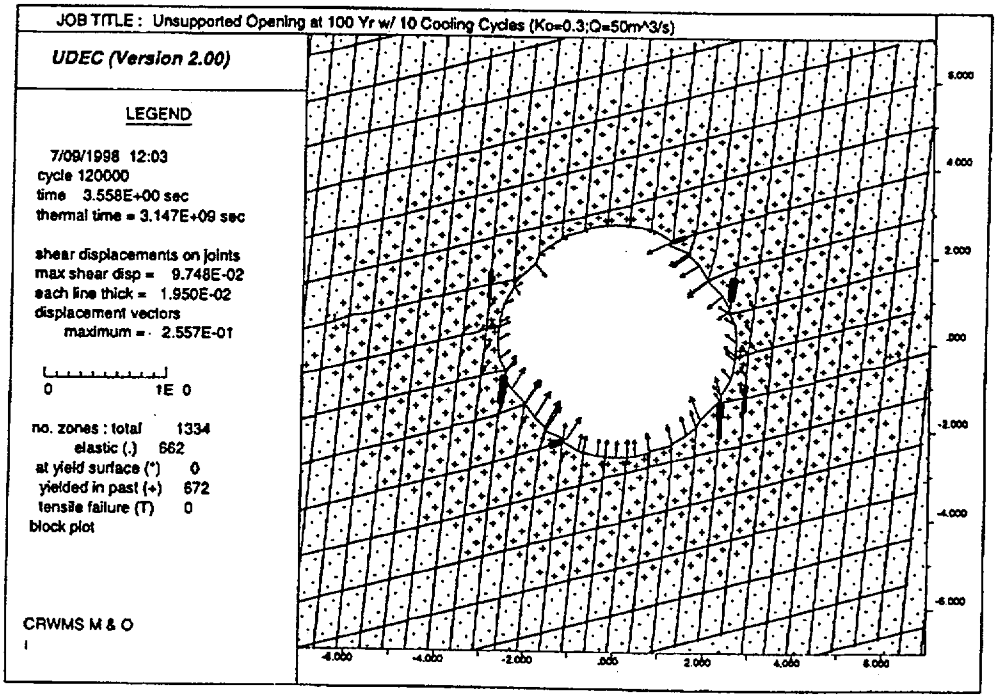

(b)

Figure 7-20 Rock Block Displacements and Potential Rock Yield around an Emplacement Drift for Case C and Ko=0.3: (a) at 10 Years; (b) at 100 Years. (Dimensions are in Meters, Displacements in Meters)

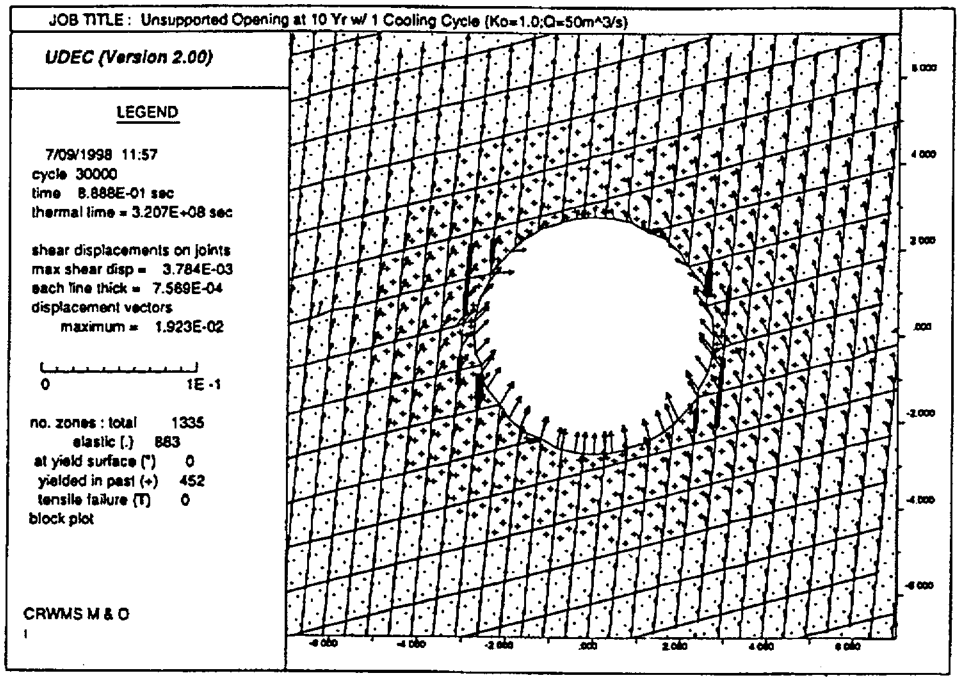

(a)

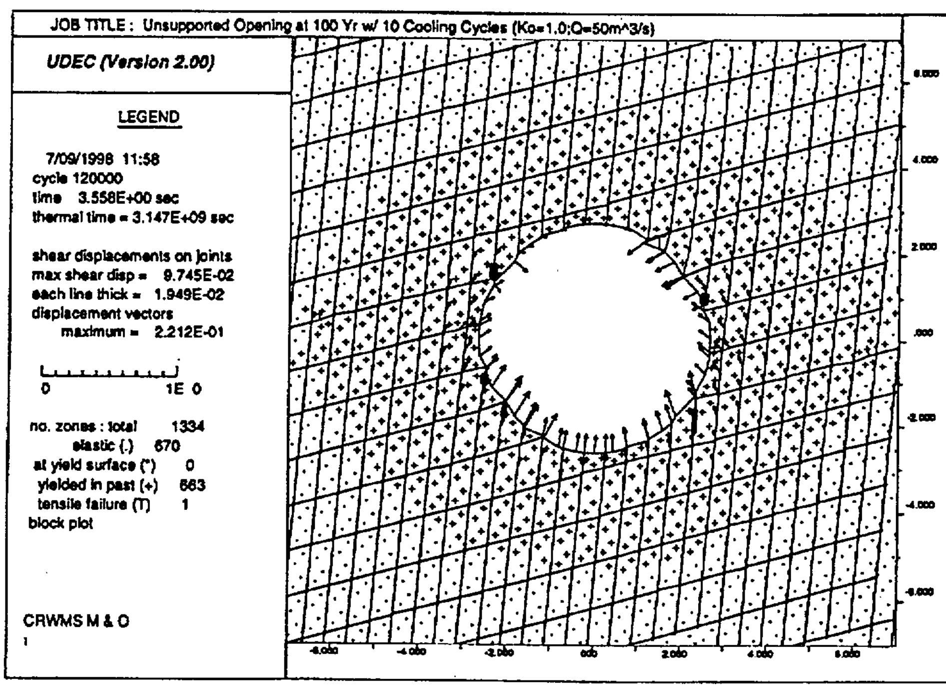

(b)

Figure 7-21 Rock Block Displacements and Potential Rock Yield around an Emplacement Drift for Case C and Ko=1.0: (a) at 10 Years; (b) at 100 Years. (Dimensions are in Meters, Displacements in Meters)

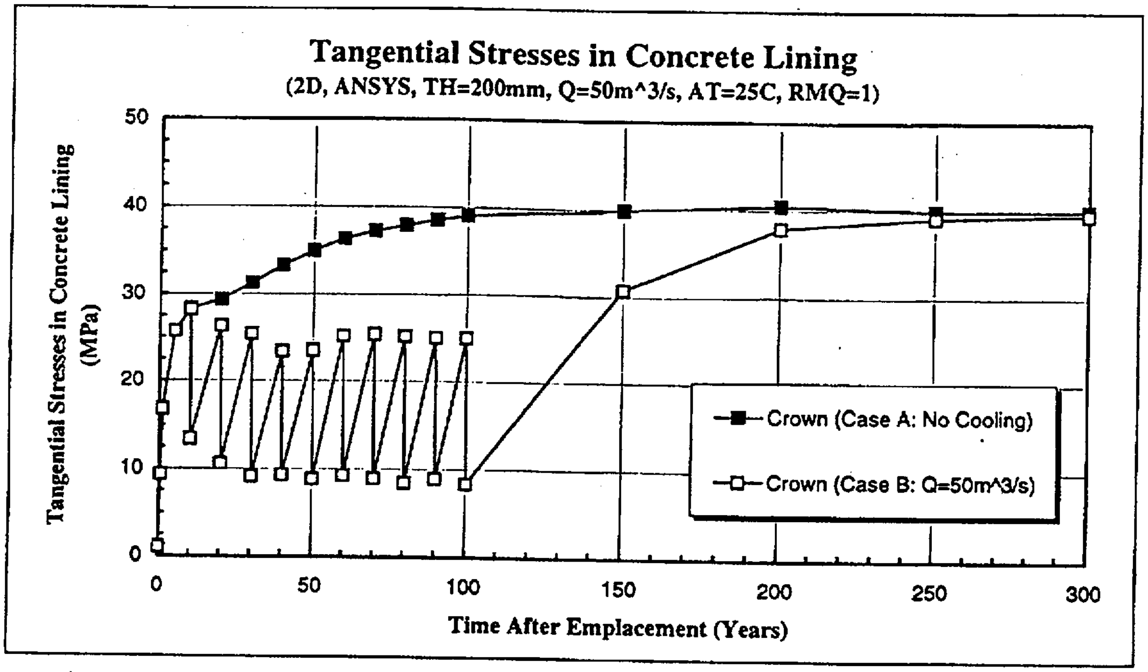

(a)

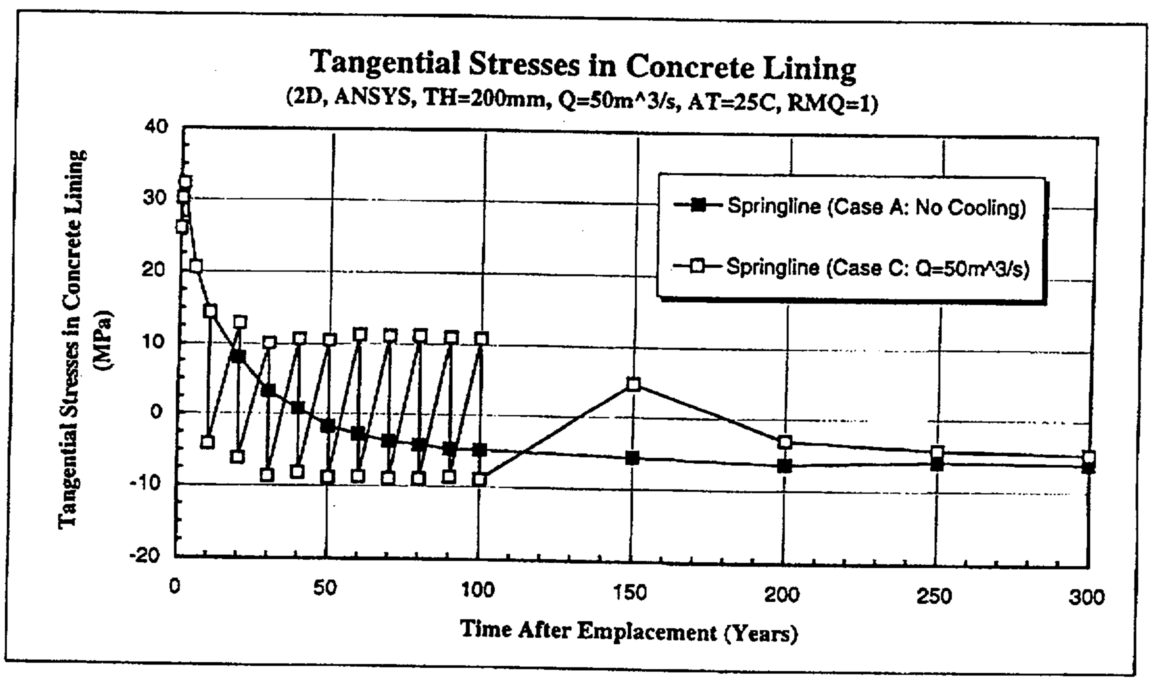

(b)

Figure 7-22 Tangential Stresses in Concrete Lining for Cases A and C and RMQ=1: (a) at Crown; (b) at Springline. (Note: Compression Is Positive. TH=Thickness, Q=Air Quantity, AT=Air Temperature, RMQ=Rock Mass Quality Category)

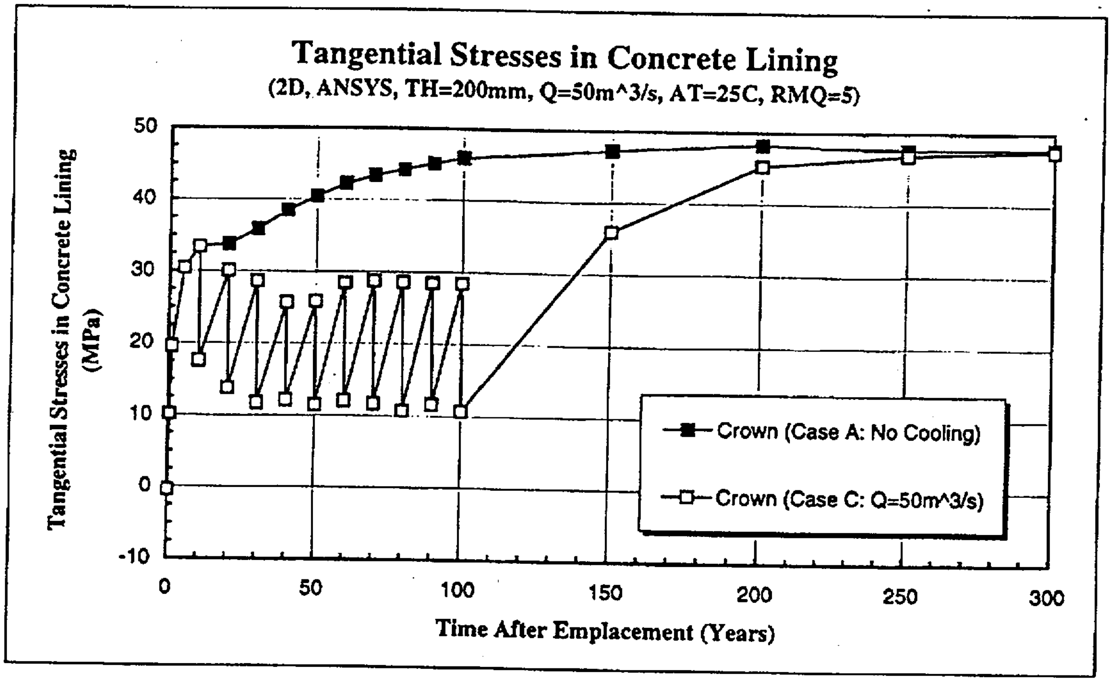

(a)

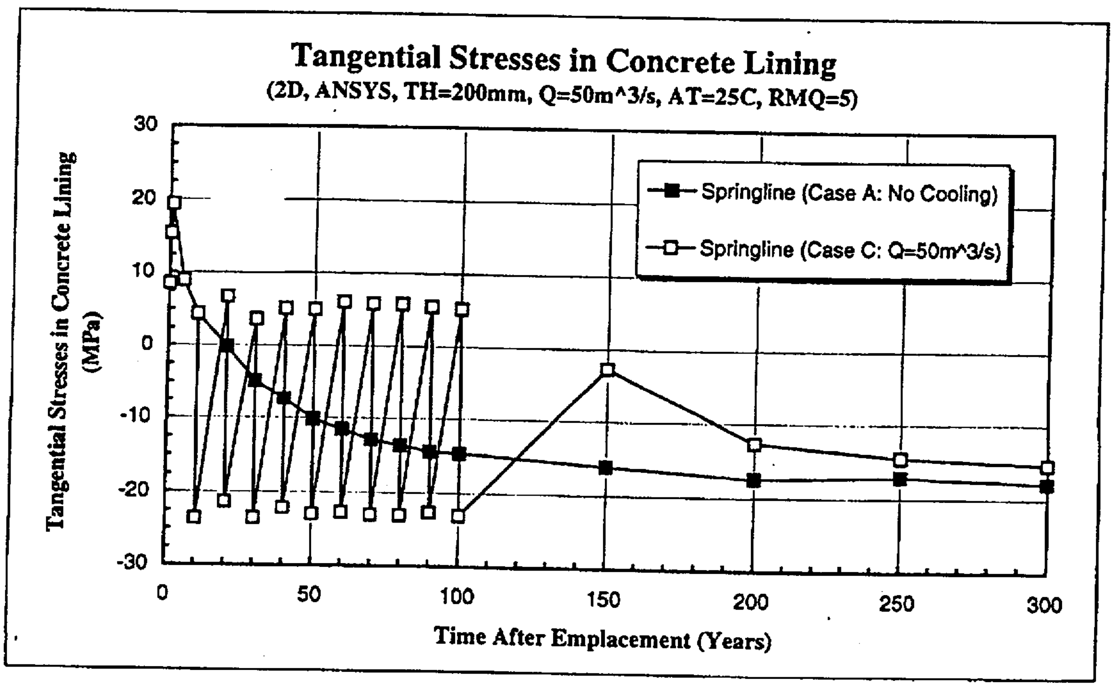

(b)

Figure 7-23 Tangential Stresses in Concrete Lining for Cases A and C and RMQ=5: (a) at Crown; (b) at Springline. (Note: Compression Is Positive. TH=Thickness, Q=Air Quantity, AT=Air Temperature, RMQ=Rock Mass Quality Category)

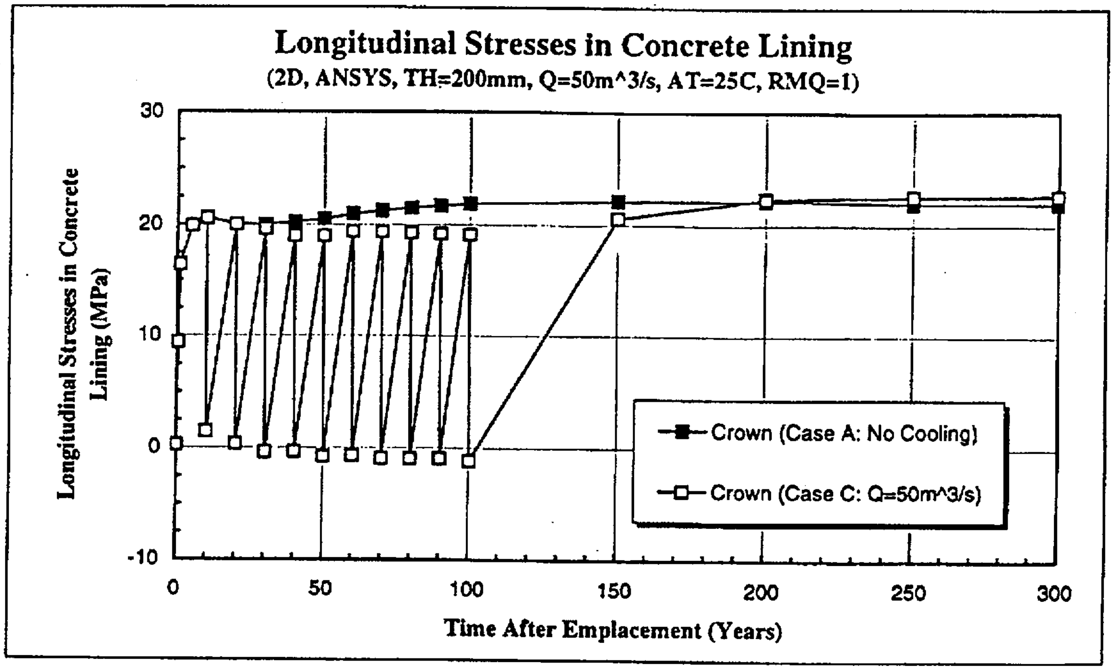

(a)

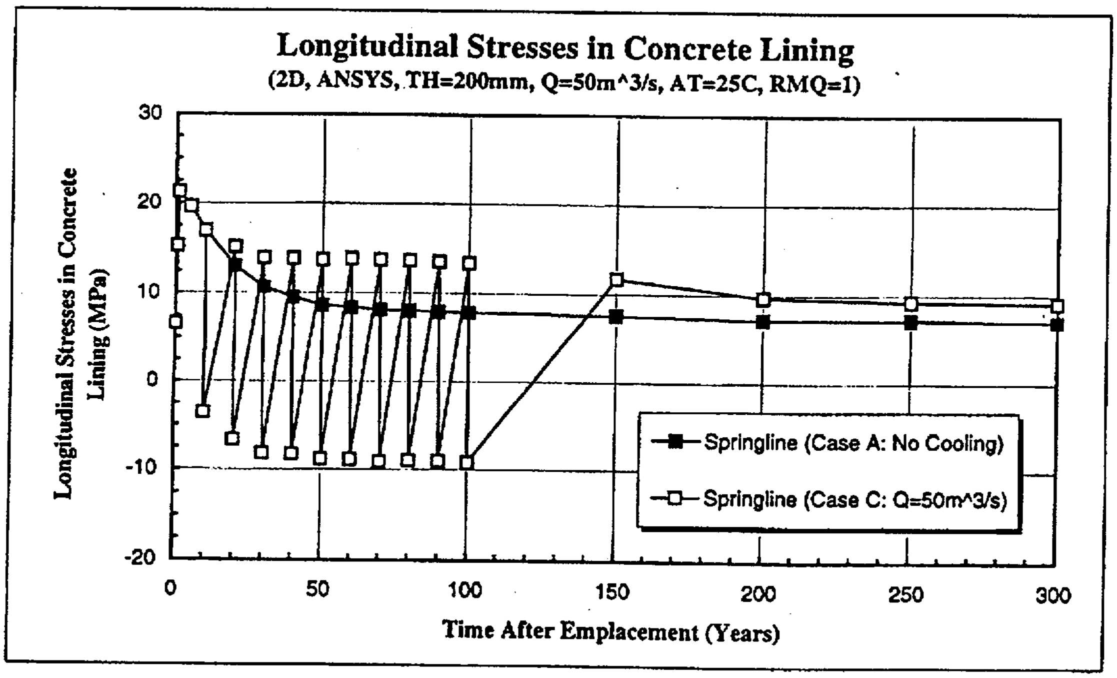

(b)

Figure 7-24 Longitudinal Stresses in Concrete Lining for Cases A and C and RMQ=1: (a) at Crown; (b) at Springline. (Note: Compression Is Positive. TH=Thickness, Q=Air Quantity, AT=Air Temperature, RMQ=Rock Mass Quality Category)

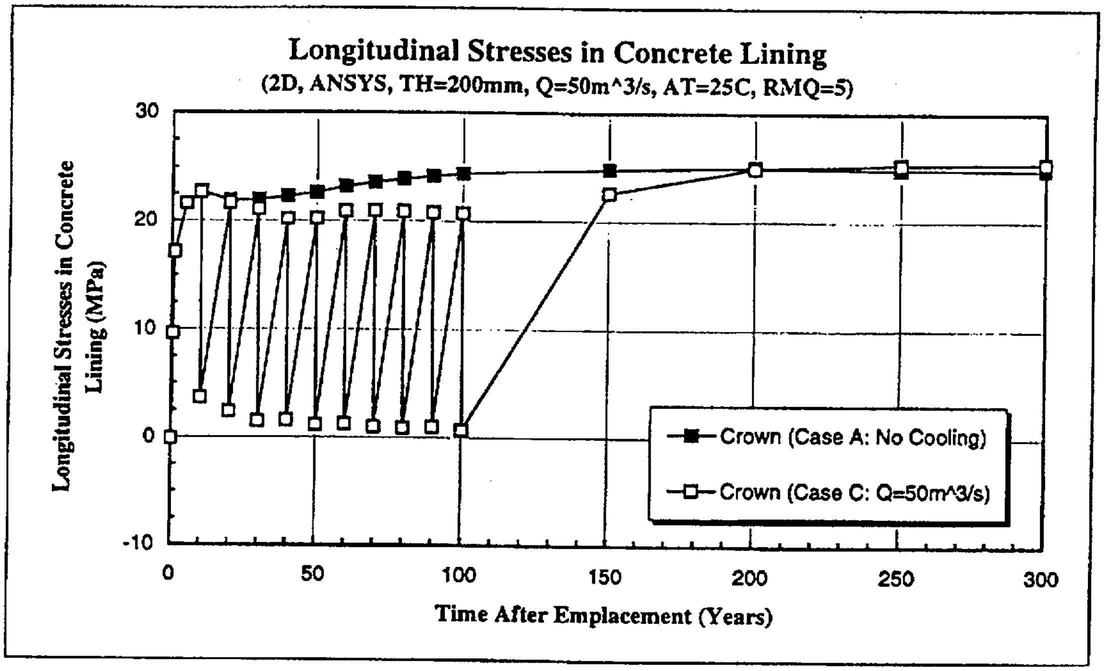

(a)

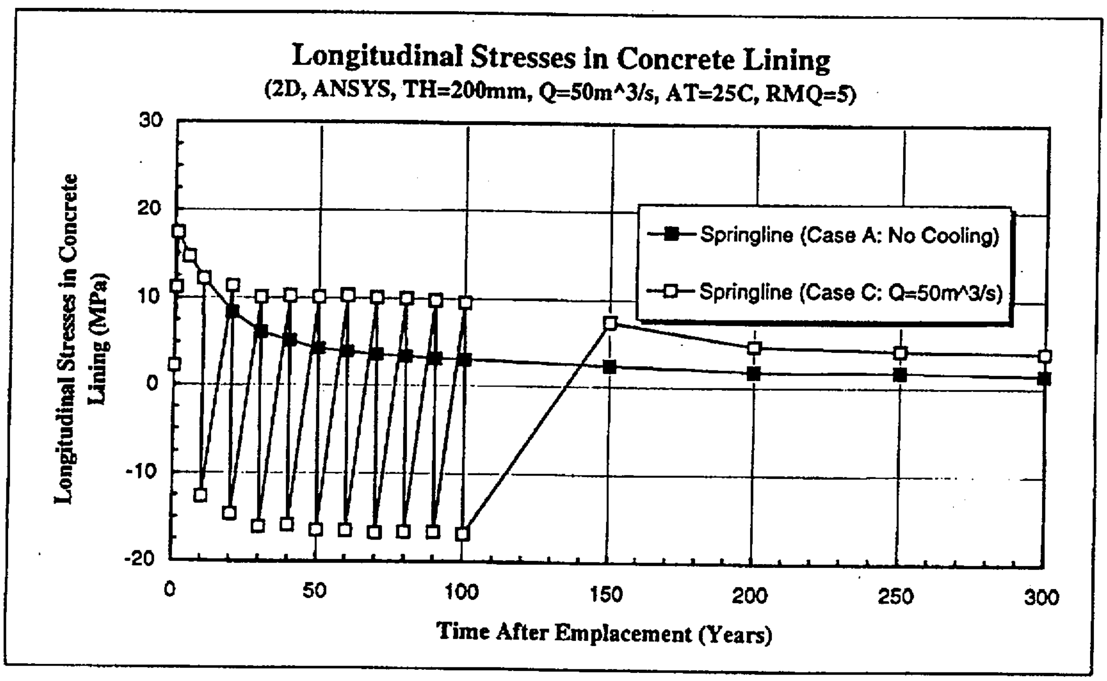

(b)

Figure 7-25 Longitudinal Stresses in Concrete Lining for Cases A and C and RMQ=5: (a) at Crown; (b) at Springline. (Note: Compression Is Positive. TH=Thickness, Q=Air Quantity, AT=Air Temperature, RMQ=Rock Mass Quality Category)

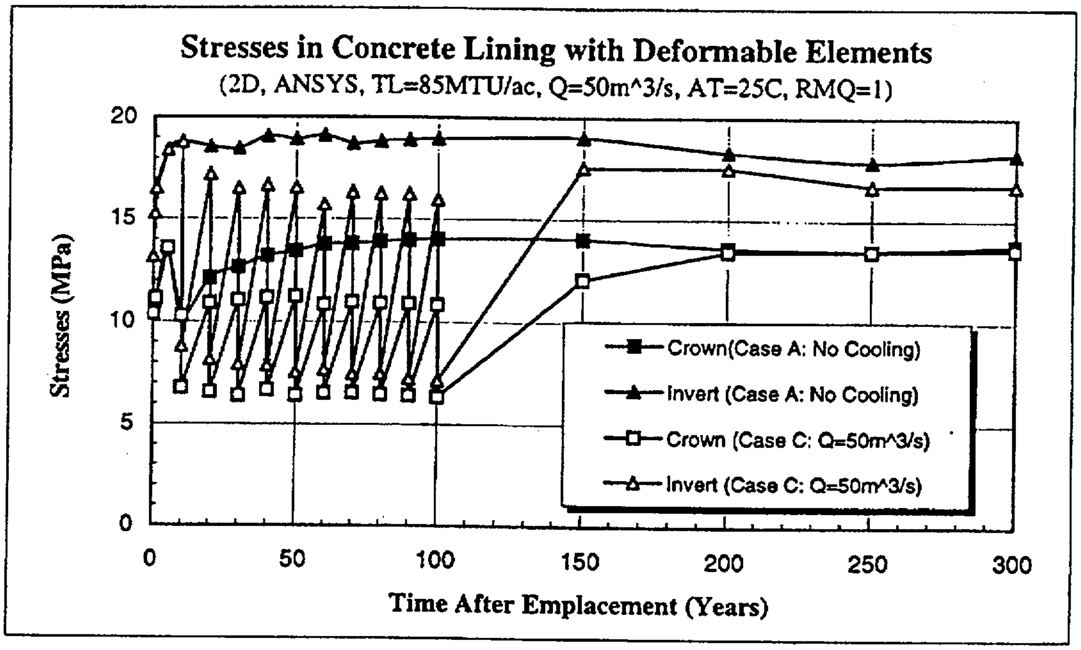

(a)

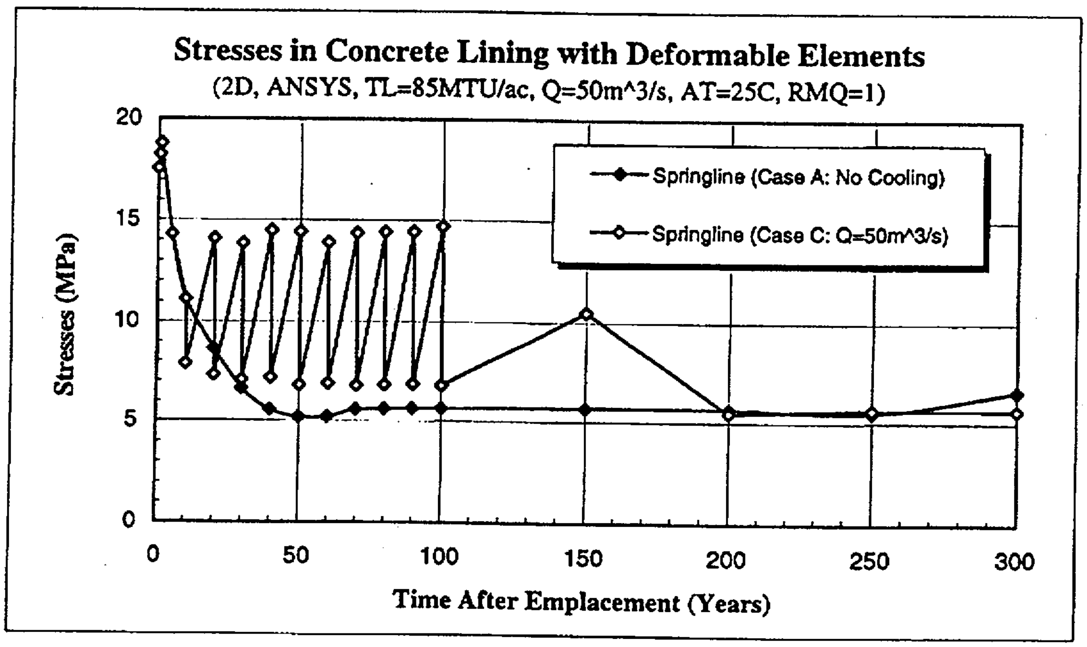

(b)

Figure 7-26 Stresses in Concrete Lining with Deformable Elements for Cases A and C and RMQ=1: (a) at Crown and Invert; (b) at Springline. (Note: Compression Is Positive. TL=Thermal Load, Q=Air Quantity, AT=Air Temperature, RMQ=Rock Mass Quality Category)

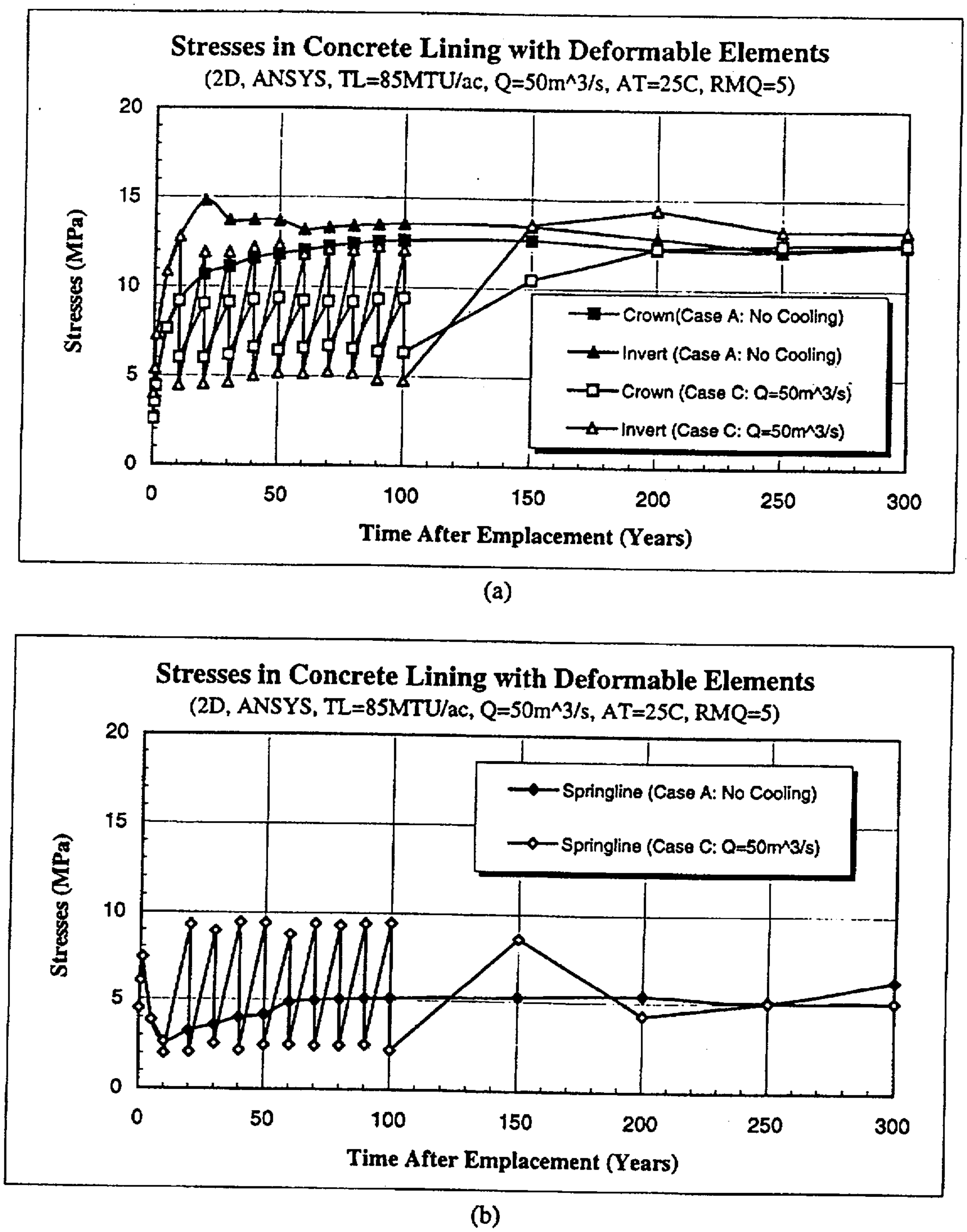

Figure 7-27 Stresses in Concrete Lining with Deformable Elements for Cases A and C and RMQ=5: (a) at Crown and Invert; (b) at Springline. (Note: Compression Is Positive. TL=Thermal Load, Q=Air Quantity, AT=Air Temperature, RMQ=Rock Mass Quality Category)

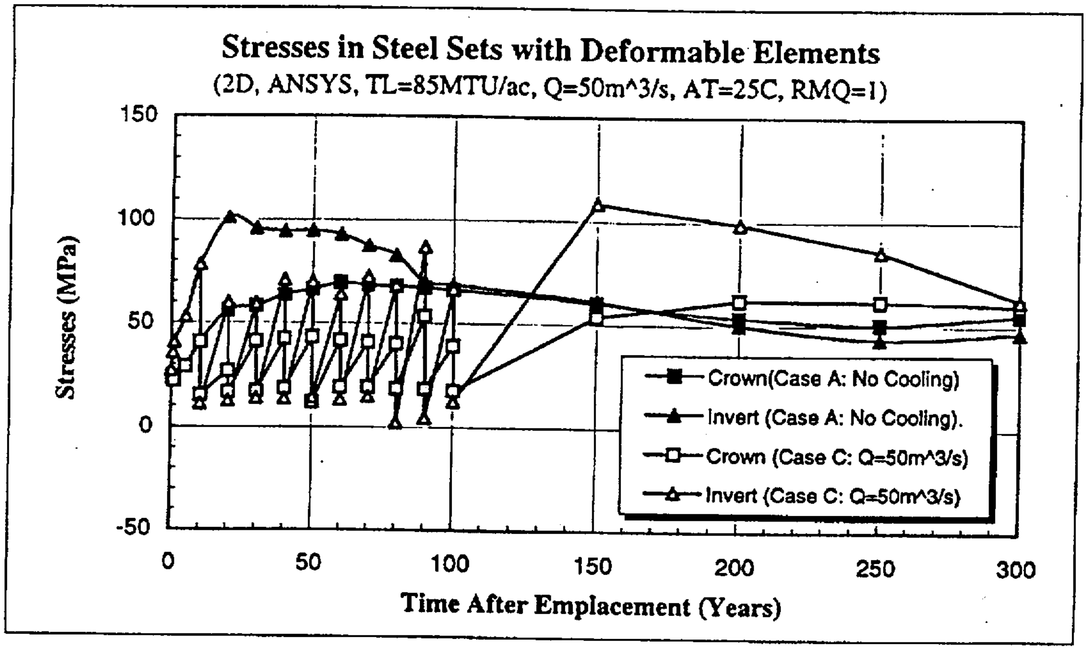

(a)

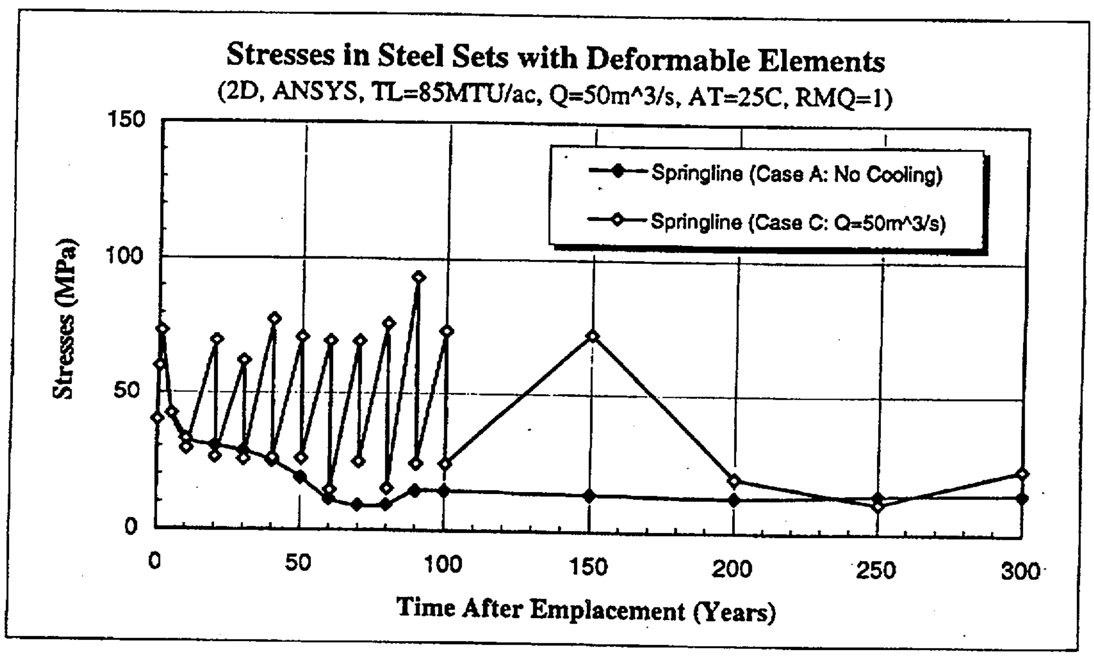

(b)

Figure 7-28 Stresses in Steel Sets with Deformable Elements for Cases A and C and RMQ=1: (a) at Crown and Invert; (b) at Springline. (Note: Compression Is Positive. TL=Thermal Load, Q=Air Quantity, AT=Air Temperature, RMQ=Rock Mass Quality Category)

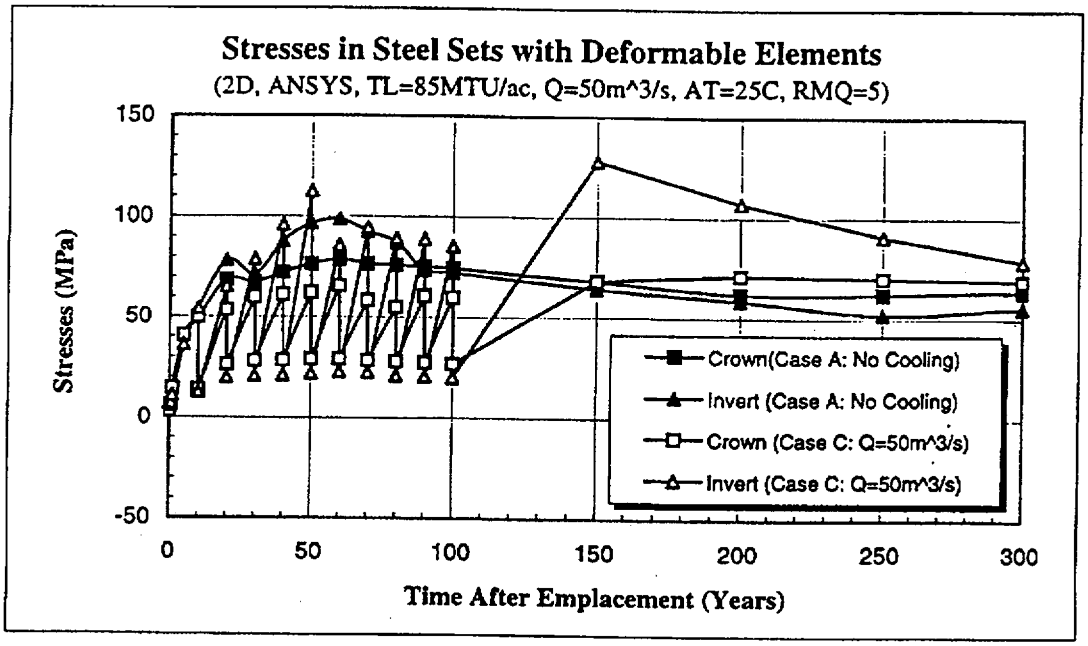

(a)

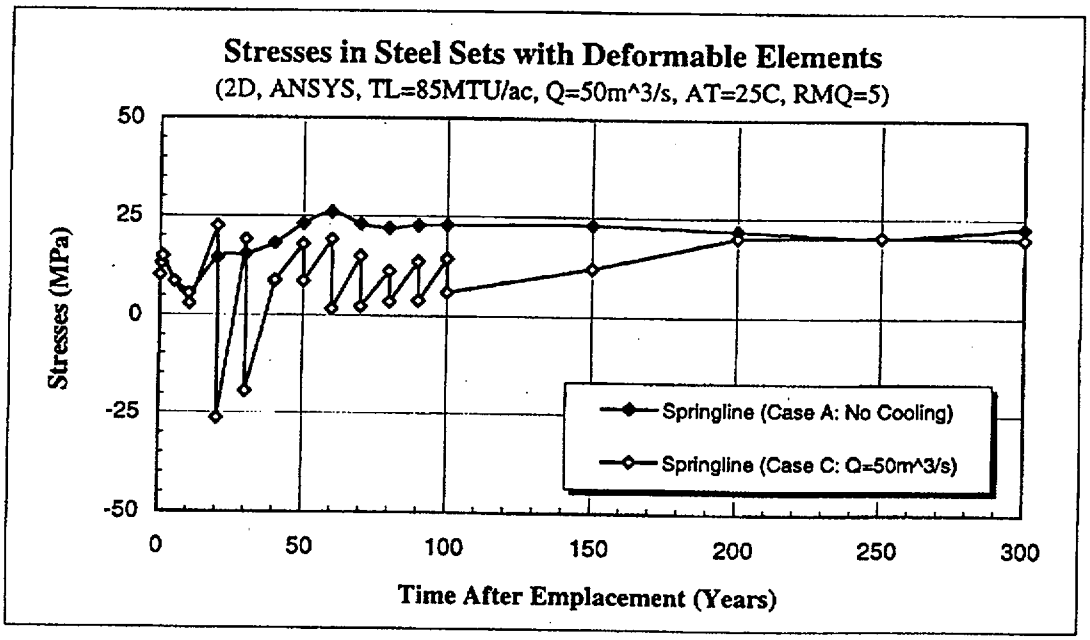

(b)

Figure 7-29 Stresses in Steel Sets with Deformable Elements for Cases A and C and RMQ=5: (a) at Crown and Invert; (b) at Springline. (Note: Compression Is Positive. TL=Thermal Load, Q=Air Quantity, AT=Air Temperature, RMQ=Rock Mass Quality Category)

ATTACHMENT I

CALCULATION OF HEAT OUTPUT DECAY VALUES OF WASTE PACKAGE

I.1 Calculation of Waste Package Spacing

The average waste package spacing is calculated based on the assumed waste stream, as listed in Table I-1 (Reference 5.4, Keys 003 and 004), and 21 PWR packages only.

The average MTU per package is equal to: 37,833.44 ÷ 4,239 = 8.93 MTU/package.

The following values are used in calculation of the average waste package spacings:

Conversion Factor:	1 acre = 4,047 m^2
Drift Spacing:	28.0 m
Thermal Load:	85 MTU/acre
WP MTU per Package:	8.93

The average waste package spacing is equal to:

$$\frac{4047m^2\ /\ acre \times 8.93MTU\ /\ package}{85MTU\ /\ acre \times 28m} = 15.18m\ /\ package$$

I.2 Calculation of Average Waste Package Heat Flux

The heat decay values for the 21 PWR waste packages are obtained from Reference 5.9 (Attachment XXXIX, pp. 1-3). These values are given in a form of heat output per assembly, as listed in Table I-2, Columns B through D. The total number of assemblies of each type of waste packages, identified as $k \leq 1.00$, $k \leq 1.13$, and $k \leq 1.45$, are 30317, 55455, and 2520, respectively (Reference 5.9, Attachment XXXIX, pp. 1-3). The averaged heat output values per waste package at a given time, for example at 0 year, is calculated as follows:

$$\textit{Heat Output per WP} = (489.13 \times 30317 + 434.28 \times 55455 + 138.32 \times 2520)/4239 = 9.26\ kW$$

Column E of Table I-2 lists the average values of WP heat output for a period of 300 years. The average heat flux of a waste package for a two-dimensional analysis is calculated by assuming that the package has a virtual length of 15.18 meters for the drift spacing of 28 meters, and its heat output smears over the side surface of that length. In addition, to use the *year* as time unit in the analysis, a conversion factor of 3.1536×10^7 sec/year is assumed to convert the units from watts (joules/sec) to joules/year. Column F of Table I-2 provides the average heat flux values over the waste package side surface, and these values are used as inputs to the ANSYS models.

The following values are involved in the calculation:

WP Diameter:	1.664 m
WP Side Surfaces:	$\pi \times 1.664 \times 15.18 = 79.36$ m^2/package
Seconds Per Year:	$365 \times 24 \times 3600 = 3.1536 \times 10^7$ sec/year

Table I-1. Assumed Waste Stream for 21 PWR Packages (Reference 5.4, Keys 003 and 004).

A	B	C	D	E	F	G	H=B*E+C*F+D*G
Time (year)	No. of Packages LG-WP 21 PWR K<=1.00	No. of Packages LG-WP 21 PWR K<=1.13	No. of Packages LG-WP 21 PWR K<=1.45	Ave. MTU/Package LG-WP 21 PWR K<=1.00	Ave. MTU/Package LG-WP 21 PWR K<=1.13	Ave. MTU/Package LG-WP 21 PWR K<=1.45	Average MTU for All 21 PWR Packages
2010	3	17	1	8.99	8.89	0.90	179.00
2011	4	27	5	9.02	8.78	8.89	317.59
2012	19	56	0	9.01	9.06	0.00	678.55
2013	29	94	9	9.15	9.02	8.65	1191.08
2014	45	150	7	8.71	9.12	7.27	1810.84
2015	50	155	1	8.96	9.02	2.54	1848.64
2016	57	131	3	9.03	9.08	5.34	1720.21
2017	43	152	3	9.06	9.08	8.00	1793.74
2018	52	133	4	9.01	9.02	8.01	1700.22
2019	49	139	7	9.04	9.10	7.72	1761.90
2020	51	138	5	9.00	8.99	8.31	1741.17
2021	62	128	3	8.99	9.06	7.01	1738.09
2022	61	131	3	9.04	9.08	8.75	1767.17
2023	59	133	12	9.03	9.01	8.85	1837.30
2024	63	118	15	9.14	9.06	8.51	1772.55
2025	58	117	4	8.83	9.08	8.84	1609.86
2026	77	94	20	8.28	8.77	6.14	1584.74
2027	114	83	7	8.68	8.78	7.20	1768.66
2028	92	109	2	8.94	8.92	4.81	1804.38
2029	89	120	3	9.02	9.01	5.96	1901.86
2030	88	129	5	8.83	8.92	5.79	1956.67
2031	112	118	3	9.04	8.94	7.52	2089.96
2032	105	118	7	8.89	8.97	6.27	2035.80
2033	72	63	3	8.92	8.91	6.63	1223.46
Total	1454	2653	132				37833.44

Table I-2. Heat Flux Values for 21 PWR Waste Packages.

A	B	C	D	E=(B*30317+C*55455+D*2520)/4239	F
Time (year)	Heat Decay Values (W/assembly)			Average Heat Output (W/package)	Average Heat Output (J/yr/m^2)
	k<=1.00	k<=1.13	k<=1.45	4239 Packages	
	30317 Assemblies	55455 Assemblies	2520 Assemblies		
	(Reference 5.9, Attachment XXXIX, pp. 1-3)				
0	489.13	434.28	138.32	9261.74	3.68E+09
1	478.42	421.61	135.29	9017.59	3.58E+09
5	442.08	384.36	125.04	8264.29	3.28E+09
10	404.24	349.27	114.37	7528.27	2.99E+09
20	343.09	294.93	97.02	6369.73	2.53E+09
30	295.20	252.66	83.27	5466.07	2.17E+09
40	257.14	219.41	72.29	4752.36	1.89E+09
50	226.51	192.36	63.47	4174.19	1.66E+09
60	201.78	170.67	56.38	3709.35	1.47E+09
70	181.78	153.07	50.63	3332.65	1.32E+09
80	165.26	138.64	46.00	3022.97	1.20E+09
90	151.72	126.98	42.24	2771.36	1.10E+09
100	140.39	117.08	39.17	2559.00	1.02E+09
150	105.93	87.72	30.27	1923.16	7.64E+08
200	88.03	73.12	26.03	1601.62	6.36E+08
250	77.14	64.39	23.60	1408.09	5.59E+08
300	69.39	58.25	21.81	1271.27	5.05E+08

ATTACHMENT II

CALCULATION OF CONVECTION HEAT TRANSFER COEFFICIENT

Parameters Used in Calculation:

Constant (π):	3.141592654	
Ventilation Air Quantity (Q):	2.5 and 50 m^3/s	(Section 4.3.10)
Drift Inside Diameter (D):	5.1 m	(For drift diameter of 5.5 m and concrete lining thickness of 0.20 m) (Sections 4.3.7 and 4.3.5)
WP Diameter (d):	1.664 m	(Section 4.3.2)
Ventilation Air Temperature (T):	25°C	(Section 4.3.10)

Air Properties Estimated Based on a Temperature of 25°C (298 K) (Reference. 5.3, p. 646):

Density (ρ):	1.1868 kg/m^3	(Section 4.3.10)
Thermal Conductivity (k):	0.02608 W/m·K	(Section 4.3.10)
Dynamic Viscosity (μ):	1.8363×10^{-5} (kg/m·s)	(Section 4.3.10)
Prandtl Number (Pr):	0.709	(Section 4.3.10)

Calculation:

Cross-Sectional Area (A):

$$A = \frac{\pi(D^2 - d^2)}{4} = \frac{3.141592654\times(5.1^2 - 1.664^2)}{4} = 18.25m^2$$

Wetted Perimeter (P):

$$P = \pi(D + d) = 3.141592654\times(5.1 + 1.664) = 21.25m$$

Hydraulic Diameter (D_h):

$$D_h = \frac{4A}{P} = \frac{4\times18.25}{21.25} = 3.44m$$

The additional equations used in calculating the convection heat transfer coefficients listed in Table II-1 are given as follows:

Air Flow Velocity (v): $v = \dfrac{Q}{A}$

Reynolds No. (Re) (Reference 5.3, Basic Heat Transfer Relations, inside front cover):

$$Re = \frac{\rho v D_h}{\mu}$$

Nusselt No. (*Nu*) (Reference 5.3, Eq. (6-4a), p. 286; n=0.4 for heating, p. 286):

$$Nu = 0.023\, Re^{0.8}\, Pr^{0.4}$$

Convection Heat Transfer Coefficient (*h*) (Reference 5.3, Eq. (5-107), p. 261):

$$h = \frac{k Nu}{D_h}$$

Table II-1. Calculation of Convection Heat Transfer Coefficients

Parameter	Value	
Air Flow Rate (m^3/s)	2.5	50
Air Flow Velocity (m/s)	0.14	2.74
Reynolds No. (dimensionless)	30414.48*	608289.65*
Nusselt No. (dimensionless)	77.57*	849.72*
Convection Heat Transfer Coefficient ($W/m^2 \cdot K$)	0.59*	6.45*

* Due to rounding these values may vary since interpolations and other calculations are contained within a spreadsheet.

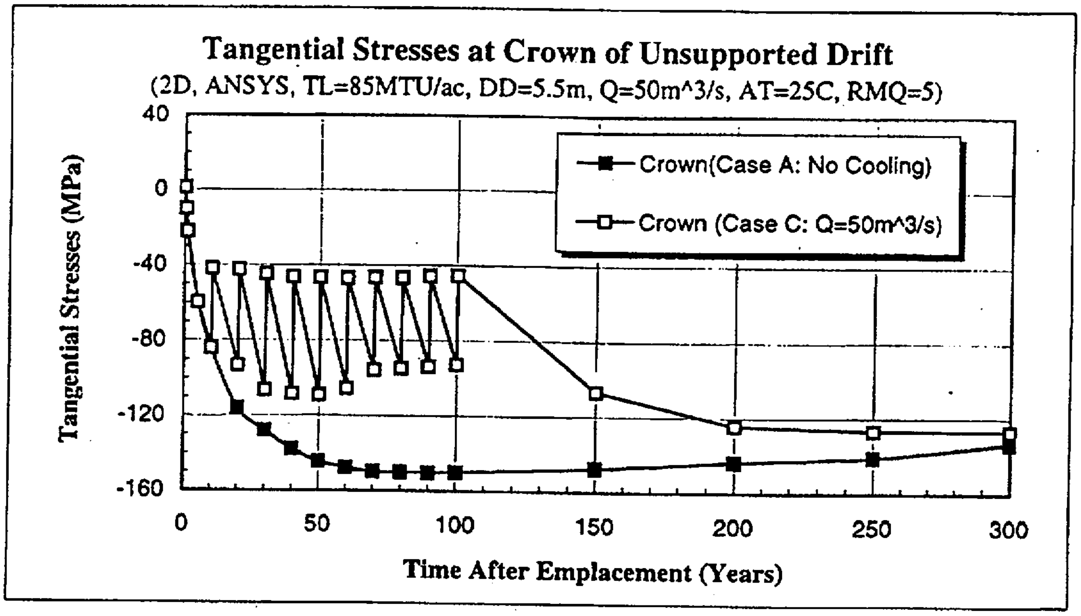

(a)

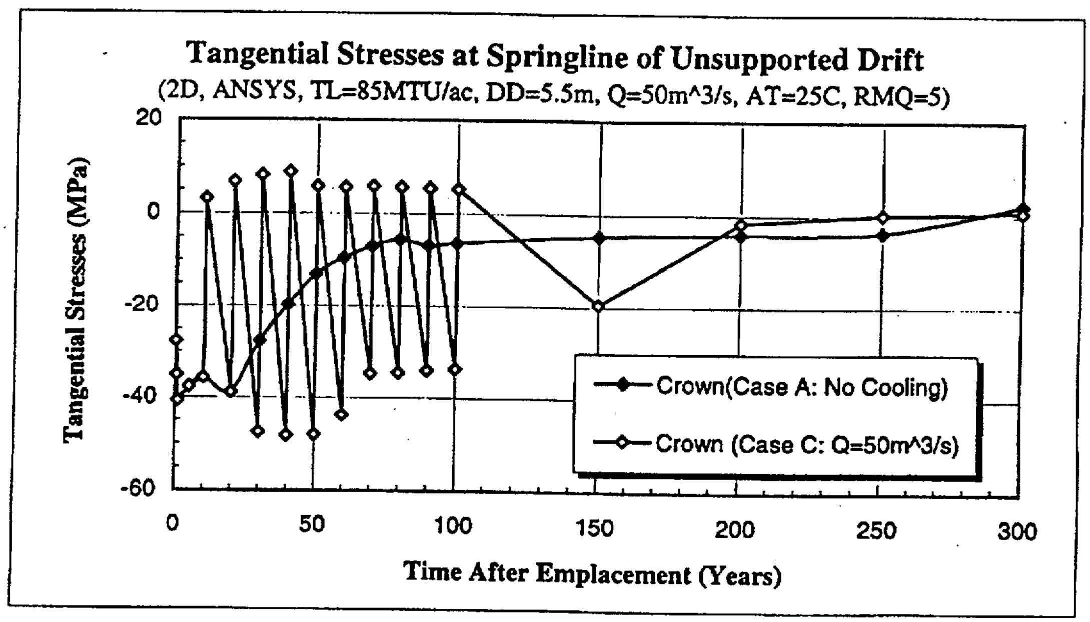

(b)

Figure 7-15 Tangential Stresses at Unsupported Drift for Cases A and C and RMQ=5: (a) Crown; (b) Springline. (Note: Compression Is Negative. TL=Thermal Load, DD=Drift Diameter, Q=Air Quantity, AT=Air Temperature, RMQ=Rock Mass Quality Category)

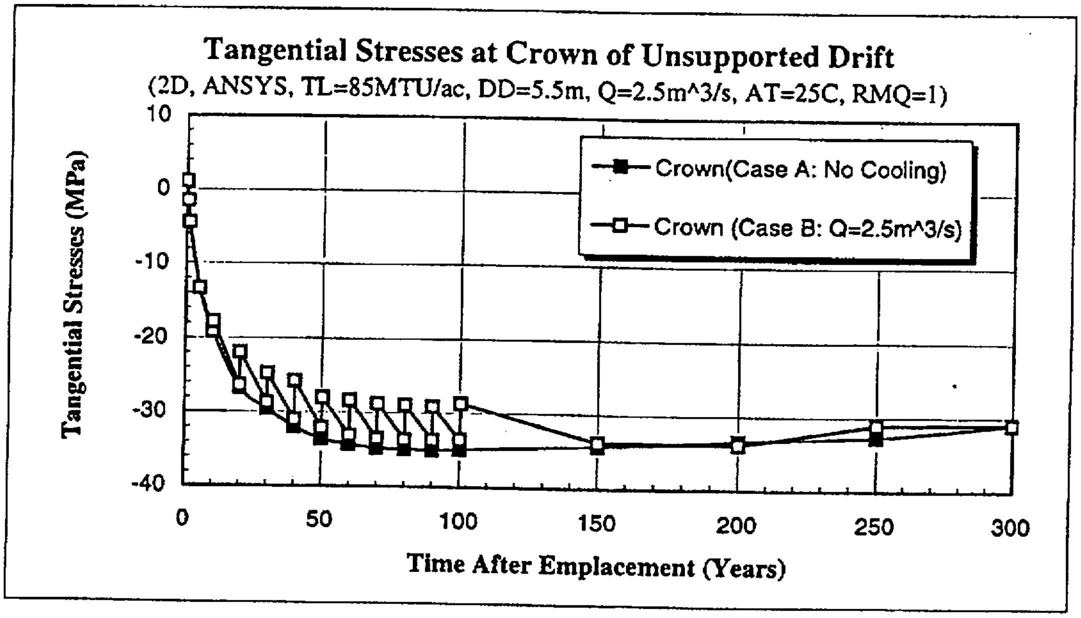

(a)

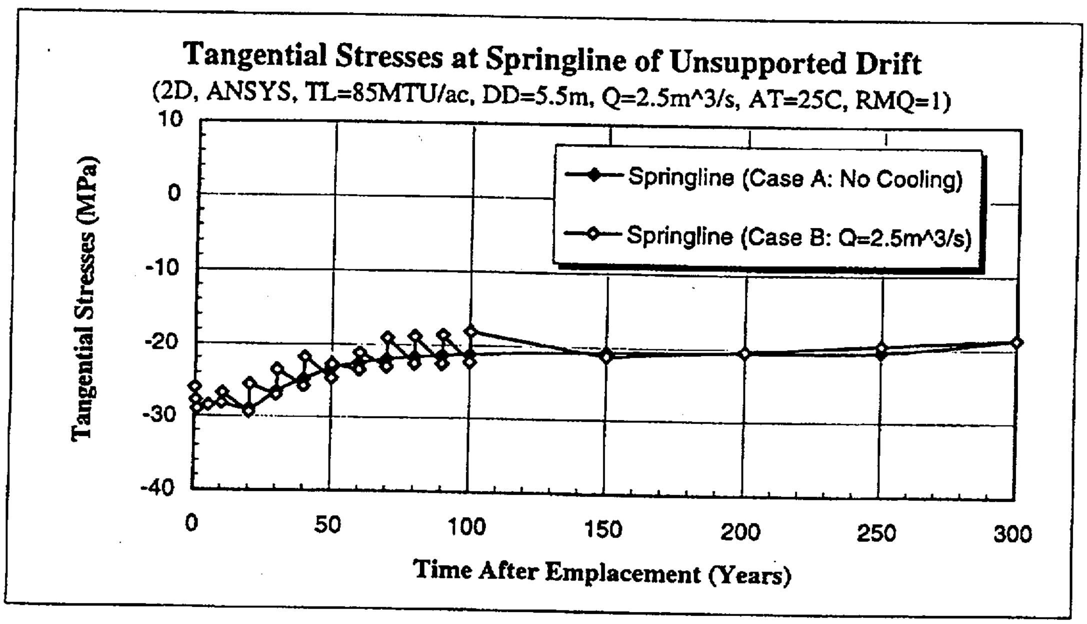

(b)

Figure 7-16 Tangential Stresses at Unsupported Drift for Cases A and B and RMQ=1: (a) Crown; (b) Springline. (Note: Compression Is Negative. TL=Thermal Load, DD=Drift Diameter, Q=Air Quantity, AT=Air Temperature, RMQ=Rock Mass Quality Category)

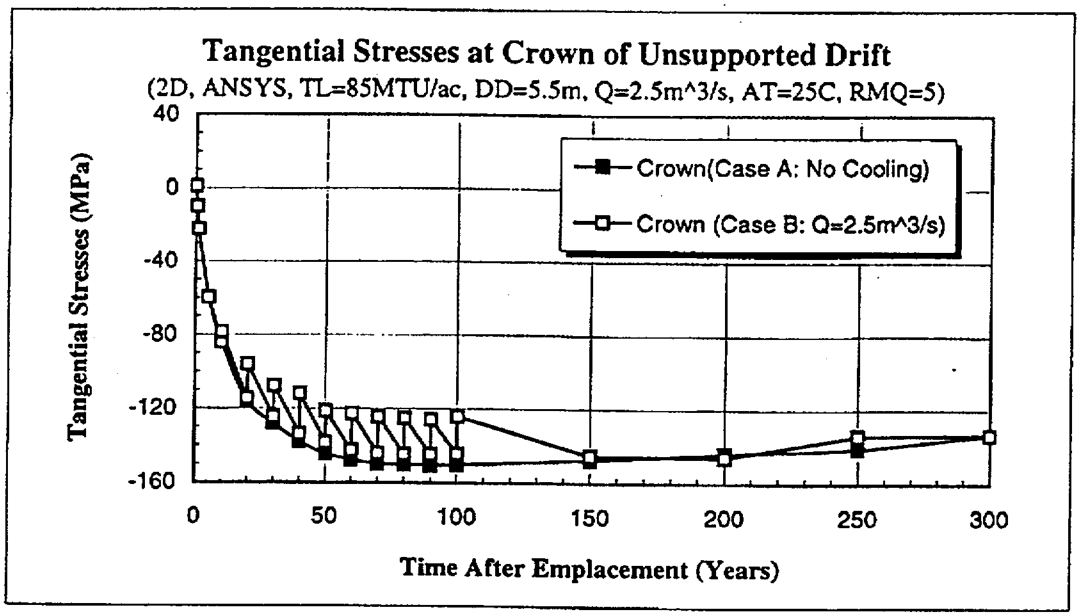

(a)

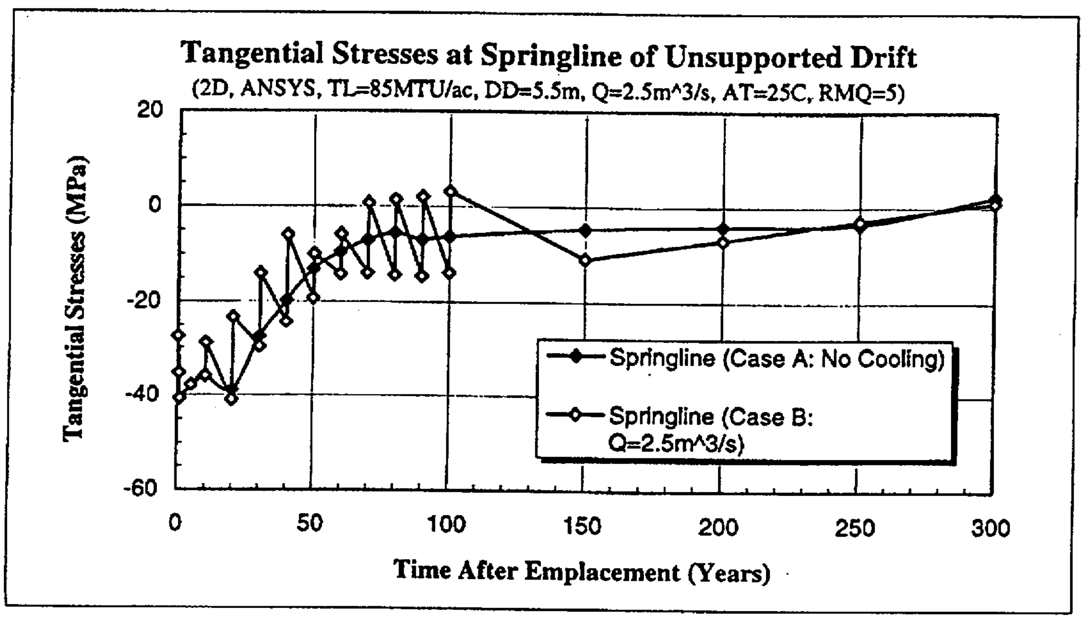

(b)

Figure 7-17 Tangential Stresses at Unsupported Drift for Cases A and C and RMQ=5: (a) Crown; (b) Springline. (Note: Compression Is Negative. TL=Thermal Load, DD=Drift Diameter, Q=Air Quantity, AT=Air Temperature, RMQ=Rock Mass Quality Category)

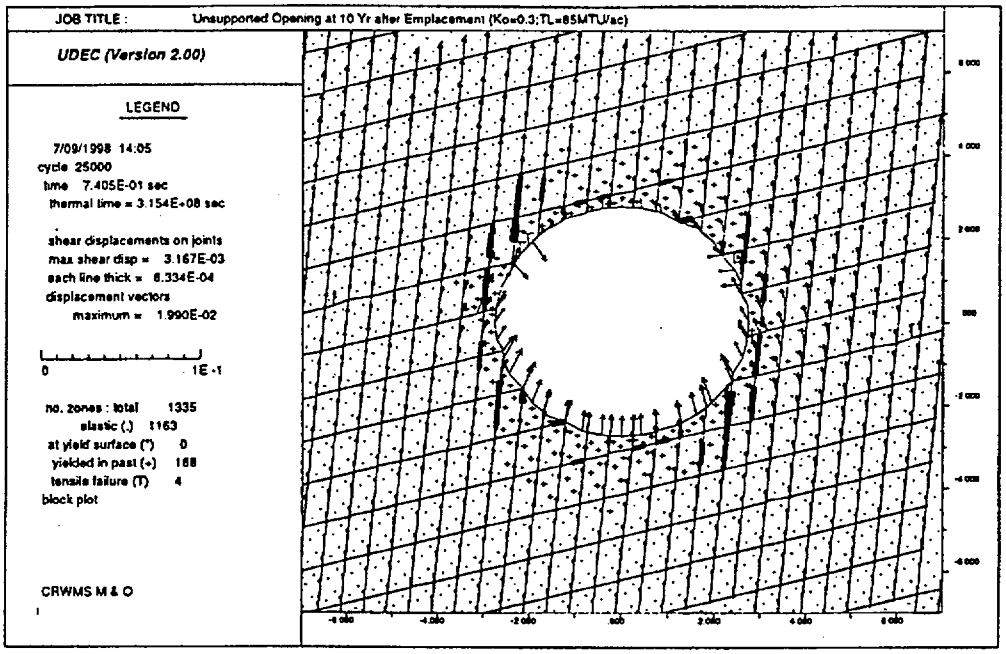

(a)

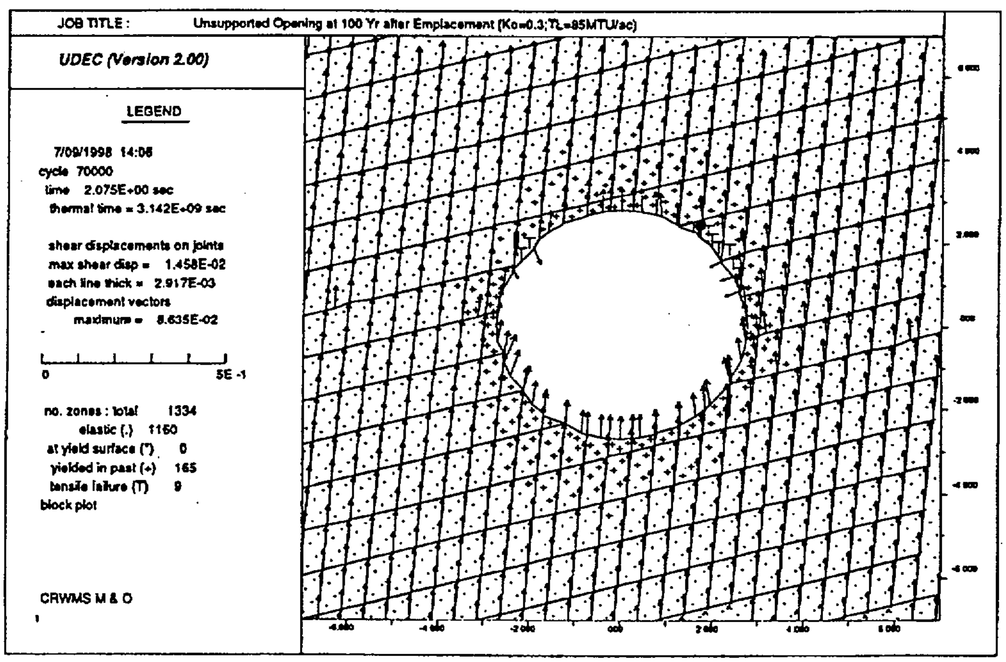

(b)

Figure 7-18 Rock Block Displacements and Potential Rock Yield around an Emplacement Drift for Case A and Ko=0.3: (a) at 10 Years; (b) at 100 Years. (Dimensions are in Meters, Displacements in Meters)

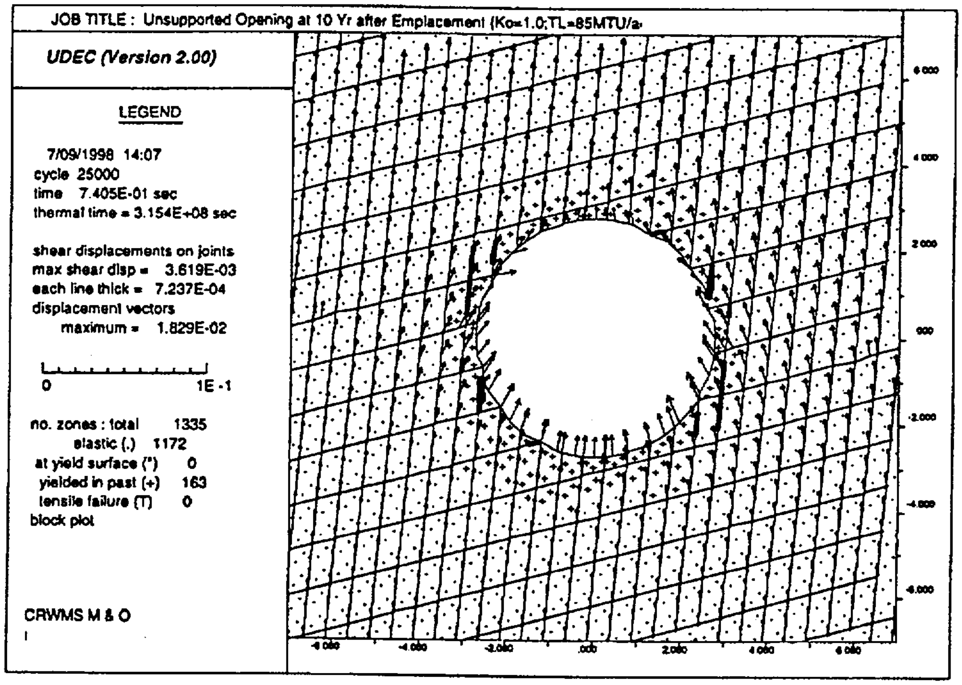

(a)

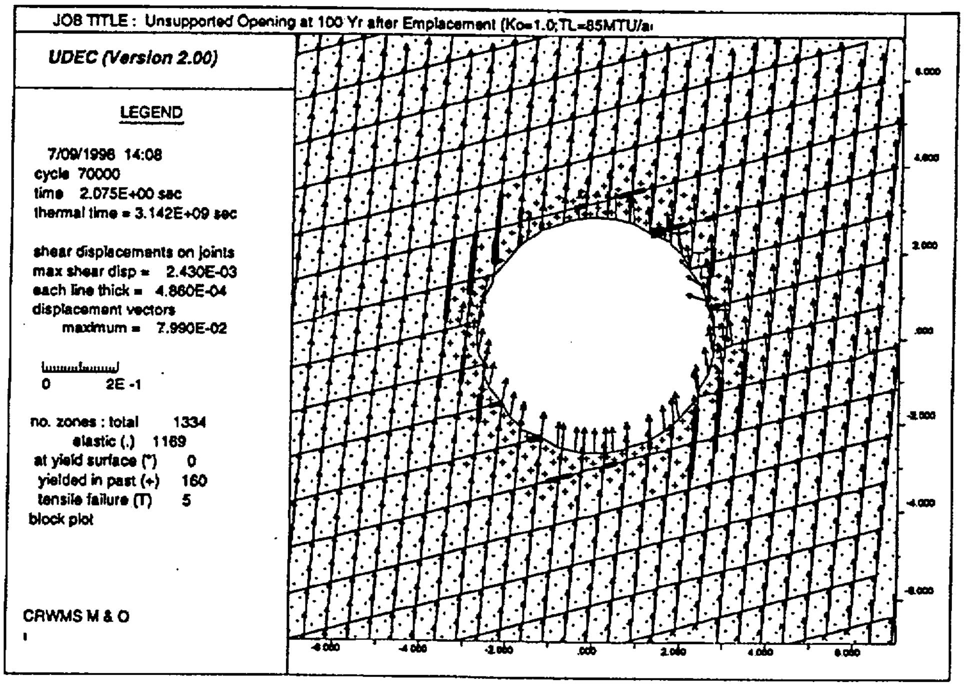

(b)

Figure 7-19 Rock Block Displacements and Potential Rock Yield around an Emplacement Drift for Case A and Ko=1.0: (a) at 10 Years; (b) at 100 Years. (Dimensions are in Meters, Displacements in Meters)

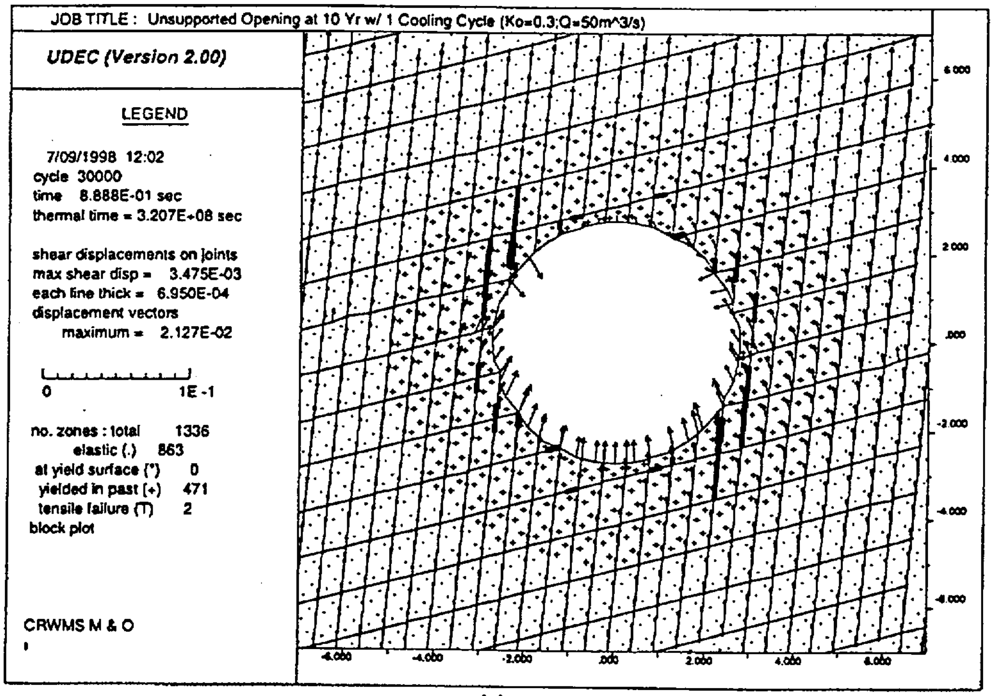

(a)

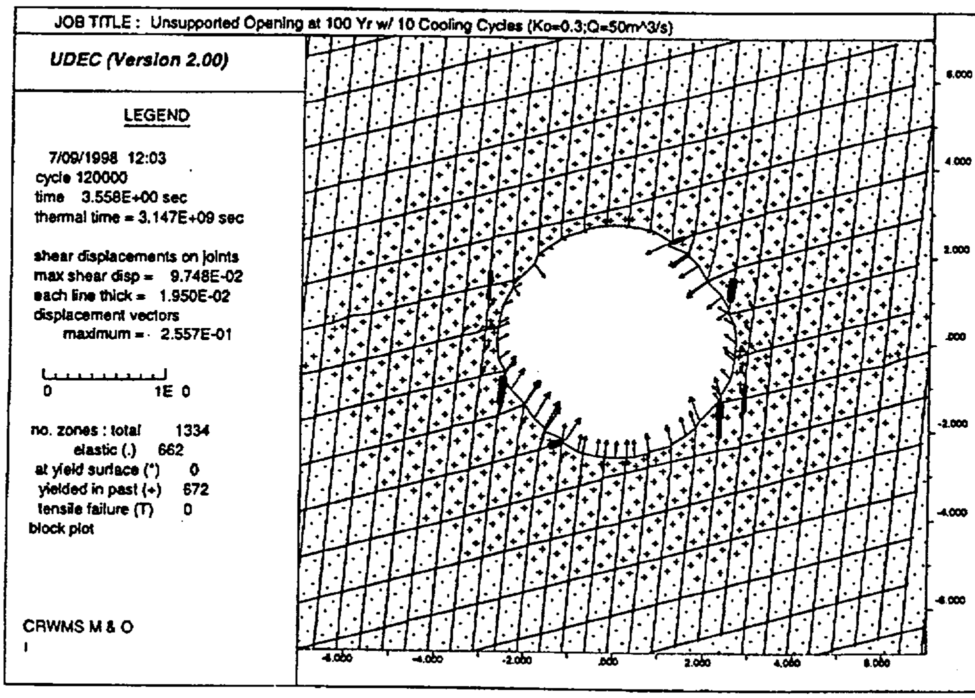

(b)

Figure 7-20 Rock Block Displacements and Potential Rock Yield around an Emplacement Drift for Case C and Ko=0.3: (a) at 10 Years; (b) at 100 Years. (Dimensions are in Meters, Displacements in Meters)

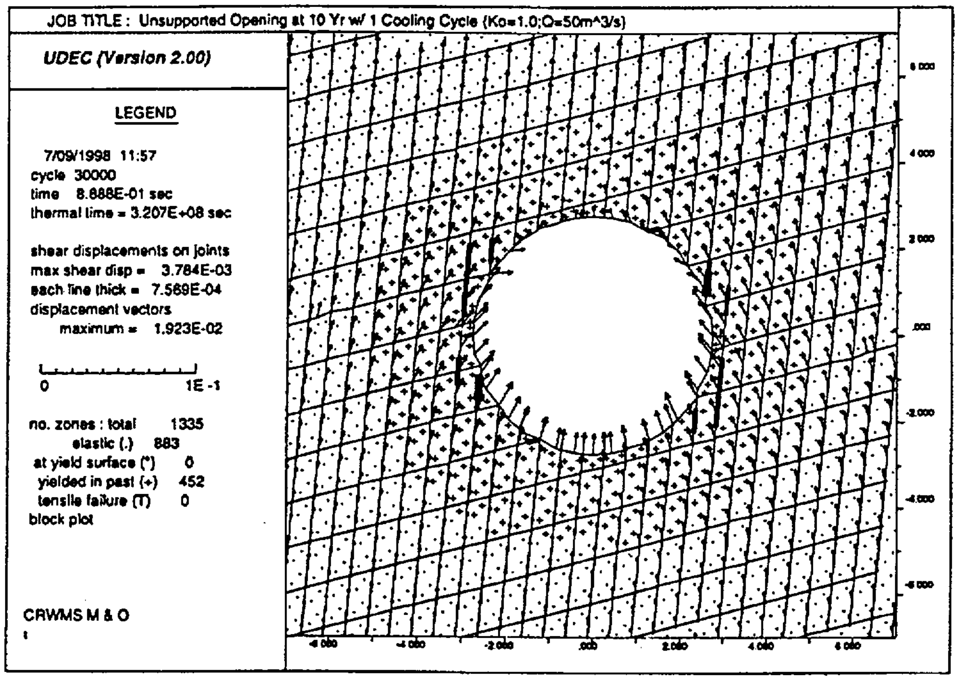

(a)

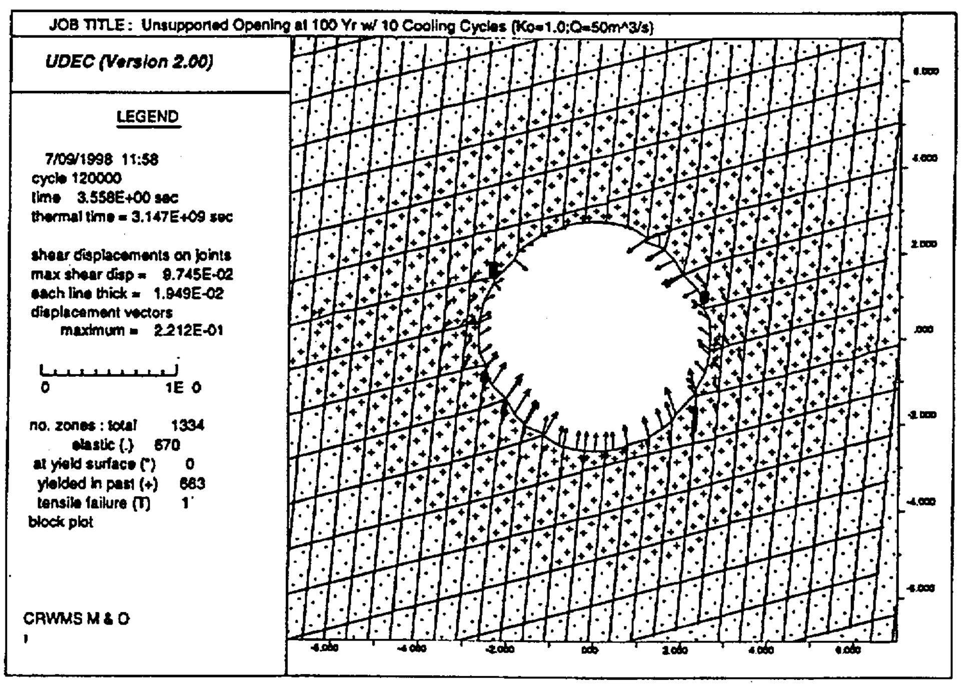

(b)

Figure 7-21 Rock Block Displacements and Potential Rock Yield around an Emplacement Drift for Case C and Ko=1.0: (a) at 10 Years; (b) at 100 Years. (Dimensions are in Meters, Displacements in Meters)

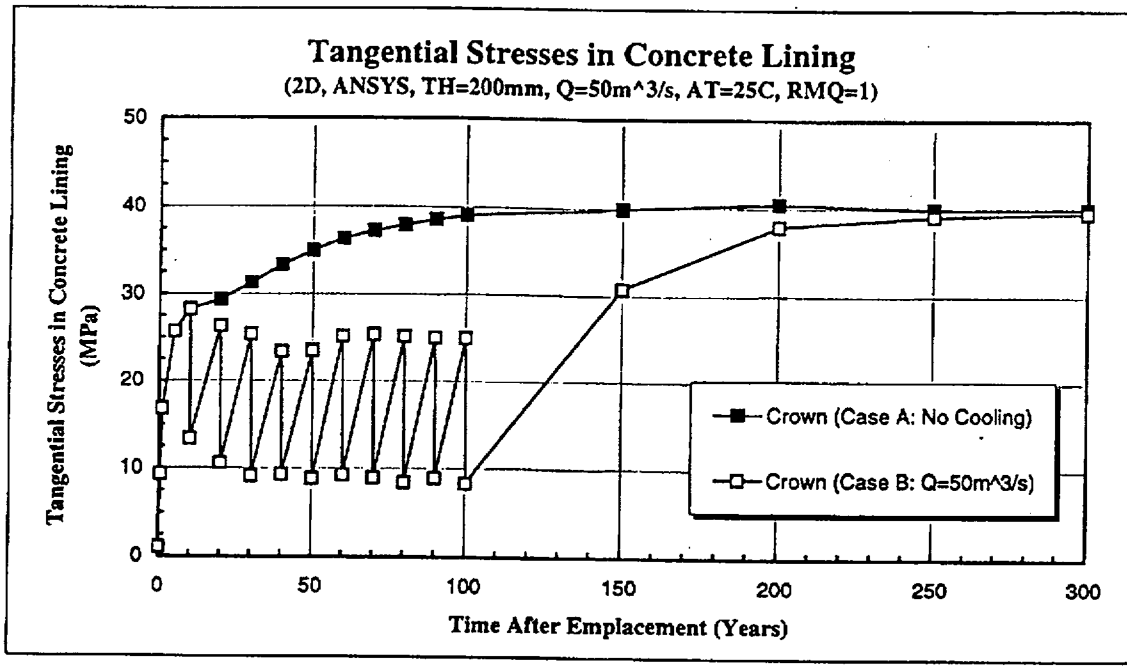

(a)

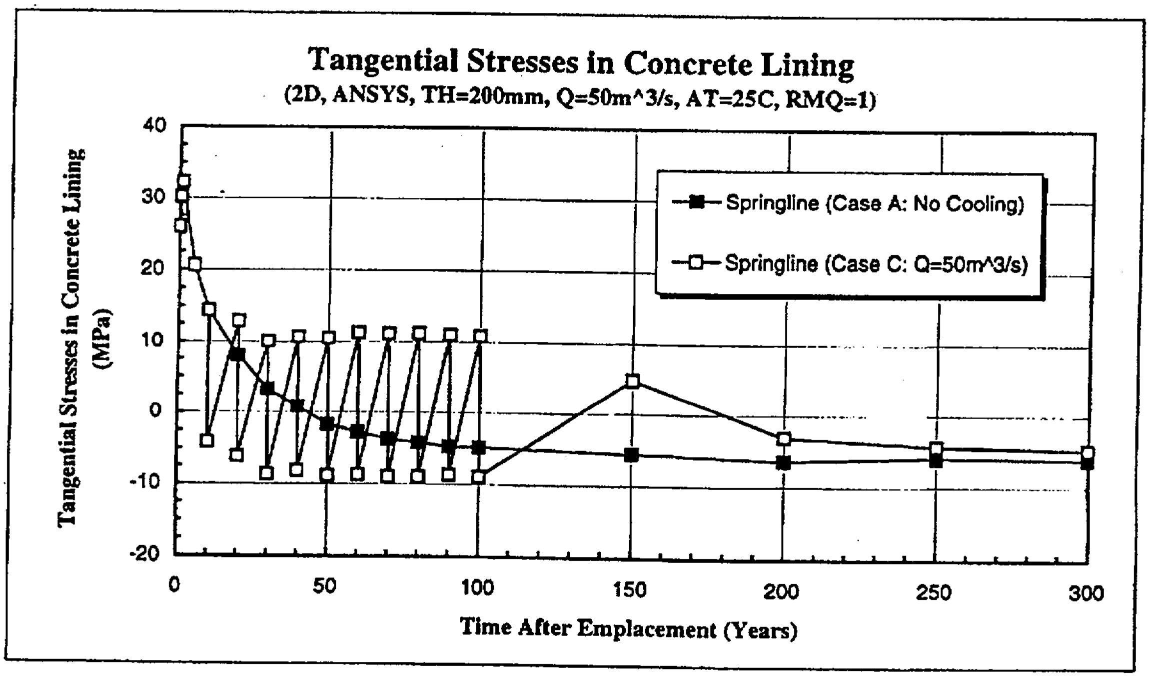

(b)

Figure 7-22 Tangential Stresses in Concrete Lining for Cases A and C and RMQ=1: (a) at Crown; (b) at Springline. (Note: Compression Is Positive. TH=Thickness, Q=Air Quantity, AT=Air Temperature, RMQ=Rock Mass Quality Category)

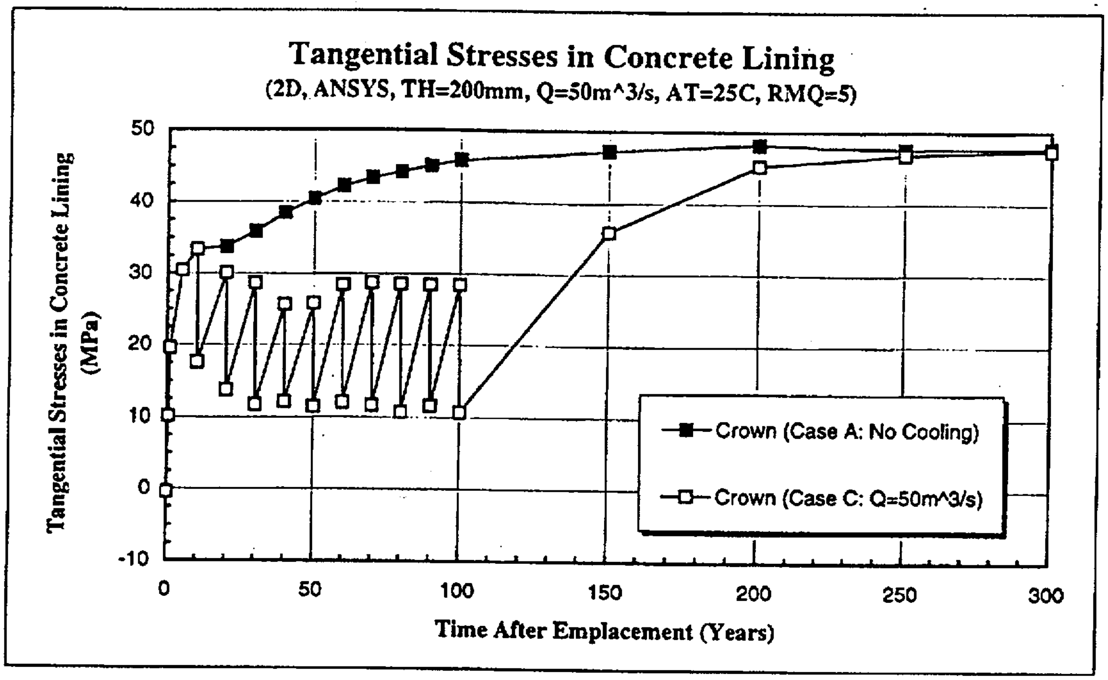

(a)

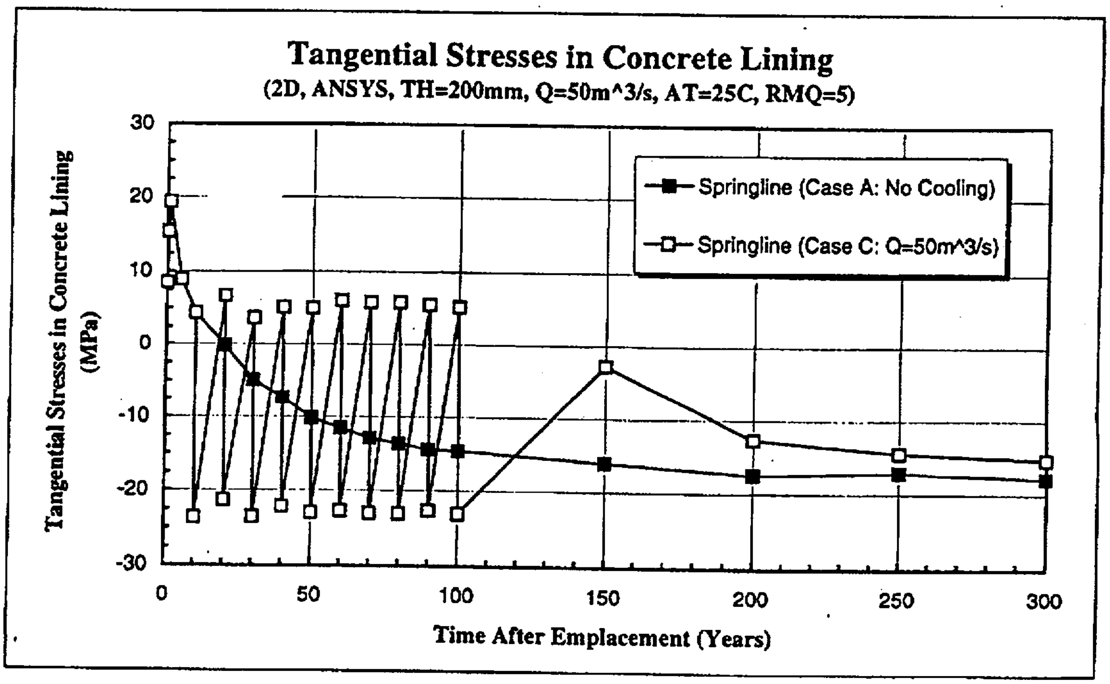

(b)

Figure 7-23 Tangential Stresses in Concrete Lining for Cases A and C and RMQ=5: (a) at Crown; (b) at Springline. (Note: Compression Is Positive. TH=Thickness, Q=Air Quantity, AT=Air Temperature, RMQ=Rock Mass Quality Category)

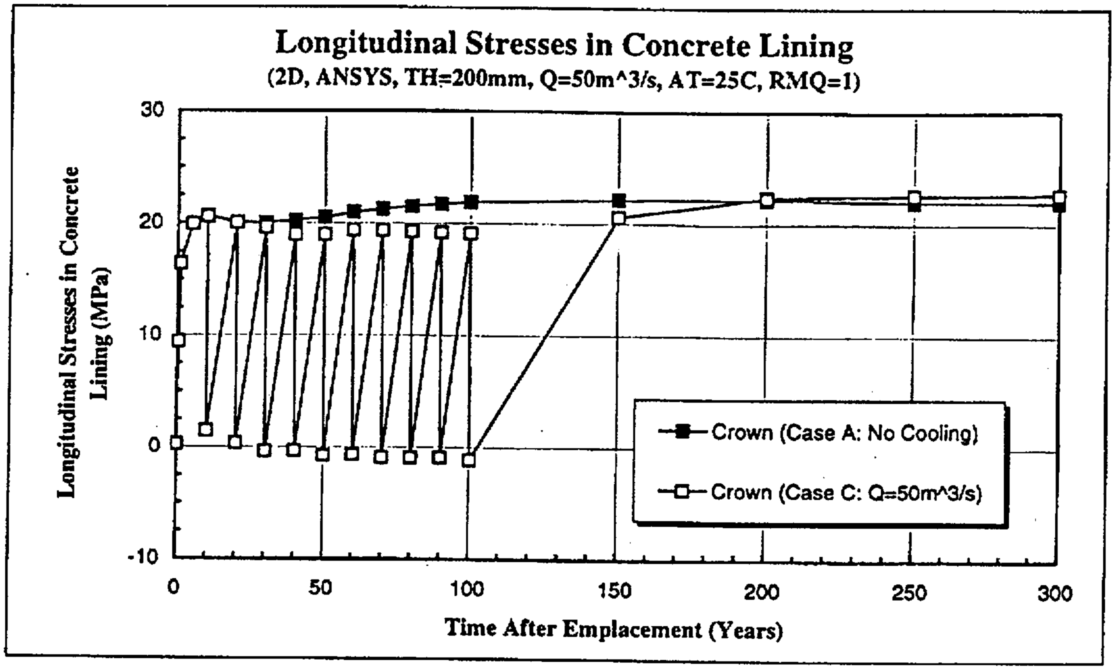

(a)

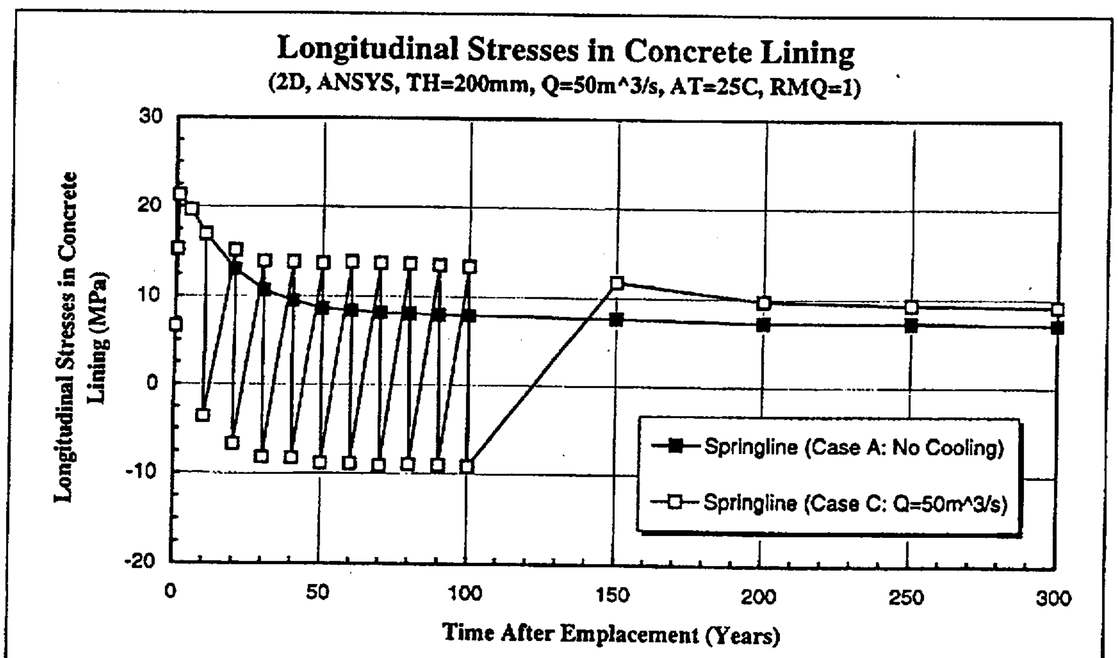

(b)

Figure 7-24 Longitudinal Stresses in Concrete Lining for Cases A and C and RMQ=1: (a) at Crown; (b) at Springline. (Note: Compression Is Positive. TH=Thickness, Q=Air Quantity, AT=Air Temperature, RMQ=Rock Mass Quality Category)

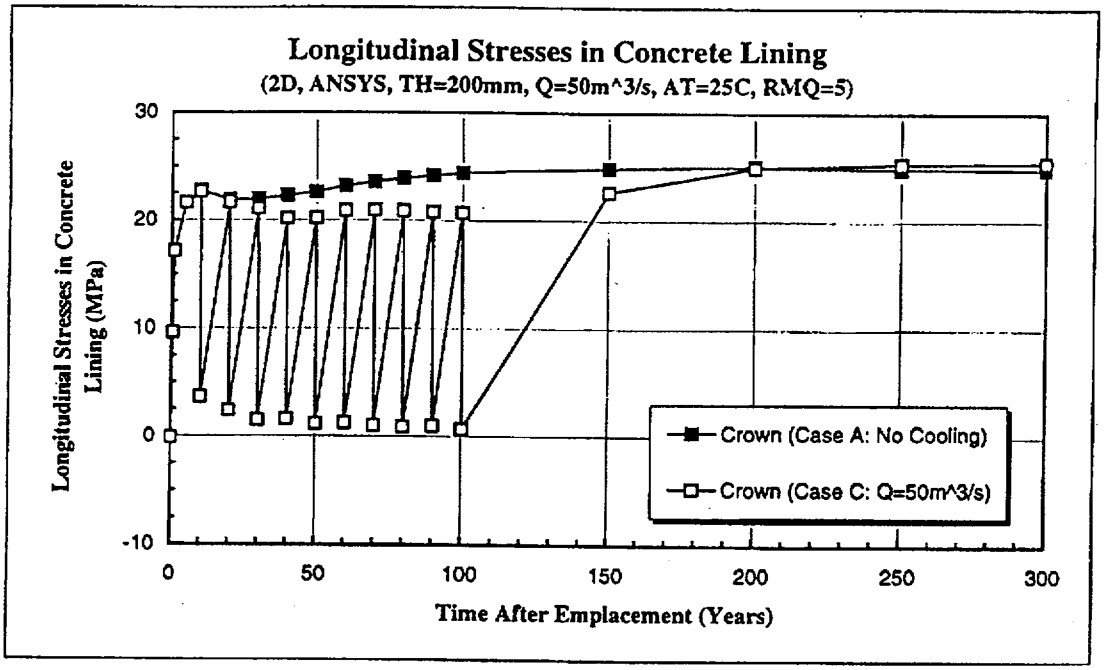

(a)

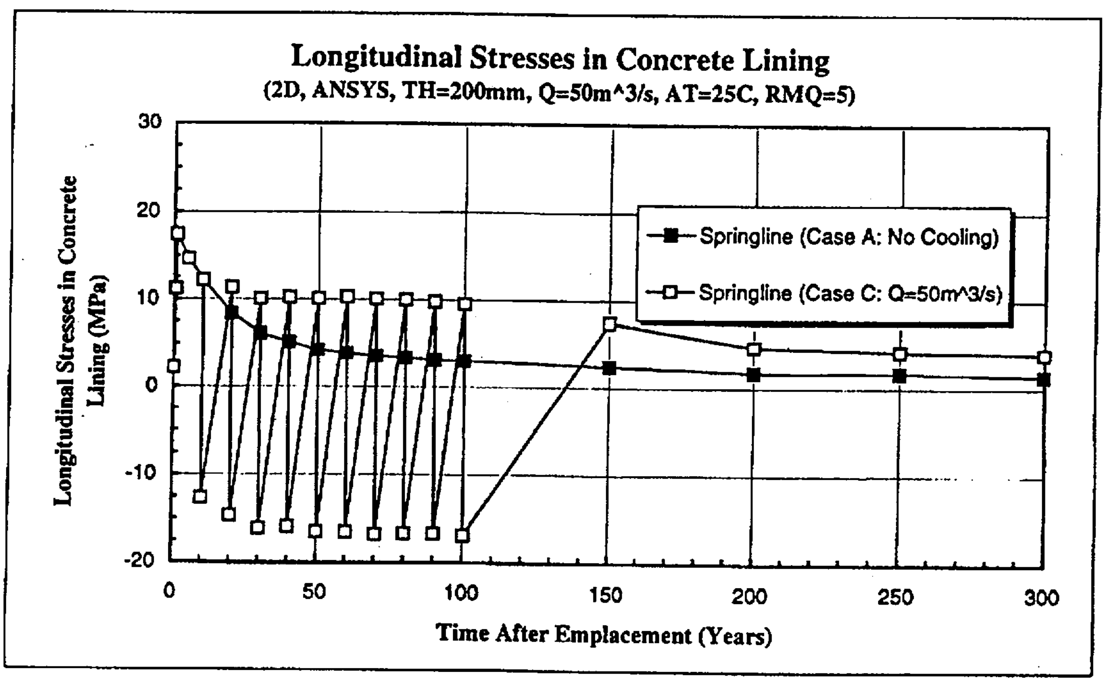

(b)

Figure 7-25 Longitudinal Stresses in Concrete Lining for Cases A and C and RMQ=5: (a) at Crown; (b) at Springline. (Note: Compression Is Positive. TH=Thickness, Q=Air Quantity, AT=Air Temperature, RMQ=Rock Mass Quality Category)

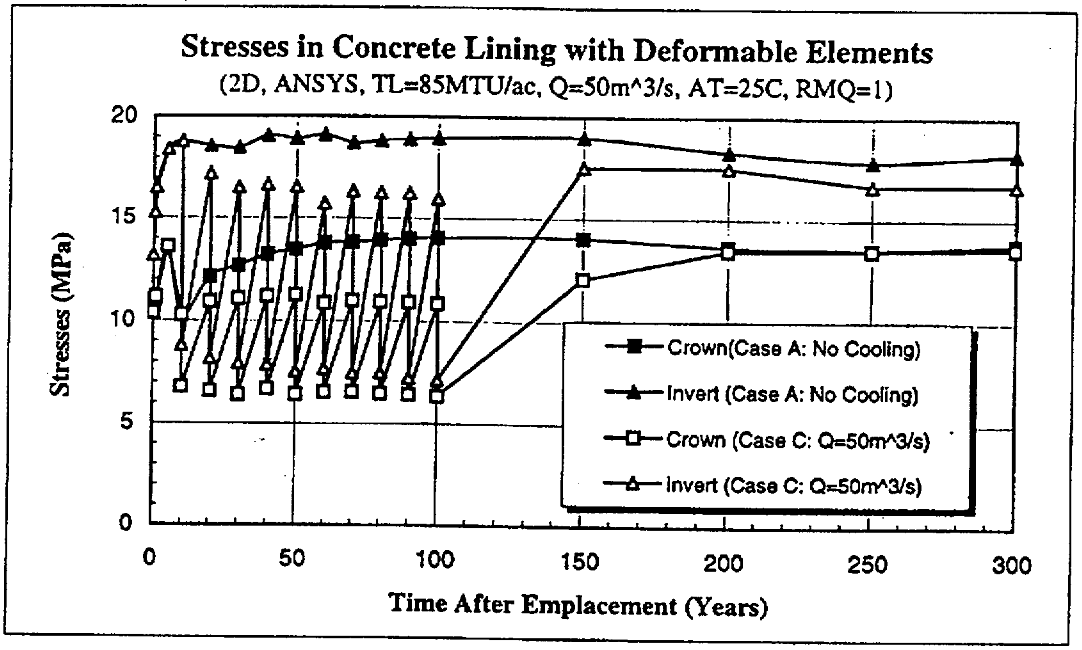

(a)

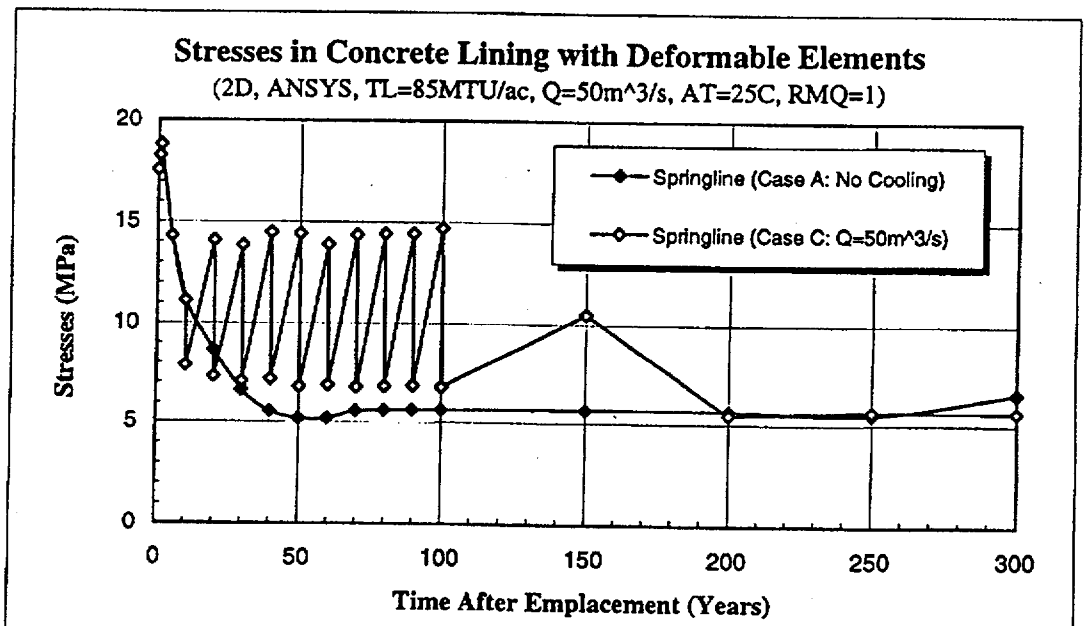

(b)

Figure 7-26 Stresses in Concrete Lining with Deformable Elements for Cases A and C and RMQ=1: (a) at Crown and Invert; (b) at Springline. (Note: Compression Is Positive. TL=Thermal Load, Q=Air Quantity, AT=Air Temperature, RMQ=Rock Mass Quality Category)

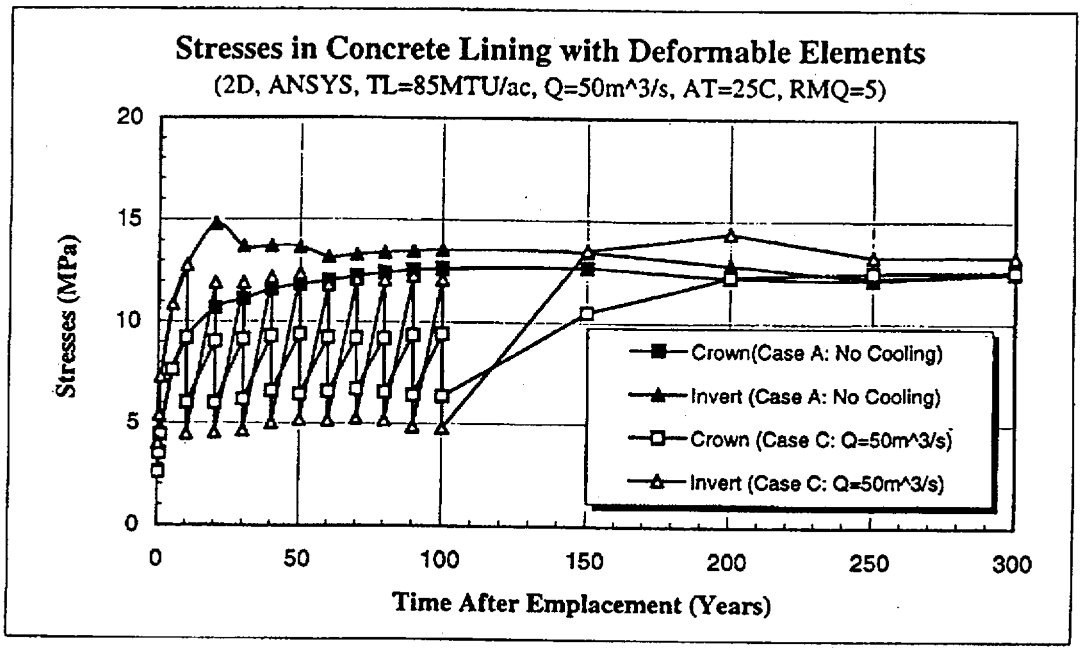

(a)

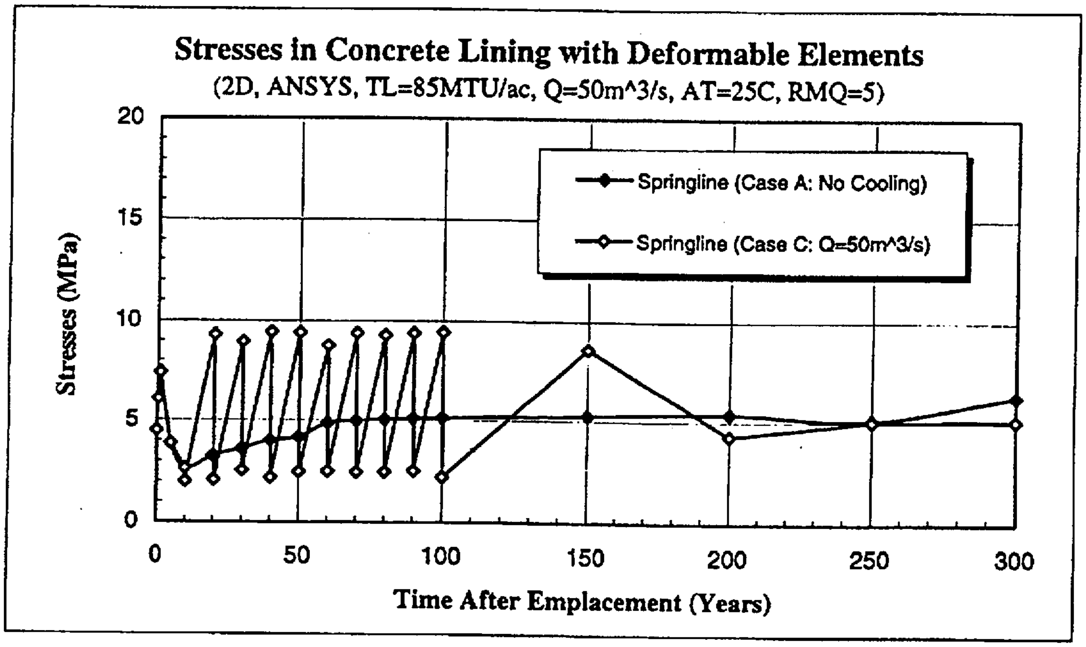

(b)

Figure 7-27 Stresses in Concrete Lining with Deformable Elements for Cases A and C and RMQ=5: (a) at Crown and Invert; (b) at Springline. (Note: Compression Is Positive. TL=Thermal Load, Q=Air Quantity, AT=Air Temperature, RMQ=Rock Mass Quality Category)

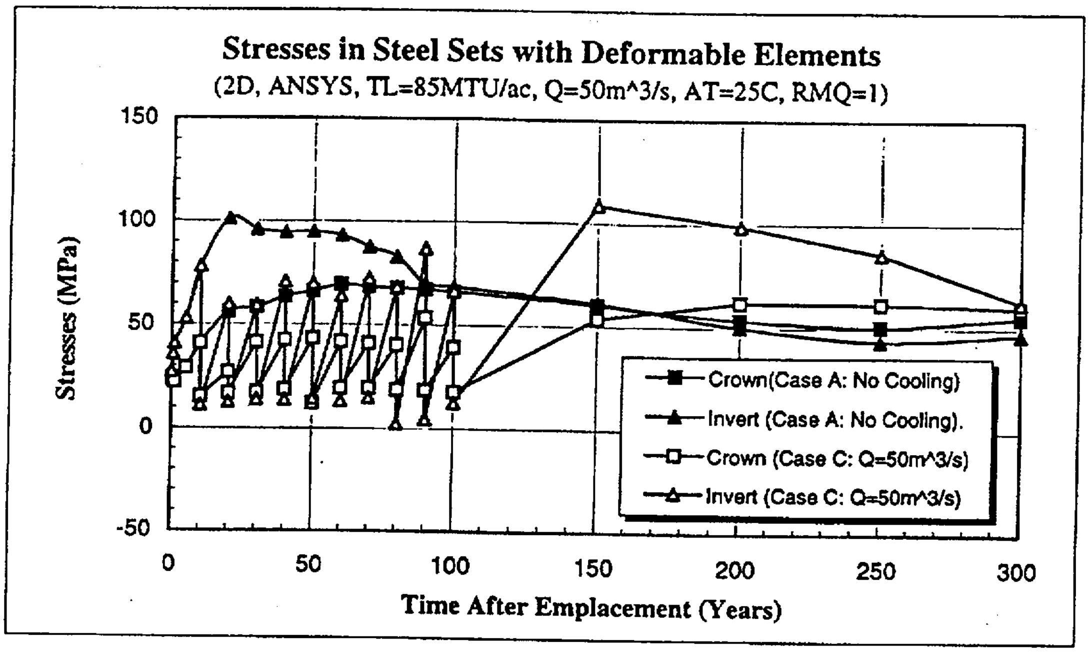

(a)

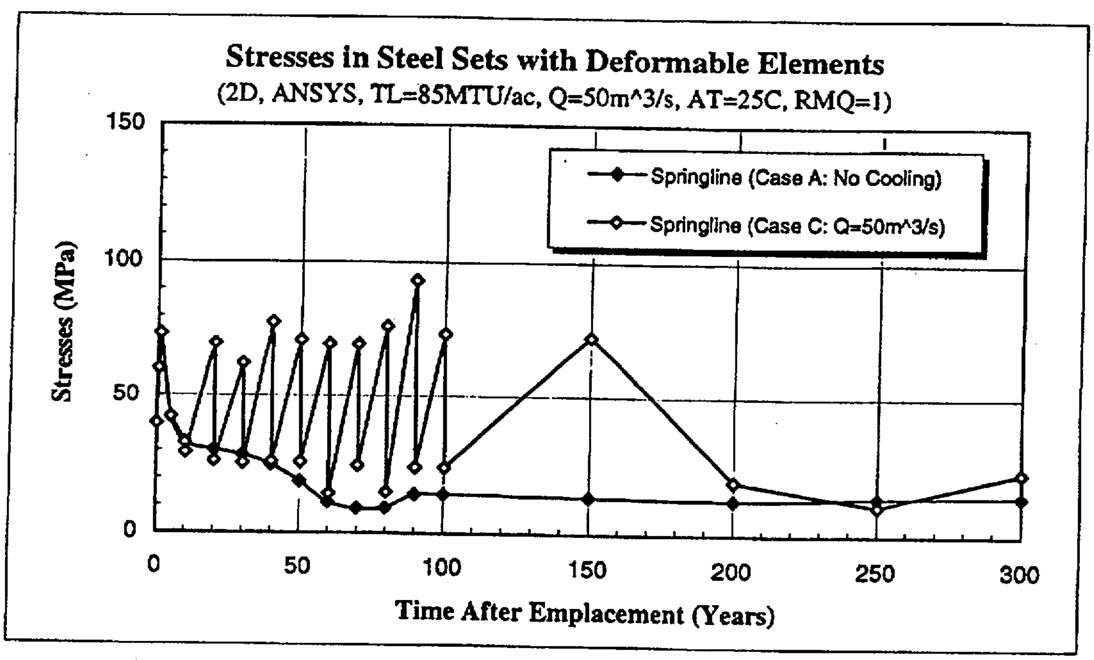

(b)

Figure 7-28 Stresses in Steel Sets with Deformable Elements for Cases A and C and RMQ=1: (a) at Crown and Invert; (b) at Springline. (Note: Compression Is Positive. TL=Thermal Load, Q=Air Quantity, AT=Air Temperature, RMQ=Rock Mass Quality Category)

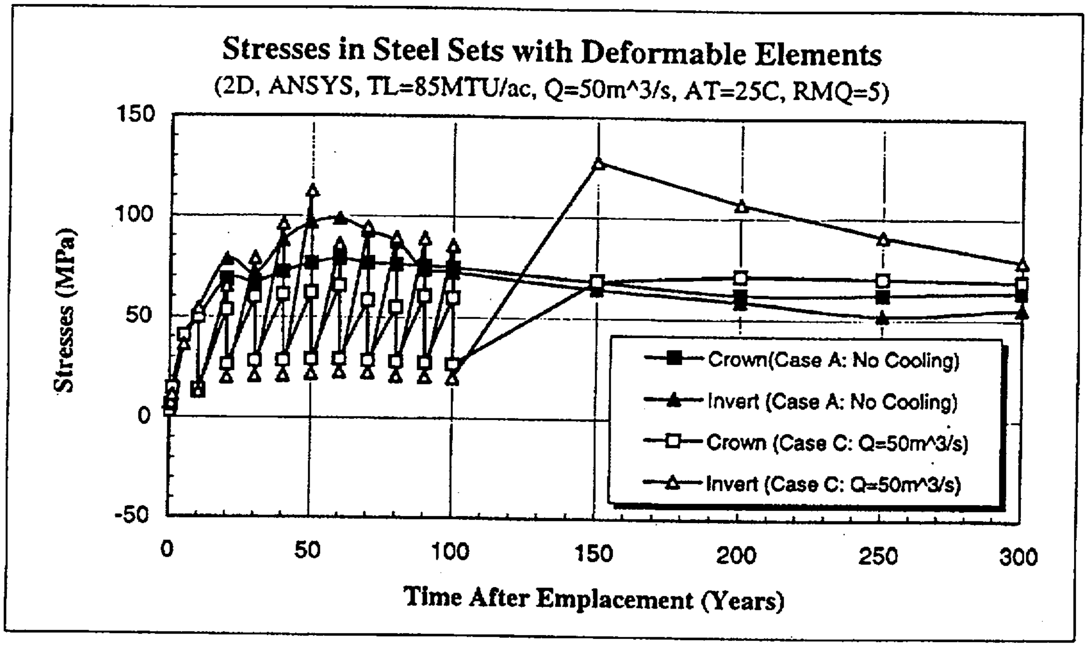

(a)

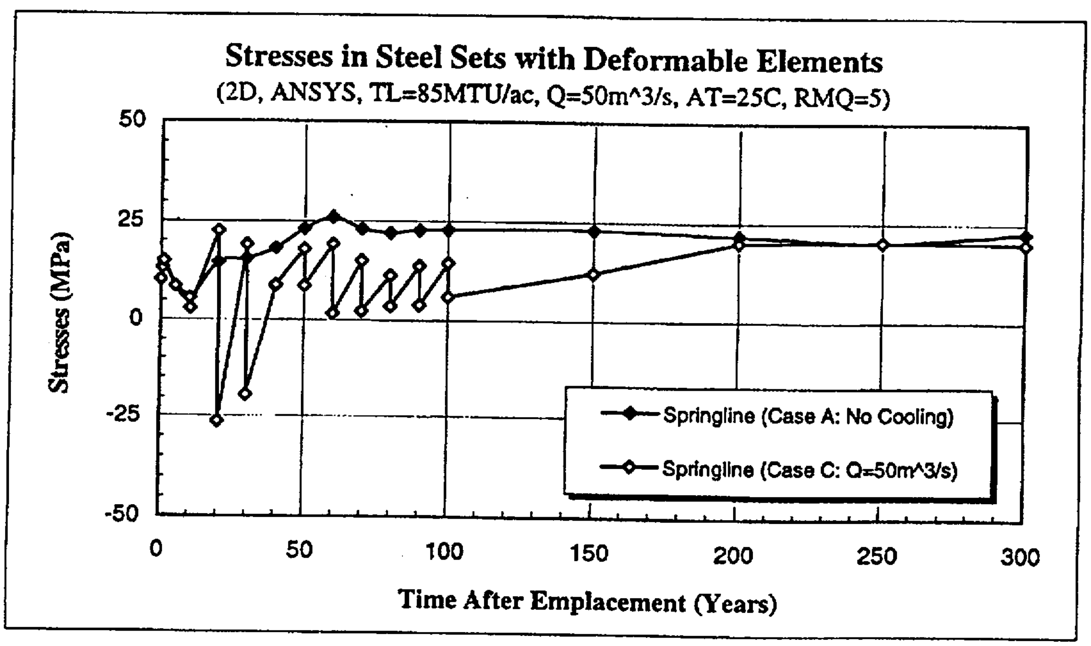

(b)

Figure 7-29 Stresses in Steel Sets with Deformable Elements for Cases A and C and RMQ=5: (a) at Crown and Invert; (b) at Springline. (Note: Compression Is Positive. TL=Thermal Load, Q=Air Quantity, AT=Air Temperature, RMQ=Rock Mass Quality Category)

ATTACHMENT I

CALCULATION OF HEAT OUTPUT DECAY VALUES OF WASTE PACKAGE

I.1 Calculation of Waste Package Spacing

The average waste package spacing is calculated based on the assumed waste stream, as listed in Table I-1 (Reference 5.4, Keys 003 and 004), and 21 PWR packages only.

The average MTU per package is equal to: 37,833.44 ÷ 4,239 = 8.93 MTU/package.

The following values are used in calculation of the average waste package spacings:

Conversion Factor:	1 acre = 4,047 m^2
Drift Spacing:	28.0 m
Thermal Load:	85 MTU/acre
WP MTU per Package:	8.93

The average waste package spacing is equal to:

$$\frac{4047m^2 / acre \times 8.93MTU / package}{85MTU / acre \times 28m} = 15.18m / package$$

I.2 Calculation of Average Waste Package Heat Flux

The heat decay values for the 21 PWR waste packages are obtained from Reference 5.9 (Attachment XXXIX, pp. 1-3). These values are given in a form of heat output per assembly, as listed in Table I-2, Columns B through D. The total number of assemblies of each type of waste packages, identified as $k \leq 1.00$, $k \leq 1.13$, and $k \leq 1.45$, are 30317, 55455, and 2520, respectively (Reference 5.9, Attachment XXXIX, pp. 1-3). The averaged heat output values per waste package at a given time, for example at 0 year, is calculated as follows:

$$Heat\ Output\ per\ WP = (489.13 \times 30317 + 434.28 \times 55455 + 138.32 \times 2520)/4239 = 9.26\ kW$$

Column E of Table I-2 lists the average values of WP heat output for a period of 300 years. The average heat flux of a waste package for a two-dimensional analysis is calculated by assuming that the package has a virtual length of 15.18 meters for the drift spacing of 28 meters, and its heat output smears over the side surface of that length. In addition, to use the *year* as time unit in the analysis, a conversion factor of 3.1536×10^7 sec/year is assumed to convert the units from watts (joules/sec) to joules/year. Column F of Table I-2 provides the average heat flux values over the waste package side surface, and these values are used as inputs to the ANSYS models.

The following values are involved in the calculation:

WP Diameter:	1.664 m
WP Side Surfaces:	$\pi \times 1.664 \times 15.18 = 79.36$ m^2/package
Seconds Per Year:	$365 \times 24 \times 3600 = 3.1536 \times 10^7$ sec/year

Table I-1. Assumed Waste Stream for 21 PWR Packages (Reference 5.4, Keys 003 and 004).

A	B	C	D	E	F	G	H=B*E+C*F+D*G
Time (year)	No. of Packages LG-WP 21 PWR K<=1.00	No. of Packages LG-WP 21 PWR K<=1.13	No. of Packages LG-WP 21 PWR K<=1.45	Ave. MTU/Package LG-WP 21 PWR K<=1.00	Ave. MTU/Package LG-WP 21 PWR K<=1.13	Ave. MTU/Package LG-WP 21 PWR K<=1.45	Average MTU for All 21 PWR Packages
2010	3	17	1	8.99	8.89	0.90	179.00
2011	4	27	5	9.02	8.78	8.89	317.59
2012	19	56	0	9.01	9.06	0.00	678.55
2013	29	94	9	9.15	9.02	8.65	1191.08
2014	45	150	7	8.71	9.12	7.27	1810.84
2015	50	155	1	8.96	9.02	2.54	1848.64
2016	57	131	3	9.03	9.08	5.34	1720.21
2017	43	152	3	9.06	9.08	8.00	1793.74
2018	52	133	4	9.01	9.02	8.01	1700.22
2019	49	139	7	9.04	9.10	7.72	1761.90
2020	51	138	5	9.00	8.99	8.31	1741.17
2021	62	128	3	8.99	9.06	7.01	1738.09
2022	61	131	3	9.04	9.08	8.75	1767.17
2023	59	133	12	9.03	9.01	8.85	1837.30
2024	63	118	15	9.14	9.06	8.51	1772.55
2025	58	117	4	8.83	9.08	8.84	1609.86
2026	77	94	20	8.28	8.77	6.14	1584.74
2027	114	83	7	8.68	8.78	7.20	1768.66
2028	92	109	2	8.94	8.92	4.81	1804.38
2029	89	120	3	9.02	9.01	5.96	1901.86
2030	88	129	5	8.83	8.92	5.79	1956.67
2031	112	118	3	9.04	8.94	7.52	2089.96
2032	105	118	7	8.89	8.97	6.27	2035.80
2033	72	63	3	8.92	8.91	6.63	1223.46
Total	1454	2653	132				37833.44

Table I-2. Heat Flux Values for 21 PWR Waste Packages.

A	B	C	D	E=(B*30317+C*55455+D*2520)/4239	F
Time (year)	Heat Decay Values (W/assembly)			Average Heat Output (W/package)	Average Heat Output (J/yr/m^2)
	k<=1.00	k<=1.13	k<=1.45	4239 Packages	
	30317 Assemblies	55455 Assemblies	2520 Assemblies		
	(Reference 5.9, Attachment XXXIX, pp. 1-3)				
0	489.13	434.28	138.32	9261.74	3.68E+09
1	478.42	421.61	135.29	9017.59	3.58E+09
5	442.08	384.36	125.04	8264.29	3.28E+09
10	404.24	349.27	114.37	7528.27	2.99E+09
20	343.09	294.93	97.02	6369.73	2.53E+09
30	295.20	252.66	83.27	5466.07	2.17E+09
40	257.14	219.41	72.29	4752.36	1.89E+09
50	226.51	192.36	63.47	4174.19	1.66E+09
60	201.78	170.67	56.38	3709.35	1.47E+09
70	181.78	153.07	50.63	3332.65	1.32E+09
80	165.26	138.64	46.00	3022.97	1.20E+09
90	151.72	126.98	42.24	2771.36	1.10E+09
100	140.39	117.08	39.17	2559.00	1.02E+09
150	105.93	87.72	30.27	1923.16	7.64E+08
200	88.03	73.12	26.03	1601.62	6.36E+08
250	77.14	64.39	23.60	1408.09	5.59E+08
300	69.39	58.25	21.81	1271.27	5.05E+08

ATTACHMENT II

CALCULATION OF CONVECTION HEAT TRANSFER COEFFICIENT

Parameters Used in Calculation:

Constant (π):	3.141592654	
Ventilation Air Quantity (Q):	2.5 and 50 m^3/s	(Section 4.3.10)
Drift Inside Diameter (D):	5.1 m	(For drift diameter of 5.5 m and concrete lining thickness of 0.20 m) (Sections 4.3.7 and 4.3.5)
WP Diameter (d):	1.664 m	(Section 4.3.2)
Ventilation Air Temperature (T):	25°C	(Section 4.3.10)

Air Properties Estimated Based on a Temperature of 25°C (298 K) (Reference. 5.3, p. 646):

Density (ρ):	1.1868 kg/m^3	(Section 4.3.10)
Thermal Conductivity (k):	0.02608 W/m·K	(Section 4.3.10)
Dynamic Viscosity (μ):	1.8363×10^{-5} (kg/m·s)	(Section 4.3.10)
Prandtl Number (Pr):	0.709	(Section 4.3.10)

Calculation:

Cross-Sectional Area (A):

$$A = \frac{\pi(D^2 - d^2)}{4} = \frac{3.141592654 \times (5.1^2 - 1.664^2)}{4} = 18.25\,m^2$$

Wetted Perimeter (P):

$$P = \pi(D + d) = 3.141592654 \times (5.1 + 1.664) = 21.25m$$

Hydraulic Diameter (D_h):

$$D_h = \frac{4A}{P} = \frac{4 \times 18.25}{21.25} = 3.44m$$

The additional equations used in calculating the convection heat transfer coefficients listed in Table II-1 are given as follows:

Air Flow Velocity (v): $$v = \frac{Q}{A}$$

Reynolds No. (Re) (Reference 5.3, Basic Heat Transfer Relations, inside front cover):

$$Re = \frac{\rho v D_h}{\mu}$$

Nusselt No. (Nu) (Reference 5.3, Eq. (6-4a), p. 286; n=0.4 for heating, p. 286):

$$Nu = 0.023\, Re^{0.8}\, Pr^{0.4}$$

Convection Heat Transfer Coefficient (h) (Reference 5.3, Eq. (5-107), p. 261):

$$h = \frac{k Nu}{D_h}$$

Table II-1. Calculation of Convection Heat Transfer Coefficients

Parameter	Value	
Air Flow Rate (m^3/s)	2.5	50
Air Flow Velocity (m/s)	0.14	2.74
Reynolds No. (dimensionless)	30414.48*	608289.65*
Nusselt No. (dimensionless)	77.57*	849.72*
Convection Heat Transfer Coefficient ($W/m^2 \cdot K$)	0.59*	6.45*

* Due to rounding these values may vary since interpolations and other calculations are contained within a spreadsheet.

DRAFT DISCLAIMER

Lawrence Livermore National Laboratory

MOL.19980105.0566

LLYMP9707016
July 9, 1997

QA: N

Larry Hayes, Manager
Scientific Program Operations
CRWMS Management & Operations Contractor
1180 Town Center Drive
Las Vegas, NV 89134

ATTN: Terry Grant

SUBJECT: Completion of Level 4 Milestone SP9320M4 (TR3E2FB23)
Thermochemical Analyses of the Drift Scale Test (WBS 1.2.3.14.2)

Enclosed is the subject milestone, which has a due date of 7/9/97. This milestone was designated as a separate milestone ID and Task B from the former SP9318M4 as requested by Mark Peters on 4/21/97.

If you have questions, contact Bill Glassley at (510) 422-6499.

Dale G. Wilder

Dale G. Wilder
TAL for Near Field Environment
Characterization

DGW/BB/bb

Enclosure

xc: R. Datta

THERMO-CHEMICAL ANALYSES OF THE DRIFT SCALE HEATER TEST: MINERALOGICAL AND GEOCHEMICAL CHARACTERICS

William Glassley
Lawrence Livermore National Laboratory

Level 4 Milestone SP9320M4
WBS 1.2.3.14.2
Summary Account TR3E2FB23

Executive Summary

Reactive transport simulations were conducted of the heating phase of the drift scale heater test. The purpose of the simulations was to determine where, and to what extent, mineralogical changes would occur in response to movement of condensate water, and how the chemical composition of the water would evolve through time. The simulations were conducted using the temperature and flow fields generated using the NUFT code simulations of the thermo-hydrological evolution of the rock surrounding the drift and wing heaters.

Initial simulations indicated that no perceptible changes in mineralogy would occur during the first four years, for those regions within which the temperature did not exceed 40°C. In addition, the region where temperatures exceed 100°C will be regions within which mineralogical changes will be dominated by either mineralogical dehydration, or vapor-phase alteration of existing mineral phases. Hence, the simulations conducted here consider those regions within which temperatures remained between 40°C and 100°C. In the simulations it was assumed that the coexisting gas phase was buffered to a CO_2 pressure of 0.01 bars, consistent with results obtained from the Single Heater Test.

The simulations were conducted for two separate domains (designated Zones 1 and 2). Zone 1 is that region above the heated drift region, that encloses the temperatures of interest, and Zone 2 is the corresponding region below the heated drift. The simulations were conducted in 2-dimensions, along a plan that encompasses the geochemical

boreholes. Thus, the results provide an indication of the chemical changes in condensate water that may be expected during the course of the heating phase of the system, and of the mineralogical evolution that may occur, as well.

The results demonstrate that large variation in water chemistry should be anticipated, with concentrations of individual cations varying by several orders of magnitude within each zone. This strong compositional zoning of the waters reflects the effect that flow path length has on reaction progress; those regions over which flow distances are short generate dilute waters, while solutions in those regions father along the flow path reach saturation in a variety of secondary minerals.

Secondary mineral development is complex, and depends upon spatial location relative to the drift and wing heaters, and upon time. The saturation state of the waters varies, but indicates that precipitation of secondary minerals should be expected above and below the drifts. The extent of precipitation is time-dependent, but will be greatest above the drift.

Counteracting the effects of mineral precipitation is mineral dissolution. This, too, exhibits complex behavior, but is consistently greatest in the immediate vicinity of the boiling front.

During cool down, reversal of the mineralogical sequence development seen during heating, is anticipated. However, nucleation effects and changes in flow pathways and velocities will lead to inhomogeneous development of secondary phases during this period.

Introduction

As described in the report on thermo-hydrological processes anticipated to develop during the course of the Drift Scale Heater Test, a boiling front and region of condensate formation will migrate outward from the heated region. The condensate will form along fractures and be imbibed into the rock, in regions where full saturation has not been achieved, or will migrate along fracture surfaces. In the latter case, water will dissolve pre-existing mineral phases that line fracture surfaces, potentially reaching saturation in a number of potential secondary mineral phases. If saturation occurs, precipitation of those phases may occur, provided kinetic barriers to nucleation do not inhibit the mineral growth process. This report describes the first suite of simulations conducted to determine the time-dependent chemical and mineralogical changes expected to develop during the course of the heating phase of the heater test. The purpose of these simulations was to provide a first prediction of the chemical and mineralogical changes that may be observed at the locations of the geochemistry boreholes.

Method

The temperature distribution, and vertical and horizontal components of the velocity field were obtained from the NUFT thermo-hydrological simulations, for the plane within which the geochemical boreholes 69, 70, 71, 72 and 73 are located, for times of 1, 2, 3, and 4 years after turn on of the heaters. This approach of taking sequential time slices through the flow field was taken because current reactive transport simulators that account for non-ideal solute and solvent behavior, and realistic dissolution and precipitation kinetics, generally do not update thermal and flow fields automatically; code enhancements to accomplish this are planned.

The data were fit to a regular mesh of 1 meter x 1 meter grid blocks. Vertical boundaries of the mesh were located at the access drift (approximately 28 meters from the drift center), and at the approximate outer edge of the outer wing heaters. This geometry provided coverage of those regions intersected by the geochemistry boreholes.

Initial, scoping simulations demonstrated that those regions where temperatures were below 40°C, were regions within which there would be virtually no detectable changes in the mineralogy. In addition, for conditions above boiling, existing reactive transport codes have limited capabilities to model fluid-rock interaction. Hence, domains were selected above (Zone 1) and below (Zone 2) the heated region where temperatures were between 40°C and 100°C, and the simulations were conducted for the flux fields within these regions (see Figures 1, 2 and 3).

The volumetric fluxes (Figure 3), in units of meters^3 of /year, were generated by reformulating the thermo-hydrologically computed vertical and horizontal velocity components using the following relationships:

$$V = Q / (\phi_m(1-\phi_f) + \phi_f),$$

where V is the fluid velocity, Q is the volumetric flux and, ϕ_m and ϕ_f are the matrix and fracture porosity, respectively, per unit rock volume. Generally, ϕ_m is much greater than ϕ_f, thus allowing the simplification that

$$V = Q / \phi_m$$

and

$$V_f = Q / \phi_f ,$$

where V_f is the fracture velocity. For the case where the fracture flux is much greater than the matrix flux, this relationship can be recast as

$$Q_f = ((\phi_m/\phi_f)V_z)*(1.48219e10 \text{ secs/year}),$$

where Q_f is the volumetric fracture flux, per unit cross sectional area (meter^2 of cross-sectional area), and V_z is the velocity component in the x or z direction.

The calculations were conducted assuming that the instantaneous flow field and temperature field obtained from the thermo-hydrological modeling, at each selected time, represented a reasonable approximation for the time-averaged flow and temperature fields for the preceding year. This approximation can over-estimate the extent of reaction at each grid block, since it assumes that each grid block experiences the defined temperature and flow field for 12 months. In reality, each location represented by the grid blocks will see a progressive change in conditions for the duration of the DST. To evaluate the extent to which this approach would provide misleading results, simulations for each year were conducted assuming that the conditions persisted for 0.1 years, 1, 2, 3, and 4 years, and the results compared. The results of these comparisons are described below.

For each year for which simulations were conducted, the initial mineralogy was the same. This approach allows the specific effects due to the evolution of the physical parameters (temperature and flow fields) to be determined. Future simulations will consider the effects of mineralogical changes that occur due to heat and fluid transfer during preceding years.

The initial mineralogy was assumed to be that which appears to be responsible for development of the compositional characteristics of water collected from Hole 16 of the Single Heater Test (Glassley and DeLoach, 1997). The mineralogy was that typical of fractures (calcite, cristobalite, kaolinite [a proxy for complex smectite/illite clays]), but also allowing for minor interaction with the Tsw2 matrix (albite and K-feldspar [proxies for alkali feldspar], quartz and cristobalite).

Particular attention was focused on the concentrations of those solutes that usually account for ca 90% of the total dissolved solids normally encountered in waters in fractures and in the saturated zone at Yucca Mountain (i.e., Ca^{++}, Na^{+}, K^{+}, SiO_2, Al^{+++}, and HCO_3^{-}), and on those mineral phases that either compose the rock (i.e., cristobalite, quartz, K-feldspar, albite, calcite) or which may reasonably be expected to occur as secondary minerals during reaction progress for the period of time the test is ongoing (i.e., chalcedony, kaolinite, diaspore, stilbite). Porosity changes, pH, and the concentrations of other solute species were also considered in the calculations.

The code used in the simulations was GIMRT (Steefel and Yabusaki, 1995), which allows direct monitoring of changes in porosity, solution composition, and dissolution or precipitation of mineral phases, as a function of temperature, pressure, fluid flux, input solution chemistry, reaction kinetics, and system geometry.

Initial water chemistry was assumed to be that of condensate in equilibrium with 0.01 bars of CO_2. Condensate was modeled as containing 1.0e-10 moles of each basis species, at a pH of 6.85 and HCO_3^{-} molality of 7.11e-6.

Mineralogical development during cool down was initially simulated in thermal fields in which temperatures decreased along the flow pathway. However, it was quickly evident that such simulations will not represent the effects of cool down, since experience has shown that nucleation effects dominate mineral development during rapid tempernature drops, as expected in the DST. As a result, we anticipate that the mineralogical sequence developed during progressive heating will be reversed, but the extent of mineralogical development will be small, and supersaturated fluids will develop.

Results

Comparison of pH distribution (Figure 4) at 0.1 and 1.0 years in Zone 1 shows that there is very little difference in the absolute values of pH over this time period. Since dissolution and precipitation of the solid minerals is modeled as a series of simultaneous hydrolysis reactions, the similarities between the pH distributions in these two time periods is mimicked by the cation and ion distribution of other species. Hence, it was decided to conduct simulations for 1 year duration, at the time periods considered. These results will then provide a conservative indication of the solution chemistries that may be encountered in the geochemistry holes. Conservative is used in this context as being a result that overestimates the extent of mineral dissolution and/or precipitation.

Simulations conducted for all time periods showed that the chemical and mineralogical changes were smoothly continuous for the duration of the heating period. Hence, only the results for the first and fourth years are presented, as they provide a thorough description of the effects to be expected in the evolution of the geochemical and mineralogical system. As the evolution is different between Zones 1 and 2, the characteristics of these zones will be discussed separately.

Zone 1

In general, the changes in solution chemistry and mineral distributions directly reflect the flux vectors. The greatest vertical fluxes of heated water occur immediately above the central drift, and to a lesser extent immediately over the wing heaters. Within these areas dissolution of primary minerals is the greatest. Since this is an area within which the path length is relatively short, it is also the region in which the concentrations of dissolved species are consistently the lowest (see Figures 5, a-d, and 6, a-d).

During the first year of heating, all dissolved basis species exhibit a ridge of maximum concentration within the upper half of Zone 1. This phenomenon reflects the fact that the solution achieves saturation in calcite, kaolinite and stilbite by this point along the flow path. For all of the species, solution composition varies by several orders of magnitude along the flow path, which is a sufficiently large contrast to allow detection by the analytical methods expected to be used in analysis of collected fluids.

During the fourth year, the solute distribution patterns are more complex, although the general tendency toward more dilute concentrations nearest the heaters persists. Ca^{++} maintains a broad compositional ridge in the middle portion of Zone 1, while K^+ and SiO_2 (aqueous) develop smoothly increasing concentration profiles away from the heaters. Na^+ develops regions of very low concentration over the wing heaters in the middle distance within the zone, which punctuate the otherwise regular increase in Na^+ away from the heaters.

The saturation state of the mineral phases is indicated by the saturation index, which is defined as the log of the ratio of the ion activity product (Q) of the respective hydrolysis reaction to the equilibrium constant (K) of the hydrolysis reaction (i.e., log[Q/K]). Values of the saturation index that are greater than zero indicate that the solution is supersaturated in the mineral phase, while values less than zero are undersaturated. Because of uncertainty associated with thermodynamic parameters used in the calculations, it is generally considered that saturation indices within 0.1 log units of zero indicate an equilibrium or saturated conditioned.

Consideration of the saturation indices for the first year of heating (Figure 7, a-f) indicate that the solution becomes saturated to supersaturated in calcite, kaolinite and stilbite in some regions within zone 1, and is consistently undersaturated in quartz, potassium feldspar and albite throughout zone 1. By the fourth year (Figure 8, a-f), most of the area within zone 1 is saturated or supersaturated with respect calcite, K-feldspar, quartz and stilbite, but remains undersaturated in albite. Kaolinite is generally undersaturated throughout the zone, with the exception of a central ridge running through the zone where the water is nearly saturated in kaolinite.

For all time periods considered, there is a net porosity increase at the base of the boiling zone, changing from an initial 2.75% to approximately 3.2-3.4%. From this maximum porosity, there is a steady and smooth decrease in absolute porosity, moving outward toward cooler regions. Nevertheless, during the first year, the porosity remains above that of the initial state for the entire area of Zone 1. However, by the fourth year, there is sufficient development of secondary mineral phases in the coolest regions of the zone, to result in a net decrease in porosity below that of the initial state, down to approximately 2.6%.

Zone 2

As in Zone 1, the changes in solution chemistry and mineral distributions correspond to the flux vectors. Immediately below the central drift, and to an even greater extent immediately below the wing heaters, large downward fluxes develop . As observed in Zone 1, these are areas where dissolution of primary minerals is the greatest because the condensate flow path lengths are relatively short and the concentrations of dissolved species are consistently the lowest (see Figures 9, a-d, and 10, a-d).

As a result, all dissolved basis species exhibit an increase in concentration with distance away from the heated region. By the fourth year, this pattern is strongly influenced by the high fluxes immediately below the wing heaters, which results in an apparent bulge in the concentration contours in the lower middle portion of the zone. For all of the species, solution composition varies by several orders of magnitude along the flow path, which is a sufficiently large contrast to allow detection by the analytical methods expected to be used in analysis of collected fluids.

Consideration of the saturation indices for the first year of heating (Figure 11, a-f) indicate that the solution becomes saturated to supersaturated only in kaolinite and stilbite in lower and central regions, respectively, within zone 2, and is consistently undersaturated in quartz, potassium feldspar and albite throughout zone 2. By the fourth year (Figure 12, a-f), calcite saturation is achieved within the central region of Zone 2, directly below the central drift, as with kaolinite and stilbite. The zone remains undersaturated in albite and K-feldspar.

As in Zone 1, there is a net porosity increase at the edge of the boiling zone, changing from an initial 2.75% to approximately 3.4%. From this maximum porosity, there is a steady and smooth decrease in absolute porosity, moving outward toward cooler regions. However, unlike Zone 1, there is no region within the zone area where the porosity decreases below initial values.

Discussion and Conclusion

These results indicate that significant changes in solution composition can be expected and detected during the course of the heating period of the Drift Scale Heater Test. These changes are expected to evolve as a function of time and location with respect to the wing heaters and central drift. It is clear by comparing the results from the different time intervals, that the duration of the experiment must be a minimum of 4 years, in order for the changes to occur along fracture surfaces in a manner that will allow thorough characterization of dissolution and precipitation effects.

These preliminary results suggest that mineralogical changes may be of such magnitude as to result in detectable modification of fracture apertures. Both above and below the drift, a complex history of mineral dissolution and precipitation can be expected. Above the heated region, calcite can be expected to precipitate, along with clay and zeolite. However, the progressive changes in the thermal and flow regimes will cause early precipitated phases to experience later dissolution in some areas, and reprecipitation at later times in other areas. Below the heated region, similar effects are expected, but the geometry is not a mirror image of that above the heaters. Instead, because of the thermal load placed on the system by the wing heaters, mineral precipitation may be concentrated immediately below the central drift. Under most conditions within the studied zones, the primary alkali feldspar components are undersaturated, and are expected to exhibit dissolution effects. Calcite, however, which is the dominant fracture lining mineral, will record a complex history of dissolution and precipitation.

During cool down, collapse of the rehydration front is slow, relative to the thermal field evolution. As a result mineralogical changes will be concentrated in an environment within which temperatures are falling, and fluid velocities are dropping. Consequently, it is theoretically possible that changes in mineralogy during the cool down phase will represent reversal of the reactions that progressed during the heat-up phase. However, experience has shown that nucleation of secondary phases during cool down of experimental systems does not usually follow an equilibrium pathway. This primarily reflects the difficulty of overcoming nucleation energy barriers. As a result, as a first approximation, it is expected that the mineralogical sequence that developed during heat up will be reversed during cool down, but the extent of recrystallization will be insufficient to eliminate the secondary phases formed during heating. In addition, because the flow fields will evolve differently during cool down, it is anticipated that nucleation effects will cause "spotty" distribution of the secondary phase development during cool down.

If these results are supported by later simulations that address the limitations described in the section on "Methods", it may be anticipated that regions above and below the drift will experience significant changes in porosity. These changes may be detectable using a variety of remote sensing techniques, and should be considered in future discussions concerning *in situ* measurements.

References

Glassley, W.E., and Laura DeLoach, 1997, Second Quarter Results of Chemical Measurements in the Single Heater Test. Milestone SP9240M4, Yucca Mountain Project, Lawrence Livermore National Laboratory, Livermore, CA.

Steefel, C.I. and Yabusaki, S.B., 1995. OS3D/GIMRT: Software for modeling multicomponent-multidimensional reactive transport. Pacific Northwest Laboratory, Richland, Washington.

Figure Captions

ıocations of the geochemistry holes and the modeled regions (Zones 1 .. Zone 1 of the 1st and 4th year of heating are shown in blue and red, ,pectively, above the region of the heaters (located at approximately -250 meters). Zone 2 of the 1st and 4th years of heating are shown in blue and red, respectively, below the region of heating. The origin for the horizontal and distance scales are the same as used inteh thermo-hydrological modeling of the DST.

Figure 2, a, b : The temperature fields for years 1 and 4. The color scales are the same for both years. The horizontal and vertical distances are based on the same zero coordinates as those used in the thermo-hydrological models.

Figure 3, a, b : Flux vectors, at 1 and 4 years. Fluxes are in units of m^3 of fluid/m^2 of cross sectional area/year. The coordinate system is the same as that used in Fig. 2.

Figure 4, a,b : pH in Zone 1 at 0.1 and 1.0 years. See Fig. 1 for the location of the figure origin.

Figure 5, a-d: Distribution of Ca^{++}, K^+, Na^+, and SiO_2 (aqueous) aqueous species in Zone 1 during the first year of heating.

Figure 6, a-d: Distribution of Ca^{++}, K^+, Na^+, and SiO_2 (aqueous) aqueous species in Zone 1 during the fourth year of heating.

Figure 7, a-f : Saturation index (log Q/K) for the minerals albite, calcite, kaolinite, K-feldspar, quartz, and stilbite, in Zone 1, during the first year of heating.

Figure 8, a-f: Saturation index (log Q/K) for the minerals albite, calcite, kaolinite, K-feldspar, quartz, and stilbite, in Zone 1, during the fourth year of heating.

Figure 9, a-d: Distribution of Ca^{++}, K^+, Na^+, and SiO_2 (aqueous) aqueous species in Zone 2 during the first year of heating.

Figure Captions

Figure 1: Respective locations of the geochemistry holes and the modeled regions (Zones 1 and 2). Zone 1 of the 1st and 4th year of heating are shown in blue and red, respectively, above the region of the heaters (located at approximately -250 meters). Zone 2 of the 1st and 4th years of heating are shown in blue and red, respectively, below the region of heating. The origin for the horizontal and distance scales are the same as used inteh thermo-hydrological modeling of the DST.

Figure 2, a, b : The temperature fields for years 1 and 4. The color scales are the same for both years. The horizontal and vertical distances are based on the same zero coordinates as those used in the thermo-hydrological models.

Figure 3, a, b : Flux vectors, at 1 and 4 years. Fluxes are in units of m^3 of fluid/m^2 of cross sectional area/year. The coordinate system is the same as that used in Fig. 2.

Figure 4, a,b : pH in Zone 1 at 0.1 and 1.0 years. See Fig. 1 for the location of the figure origin.

Figure 5, a-d: Distribution of Ca^{++}, K^+, Na^+, and SiO_2 (aqueous) aqueous species in Zone 1 during the first year of heating.

Figure 6, a-d: Distribution of Ca^{++}, K^+, Na^+, and SiO_2 (aqueous) aqueous species in Zone 1 during the fourth year of heating.

Figure 7, a-f : Saturation index (log Q/K) for the minerals albite, calcite, kaolinite, K-feldspar, quartz, and stilbite, in Zone 1, during the first year of heating.

Figure 8, a-f: Saturation index (log Q/K) for the minerals albite, calcite, kaolinite, K-feldspar, quartz, and stilbite, in Zone 1, during the fourth year of heating.

Figure 9, a-d: Distribution of Ca^{++}, K^+, Na^+, and SiO_2 (aqueous) aqueous species in Zone 2 during the first year of heating.

Figure 10, a-d: Distribution of Ca^{++}, K^{+}, Na^{+}, and SiO_2 (aqueous) aqueous species in Zone 2 during the fourth year of heating.

Figure 11, a-f : Saturation index (log Q/K) for the minerals albite, calcite, kaolinite, K-feldspar, quartz, and stilbite, in Zone 2, during the first year of heating.

Figure 12, a-f: Saturation index (log Q/K) for the minerals albite, calcite, kaolinite, K-feldspar, quartz, and stilbite, in Zone 2, during the fourth year of heating.

LOCATIONS OF BOREHOLES AND STUDIED ZONES

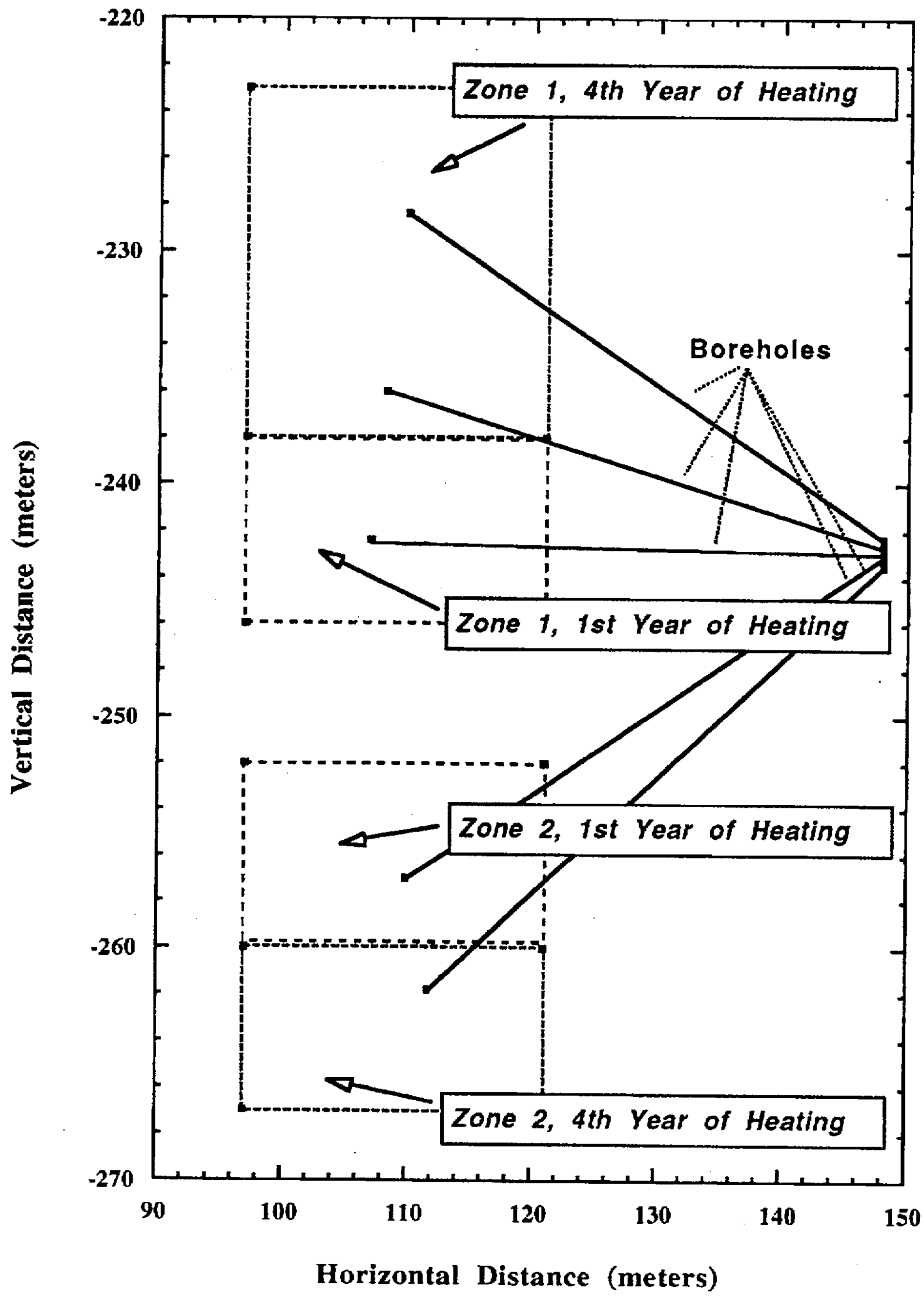

Fig. 1

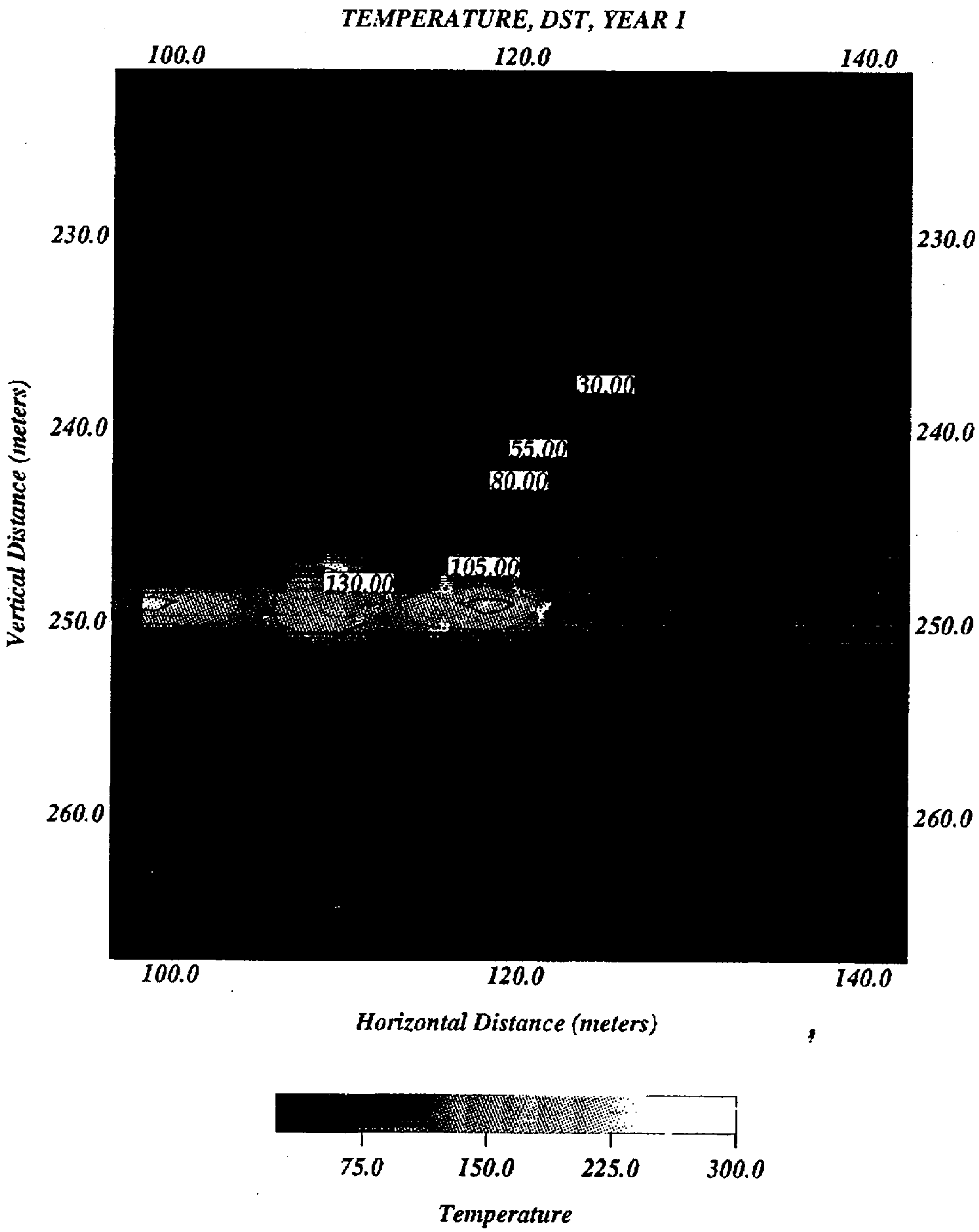
TEMPERATURE, DST, YEAR 1
100.0
120.0
140.0
230.0
240.0
250.0
260.0
30.00
55.00
80.00
105.00
130.00
Vertical Distance (meters)
Horizontal Distance (meters)
75.0
150.0
225.0
300.0
Temperature

Figure 2a

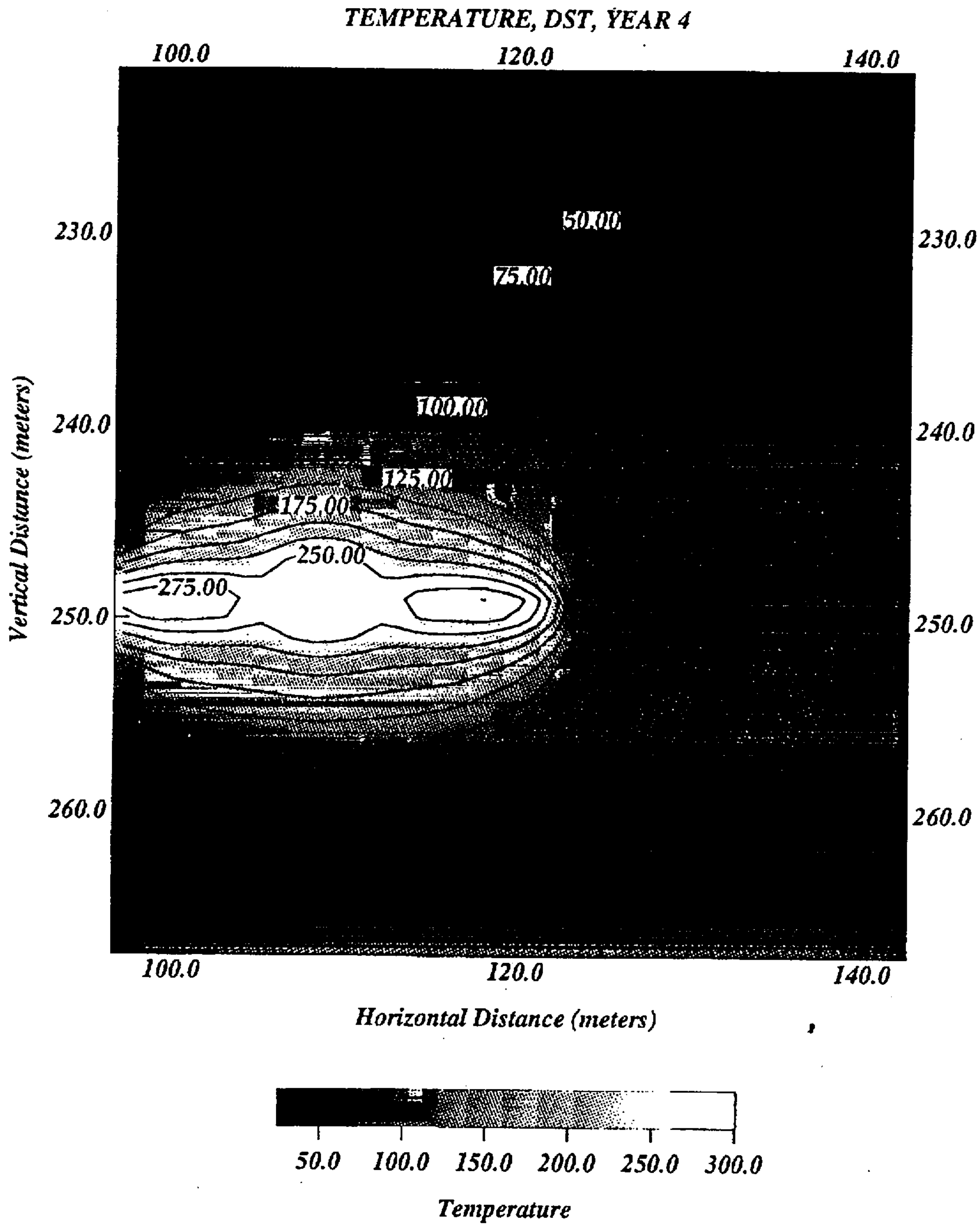

TEMPERATURE, DST, YEAR 4
100.0
120.0
140.0
230.0
240.0
250.0
260.0
Vertical Distance (meters)
50.00
75.00
100.00
125.00
175.00
250.00
275.00
Horizontal Distance (meters)
50.0
100.0
150.0
200.0
250.0
300.0
Temperature

Figure 2b

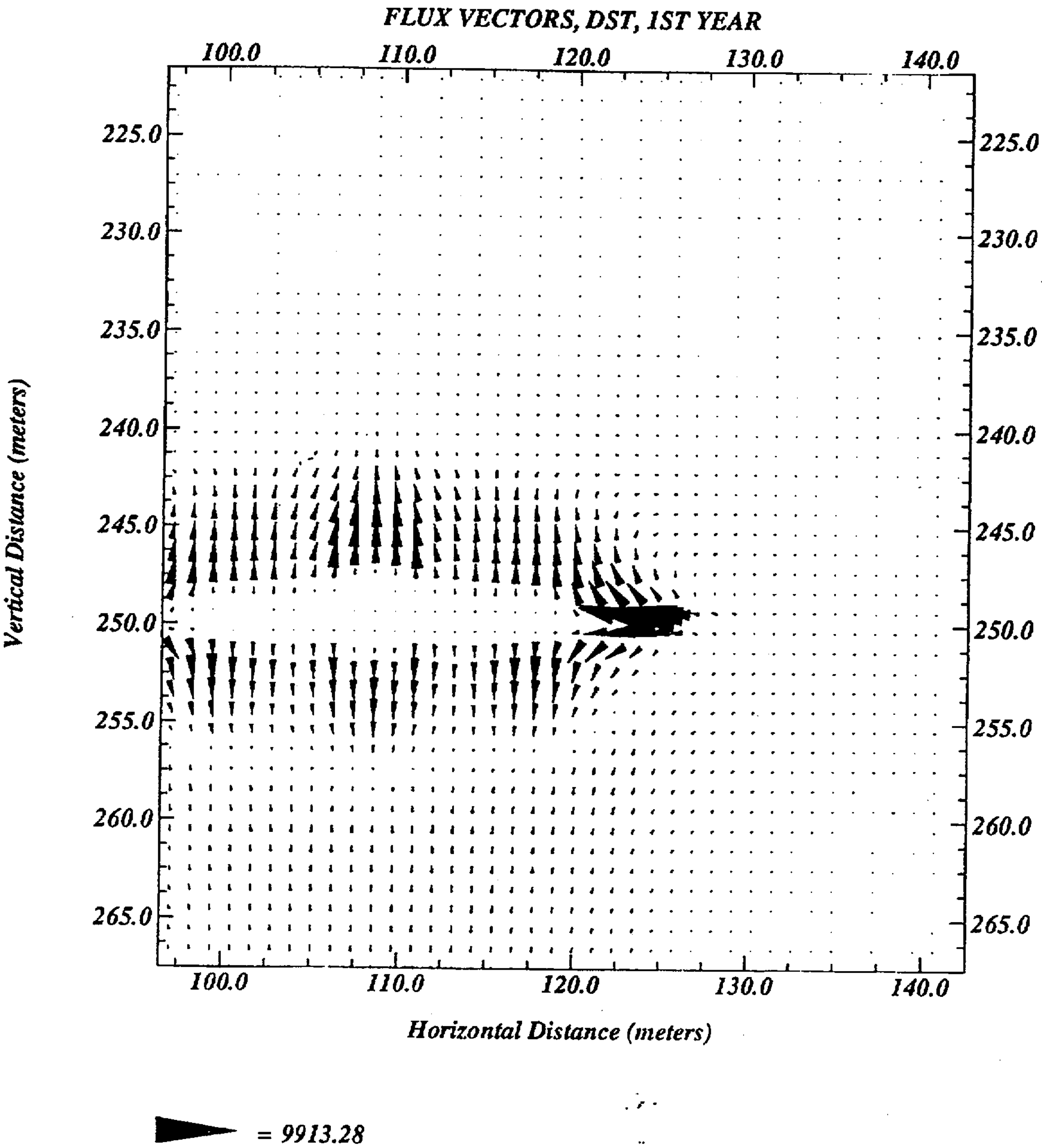
FLUX VECTORS, DST, 1ST YEAR
100.0
110.0
120.0
130.0
140.0
225.0
230.0
235.0
240.0
245.0
250.0
255.0
260.0
265.0
Vertical Distance (meters)
Horizontal Distance (meters)
= 9913.28

Figure 3a

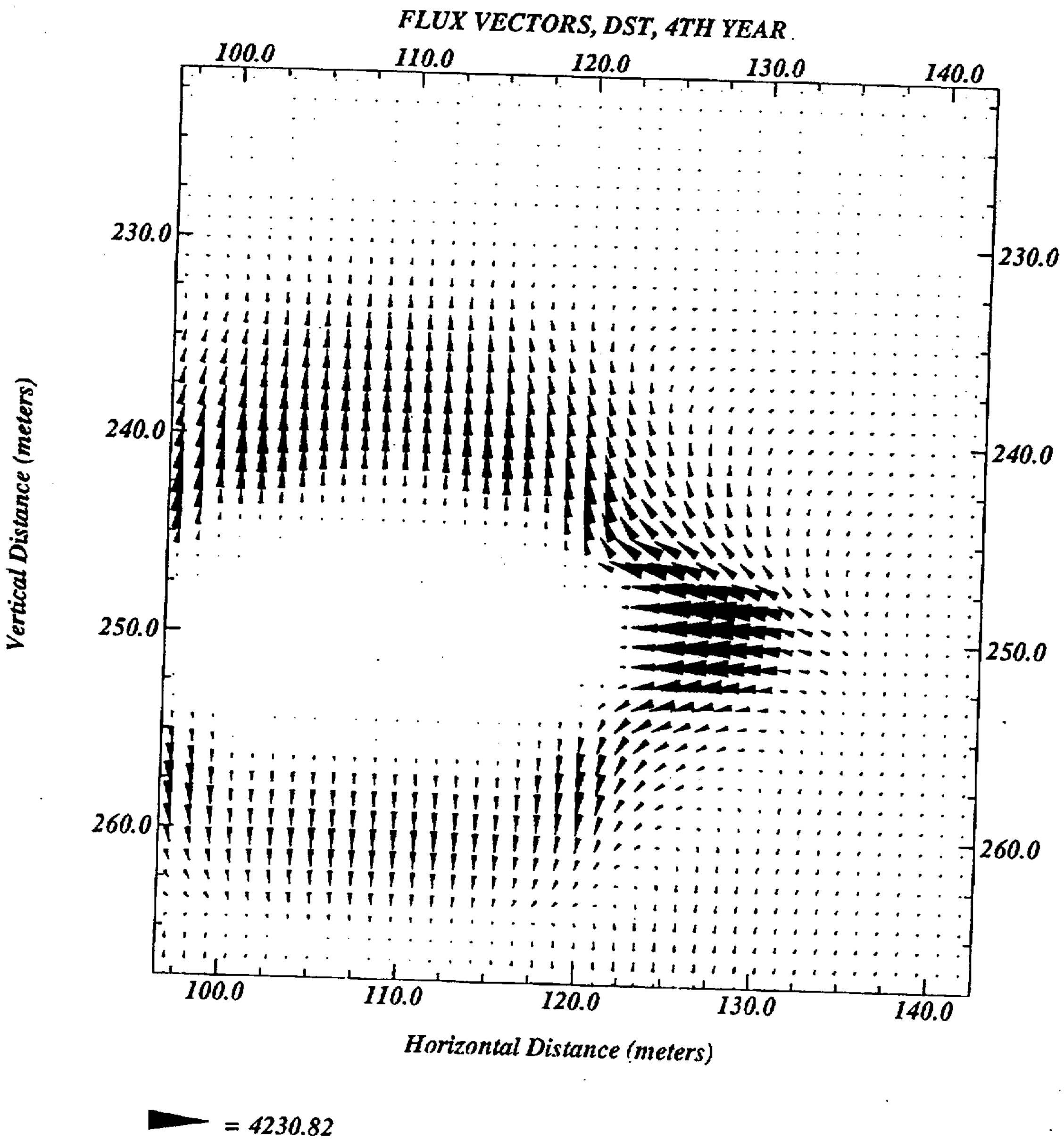

FLUX VECTORS, DST, 4TH YEAR
100.0
110.0
120.0
130.0
140.0
230.0
240.0
250.0
260.0
Vertical Distance (meters)
Horizontal Distance (meters)
= 4230.82

Figure 3b

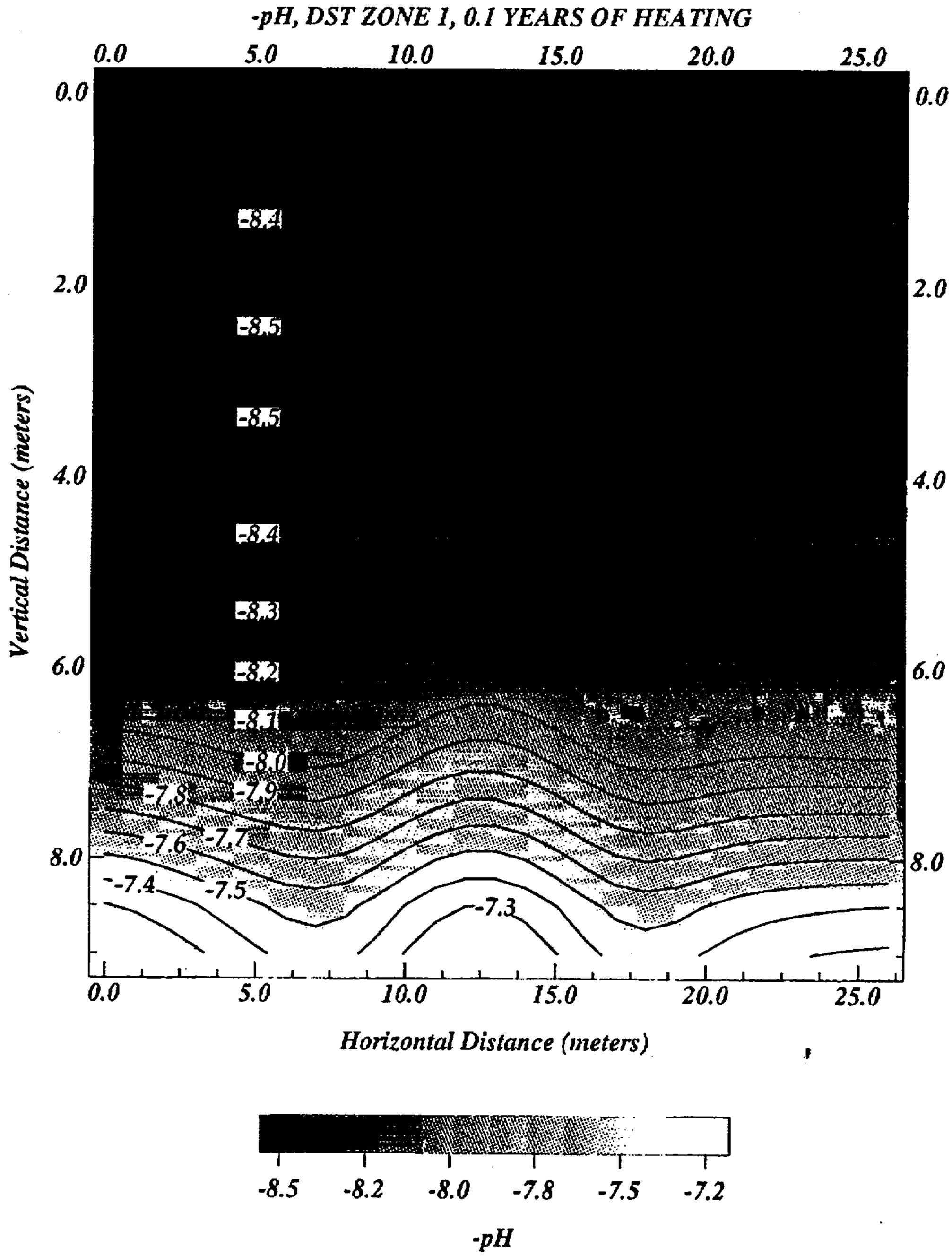

-pH, DST ZONE 1, 0.1 YEARS OF HEATING
0.0
5.0
10.0
15.0
20.0
25.0
0.0
2.0
4.0
6.0
8.0
Vertical Distance (meters)
-8.4
-8.5
-8.5
-8.4
-8.3
-8.2
-8.1
-8.0
-7.8
-7.9
-7.6
-7.7
-7.4
-7.5
-7.3
Horizontal Distance (meters)
-8.5
-8.2
-8.0
-7.8
-7.5
-7.2
-pH

Figure 4a

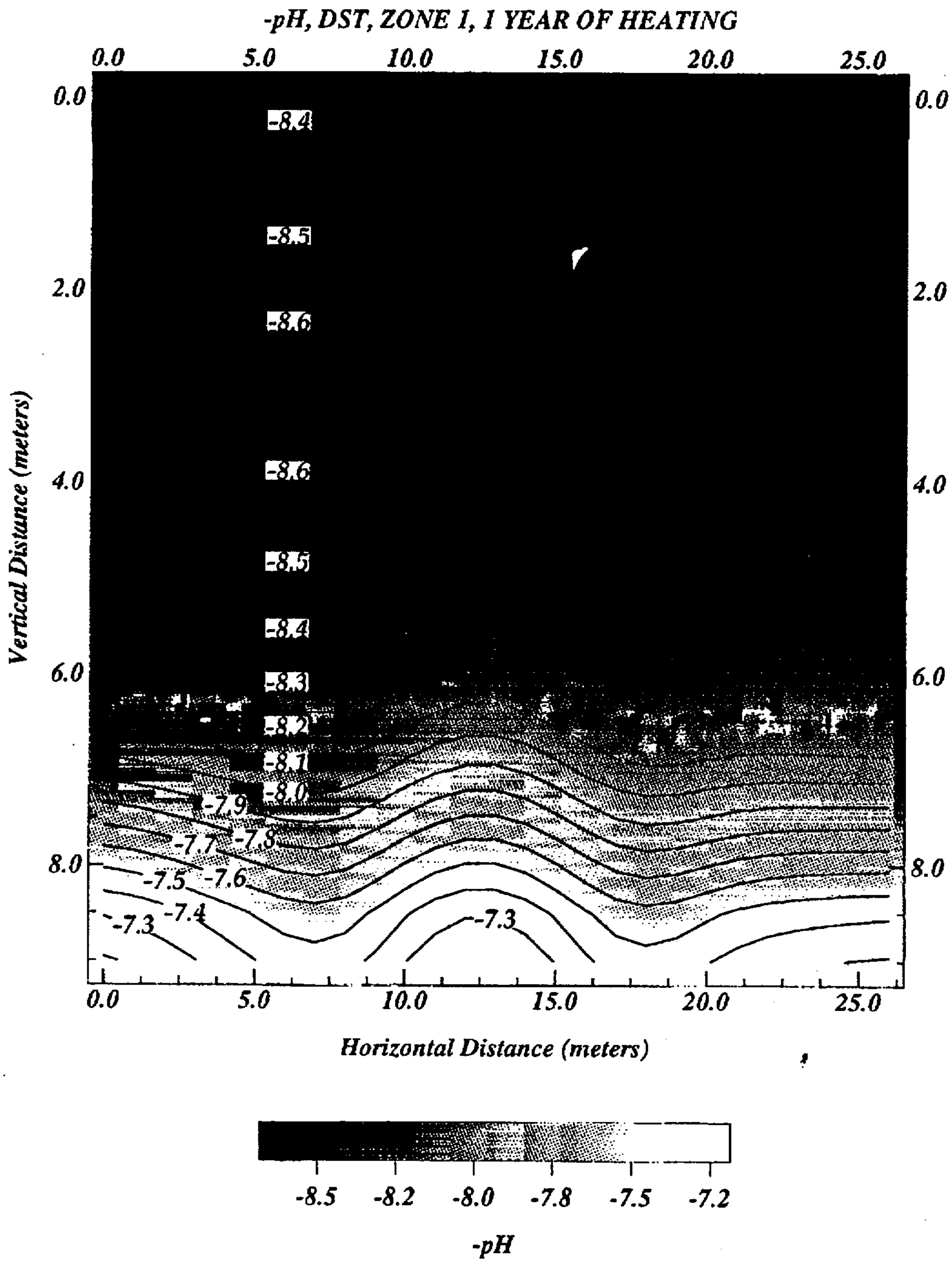

-pH, DST, ZONE 1, 1 YEAR OF HEATING
0.0 5.0 10.0 15.0 20.0 25.0
-8.4
-8.5
-8.6
-8.6
-8.5
-8.4
-8.3
-8.2
-8.1
-8.0
-7.9
-7.8
-7.7
-7.6
-7.5
-7.4
-7.3
-7.3
Vertical Distance (meters)
0.0 2.0 4.0 6.0 8.0
Horizontal Distance (meters)
-8.5 -8.2 -8.0 -7.8 -7.5 -7.2
-pH

Figure 4b

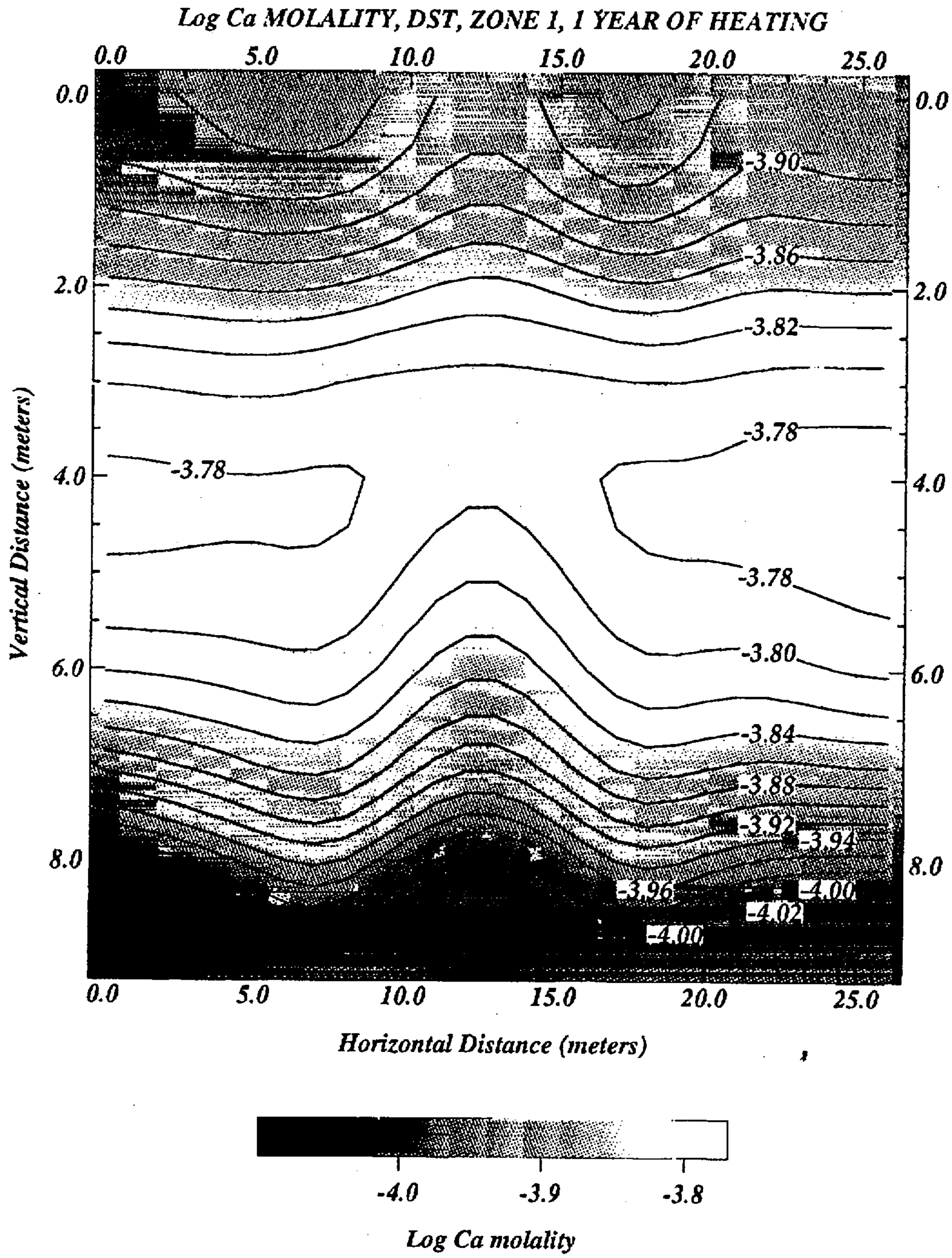
Log Ca MOLALITY, DST, ZONE 1, 1 YEAR OF HEATING
0.0
5.0
10.0
15.0
20.0
25.0
-3.90
-3.86
-3.82
-3.78
-3.78
-3.78
-3.80
-3.84
-3.88
-3.92
-3.94
-3.96
-4.00
-4.02
-4.00
0.0
2.0
4.0
6.0
8.0
Vertical Distance (meters)
Horizontal Distance (meters)
-4.0
-3.9
-3.8
Log Ca molality

Figure 5a

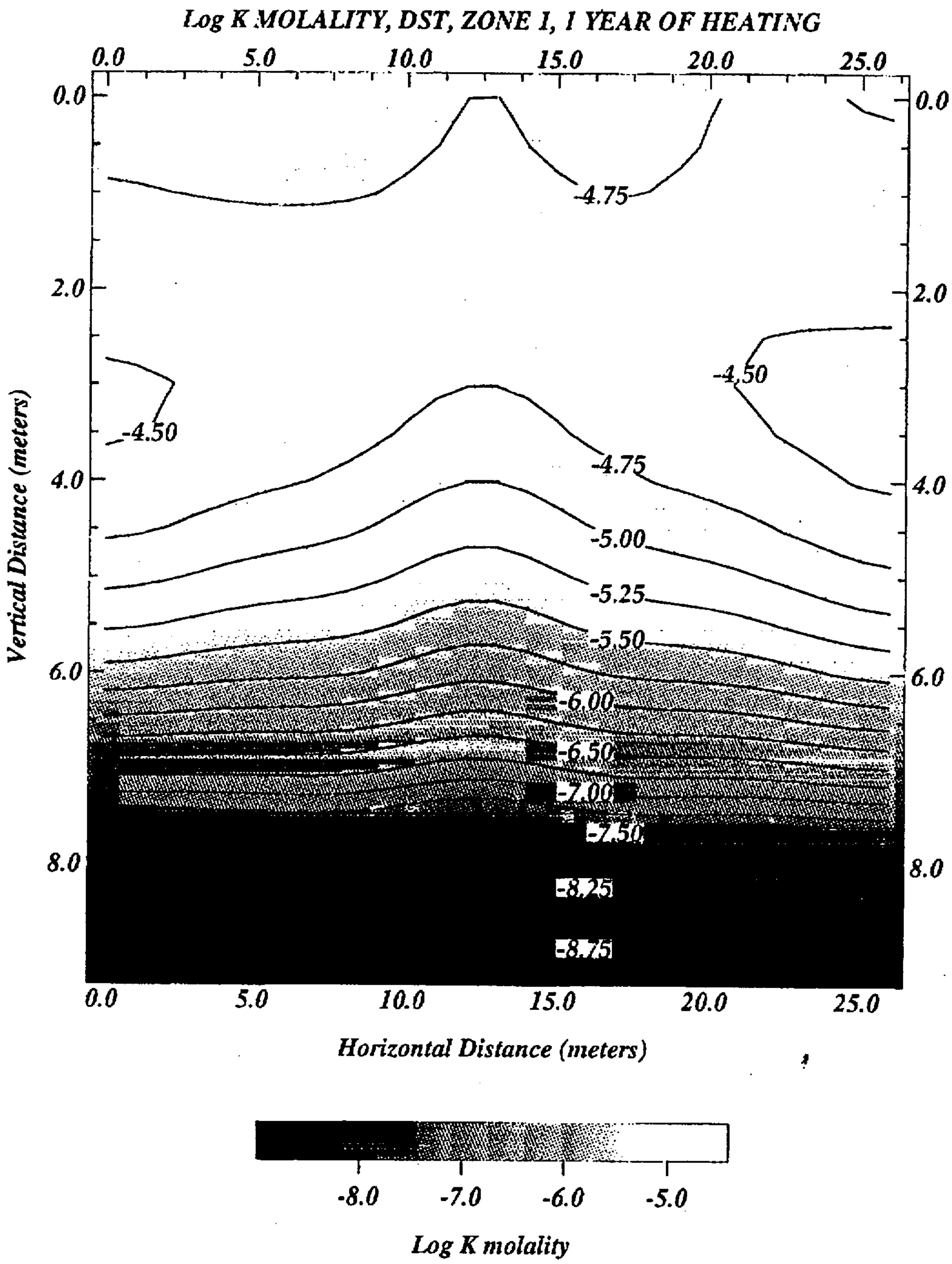
Log K MOLALITY, DST, ZONE 1, 1 YEAR OF HEATING
0.0
5.0
10.0
15.0
20.0
25.0
0.0
2.0
4.0
6.0
8.0
Vertical Distance (meters)
-4.75
-4.50
-4.50
-4.75
-5.00
-5.25
-5.50
-6.00
-6.50
-7.00
-7.50
-8.25
-8.75
Horizontal Distance (meters)
-8.0
-7.0
-6.0
-5.0
Log K molality

Figure 5b

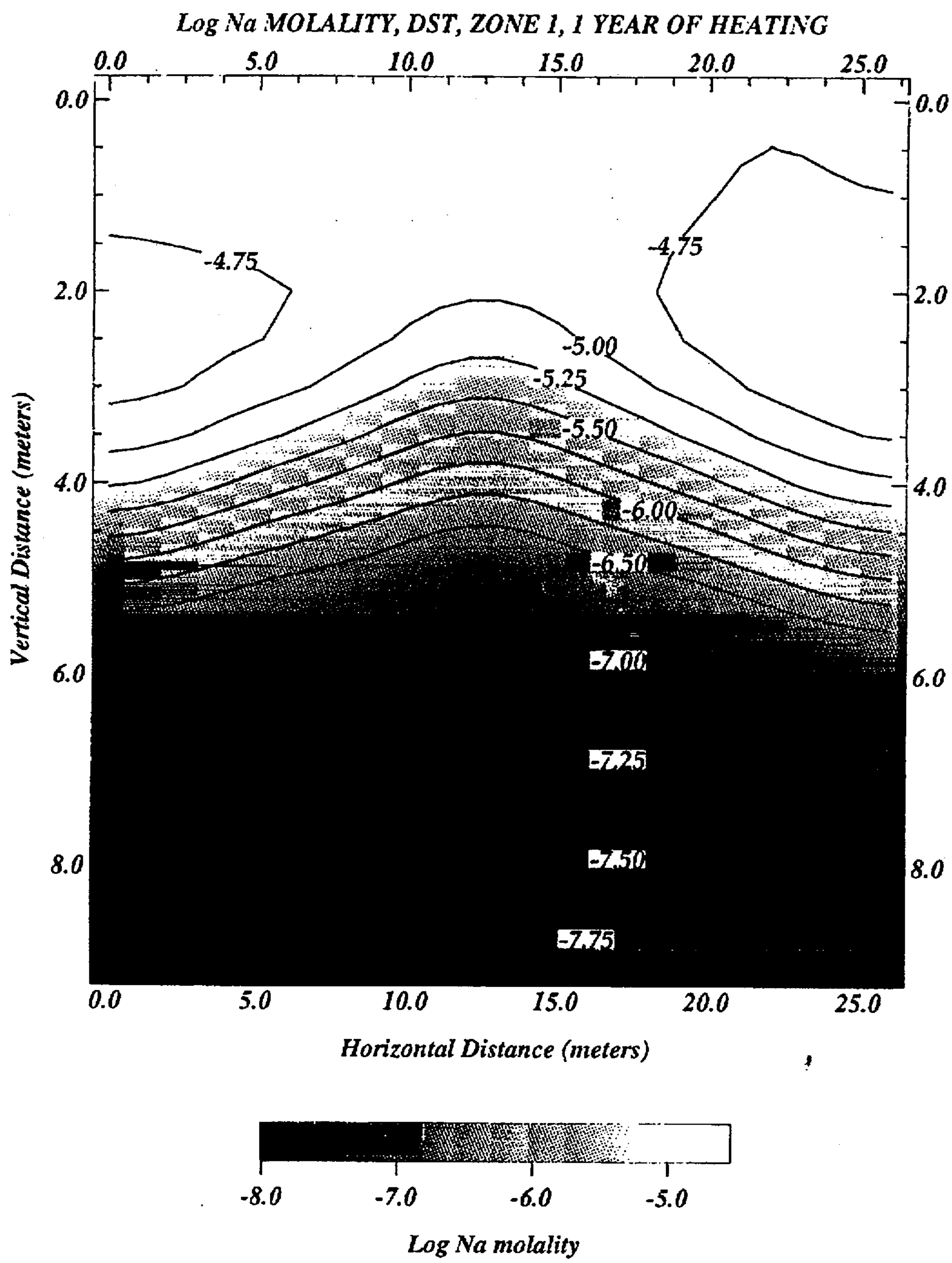
Log Na MOLALITY, DST, ZONE 1, 1 YEAR OF HEATING
0.0
5.0
10.0
15.0
20.0
25.0
0.0
2.0
4.0
6.0
8.0
Vertical Distance (meters)
-4.75
-4.75
-5.00
-5.25
-5.50
-6.00
-6.50
-7.00
-7.25
-7.50
-7.75
Horizontal Distance (meters)
-8.0
-7.0
-6.0
-5.0
Log Na molality

Figure 5c

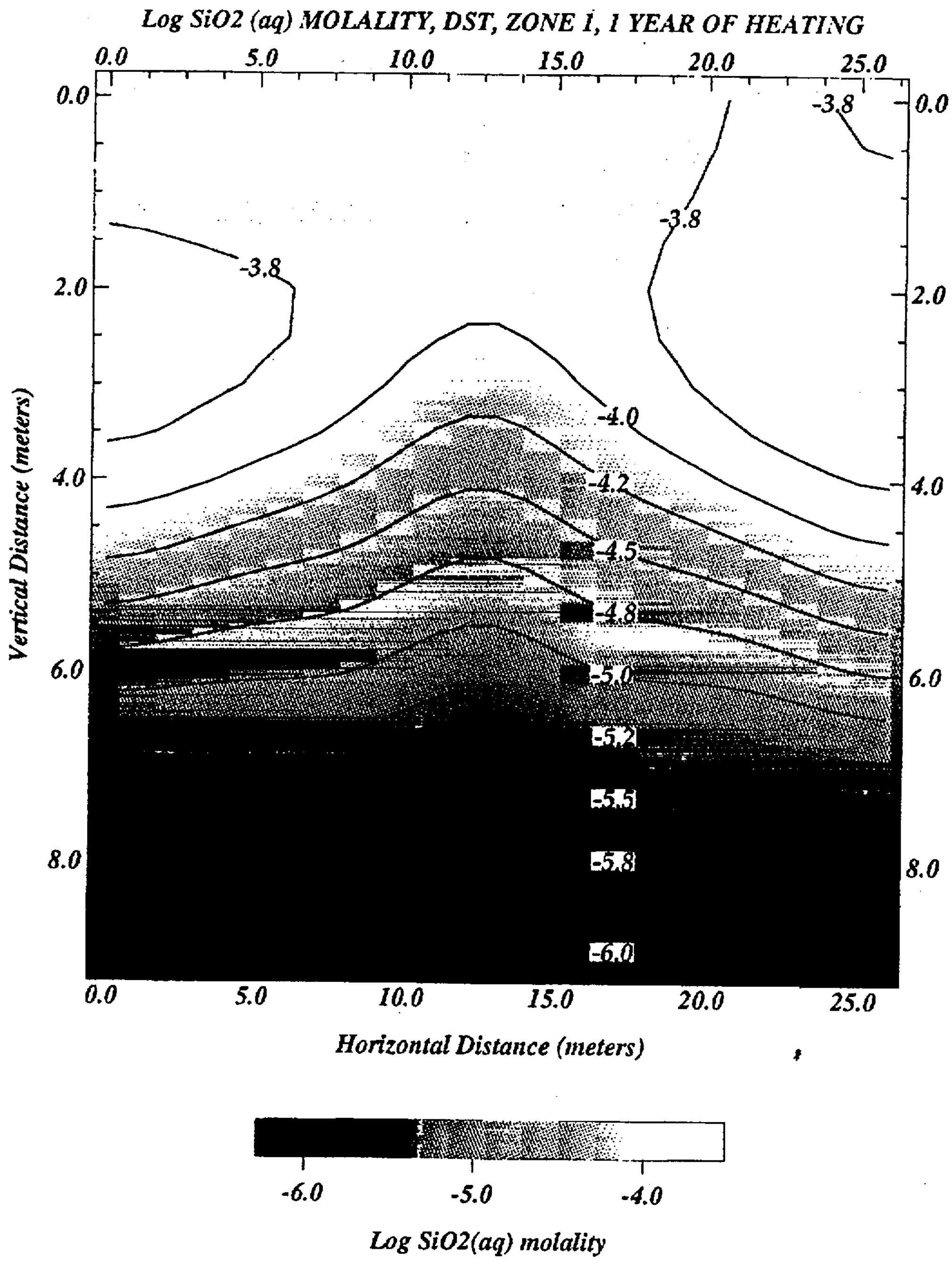
Log SiO2 (aq) MOLALITY, DST, ZONE 1, 1 YEAR OF HEATING
0.0
5.0
10.0
15.0
20.0
25.0
0.0
2.0
4.0
6.0
8.0
-3.8
-3.8
-3.8
-4.0
-4.2
-4.5
-4.8
-5.0
-5.2
-5.5
-5.8
-6.0
Vertical Distance (meters)
Horizontal Distance (meters)
-6.0
-5.0
-4.0
Log SiO2(aq) molality

Figure 5d

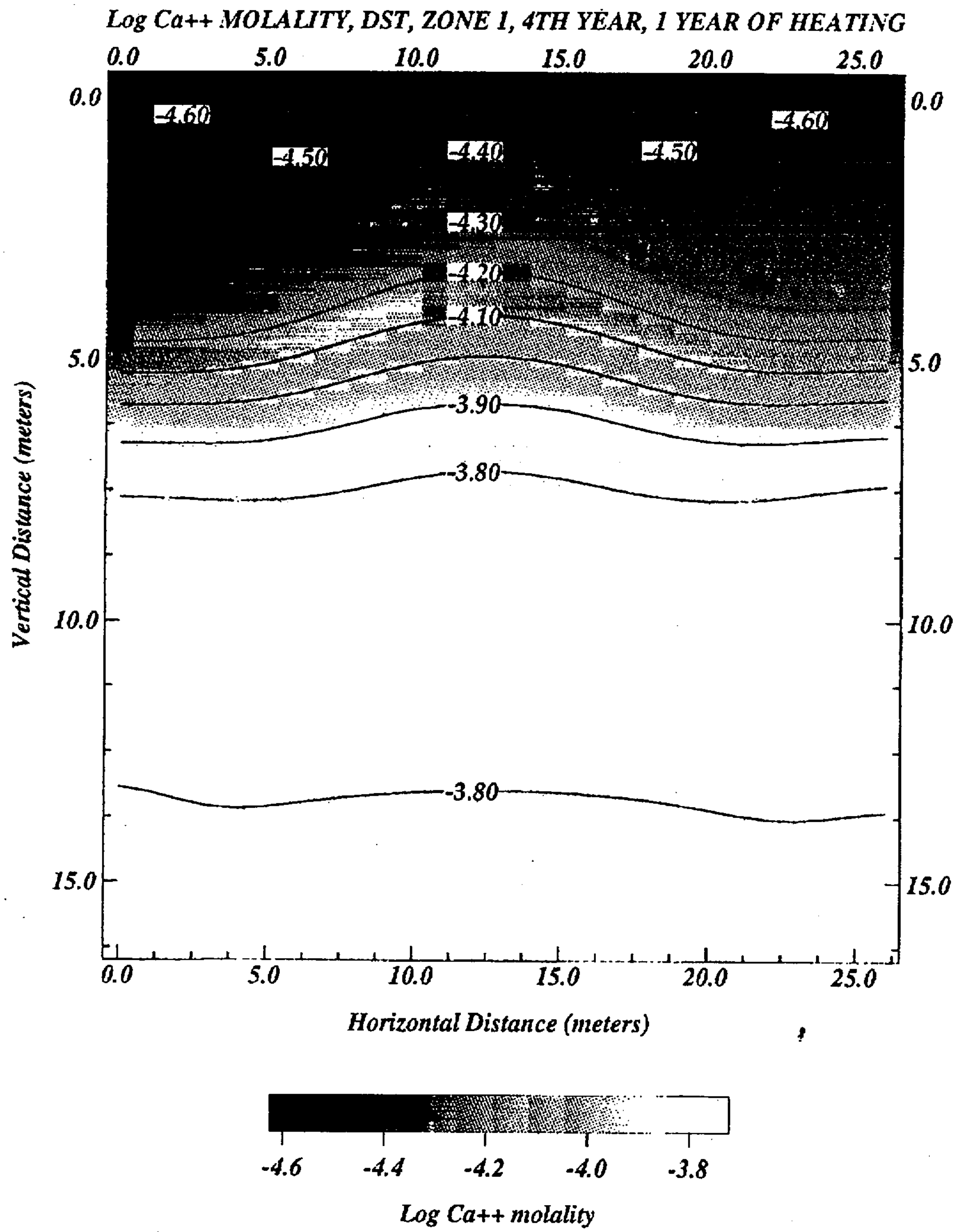
Log Ca++ MOLALITY, DST, ZONE 1, 4TH YEAR, 1 YEAR OF HEATING
0.0
5.0
10.0
15.0
20.0
25.0
-4.60
-4.50
-4.40
-4.30
-4.20
-4.10
-3.90
-3.80
Vertical Distance (meters)
Horizontal Distance (meters)
-4.6
-4.4
-4.2
-4.0
-3.8
Log Ca++ molality

Figure 6a

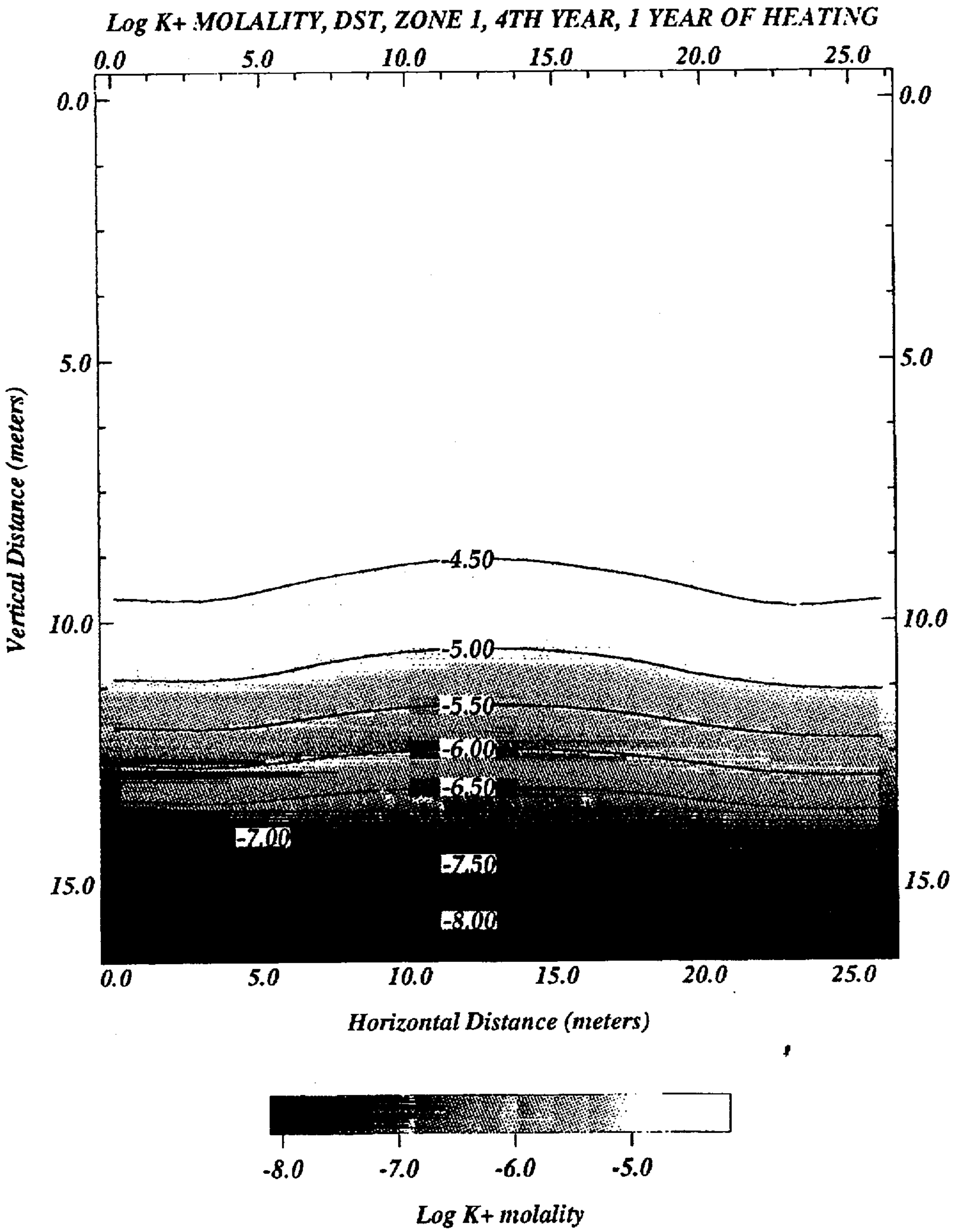

Log K+ MOLALITY, DST, ZONE 1, 4TH YEAR, 1 YEAR OF HEATING
0.0
5.0
10.0
15.0
20.0
25.0
Vertical Distance (meters)
-4.50
-5.00
-5.50
-6.00
-6.50
-7.00
-7.50
-8.00
Horizontal Distance (meters)
-8.0
-7.0
-6.0
-5.0
Log K+ molality

Figure 6b

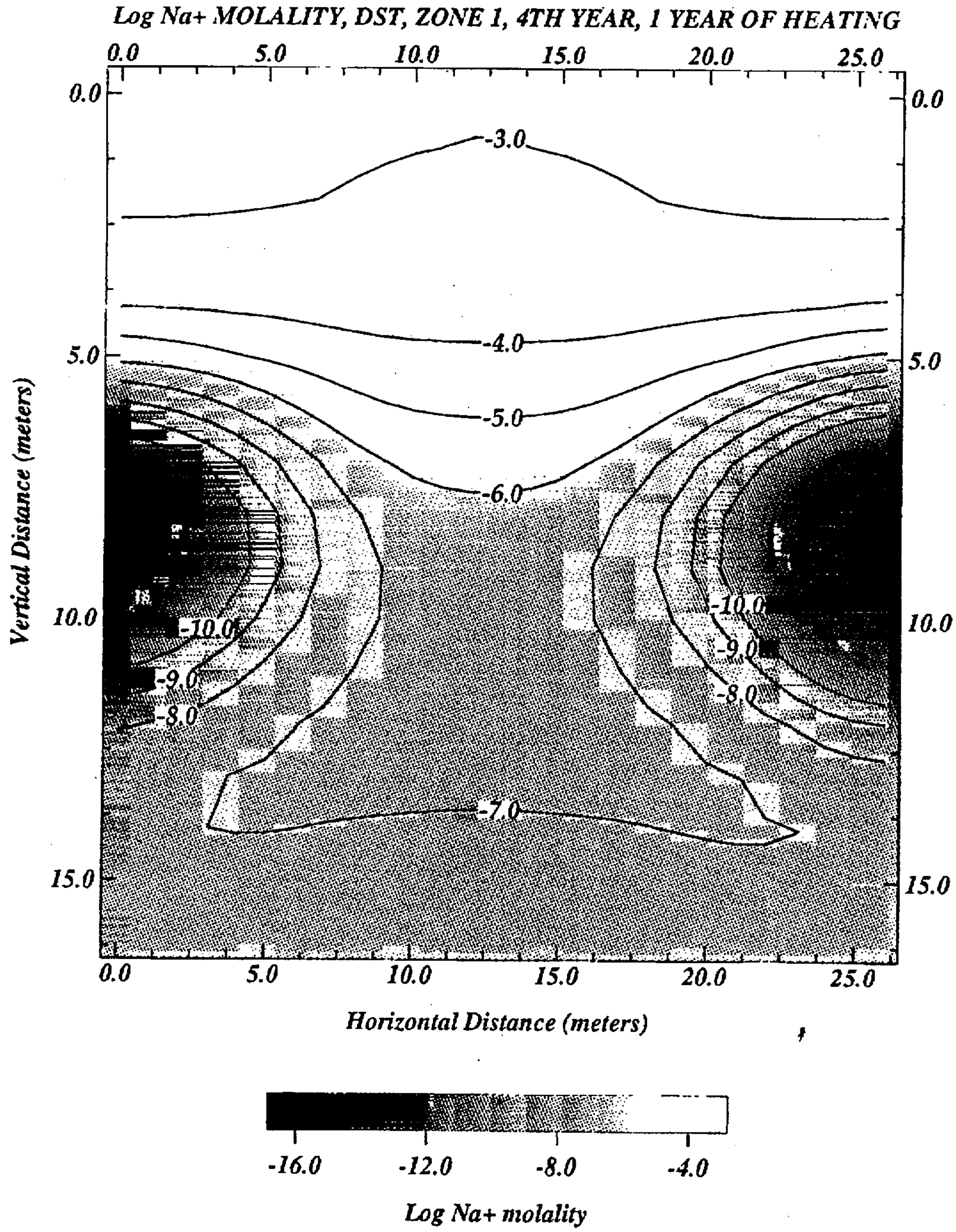

Log Na+ MOLALITY, DST, ZONE 1, 4TH YEAR, 1 YEAR OF HEATING
0.0
5.0
10.0
15.0
20.0
25.0
-3.0
-4.0
-5.0
-6.0
-7.0
-8.0
-9.0
-10.0
Vertical Distance (meters)
Horizontal Distance (meters)
-16.0
-12.0
-8.0
-4.0
Log Na+ molality

Figure 6c

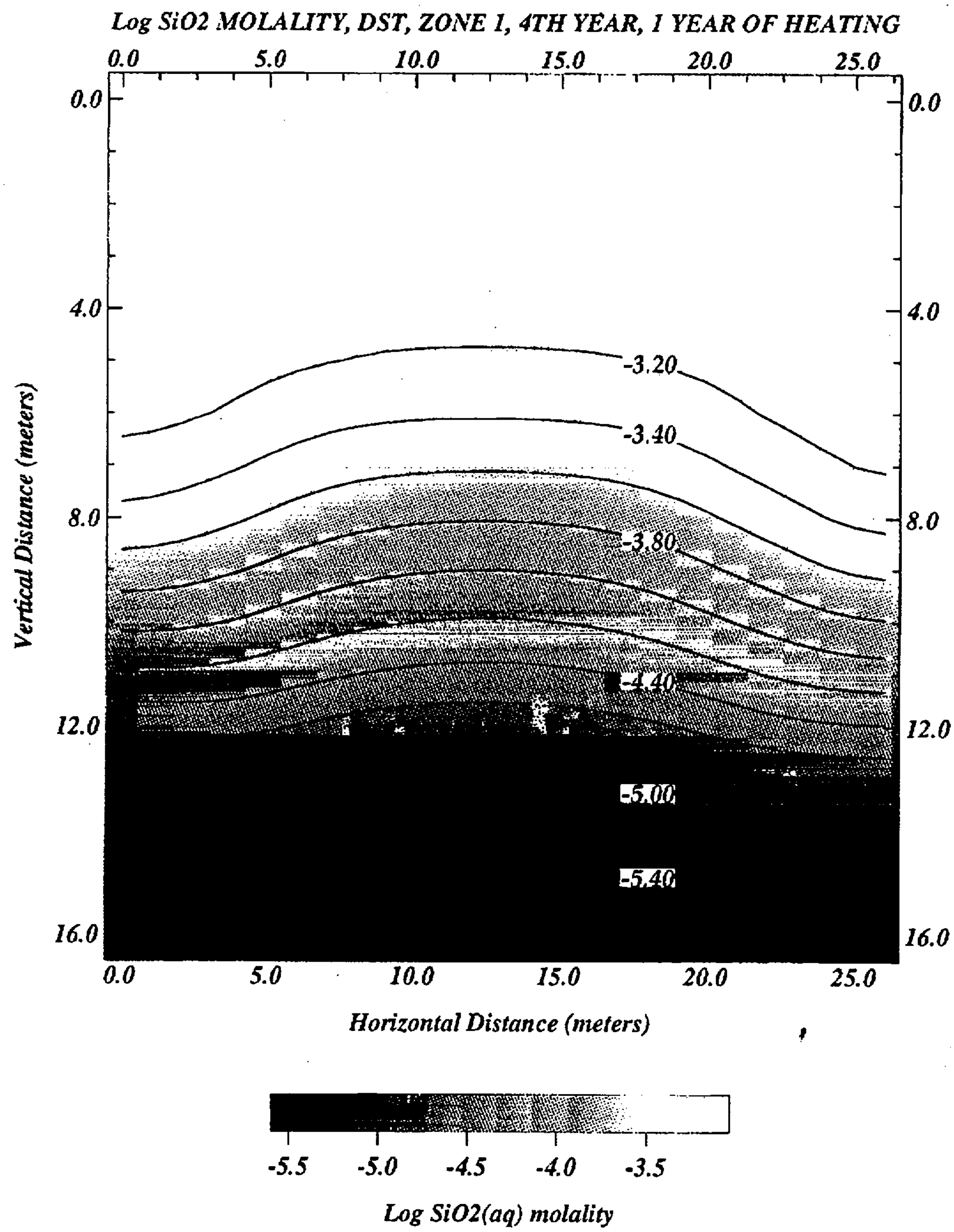
Log SiO2 MOLALITY, DST, ZONE 1, 4TH YEAR, 1 YEAR OF HEATING
0.0
5.0
10.0
15.0
20.0
25.0
0.0
4.0
8.0
12.0
16.0
-3.20
-3.40
-3.80
-4.40
-5.00
-5.40
Vertical Distance (meters)
Horizontal Distance (meters)
-5.5
-5.0
-4.5
-4.0
-3.5
Log SiO2(aq) molality

Figure 6d

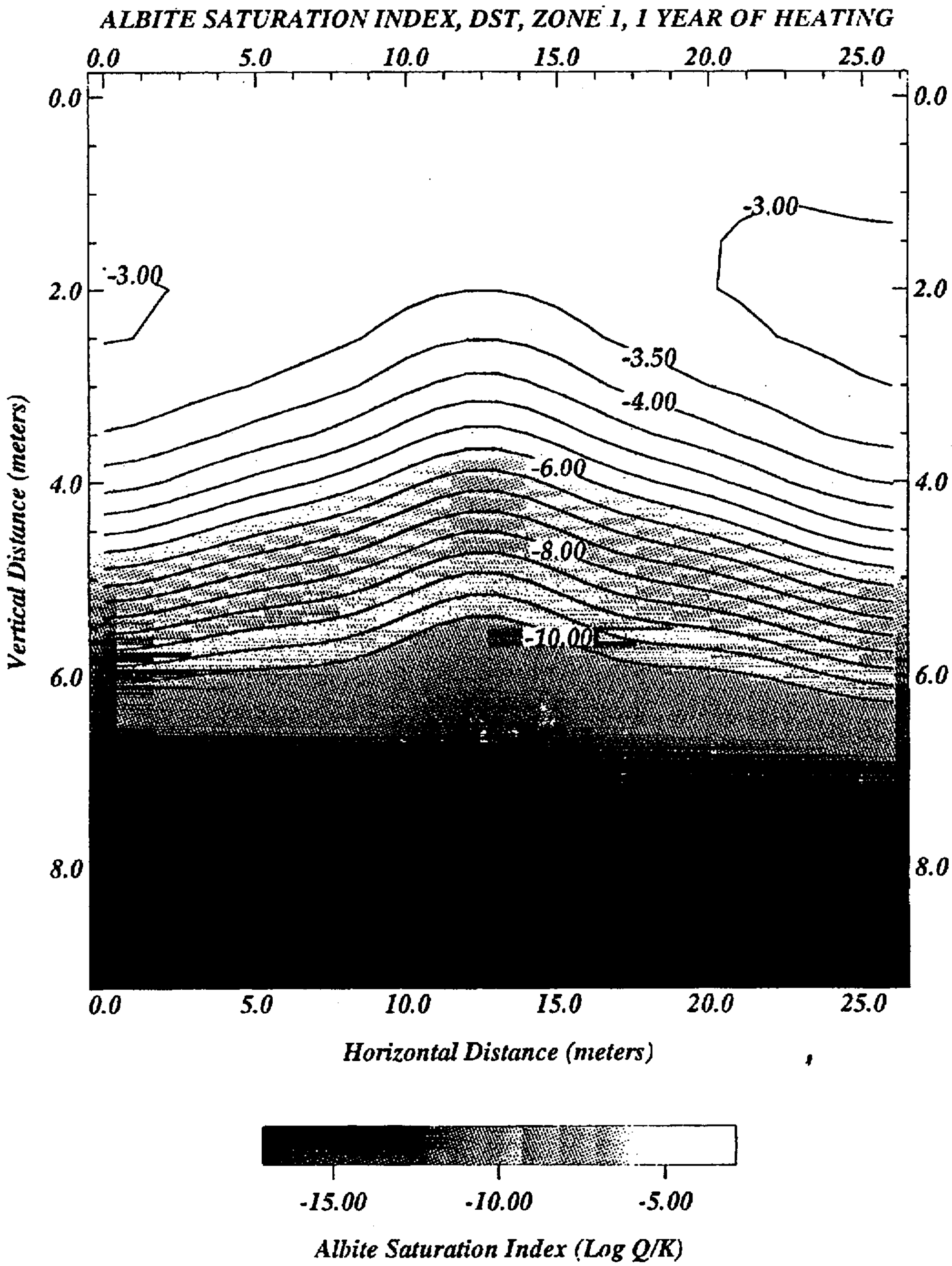

ALBITE SATURATION INDEX, DST, ZONE 1, 1 YEAR OF HEATING
0.0
5.0
10.0
15.0
20.0
25.0
0.0
2.0
4.0
6.0
8.0
-3.00
-3.00
-3.50
-4.00
-6.00
-8.00
-10.00
Vertical Distance (meters)
Horizontal Distance (meters)
-15.00
-10.00
-5.00
Albite Saturation Index (Log Q/K)

Figure 7a

CALCITE SATURATION INDEX, DST, ZONE 1, 1 YEAR OF HEATING

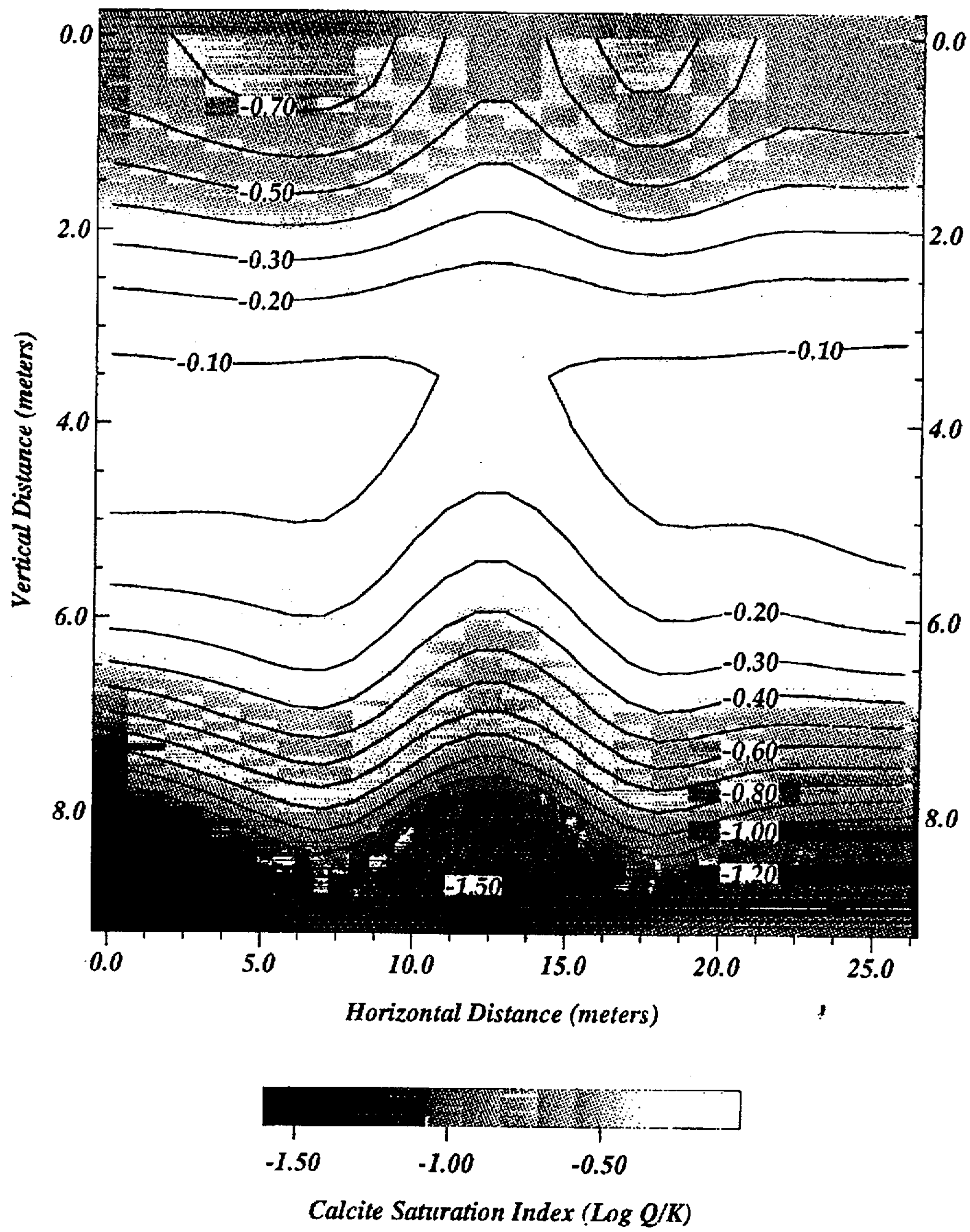

Figure 7b

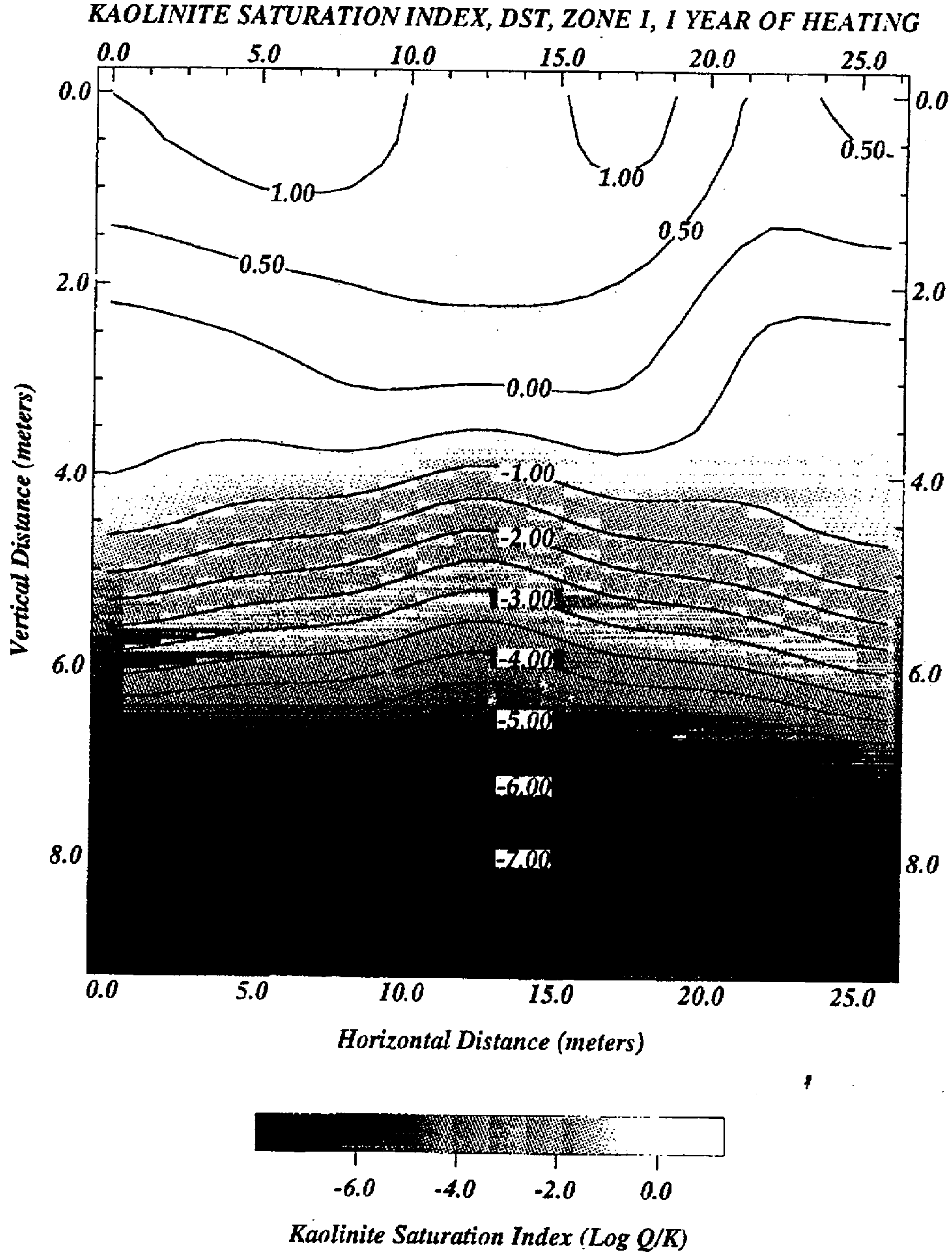
KAOLINITE SATURATION INDEX, DST, ZONE 1, 1 YEAR OF HEATING
0.0
5.0
10.0
15.0
20.0
25.0
1.00
0.50
0.00
-1.00
-2.00
-3.00
-4.00
-5.00
-6.00
-7.00
Vertical Distance (meters)
2.0
4.0
6.0
8.0
Horizontal Distance (meters)
-6.0
-4.0
-2.0
Kaolinite Saturation Index (Log Q/K)

Figure 7c

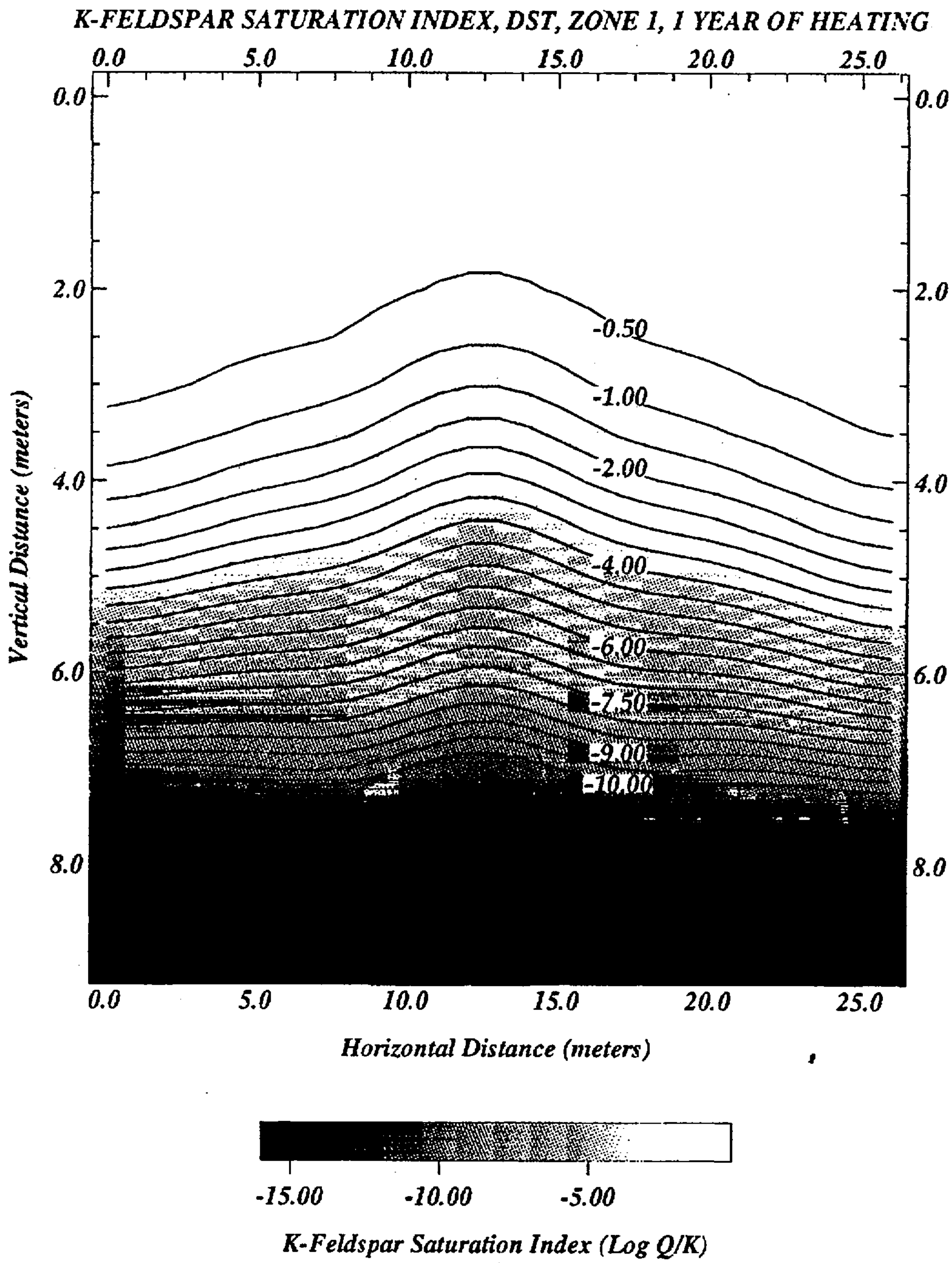

K-FELDSPAR SATURATION INDEX, DST, ZONE 1, 1 YEAR OF HEATING
0.0
5.0
10.0
15.0
20.0
25.0
2.0
4.0
6.0
8.0
-0.50
-1.00
-2.00
-4.00
-6.00
-7.50
-9.00
-10.00
Vertical Distance (meters)
Horizontal Distance (meters)
-15.00
-10.00
-5.00
K-Feldspar Saturation Index (Log Q/K)

Figure 7d

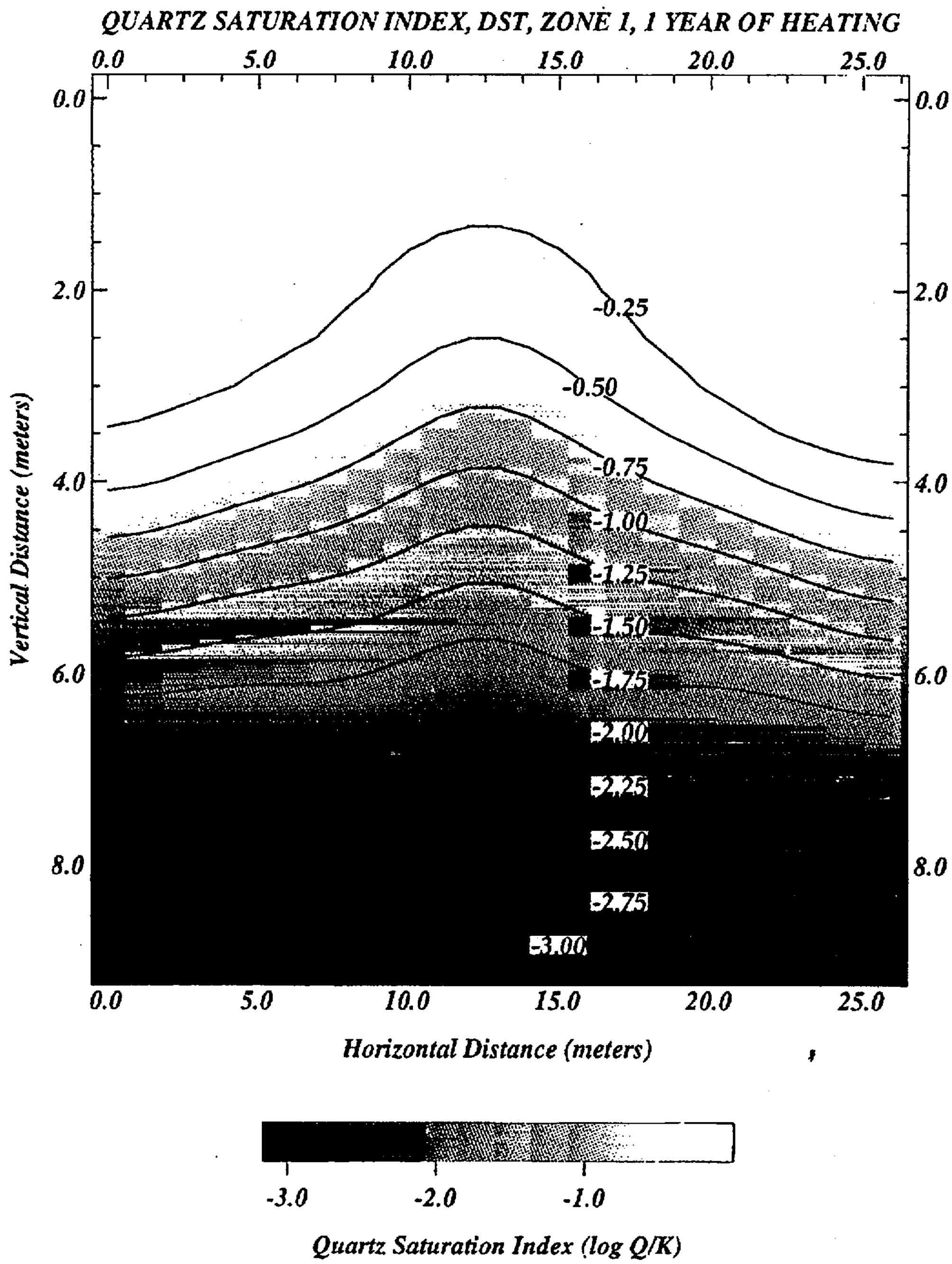

QUARTZ SATURATION INDEX, DST, ZONE 1, 1 YEAR OF HEATING
0.0
5.0
10.0
15.0
20.0
25.0
0.0
2.0
4.0
6.0
8.0
Vertical Distance (meters)
-0.25
-0.50
-0.75
-1.00
-1.25
-1.50
-1.75
-2.00
-2.25
-2.50
-2.75
-3.00
Horizontal Distance (meters)
-3.0
-2.0
-1.0
Quartz Saturation Index (log Q/K)

Figure 7e

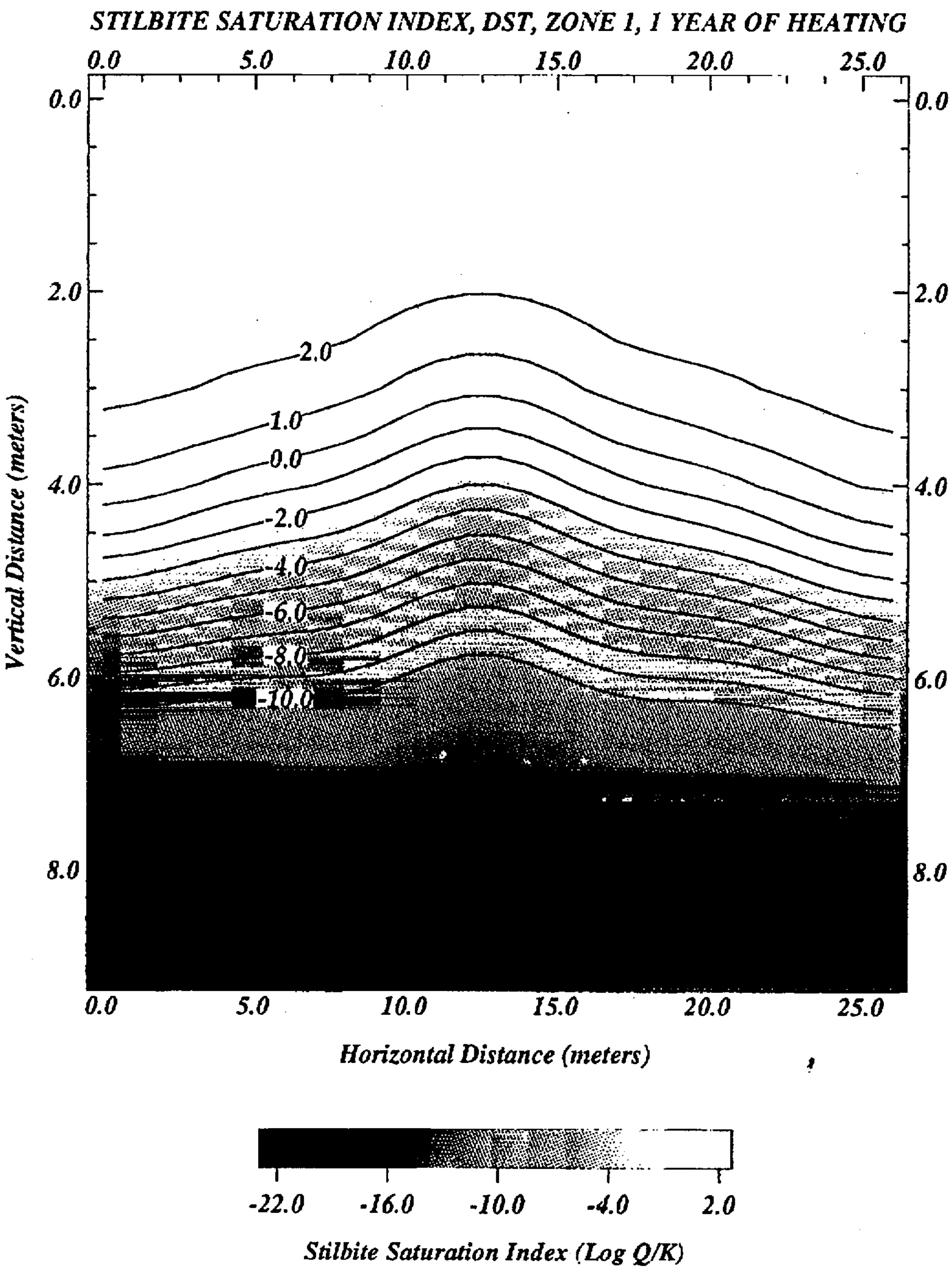
STILBITE SATURATION INDEX, DST, ZONE 1, 1 YEAR OF HEATING
0.0
5.0
10.0
15.0
20.0
25.0
0.0
2.0
4.0
6.0
8.0
2.0
1.0
0.0
-2.0
-4.0
-6.0
-8.0
-10.0
Vertical Distance (meters)
Horizontal Distance (meters)
-22.0
-16.0
-10.0
-4.0
2.0
Stilbite Saturation Index (Log Q/K)

Figure 7f

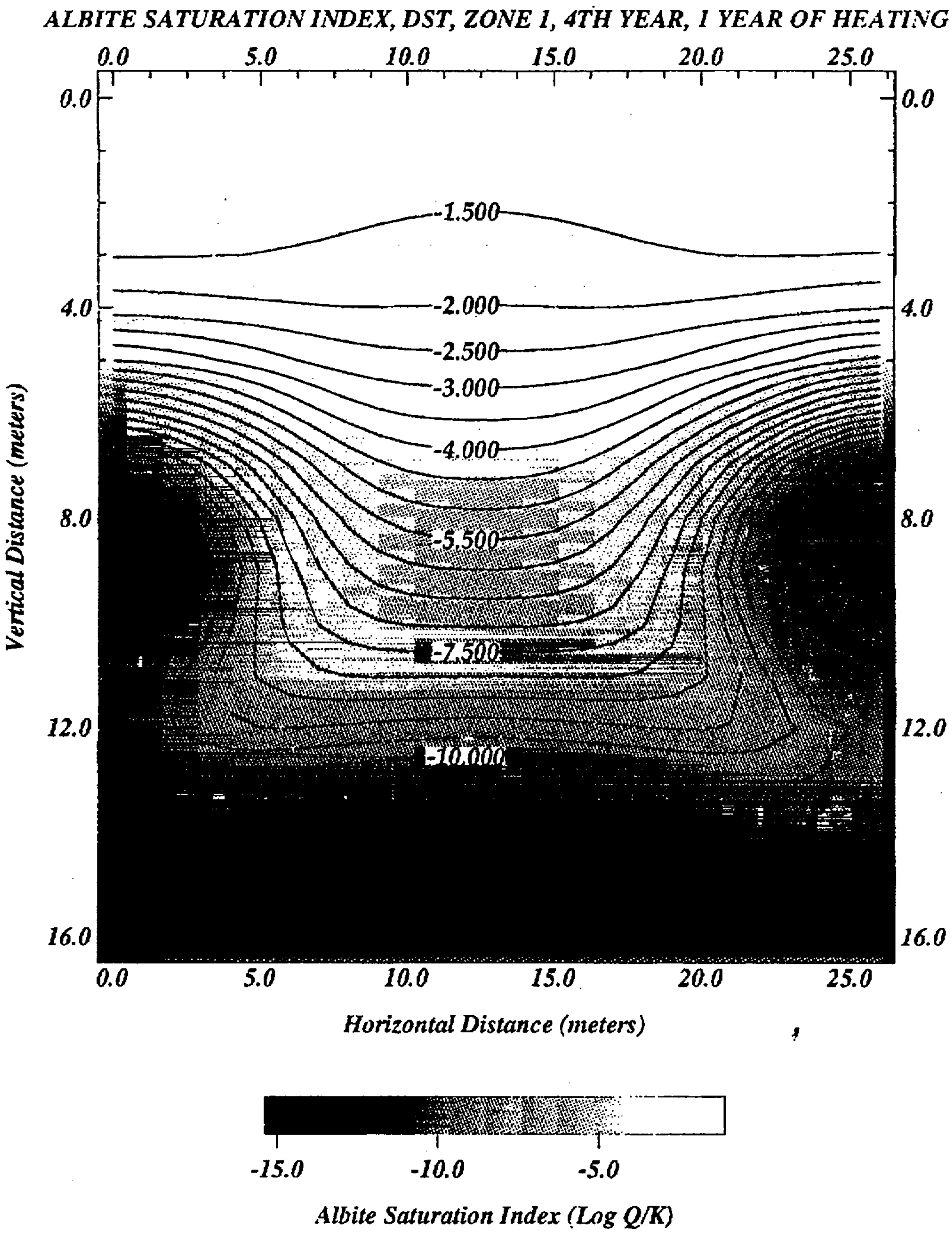
ALBITE SATURATION INDEX, DST, ZONE 1, 4TH YEAR, 1 YEAR OF HEATING
0.0
5.0
10.0
15.0
20.0
25.0
0.0
4.0
8.0
12.0
16.0
-1.500
-2.000
-2.500
-3.000
-4.000
-5.500
-7.500
-10.000
Vertical Distance (meters)
Horizontal Distance (meters)
-15.0
-10.0
-5.0
Albite Saturation Index (Log Q/K)

Figure 8a

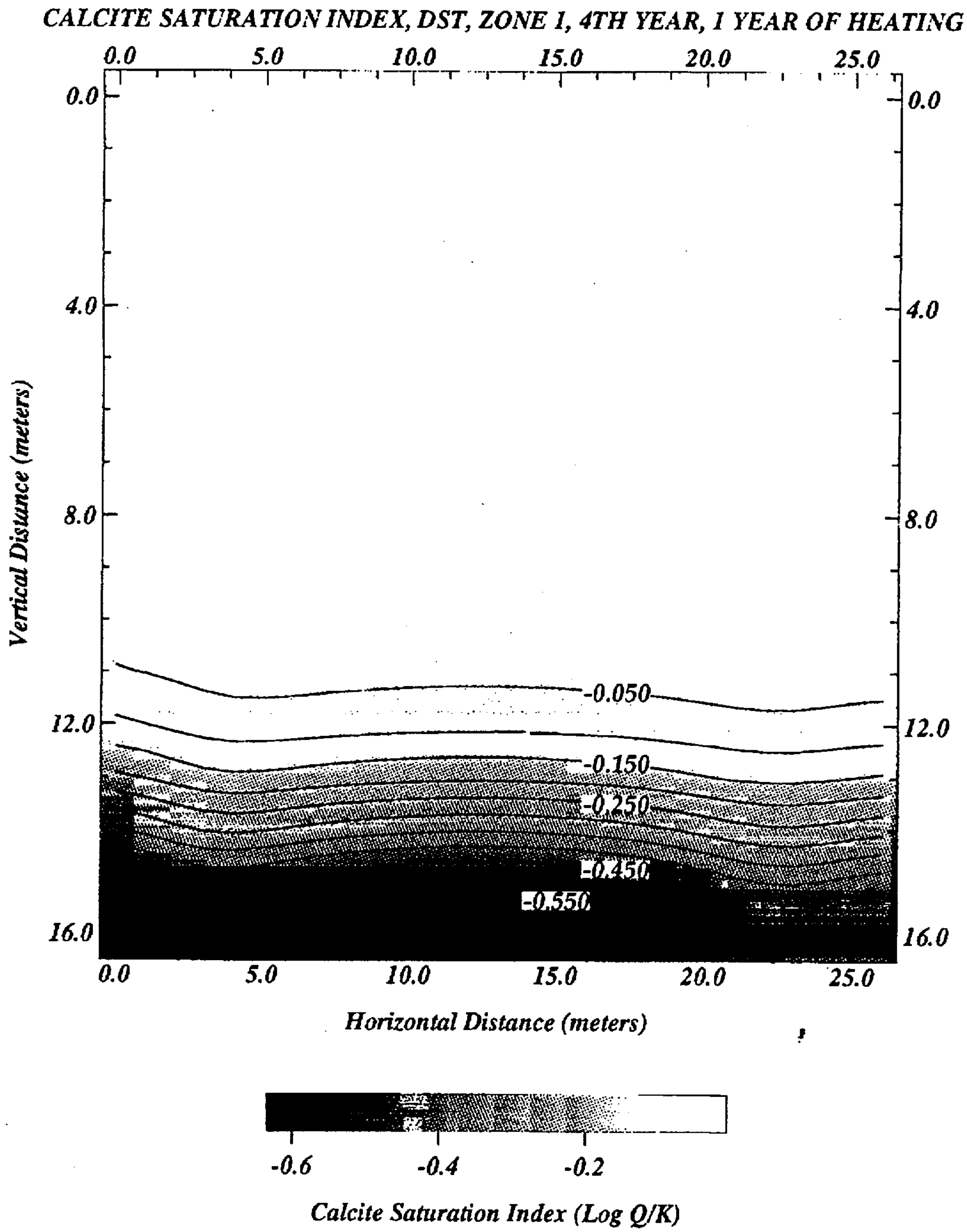
CALCITE SATURATION INDEX, DST, ZONE 1, 4TH YEAR, 1 YEAR OF HEATING
0.0
5.0
10.0
15.0
20.0
25.0
0.0
4.0
8.0
12.0
16.0
Vertical Distance (meters)
-0.050
-0.150
-0.250
-0.450
-0.550
Horizontal Distance (meters)
-0.6
-0.4
-0.2
Calcite Saturation Index (Log Q/K)

Figure 8b

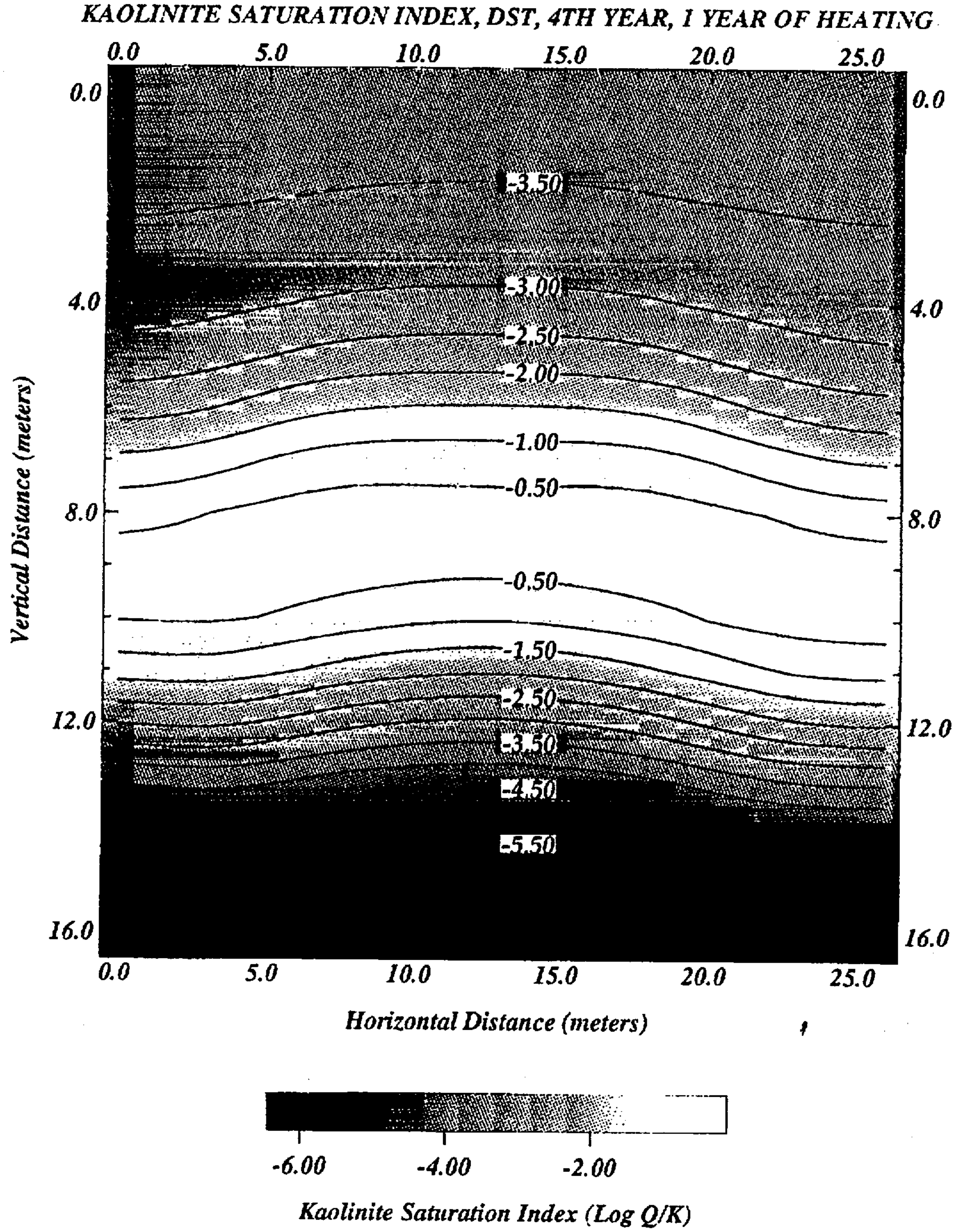

KAOLINITE SATURATION INDEX, DST, 4TH YEAR, 1 YEAR OF HEATING
0.0
5.0
10.0
15.0
20.0
25.0
0.0
4.0
8.0
12.0
16.0
Vertical Distance (meters)
Horizontal Distance (meters)
-3.50
-3.00
-2.50
-2.00
-1.00
-0.50
-0.50
-1.50
-2.50
-3.50
-4.50
-5.50
-6.00
-4.00
-2.00
Kaolinite Saturation Index (Log Q/K)

Figure 8c

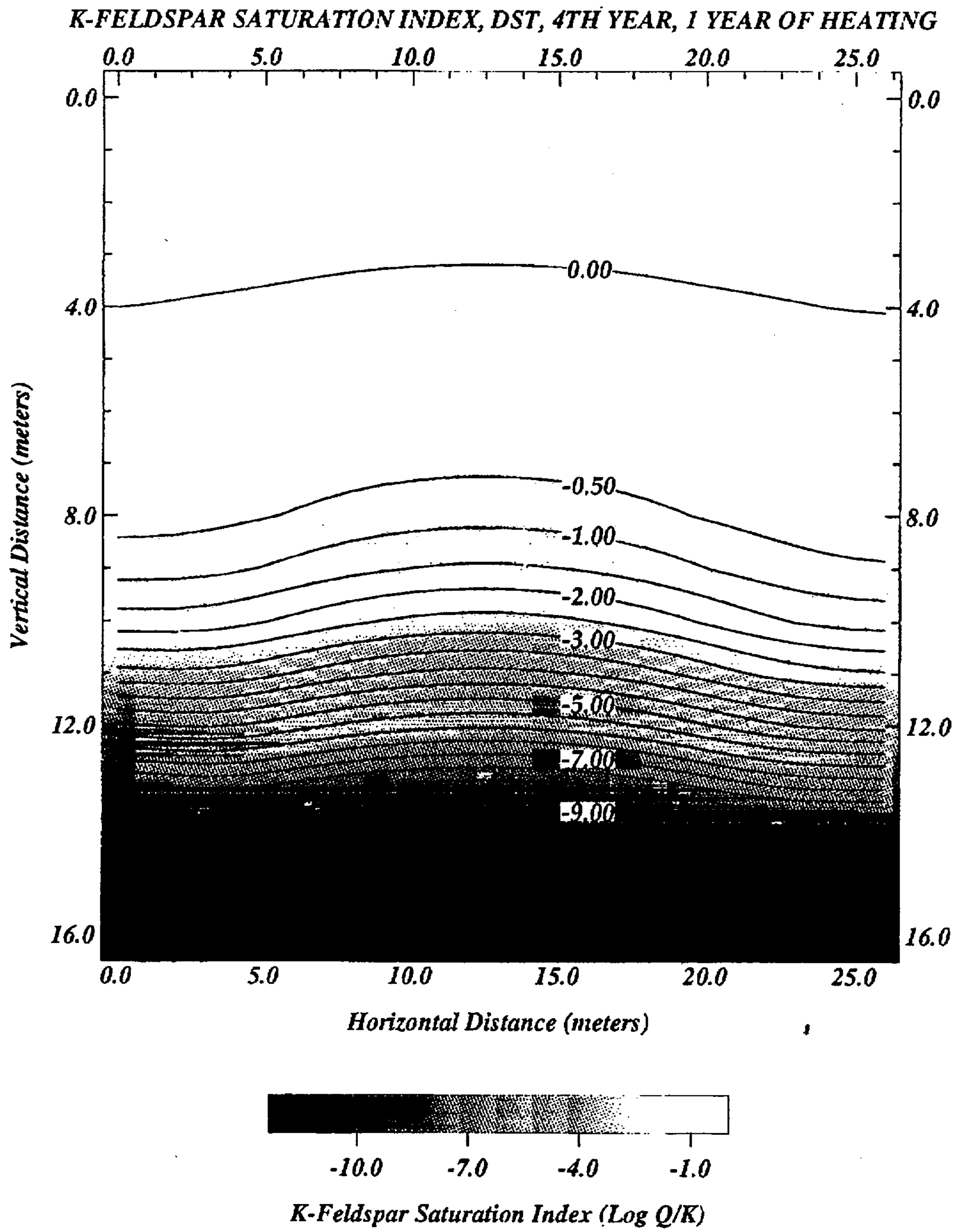
K-FELDSPAR SATURATION INDEX, DST, 4TH YEAR, 1 YEAR OF HEATING
0.0
5.0
10.0
15.0
20.0
25.0
0.0
4.0
8.0
12.0
16.0
0.00
-0.50
-1.00
-2.00
-3.00
-5.00
-7.00
-9.00
Vertical Distance (meters)
Horizontal Distance (meters)
-10.0
-7.0
-4.0
-1.0
K-Feldspar Saturation Index (Log Q/K)

Figure 8d

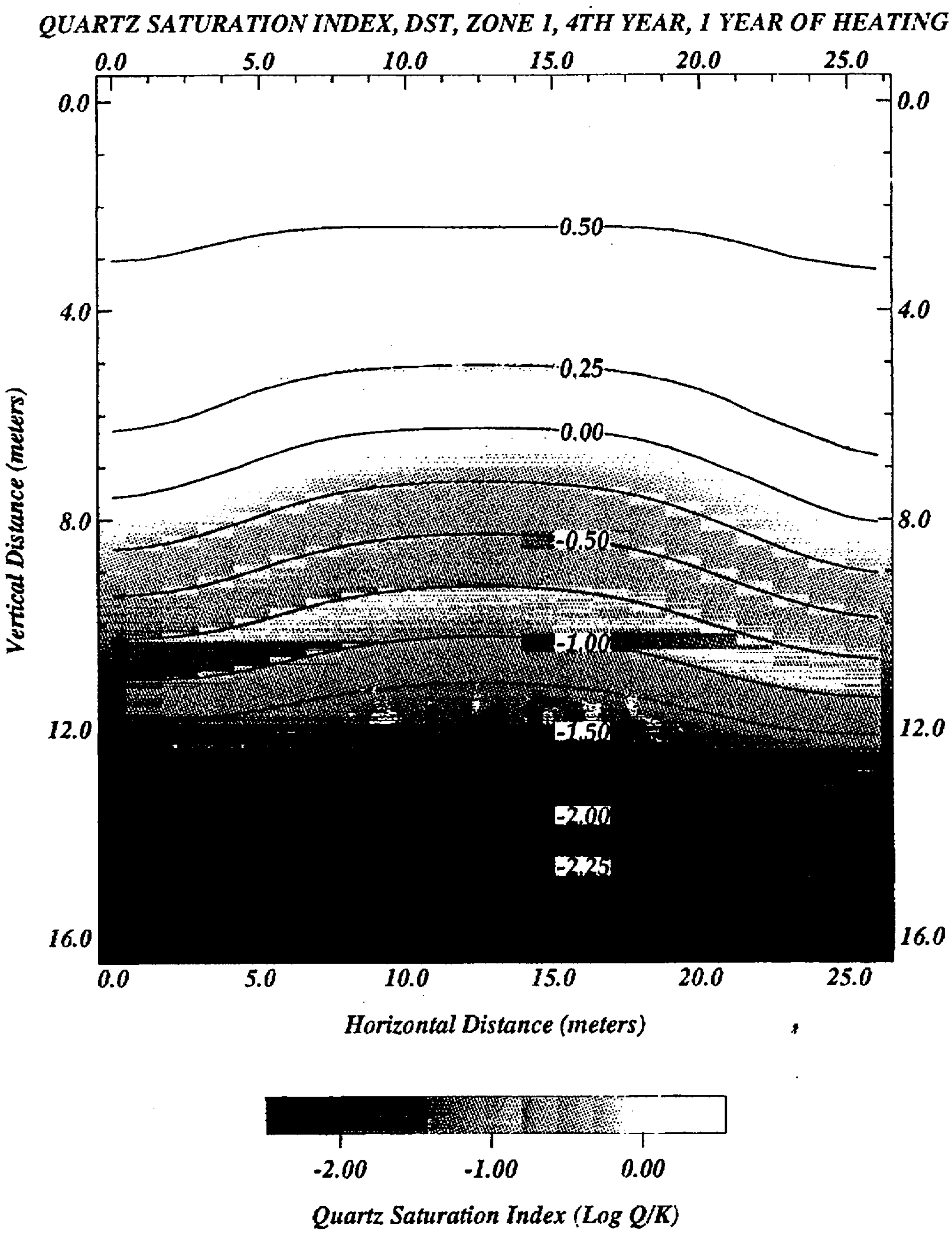
QUARTZ SATURATION INDEX, DST, ZONE 1, 4TH YEAR, 1 YEAR OF HEATING
0.0
5.0
10.0
15.0
20.0
25.0
4.0
8.0
12.0
16.0
0.50
0.25
0.00
-0.50
-1.00
-1.50
-2.00
-2.25
Vertical Distance (meters)
Horizontal Distance (meters)
-2.00
-1.00
0.00
Quartz Saturation Index (Log Q/K)

Figure 8e

STILBITE SATURATION INDEX, DST, ZONE 1, 4TH YEAR, 1 YEAR OF HEATING

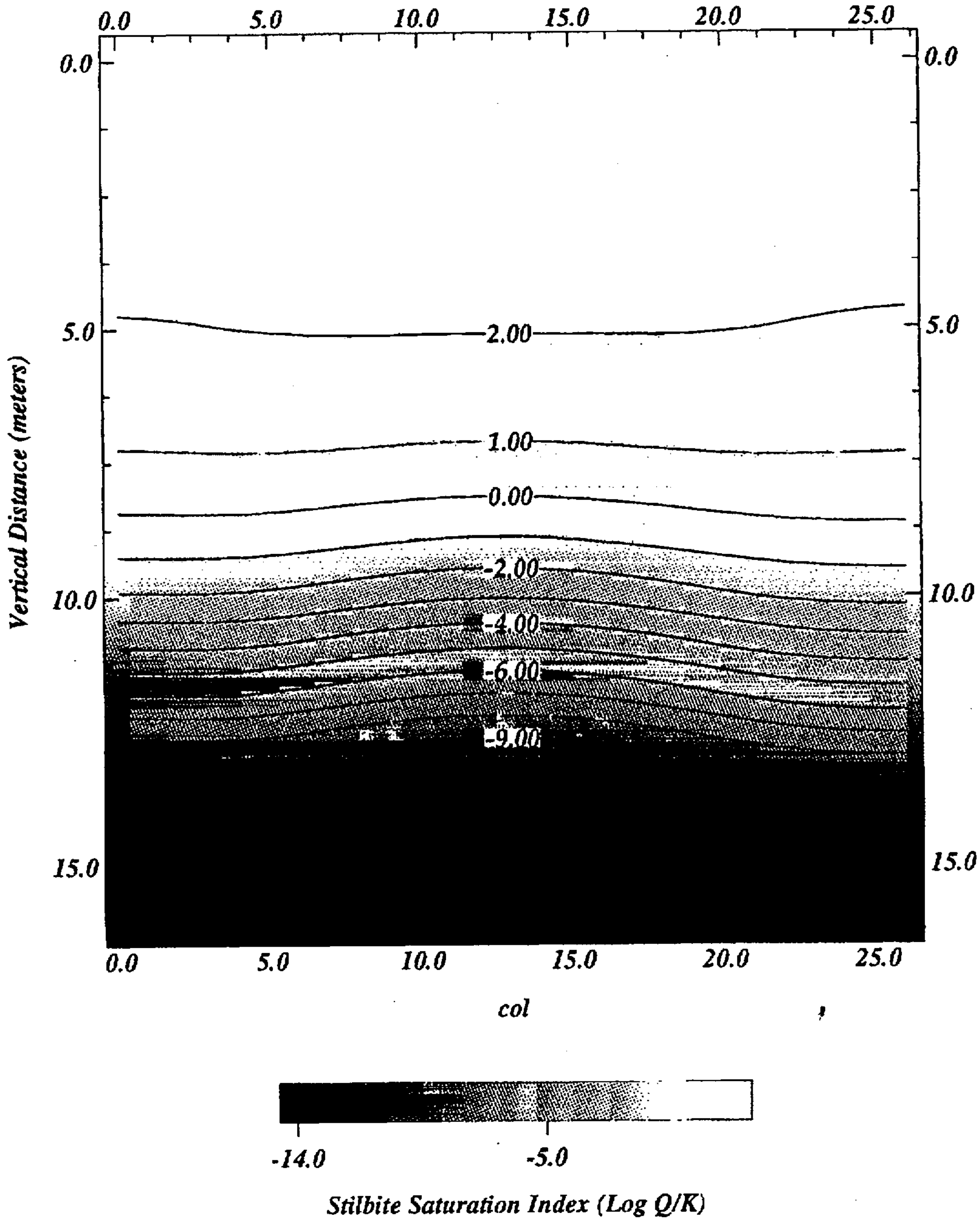

Figure 8f

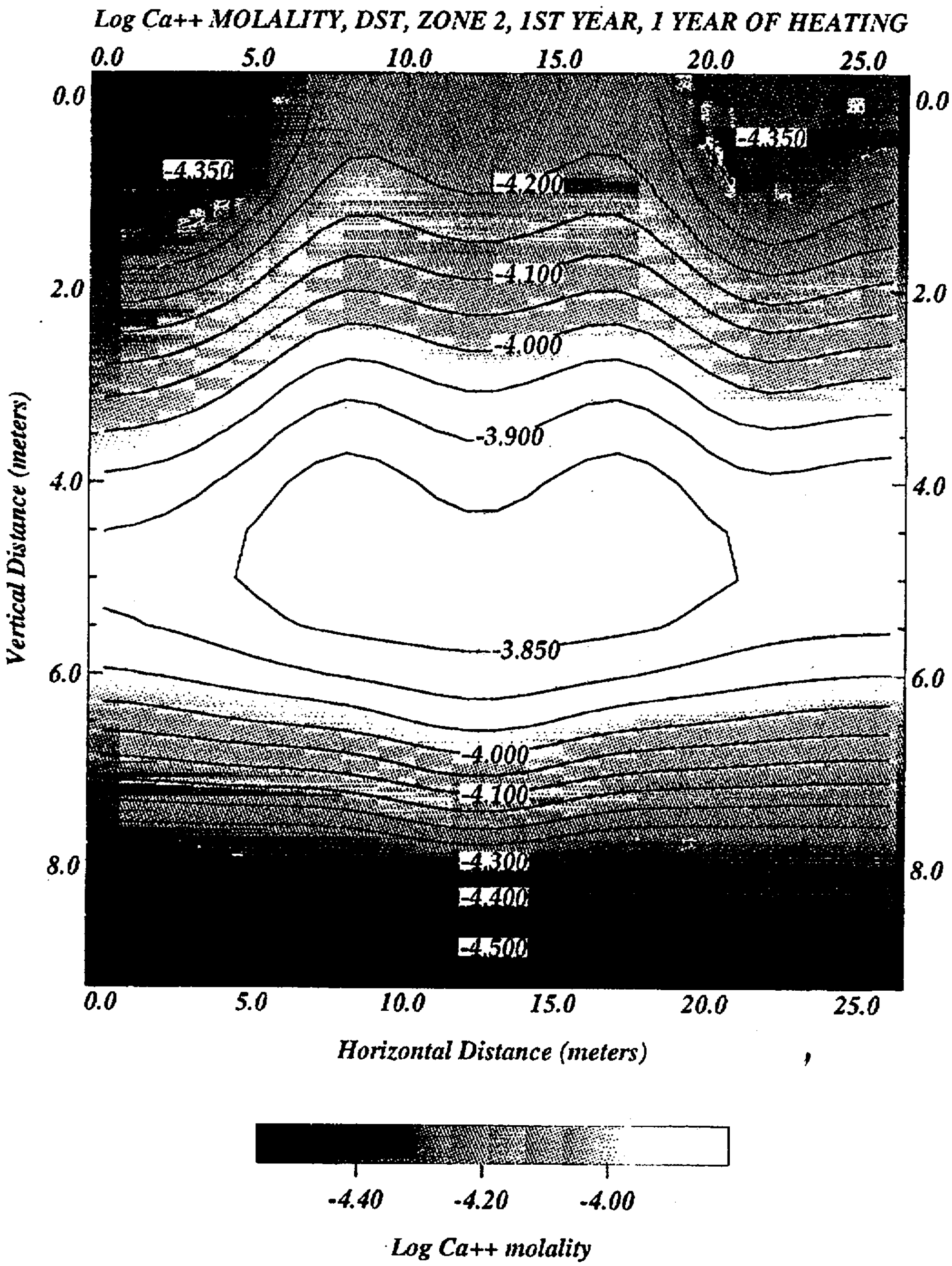

Log Ca++ MOLALITY, DST, ZONE 2, 1ST YEAR, 1 YEAR OF HEATING
0.0
5.0
10.0
15.0
20.0
25.0
-4.350
-4.200
-4.100
-4.000
-3.900
-3.850
-4.300
-4.400
-4.500
2.0
4.0
6.0
8.0
Vertical Distance (meters)
Horizontal Distance (meters)
-4.40
-4.20
-4.00
Log Ca++ molality

Figure 9a

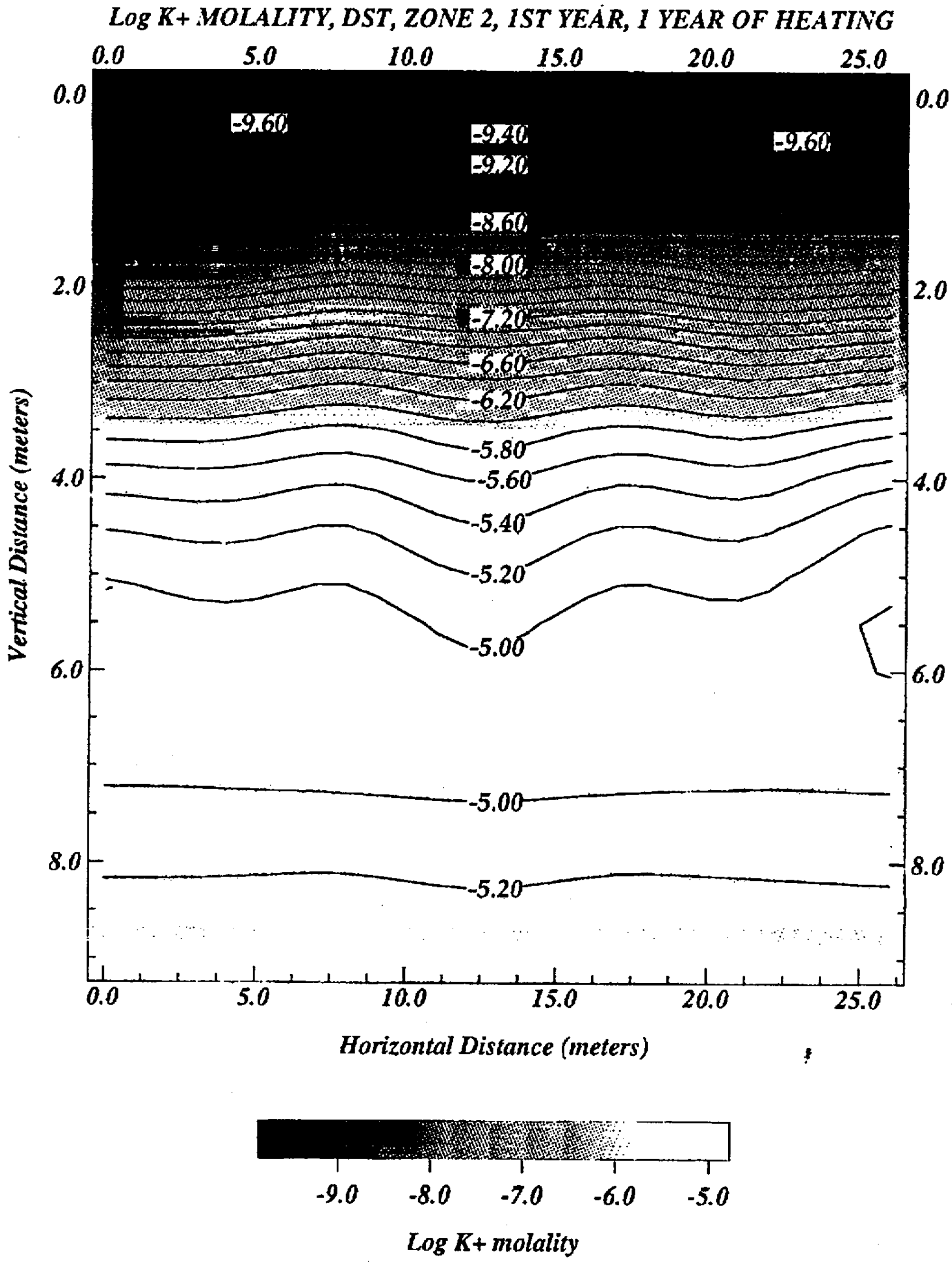
Log K+ MOLALITY, DST, ZONE 2, 1ST YEAR, 1 YEAR OF HEATING
0.0
5.0
10.0
15.0
20.0
25.0
-9.60
-9.40
-9.20
-9.60
-8.60
-8.00
-7.20
-6.60
-6.20
-5.80
-5.60
-5.40
-5.20
-5.00
-5.00
-5.20
0.0
2.0
4.0
6.0
8.0
Vertical Distance (meters)
Horizontal Distance (meters)
-9.0
-8.0
-7.0
-6.0
-5.0
Log K+ molality

Figure 9b

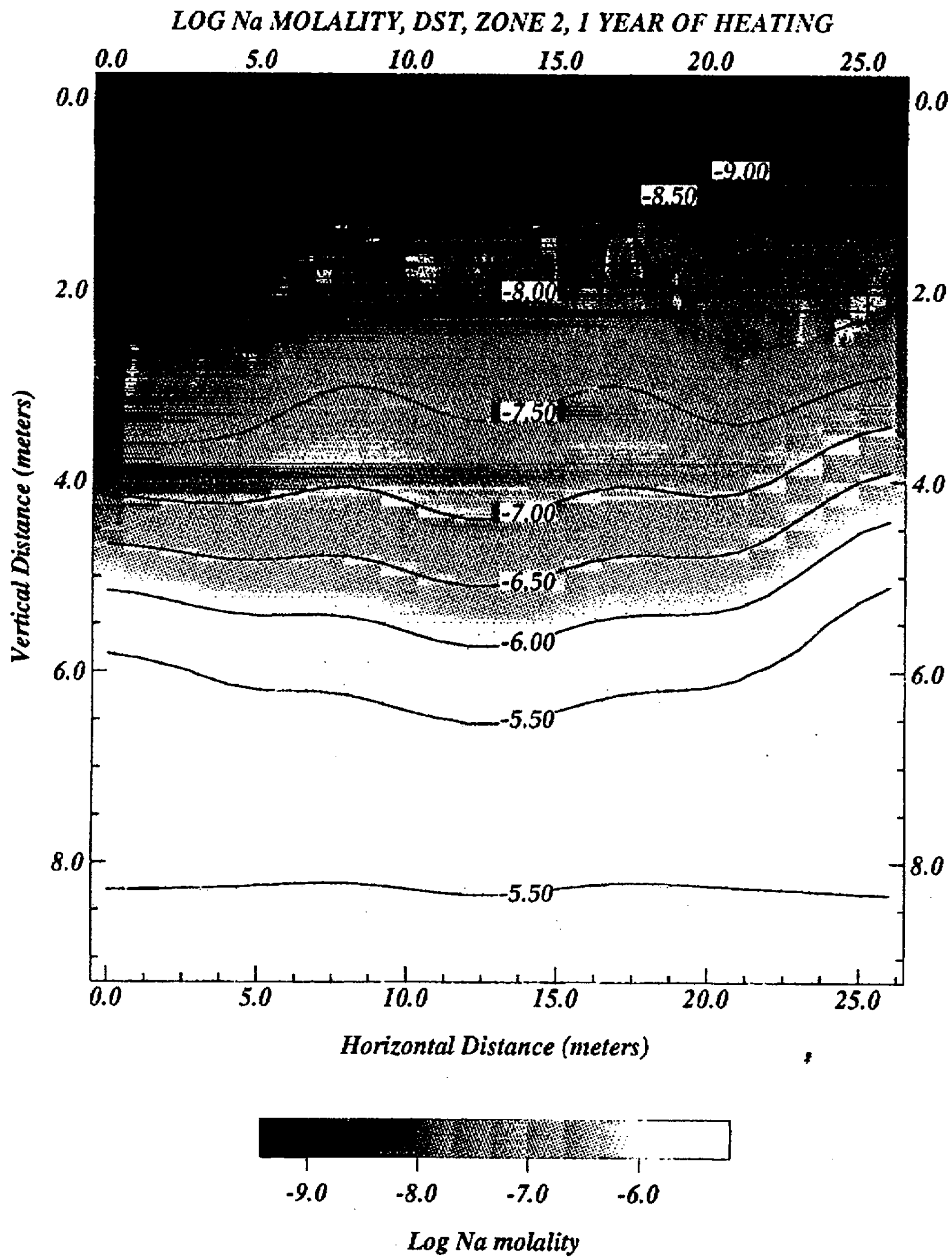

LOG Na MOLALITY, DST, ZONE 2, 1 YEAR OF HEATING
0.0
5.0
10.0
15.0
20.0
25.0
-9.00
-8.50
-8.00
-7.50
-7.00
-6.50
-6.00
-5.50
-5.50
0.0
2.0
4.0
6.0
8.0
Vertical Distance (meters)
Horizontal Distance (meters)
-9.0
-8.0
-7.0
-6.0
Log Na molality

Figure 9c

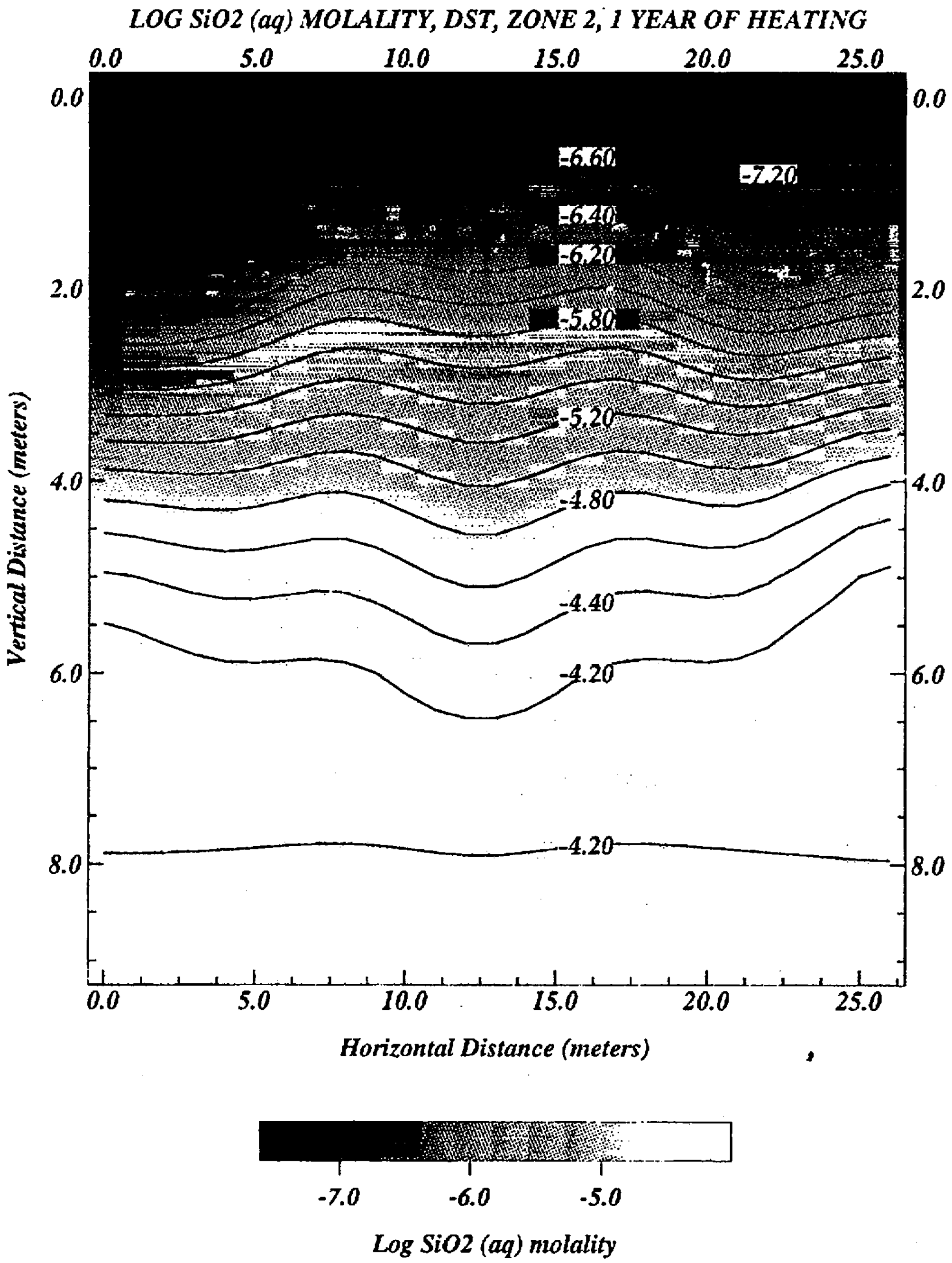
LOG SiO2 (aq) MOLALITY, DST, ZONE 2, 1 YEAR OF HEATING
0.0
5.0
10.0
15.0
20.0
25.0
-6.60
-7.20
-6.40
-6.20
-5.80
-5.20
-4.80
-4.40
-4.20
-4.20
Vertical Distance (meters)
0.0
2.0
4.0
6.0
8.0
Horizontal Distance (meters)
-7.0
-6.0
-5.0
Log SiO2 (aq) molality

Figure 9d

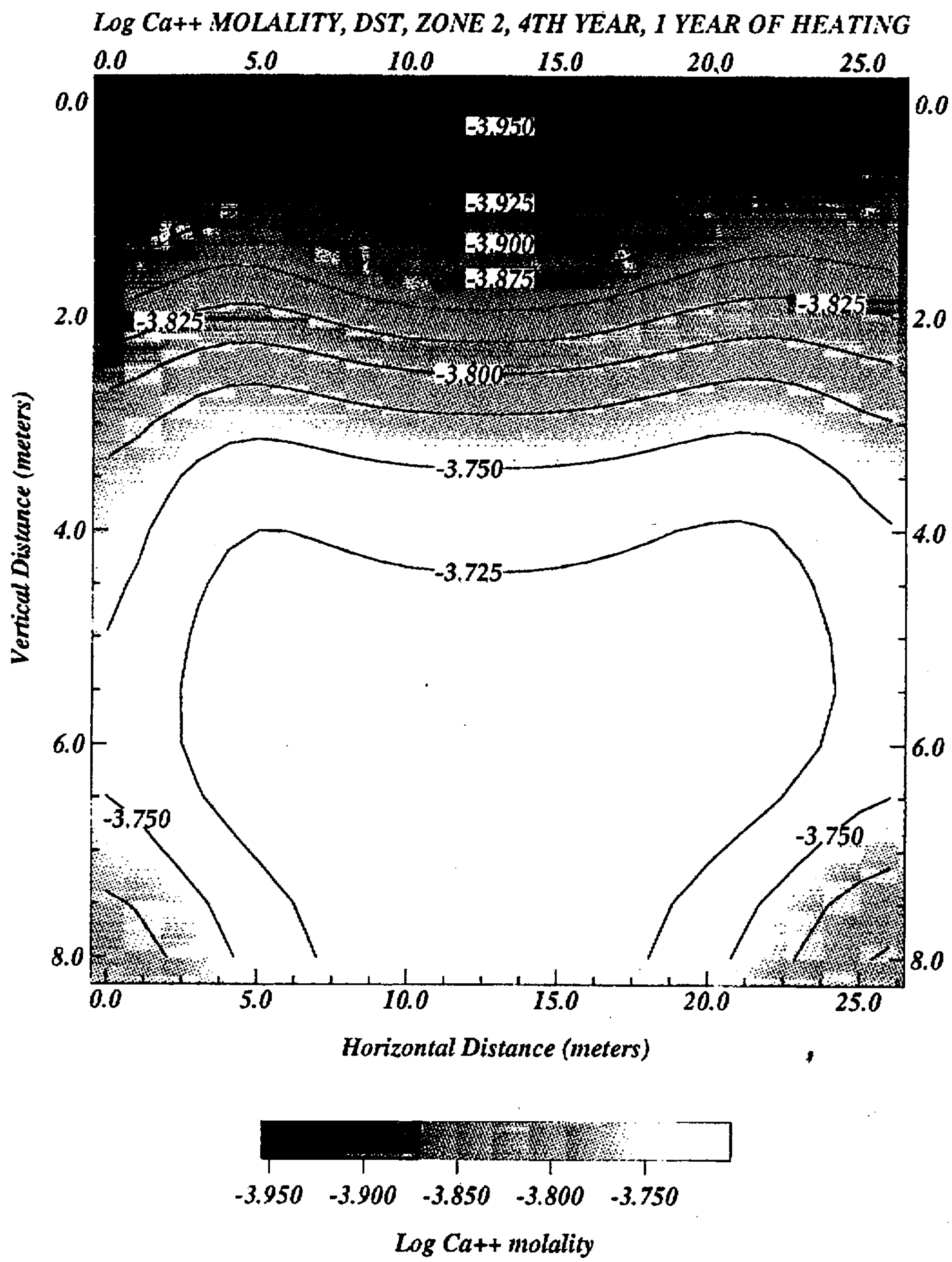

Log Ca++ MOLALITY, DST, ZONE 2, 4TH YEAR, 1 YEAR OF HEATING
0.0
5.0
10.0
15.0
20.0
25.0
0.0
2.0
4.0
6.0
8.0
-3.950
-3.925
-3.900
-3.875
-3.825
-3.825
-3.800
-3.750
-3.725
-3.750
-3.750
Vertical Distance (meters)
Horizontal Distance (meters)
-3.950
-3.900
-3.850
-3.800
-3.750
Log Ca++ molality

Figure 10a

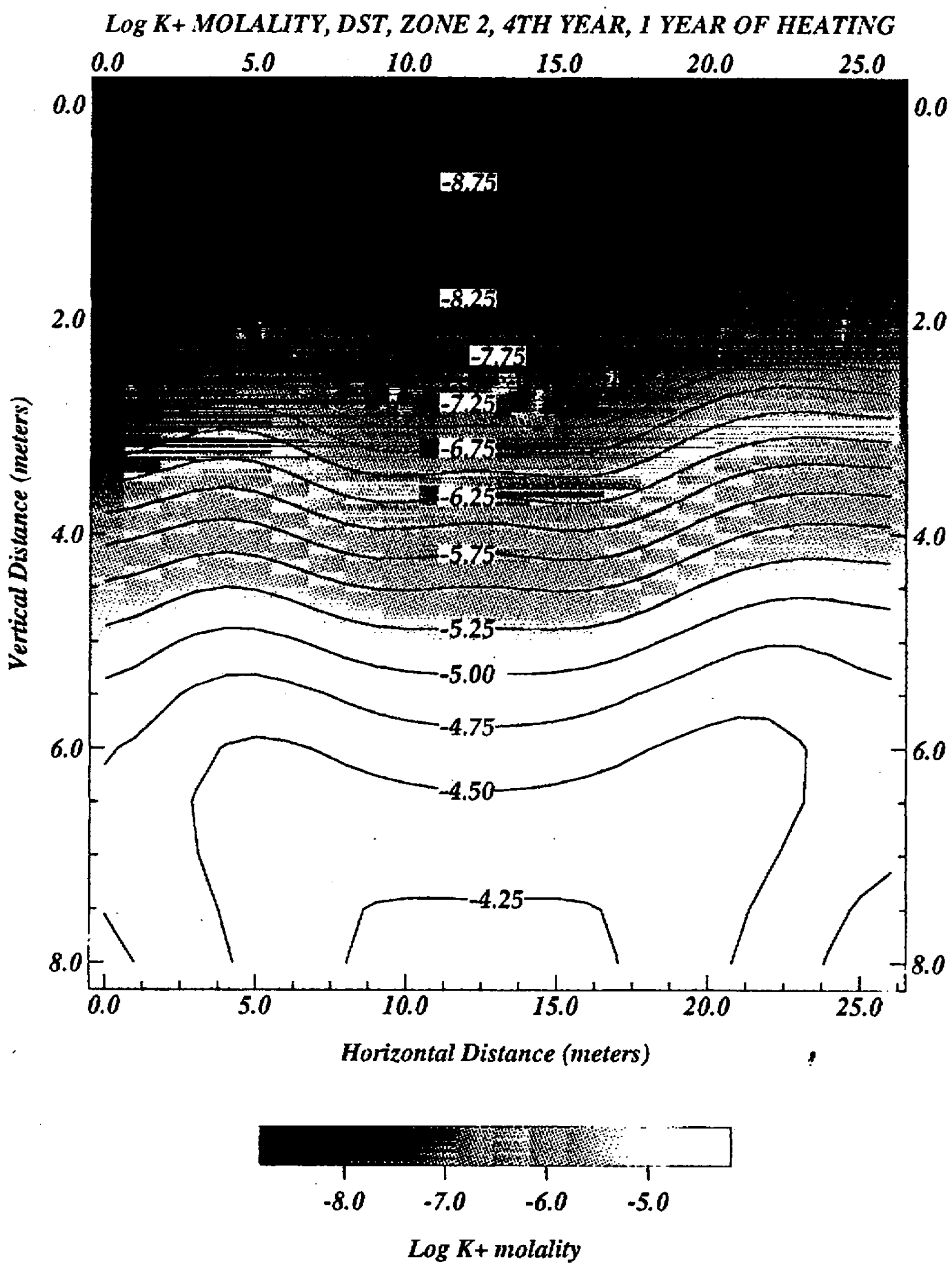

Log K+ MOLALITY, DST, ZONE 2, 4TH YEAR, 1 YEAR OF HEATING
0.0
5.0
10.0
15.0
20.0
25.0
0.0
2.0
4.0
6.0
8.0
-8.75
-8.25
-7.75
-7.25
-6.75
-6.25
-5.75
-5.25
-5.00
-4.75
-4.50
-4.25
Vertical Distance (meters)
Horizontal Distance (meters)
-8.0
-7.0
-6.0
-5.0
Log K+ molality

Figure 10b

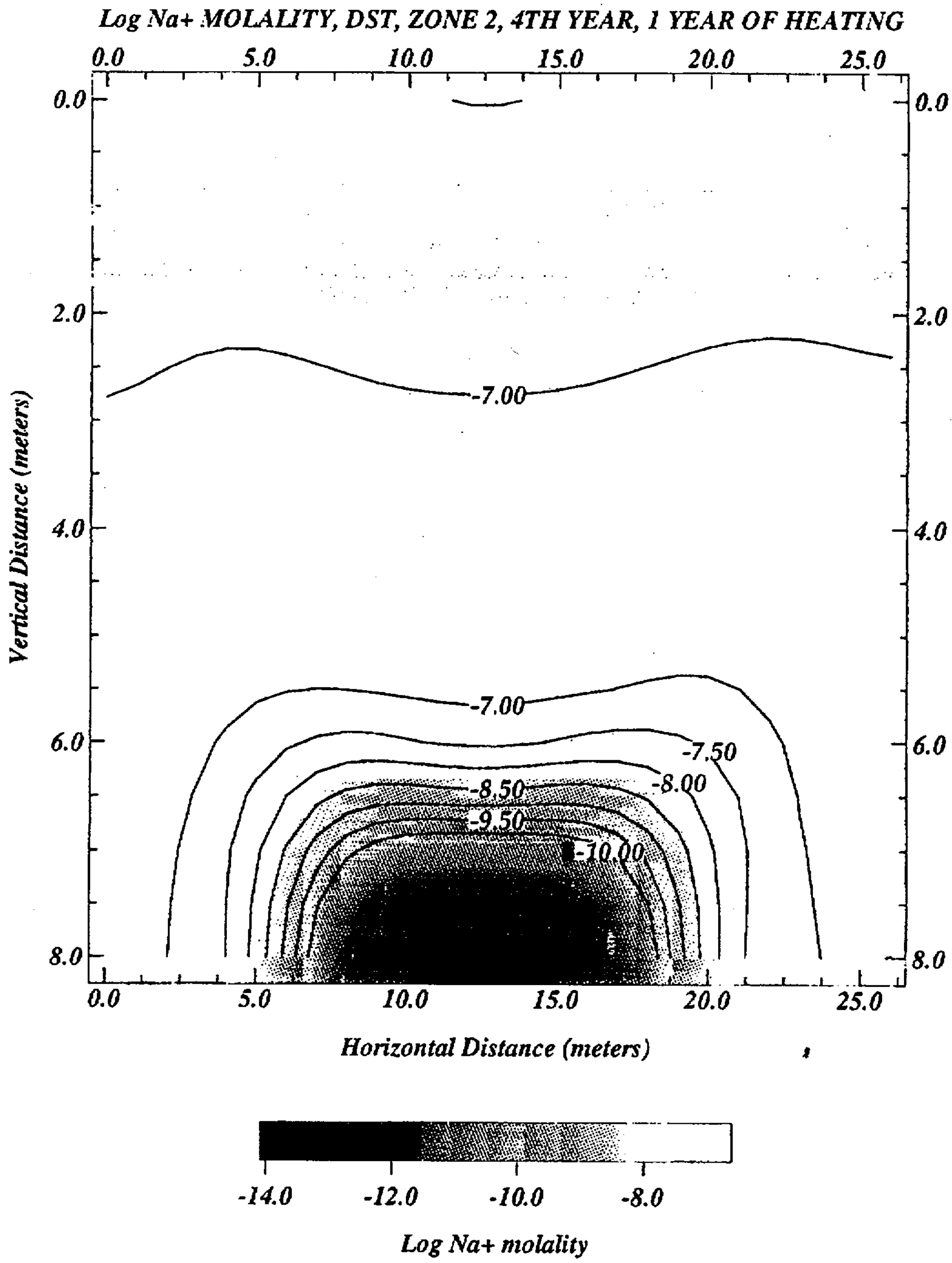
Log Na+ MOLALITY, DST, ZONE 2, 4TH YEAR, 1 YEAR OF HEATING
0.0
5.0
10.0
15.0
20.0
25.0
0.0
2.0
4.0
6.0
8.0
-7.00
-7.00
-7.50
-8.00
-8.50
-9.50
-10.00
Vertical Distance (meters)
Horizontal Distance (meters)
-14.0
-12.0
-10.0
-8.0
Log Na+ molality

Figure 10c

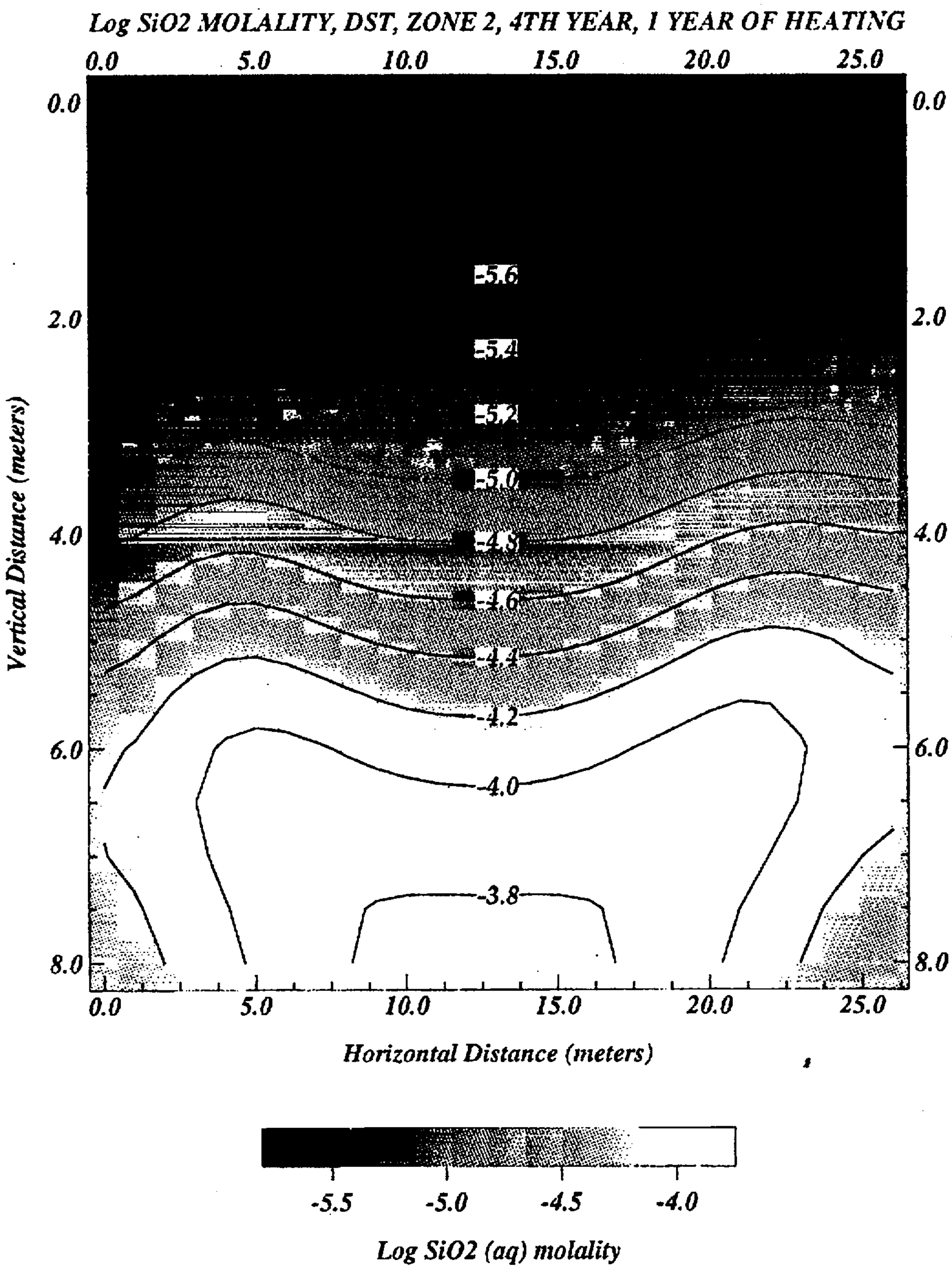
Log SiO2 MOLALITY, DST, ZONE 2, 4TH YEAR, 1 YEAR OF HEATING
0.0
5.0
10.0
15.0
20.0
25.0
0.0
2.0
4.0
6.0
8.0
-5.6
-5.4
-5.2
-5.0
-4.8
-4.6
-4.4
-4.2
-4.0
-3.8
Vertical Distance (meters)
Horizontal Distance (meters)
-5.5
-5.0
-4.5
-4.0
Log SiO2 (aq) molality

Figure 10d

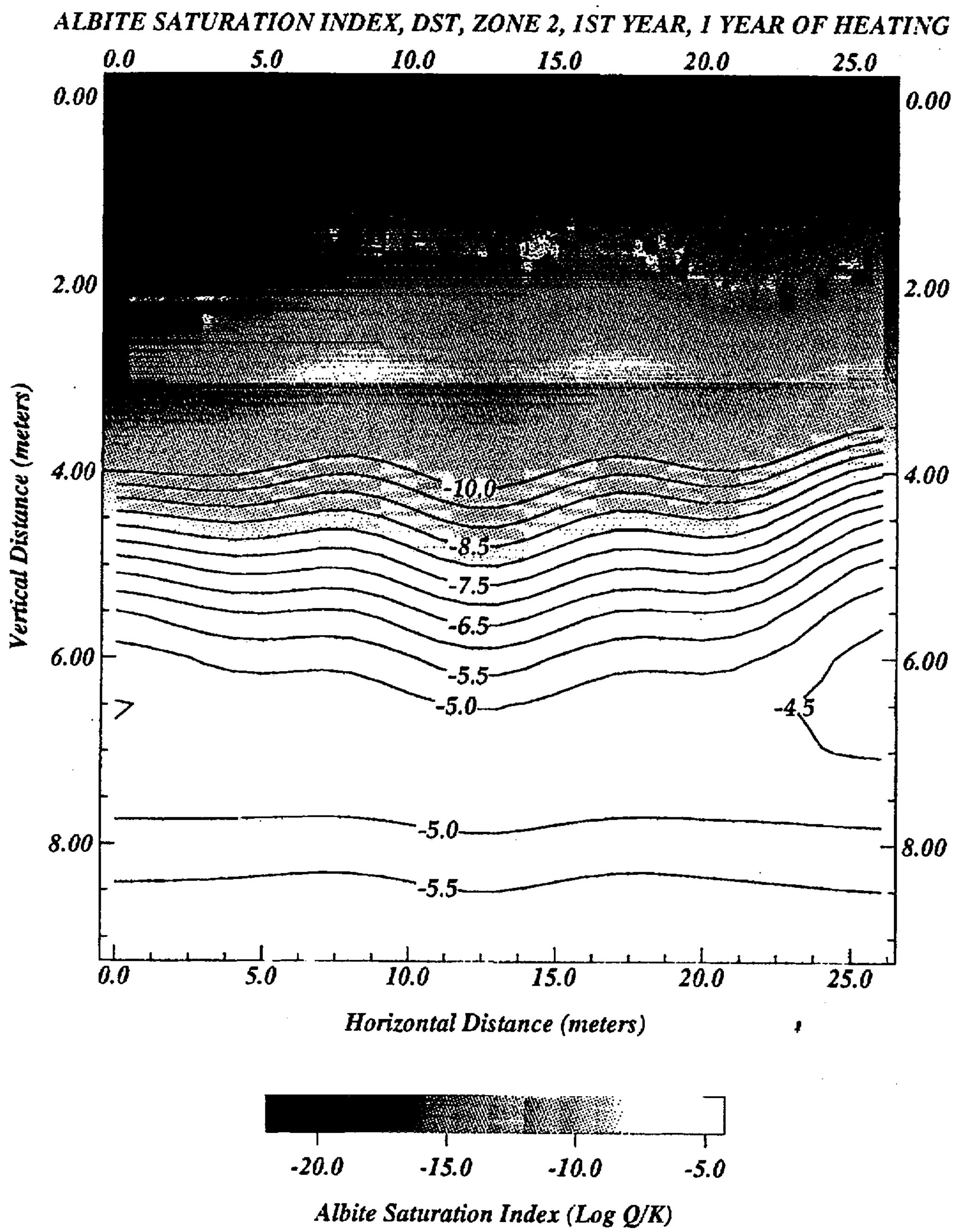
ALBITE SATURATION INDEX, DST, ZONE 2, 1ST YEAR, 1 YEAR OF HEATING
0.0
5.0
10.0
15.0
20.0
25.0
0.00
2.00
4.00
6.00
8.00
Vertical Distance (meters)
-10.0
-8.5
-7.5
-6.5
-5.5
-5.0
-4.5
-5.0
-5.5
Horizontal Distance (meters)
-20.0
-15.0
-10.0
-5.0
Albite Saturation Index (Log Q/K)

Figure 11a

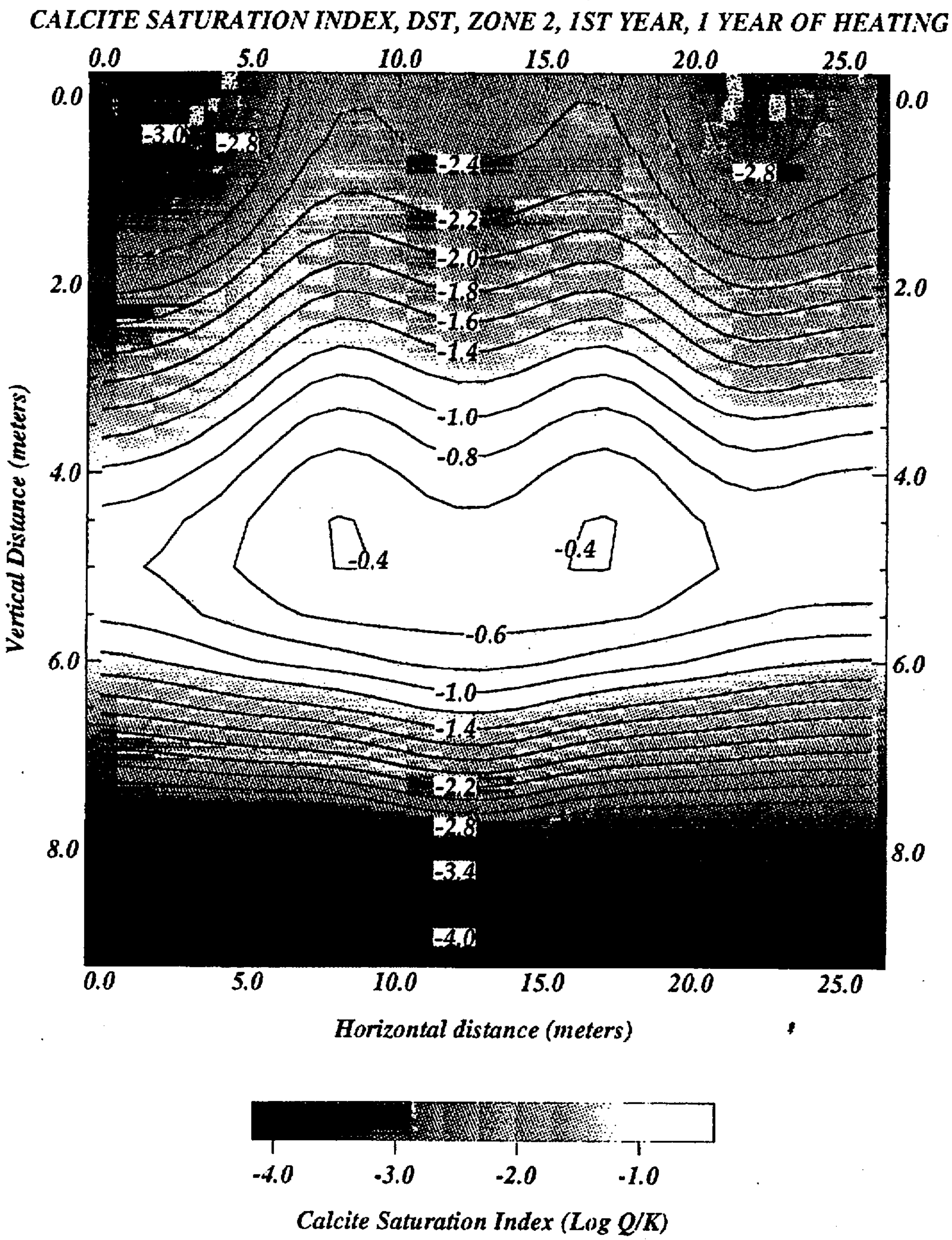

CALCITE SATURATION INDEX, DST, ZONE 2, 1ST YEAR, 1 YEAR OF HEATING
0.0
5.0
10.0
15.0
20.0
25.0
0.0
2.0
4.0
6.0
8.0
Vertical Distance (meters)
-3.0
-2.8
-2.4
-2.2
-2.0
-1.8
-1.6
-1.4
-1.0
-0.8
-0.4
-0.4
-0.6
-1.0
-1.4
-2.2
-2.8
-3.4
-4.0
Horizontal distance (meters)
-4.0
-3.0
-2.0
-1.0
Calcite Saturation Index (Log Q/K)

Figure 11b

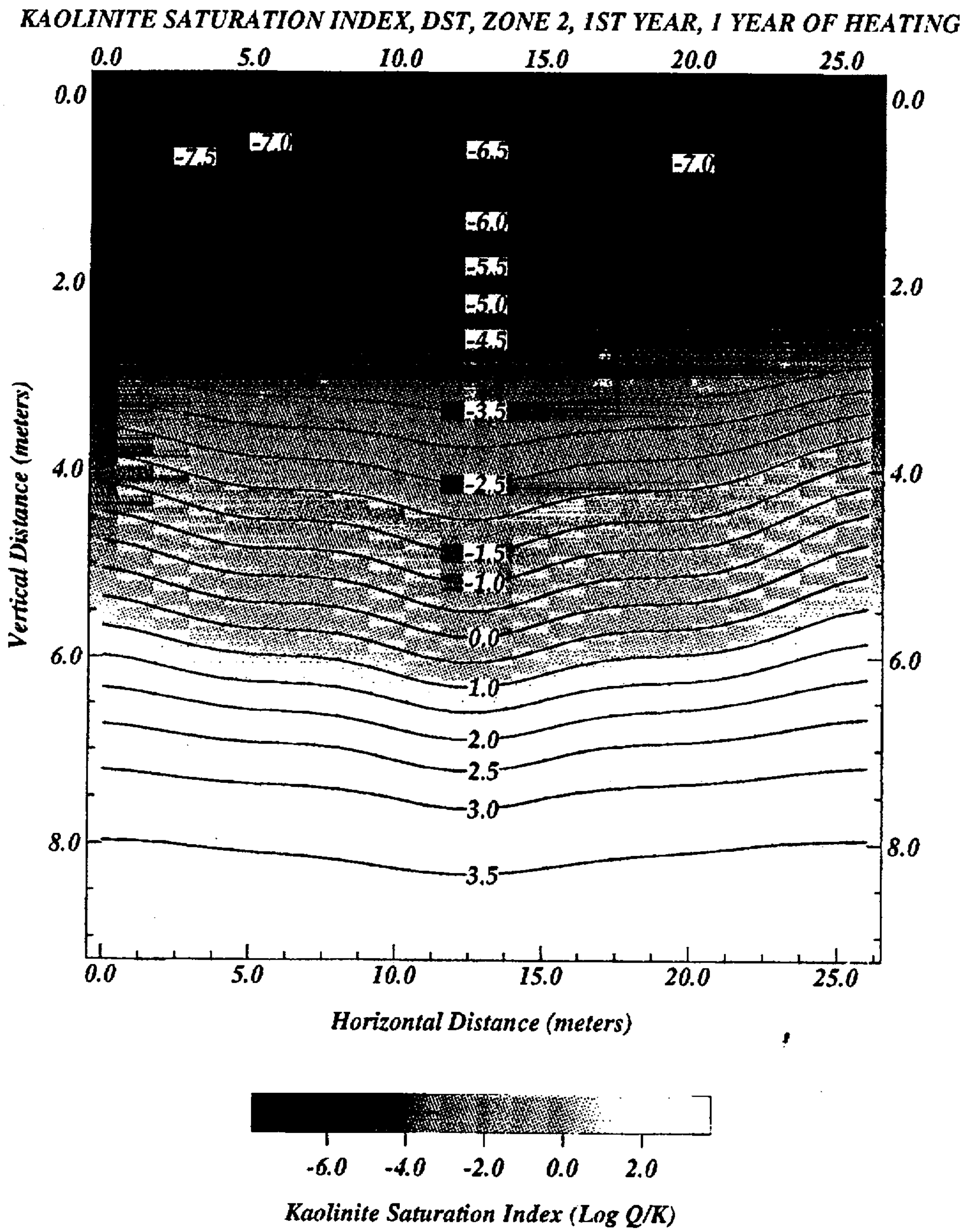

KAOLINITE SATURATION INDEX, DST, ZONE 2, 1ST YEAR, 1 YEAR OF HEATING
0.0
5.0
10.0
15.0
20.0
25.0
-7.5
-7.0
-6.5
-7.0
-6.0
-5.5
-5.0
-4.5
-3.5
-2.5
-1.5
-1.0
0.0
1.0
2.0
2.5
3.0
3.5
0.0
2.0
4.0
6.0
8.0
Vertical Distance (meters)
Horizontal Distance (meters)
-6.0
-4.0
-2.0
0.0
2.0
Kaolinite Saturation Index (Log Q/K)

Figure 11c

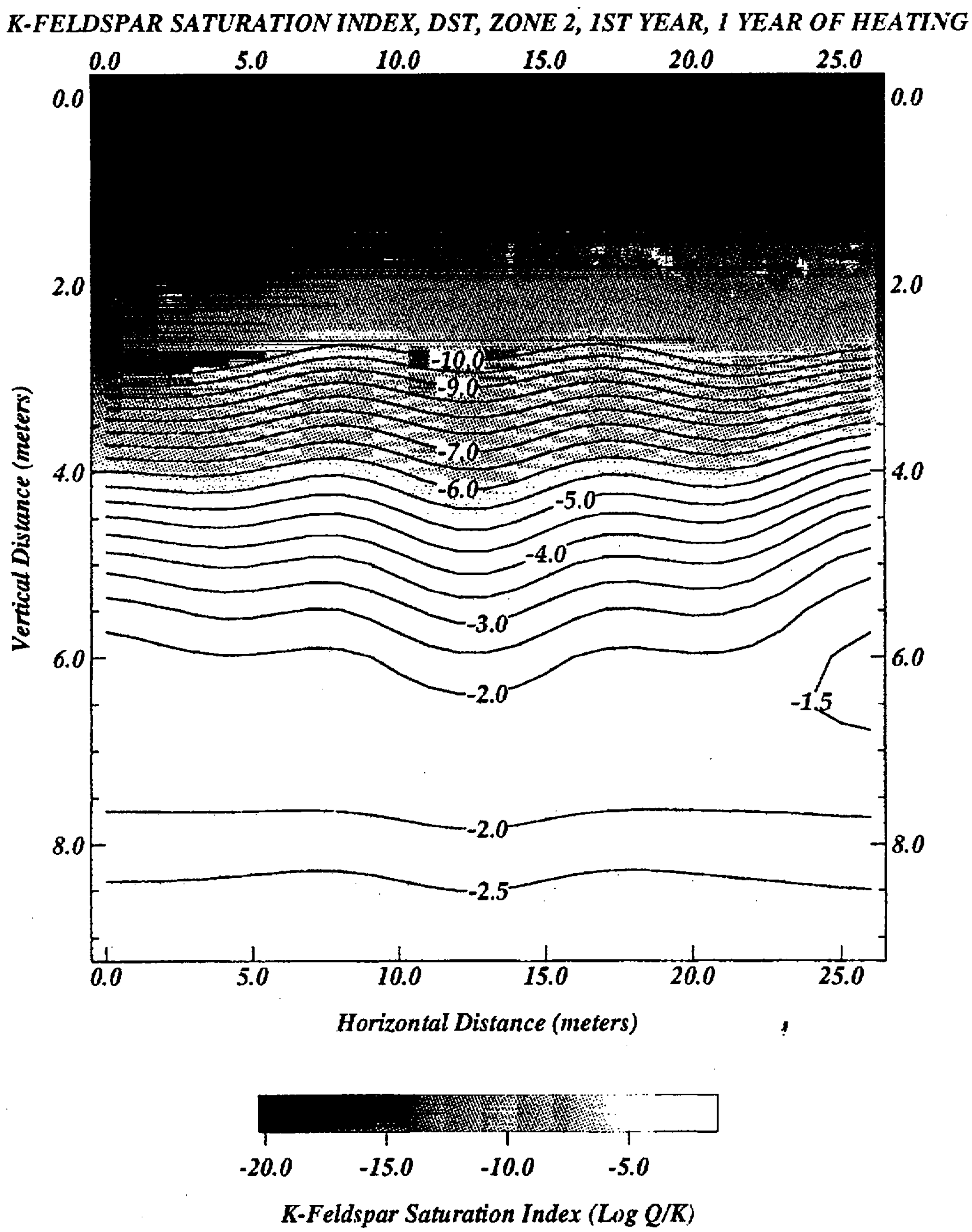
K-FELDSPAR SATURATION INDEX, DST, ZONE 2, 1ST YEAR, 1 YEAR OF HEATING
0.0
5.0
10.0
15.0
20.0
25.0
0.0
2.0
4.0
6.0
8.0
Vertical Distance (meters)
-10.0
-9.0
-7.0
-6.0
-5.0
-4.0
-3.0
-2.0
-1.5
-2.0
-2.5
Horizontal Distance (meters)
-20.0
-15.0
-10.0
-5.0
K-Feldspar Saturation Index (Log Q/K)

Figure 11d

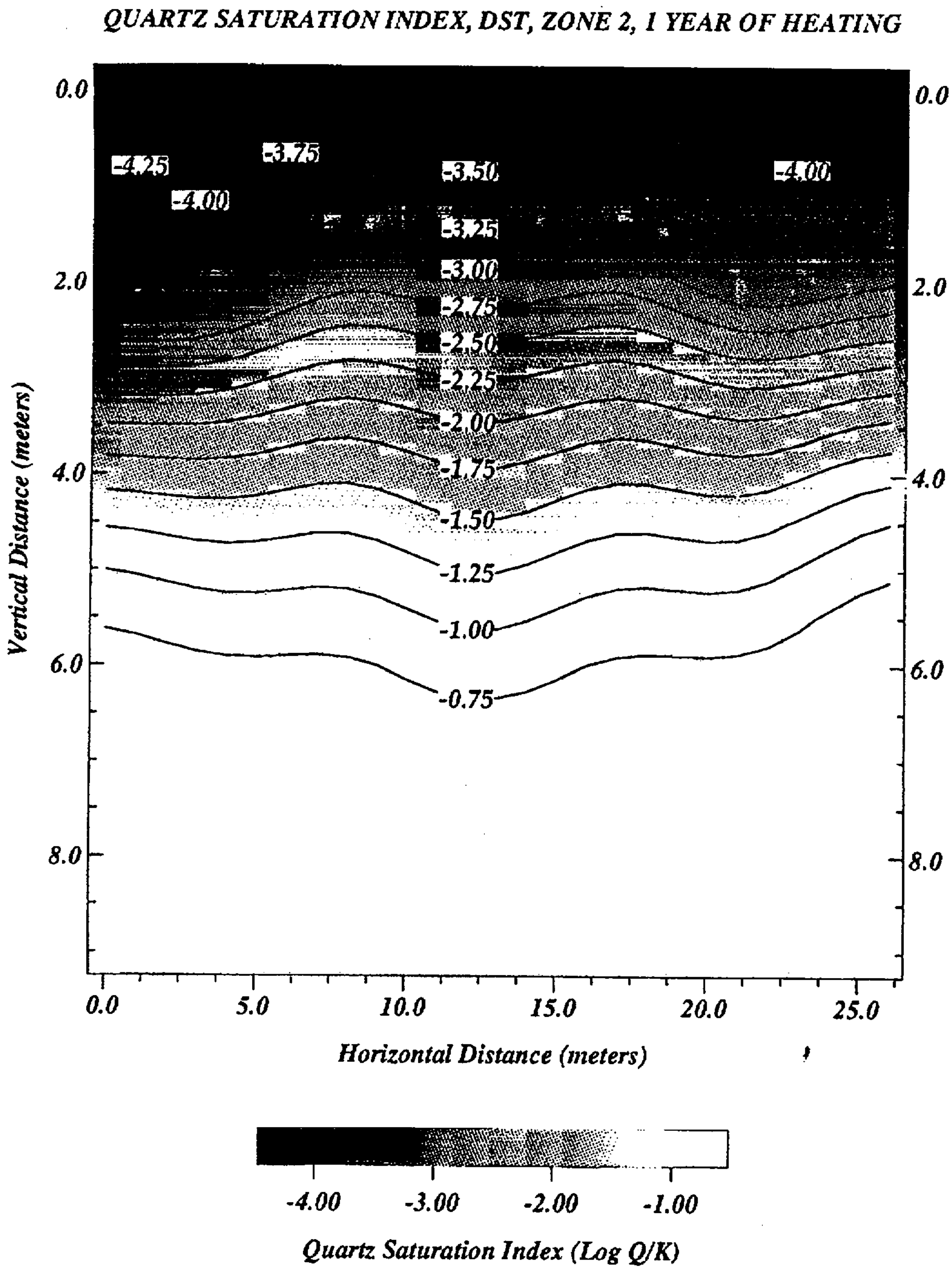

QUARTZ SATURATION INDEX, DST, ZONE 2, 1 YEAR OF HEATING
-4.25
-3.75
-4.00
-3.50
-4.00
-3.25
-3.00
-2.75
-2.50
-2.25
-2.00
-1.75
-1.50
-1.25
-1.00
-0.75
0.0
2.0
4.0
6.0
8.0
Vertical Distance (meters)
0.0
5.0
10.0
15.0
20.0
25.0
Horizontal Distance (meters)
-4.00
-3.00
-2.00
-1.00
Quartz Saturation Index (Log Q/K)

Figure 11e

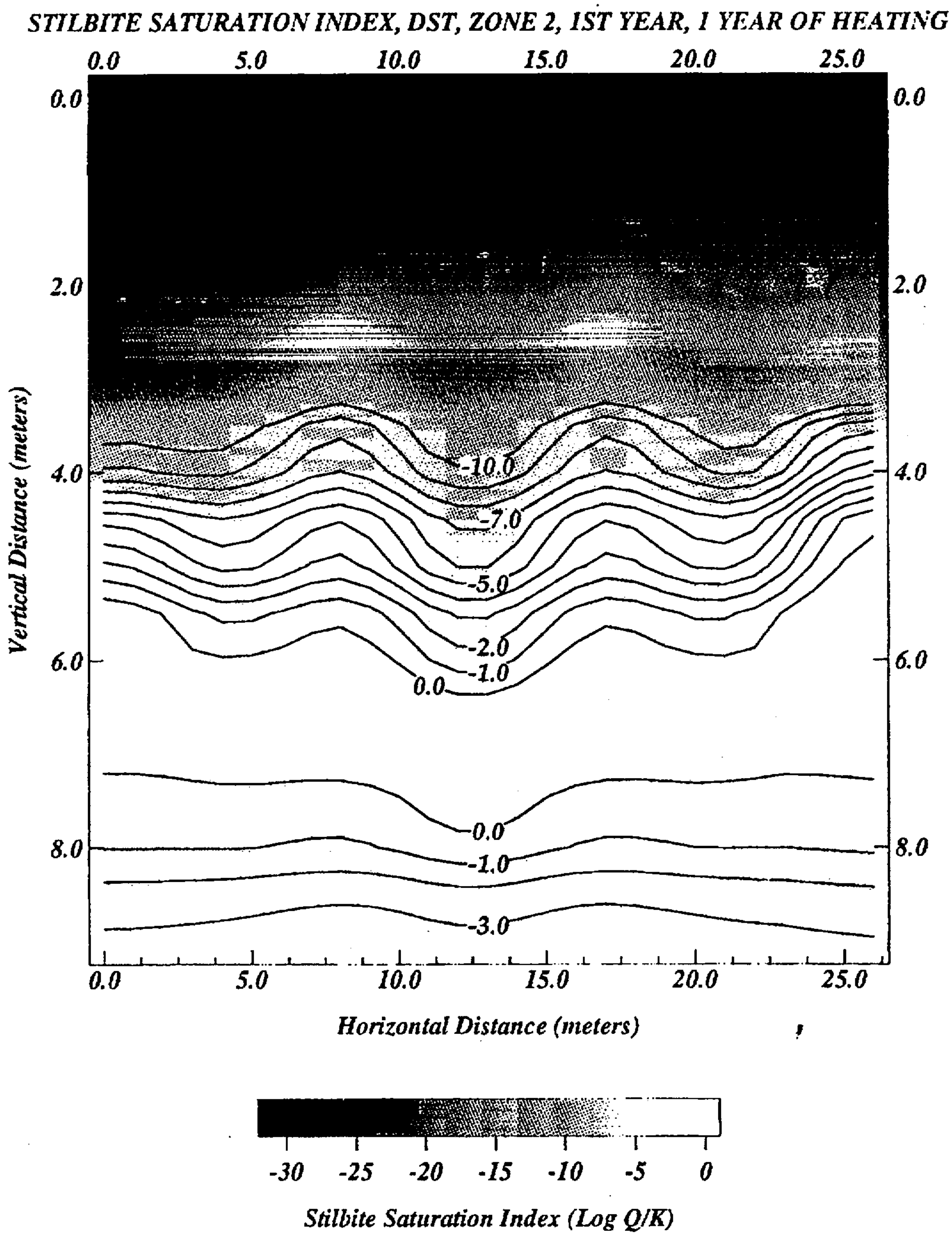
STILBITE SATURATION INDEX, DST, ZONE 2, 1ST YEAR, 1 YEAR OF HEATING
0.0
5.0
10.0
15.0
20.0
25.0
Vertical Distance (meters)
2.0
4.0
6.0
8.0
-10.0
-7.0
-5.0
-2.0
-1.0
0.0
0.0
-1.0
-3.0
Horizontal Distance (meters)
-30
-25
-20
-15
-10
-5
0
Stilbite Saturation Index (Log Q/K)

Figure 11f

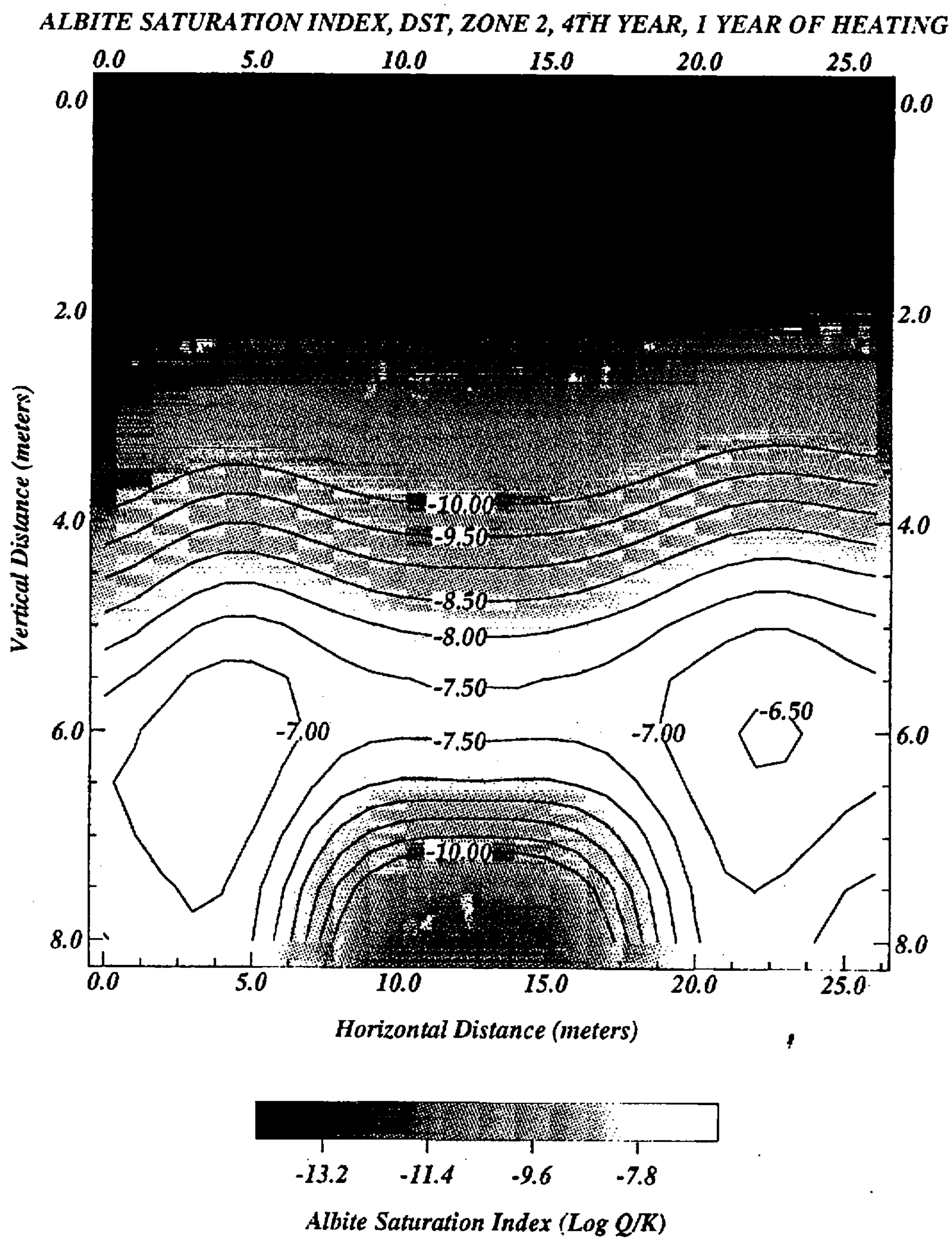
ALBITE SATURATION INDEX, DST, ZONE 2, 4TH YEAR, 1 YEAR OF HEATING
0.0
5.0
10.0
15.0
20.0
25.0
0.0
2.0
4.0
6.0
8.0
Vertical Distance (meters)
-10.00
-9.50
-8.50
-8.00
-7.50
-7.00
-7.50
-7.00
-6.50
-10.00
Horizontal Distance (meters)
-13.2
-11.4
-9.6
-7.8
Albite Saturation Index (Log Q/K)

Figure 12a

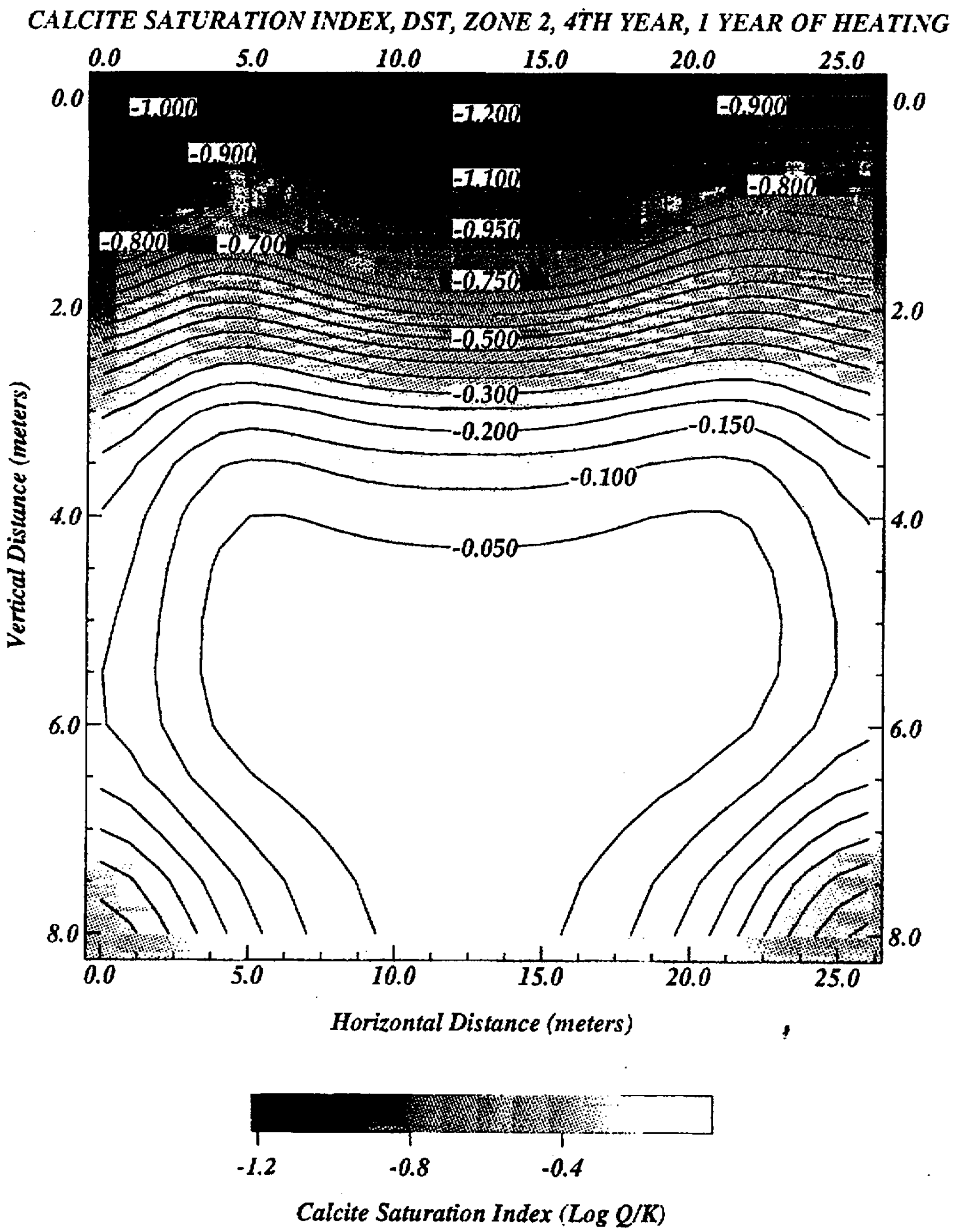
CALCITE SATURATION INDEX, DST, ZONE 2, 4TH YEAR, 1 YEAR OF HEATING
-1.000
-1.200
-0.900
-0.900
-1.100
-0.800
-0.950
-0.800
-0.700
-0.750
-0.500
-0.300
-0.200
-0.150
-0.100
-0.050
Vertical Distance (meters)
Horizontal Distance (meters)
-1.2
-0.8
-0.4
Calcite Saturation Index (Log Q/K)

Figure 12b

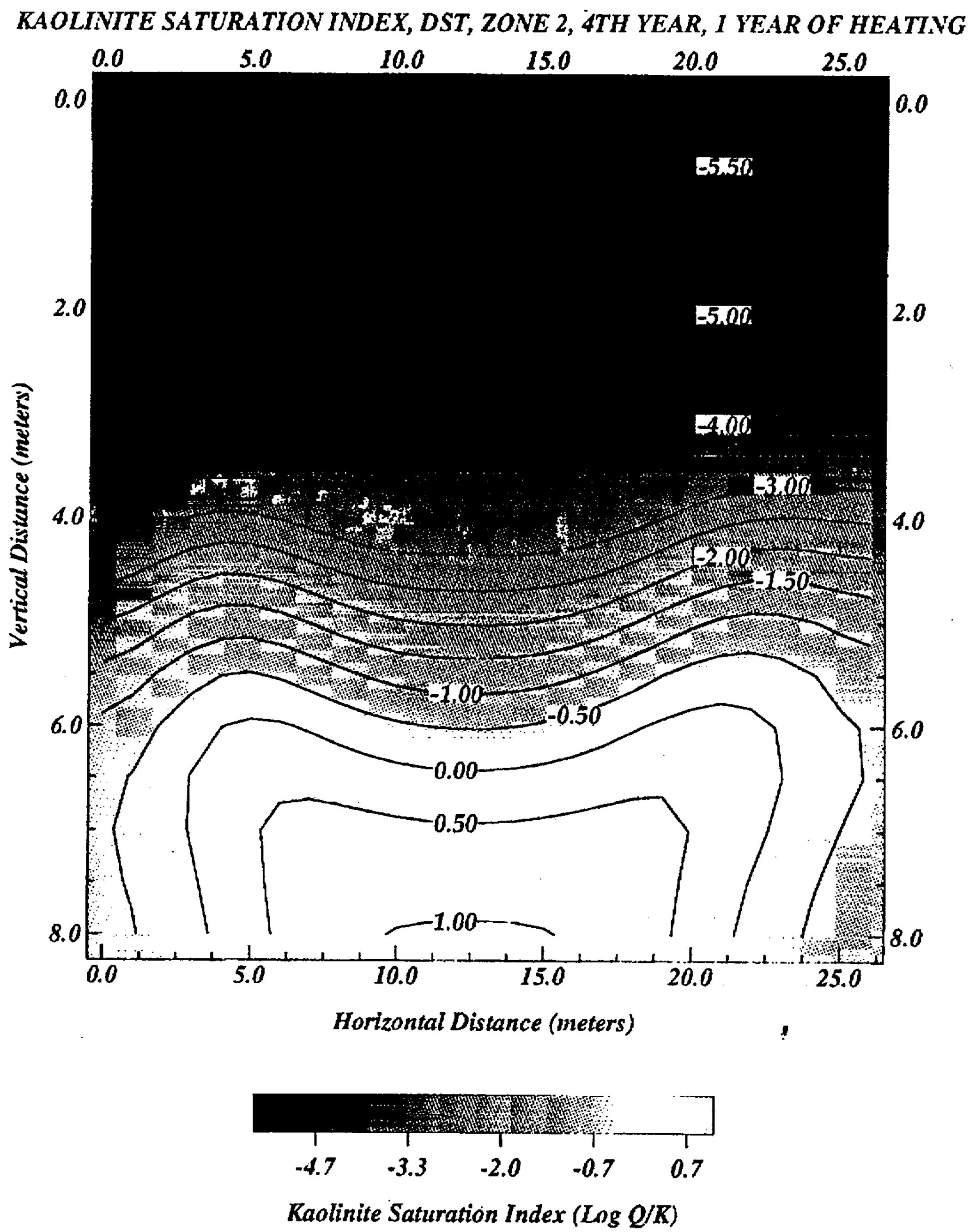
KAOLINITE SATURATION INDEX, DST, ZONE 2, 4TH YEAR, 1 YEAR OF HEATING
0.0
5.0
10.0
15.0
20.0
25.0
0.0
2.0
4.0
6.0
8.0
-5.50
-5.00
-4.00
-3.00
-2.00
-1.50
-1.00
-0.50
0.00
0.50
1.00
Vertical Distance (meters)
Horizontal Distance (meters)
-4.7
-3.3
-2.0
-0.7
0.7
Kaolinite Saturation Index (Log Q/K)

Figure 12c

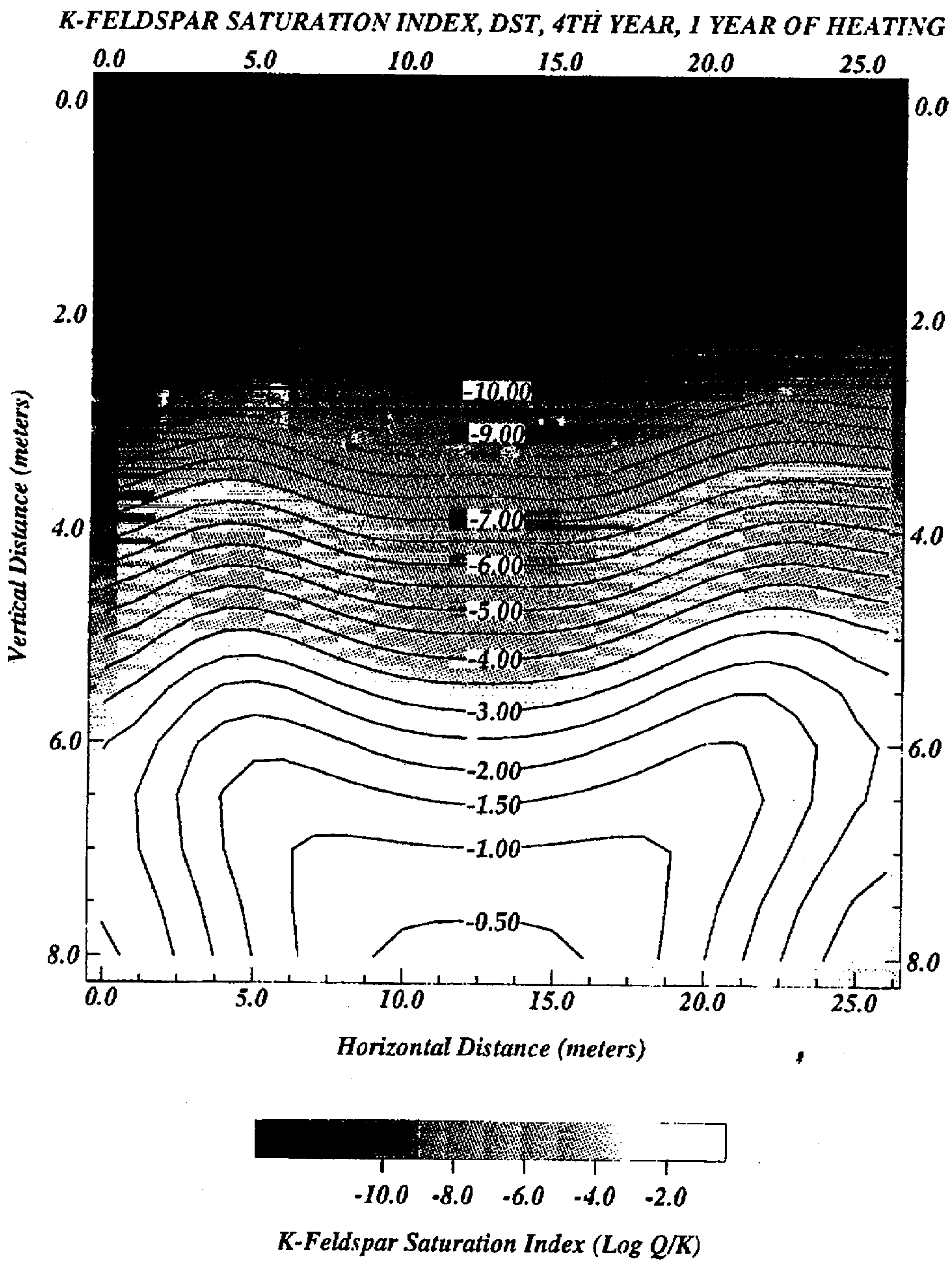

K-FELDSPAR SATURATION INDEX, DST, 4TH YEAR, 1 YEAR OF HEATING
0.0
5.0
10.0
15.0
20.0
25.0
0.0
2.0
4.0
6.0
8.0
-10.00
-9.00
-7.00
-6.00
-5.00
-4.00
-3.00
-2.00
-1.50
-1.00
-0.50
Vertical Distance (meters)
Horizontal Distance (meters)
-10.0
-8.0
-6.0
-4.0
-2.0
K-Feldspar Saturation Index (Log Q/K)

Figure 12d

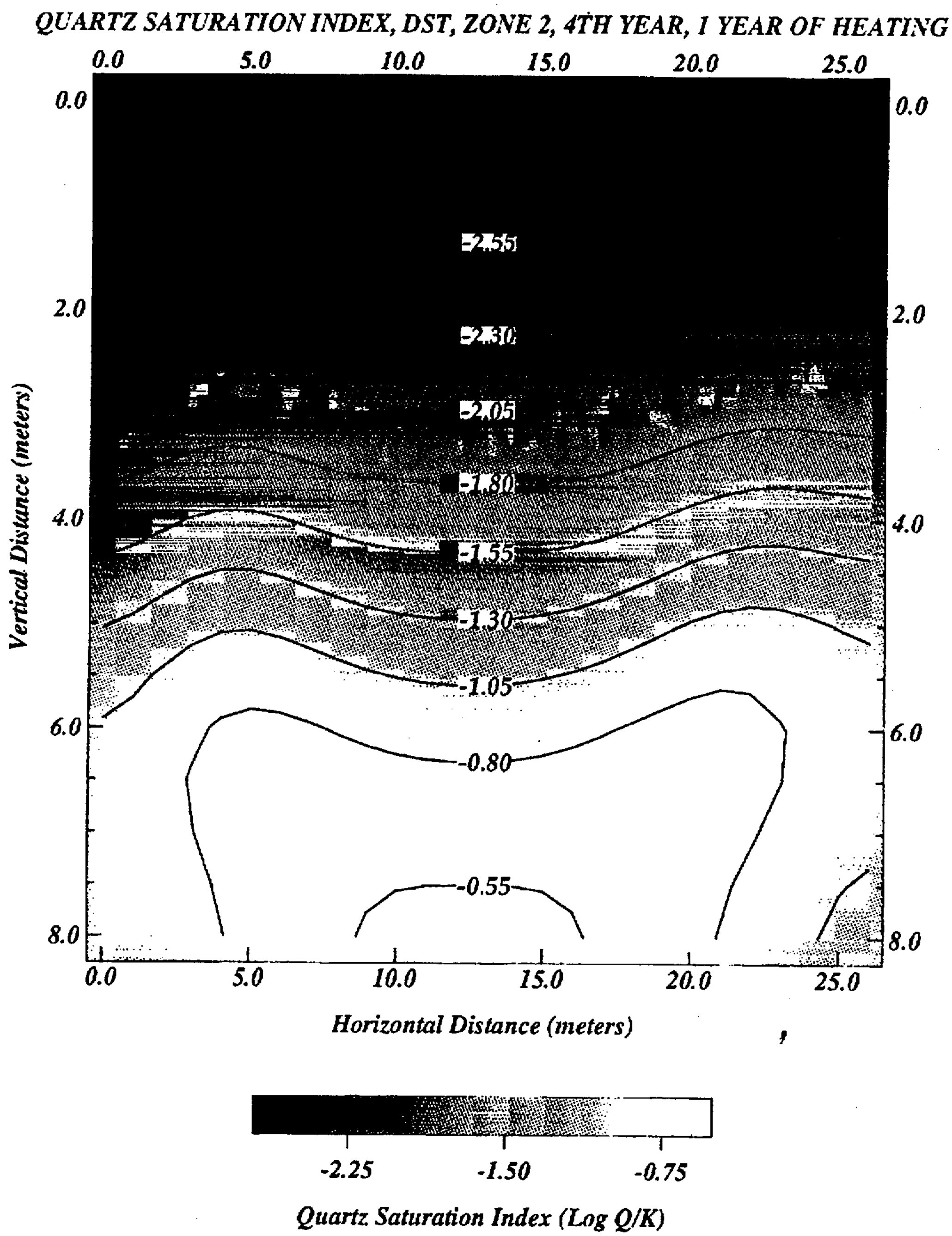
QUARTZ SATURATION INDEX, DST, ZONE 2, 4TH YEAR, 1 YEAR OF HEATING
0.0
5.0
10.0
15.0
20.0
25.0
0.0
2.0
4.0
6.0
8.0
-2.55
-2.30
-2.05
-1.80
-1.55
-1.30
-1.05
-0.80
-0.55
Vertical Distance (meters)
Horizontal Distance (meters)
-2.25
-1.50
-0.75
Quartz Saturation Index (Log Q/K)

Figure 12e

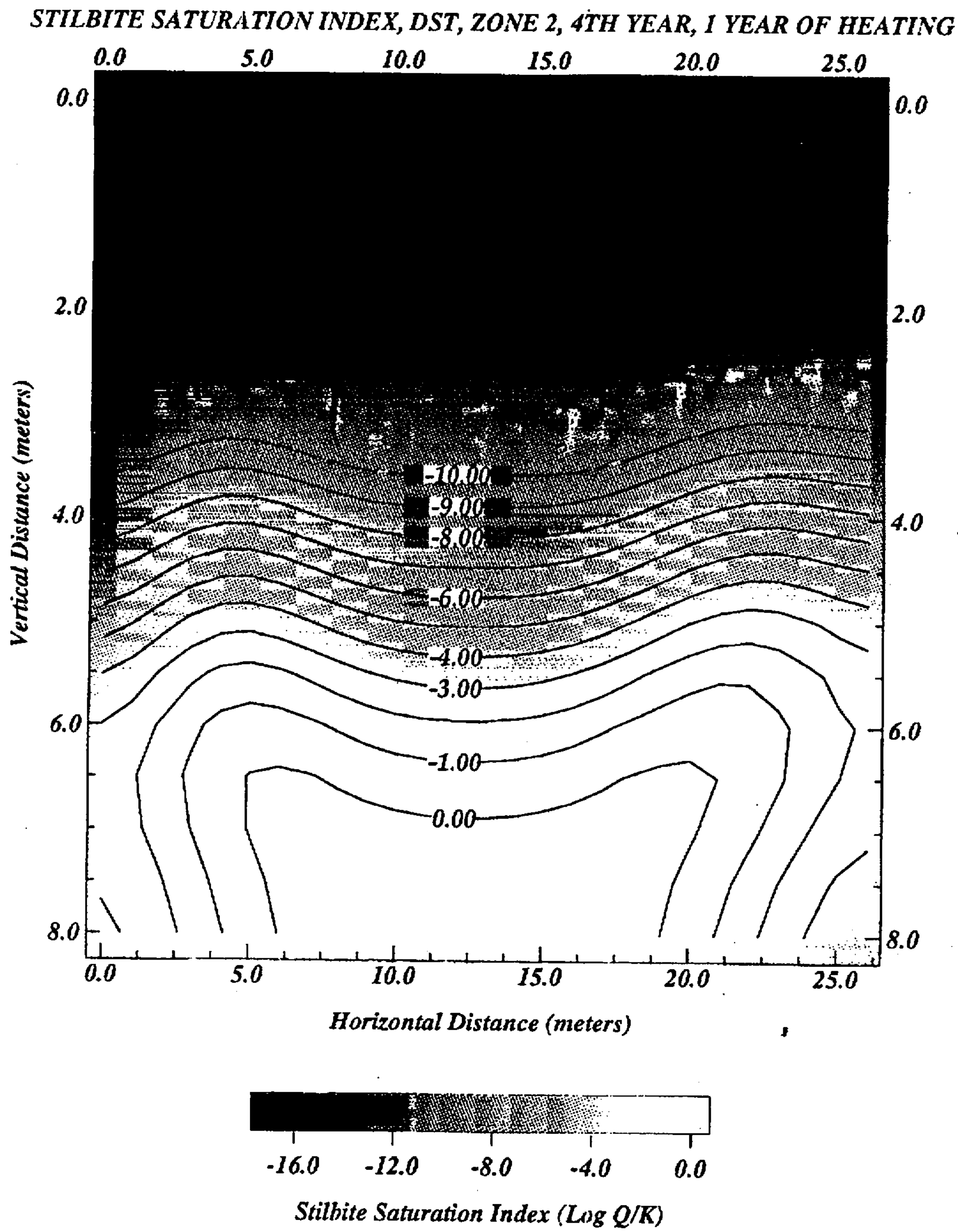

STILBITE SATURATION INDEX, DST, ZONE 2, 4TH YEAR, 1 YEAR OF HEATING
0.0
5.0
10.0
15.0
20.0
25.0
0.0
2.0
4.0
6.0
8.0
-10.00
-9.00
-8.00
-6.00
-4.00
-3.00
-1.00
0.00
Vertical Distance (meters)
Horizontal Distance (meters)
-16.0
-12.0
-8.0
-4.0
0.0
Stilbite Saturation Index (Log Q/K)

Figure 12f